

Proteomic Study in a Hematological Malignancy: B-cell Acute Lymphoblastic Leukemia

By

Sutapa Saha

LIFE 05200704001

Saha Institute of Nuclear Physics, Kolkata

*A thesis submitted to the
Board of Studies in Life Sciences*

*In partial fulfillment of requirements
For the Degree of*

DOCTOR OF PHILOSOPHY

of

HOMI BHABHA NATIONAL INSTITUTE



September, 2011

Homi Bhabha National Institute

Recommendations of the Viva Voce Board

As members of the Viva Voce Board, we certify that we have read the dissertation prepared by **Sutapa Saha** entitled “**Proteomic Study in a Hematological Malignancy: B-cell Acute Lymphoblastic Leukemia**” and recommend that it may be accepted as fulfilling the dissertation requirement for the Degree of Doctor of Philosophy.

P. Mitra
Chairman - <Name> Date: 28/3/12

Debit Chakrabarti
Guide / Convener - <Name> Date: 28/3/12

S. Saha
Member 1 - <Name> Date: 28/3/12

S. Saha
Member 2 - <Name> Date: 28/3/12

S. Saha
Member 3 - <Name> Date: 28/3/12

Final approval and acceptance of this dissertation is contingent upon the candidate's submission of the final copies of the dissertation to HBNI. I hereby certify that I have read this dissertation prepared under my direction and recommend that it may be accepted as fulfilling the dissertation requirement.


Date: 28/3/12

Place: Calcutta

Debit Chakrabarti

STATEMENT BY AUTHOR

This dissertation has been submitted in partial fulfilment of requirements for an advanced degree at Homi Bhabha National Institute (HBNI) and is deposited in the Library to be made available to borrowers under rules of the HBNI. Brief quotations from this dissertation are allowable without special permission, provided that accurate acknowledgement of source is made. Requests for permission for extended quotation from or reproduction of this manuscript in whole or in part may be granted by the Competent Authority of HBNI when in his or her judgment the proposed use of the material is in the interests of scholarship. In all other instances, however, permission must be obtained from the author.



Sutapa Saha

DECLARATION

I, hereby declare that the investigation presented in the thesis has been carried out by me. The work is original and has not been submitted earlier as a whole or in part for a degree / diploma at this or any other Institution / University.



Sutapa Saha

Dedicated To

*My Mother **Smt. Purnima Saha***

&

*Father **Sri Jagadish Chandra Saha***

ACKNOWLEDGEMENTS

This thesis was not possible without the support of my mentor, seniors, friends and colleagues I have the opportunity to thank here. First of all, I would like to thank Prof. Abhijit Chakrabarti for supervising this thesis. He guided me to channelize creative imagination into sound experimental work and tackle the really interesting questions. His enthusiasm and inspiration helped to make research enjoyable for me. I owe him lots of gratitude for all the encouragement, advices constructive criticisms, everlasting moral support and kindness. I would like to thank him for motivating me to think independently that helped me develop a sense of self-belief and made way for the successful completion of this endeavour.

I extend my thanks to Prof. Bikash Sinha, former Director, SINP, Prof. Milan K. Sanyal, Director, SINP, Prof. Jiban K. Dattagupta, former Head, Structural Genomics Section and Prof. Subrata Banerjee, Head, Structural Genomics Division, SINP for providing the institute Junior Research Fellowship [2004-2006], Senior Research Fellowship [2006-2011] and necessary facilities with excellent infrastructure to carry out my research work.

I express my sincere gratitude to my doctoral committee members, Prof. J K Dattagupta, Prof. P Mitra, Dr. A. Chakrabarti, Prof. Dipak dasgupta, and Dr. U. Sen who monitored my work.

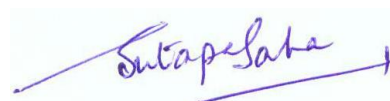
I owe a special note of appreciation to all my teachers who taught specialization courses during the Post-M.Sc course, 2004-2005 at SINP. I also wish to put on record my sincere thanks to Dr. Debashis Mukhopadhyay, Dr. Oishee Chakrabarti, Dr. Durjay Majumdar, Dr. Amitava Sengupta, Dr. Dipankar Bhattacharya, Dr. Sumanta Basu and Dr. Madhumita Chakraborty, who helped me with their intellectual inputs on many occasions and for various scientific and technical insights and interesting discussions on a number of key points during the dissertation.

Warm thanks to all the members of my lab, Avik, Suchismita, Shilpita and Madhurima for their constant support and for making the lab a wonderful place to work in. Thanks to the entire SINP student community for making my stay here pleasant and memorable. Special thanks to Suman, Dipankar, Soumyajit, Kaushik, Mithu, Anita, Eashita, Nandini, Arunabha and Shounak. I will remember very fondly our association and thank you for being fellow travellers in this journey.

I also acknowledge the technicians and staff of Administration, Accounts, Library, Workshop, Stores, Purchase, and Security for their cooperation and help.

Thanks to Dr Debasis Banerjee and Dr Sarmila Chandra for their help in collection of blood and bone marrow samples from leukemic patients.

Finally, my heartfelt gratitude goes to my family who made it all possible. My Ma, Baba, Didi, Esdee my brother Jayanta have sacrificed much and their devotion to my studies and career have brought me this far. I thank almighty for the endurance and blessings.



Sutapa Saha

CONTENTS

	<i>Page No.</i>
SYNOPSISi
LIST OF FIGURESxvii
LIST OF TABLESxxi
CHAPTER 1	An Introduction to Proteomic Study in a Hematological
	Malignancy: B-cell Acute Lymphoblastic Leukemia (B-ALL)1
CHAPTER 2	Differentially regulated CD19+ cell proteome in B-ALL72
CHAPTER 3	Altered plasma levels of proteolysis-modulating, carrier
	and acute phase proteins in B-ALL118
CHAPTER 4	Comparison of membrane and hemoglobin-depleted-cytosol
	proteomes of erythrocytes from normal, B-ALL and
	hereditary spherocytosis (HS) blood.152
REFERENCES165
CONCLUDING REMARKS184

CONTENTS (in detail.....)

<u>Topic</u>	<u>Page No.</u>
SYNOPSISi
LIST OF FIGURESxvii
LIST OF TABLESxxi
<hr/>	
CHAPTER 1	<u>An Introduction to Proteomic Study in a Hematological</u>
	<u>Malignancy: B-cell Acute Lymphoblastic Leukemia (B-ALL)</u>1
	<i>1.1 Development of B Lymphocytes</i>2
	<i>1.1.1 B cell Ontogeny</i>4
	<i>1.1.2 Markers of B cell Differentiation</i>5
	<i>1.1.3 Factors Regulating B cell Development</i>6
	<i>1.1.4 Regulation of B cell Development by the Pre-BCR and BCR</i>11
	<i>1.1.5 Signalling Defects and Clinical Disease</i>14
	<i>1.2 B- cell Acute Lymphoblastic Leukemia</i>15
	<i>1.2.1 Molecular genetic alterations in B-ALL</i>22
	<i>1.2.2 Immunophenotypic characterization of B-ALL</i>28
	<i>1.2.3 Therapeutic strategies for the treatment of B-ALL</i>31
	<i>1.3 Proteomics based on Two-Dimensional Gel</i>
	<i>Electrophoresis (2DGE), Differential In-Gel Electrophoresis (DIGE)</i>
	<i>and Mass Spectrometry</i>35
	<i>1.3.1. Gel Based Proteomics</i>36
	<i>1.3.1.1 Sample Preparation</i>38
	<i>1.3.1.2 Iso electric focusing using IPG</i>39
	<i>1.3.1.3 SDS-PAGE</i>39
	<i>1.3.1.4 Protein Detection Methods</i>40
	<i>1.3.1.5 Image Acquisition and Analysis</i>42

1.3.2 Differential In-Gel Electrophoresis (DIGE)43
1.3.3 Spot Picking and In-Gel Digestion for Mass Spectrometry45
1.3.4 Biological Mass Spectrometry46
1.3.4.1 MALDI TOF and MALDI TOF/TOF47
1.3.4.2 TOF Ion Optics49
1.3.4.3 The Tandem Mass Spectrometry: MALDI TOF/TOF50
1.3.4.4 Data Analysis Softwares53
1.4 Proteomics of B cell malignancies54
1.4.1 2-D gel electrophoresis studies of B-cell malignancies56
1.4.2 Shotgun proteomic studies on B-cell malignancies59
1.4.3 Subcellular proteomic studies of B-cell malignancies62
1.4.4 Phosphoproteomics studies of B-cell malignancies65
1.4.5 Identification of potential biomarkers in B-cell malignancies66
1.5 Motivation and aim of the present study 68
<hr/>	
CHAPTER 2	<u>Differentially regulated CD19+ cell proteome in B-ALL</u>72
	2.1 Introduction73
	2.2 Materials and Methods76
	2.2.1 B-ALL patient samples and enrichment of CD19+ cells76
	2.2.2 Two dimensional gel electrophoresis, staining and image analysis78
	2.2.3 Data analysis79
	2.2.4 CyDye labelling, Differential Gel Electrophoresis (2D-DIGE) and image analysis80
	2.2.5 In-Gel tryptic digestion and mass spectrometry80
	2.2.6 Western Immunoblotting81
	2.3 Results82
	2.3.1 Identification of differentially expressed proteins in B-ALL

	<i>CD19+ cells</i>82
	<i>2.3.2 PCA analysis</i>88
	<i>2.3.3 Two dimensional DIGE analysis of differentially expressed Proteins</i>90
	<i>2.3.4 Multifunctional nucleophosmin showed interesting expression pattern in B-ALL CD19+ cells</i>92
	<i>2.3.5 Gene Ontology Annotation</i>92
	2.4 Discussion95
<hr/>		
CHAPTER 3	<u>Altered plasma levels of proteolysis-modulating, carrier and acute phase proteins in B-ALL</u>118
	3.1. Introduction119
	3.2. Materials and Methods120
	<i>3.2.1. Plasma fractionation with ammonium sulfate</i>120
	<i>3.2.2 Two dimensional gel electrophoresis and Image Analysis</i>121
	<i>3.2.3. In-Gel tryptic digestion and mass spectrometry</i>122
	<i>3.2.4. Western immunoblotting</i>123
	3.3. Results123
	<i>3.3.1. Separation of pre-fractionated plasma proteins using 2DE</i>123
	<i>3.3.2. Identification of plasma proteins by tandem mass spectrometry</i>126
	<i>3.3.3. Display of differentially regulated proteins in B-ALL plasma</i>136
	<i>3.3.4. Validation by western immunoblotting</i>144
	3.4. Discussion146
<hr/>		
CHAPTER 4	<u>Comparison of membrane and hemoglobin-depleted-cytosol proteomes of erythrocytes from normal, B-ALL and hereditary spherocytosis (HS) blood.</u>152
	4.1. Introduction153

4.2. Materials and Methods154
4.2.1. Materials154
4.2.2. Sample Collection154
4.2.3. Hemoglobin depletion154
4.2.4. Two-Dimensional Gel Electrophoresis of erythrocyte cytosol155
4.2.5. Two-Dimensional Gel electrophoresis of Erythrocyte ghost155
4.2.6. MALDI ToF/ToF mass spectrometry155
4.2.7. Statistical Analysis156
4.2.8. Transmission Electron Microscopy of erythrocyte ghost	
Preparations157
4.3. Results157
4.3.1. Differences in the erythrocyte cytosolic proteomes of B-ALL,	
HS and normal157
4.3.2. Differences in erythrocyte membrane proteomes of B-ALL,	
HS and normal158
4.3.3. Alterations in HS erythrocyte ghost morphology160
4.4. Discussion161
REFERENCES165
CONCLUDING REMARKS184

ABBREVIATIONS

μHC	μ Heavy Chain
2DGE	Two-Dimensional Gel Electrophoresis
5-LO	5-Lipoxygenase
ADCC	Antibody Dependent Cell Mediated Cytotoxicity
AHSG	α2-HS-glycoprotein
AIF	Apoptosis Inducing factor
AK	Adenylate Kinase
ALDH	Aldehyde Dehydrogenase
AML	Acute Myeloid Leukemia
APP	Acute Phase Plasma Protein
APR	Acute Phase Response
ATRA	all-trans-retinoic acid
AZC	5-Azacytidine
B-ALL	B-cell Acute lymphoblastic Leukemia
BCP	B cell Precursor
BCR	B cell Receptor
BLNK	B-cell Linker Protein
BM	Bone Marrow
Btk	Bruton's tyrosine kinase
CBB	Coomassie Brilliant Blue
CBF	Core-Binding Factor
CD	Cluster of Differentiation
CHAPS	3-[(3-cholamidopropyl) dimethylammonio]-1-propanesulfonate
CHCA	α-Cyano-4-Hydroxycinnamic Acid
cICAT	Cleavable Form of ICAT
CID	Collision Induced Dissociation
CKIP	Casein Kinase Interacting Protein
CLL	Chronic Lymphocytic Leukemia
CLP	Common Lymphoid Progenitor
CML	Chronic Myeloid Leukemia
COX	Cytochrome Oxidase
CSC	Cancer Stem Cell
CyDye	Cyanide Dye
DAG	Diacylglycerol
DC	Dendritic Cell
DHB	2,5-Dihydroxybenzoic Acid
DIA	Differential In gel Analysis
DIGE	Differential In-Gel Electrophoresis
EBF	Early B cell Factor
EI	Electron Impact
eIF	Eukaryotic Initiation Factor
ELP	Early Lymphoid Progenitor
ERAD	ER-Associated Protein Degradation
ESI-MS	Electro Spray Ionization Mass Spectrometry
FAB	French American British Classification of Leukemia
FABP	Fatty Acid Binding Protein
FACS	Fluorescence Activated Cell Sorting

Fo	Follicular Zone
G3PD	Glyceraldehyde 3 Phosphate Dehydrogenase
GO	Gene ontology
GRP	Glucose Regulated Protein
Grx	Glutaredoxin
GSH	Reduced Glutathione
GST	Glutathione-S-Transferase
HCLS1	Haematopoietic Lineage Cell Specific Protein HS1
HS	Hereditary Spherocytosis
HSC	Hematopoietic Stem Cell
HSP	Heat Shock Protein
ICAT	Isotope-Coded Affinity Tag
IEF	Isoelectric Focusing
Ig	Immunoglobulin
IL-7R	Interleukin-7 Receptor
INF	Interferon
IP3	Inositol Triphosphate
IPG	Immobilized pH Gradient
iPPtase	Inorganic Pyrophosphatase
IRF	Interferon Regulatory Factor
IS	Internal Standard
ITAM	Immunoreceptor Tyrosine Activation Motif
ITIM	Immunoreceptor Tyrosine Inhibition Motif
iTRAQ	Isobaric Tagging for Relative and Absolute Quantification
JNK	c-Jun NH2- terminal kinase
LAT	Linker for activation of T-cells
LC	Light Chain
Lca	Clathrin Light Chain
LCP	Lymphocyte Cytosolic Protein
LMPP	Lymphoid Primed MPP
LN	Lymph Node
LSK	lin ⁻ , Sca-1 ⁺ , c-Kit ^{high}
MACS	Magnetically Assisted Cell Sorting
MALDI	Matrix assisted Laser Desorption Ionization
MBH	Membrane Bound Hemoglobin
MCL	Mantle Cell Lymphoma
miR	microRNA
MLL	Mixed-Lineage Leukaemia Protein
MNC	Mononuclear Cell
MPO	Myeloperoxidase
MPP	Multipotent Progenitor
MRD	Minimal Residual Disease
MS	Mass Spectrometry
MSDB	Mascot Search Database
MudPIT	Multi-Dimensional LC-MS/MS
MZ	Marginal Zone
NDPK	Nucleoside Di-Phosphate Kinase
NK	Natural Killer Cell
NPM	Nucleophosmin
PACAP	Pituitary Adenylate Cyclase Activating Polypeptide

PAGE	Polyacrylamide Gel Electrophoresis
PB	Peripheral Blood
PBMC	Peripheral Blood Mononuclear Cell
PC	Principal Component
PCA	Principal Component Analysis
PCNA	Proliferating Cell Nuclear Antigen
PH	Pleckstrin Homology Domain
PIP2	Phosphatidylinositol 4,5-bisphosphate
PIP3	Phosphatidylinositol 3,4,5-triphosphate
PKB	Protein Kinase B; also referred to as AKT
PKC	Protein Kinase C
PMF	Peptide Mass Fingerprint
PPM RD	Parts Per Million Relative Density
PRDX	Peroxiredoxin
Pro-B cell	B cell Progenitor
PTK	Protein Tyrosine Kinase
PTM	Post Translational Modification
PTPRC	Receptor-type Tyrosine-Protein Phosphatase C
RB	Retinoblastoma Protein
RBP	Retinol Binding Protein
SCF	Stem Cell Factor
SDS	Sodium Dodecyl Sulfate
SELDI	Surface Enhanced Laser Desorption Ionization
SETDB	SET domain bifurcated
SHIP	Phosphatidylinositol-3,4,5-Trisphosphate 5-Phosphatase
SILAC	Stable Isotope Labelling of Amino Acids in Culture
SLC	Surrogate Light Chain
SLP	Stomatin-like protein
SNP	Single Nucleotide Polymorphism
SOCS	Suppressor of Cytokine Signalling
SOD	Superoxide Dismutase
SRM	Selective Reaction Monitoring
ST13	Suppressor of Tumorigenicity 13
STMN	Stathmin
STRING	Search Tool for the Retrieval of Interacting Genes/Proteins
TBS	Tris-buffer-saline
TBST	TBS with Tween-20
TCA	Trichloroacetic Acid
TCP	T-complex protein
TCR	T-cell Receptor
TCTP	Translationally Controlled Tumor Protein
TdT	Terminal Deoxy Nucleotidyl Transferase
TEM	Transmission Electron Microscopy
TF	Transcription Factor
ToF	Time of Flight
Trx	Thioredoxin
TSLP	Thymic Stromal Lymphopoietin
UCTH	Ubiquitin Carboxyl Terminal Hydrolase
UPR	Unfolded Protein Response
XLA	X-linked Agammaglobulinemia

Synopsis of

Proteomic Study in a Hematological Malignancy: B-cell Acute Lymphoblastic Leukemia

A Thesis to be submitted by

Sutapa Saha

for the award of the degree of

Doctor of Philosophy



Structural Genomics Division

Saha Institute of Nuclear Physics, Kolkata, India

July, 2011

1. Introduction

B-cell acute lymphoblastic leukaemia (B-ALL) is the most common cancer in children and constitutes the major class of lymphoid leukemia. It is a clonal malignant disease that originates from genetic changes in the hematopoietic stem cell and is characterized by an accumulation of blast B-cells that fail to differentiate, resulting in suppression of normal haematopoiesis (1). Although contemporary treatments cure more than 80% of children with B-ALL, some patients fall in high risk and/or poor prognosis classes requiring intensive treatment, others exhibit drug resistance and many patients still develop serious acute and late complications owing to the side effects of the treatments. Furthermore, the survival rate for adults with B-ALL remains below 40% despite the use of transplantation, and treatment outcome is poor among patients who relapse on current front-line ALL regimens (2). Human plasma, the most readily obtainable patient specimen, contains a dynamic load of mediators of various cellular responses, and thus comprehensively samples the state of the body in disease (3). B-ALL malignancies are presented with mild to severe anemia, which indicate possibilities of altered erythrocyte metabolism depending on the clonality of the leukemic stem cells (4).

Although identification of the genetic abnormalities has led to an improved understanding of B-ALL pathophysiology, the mechanisms responsible for the B-cell developmental arrest are unknown. Nevertheless, the primary oncogenic events seem to require secondary cooperative changes to generate a fully transformed cell. The proteome of a cell is dynamic unlike its genome, as it shows characteristic perturbations in response to disease and physiological state of the cell. A thorough comparison of the proteomic profiles of normal and malignant cells can not only point out candidate diagnostic markers and/or therapeutic targets of the malignancy, but also throw light on the mechanism of transformation of the cells from normal to malignant state. Identification of disease specific markers helps in diagnostic and prognostic monitoring of the malignancy and the associated minimal residual disease, but, disease regulated proteins in B-ALL are still unclear.

2. Motivation

Proteomic studies for the identification of proteins aberrantly expressed in malignant B-cells can potentially be used to develop new diagnostic, prognostic or therapeutic targets. The knowledge that transcriptome data produces on genome-wide expression does not necessarily translate through to protein expression. Two-dimensional gel electrophoresis (2DGE) offers in essence a 2-step approach to separating complex protein mixtures in exquisite detail. The separation of proteins in 2D gels is associated with a substantial analytical variability. The use of Difference-In-Gel-Electrophoresis (DIGE) technology with internal standard, that exploits fluorescent labeling techniques with fluorescent cyanide (Cy) dyes to label proteins prior to 2-DE, minimizes the consequences of inter-gel variations. Digesting the protein spot bound to the gel using specific endoproteases like trypsin using ‘In-gel tryptic digestion’ generates ‘Peptide Mass Fingerprint’ (PMF) on a mass spectrometer. PMF and peptide sequences deduced from tandem mass spectra generated by MALDI-ToF/ToF subsequently lead to the identification of the protein spots based on theoretical peptide map database matches.

Given that the proteome is strongly influenced by cell differentiation, a simple comparison of mononuclear cells (MNCs) from different patients is likely to result in the identification of proteins whose apparent change in expression actually reflects a difference in the cellular composition of the specimens. Polypeptide differences between abnormally proliferating cells could be lineage related or could reflect, in part, the selective activation of genes that are not expressed in normal cells (5). To prevent such a complication and eliminate such population-shift effects, we isolated B-lymphoblasts on the basis of their surface expression of CD19 using Magnetically-Assisted-Cell-Sorting (MACS) and Fluorescence-Activated-Cell-Sorting (FACS).

The protein content of blood plasma is dominated by a handful of proteins such as albumin, immunoglobulins, and lipoproteins present across an extraordinary dynamic range of concentration. This exceeds the analytical capabilities of traditional proteomic methods,

making detection of lower abundance serum proteins extremely challenging. Reduction of sample complexity is thus an essential first step in the analysis of plasma proteome (6). We used pre-fractionation of plasma proteins with ammonium sulfate (7), to reduce concentrations of high-abundance components and enrich lower abundant components in plasma 2DE profiles, thereby facilitating the identification of disease markers.

Proteomic analysis of erythrocyte cytosol had been handicapped by the large abundance of hemoglobin, masking majority of the other cytosolic proteins. We have used cation exchange chromatography to deplete hemoglobin very efficiently and specifically (8), and subsequently studied the hemoglobin depleted erythrocyte cytosol proteome.

3. Objective(s) and Scope

The primary objective of this study was to identify differentially regulated proteins in B-ALL that; a) may contribute to our understanding of B-cell malignancies; b) can be used for diagnosis or prognosis and c) can be potential therapeutic targets.

Significant differences between primary tumour cells and immortalised cell lines (9), emphasizes the importance of obtaining protein profiling data from primary malignant B-cells, rather than immortalised cell lines. Comparative proteome analysis with background-matched CD19⁺ cell fractions obtained from fresh clinical specimens, using two-dimensional gel electrophoresis and MALDI-ToF/ToF tandem mass spectrometry, leads to the identification of many proteins differentially regulated in B-ALL compared to normal controls. For a comprehensive analysis of the large proteome dataset and proper selection of significantly altered protein, a combination of univariate and multivariate statistics is employed.

Multifactorial statistical analysis enlightens on the variation of each of the differentially regulated proteins with respect to that in others in a holistic perspective and might be helpful in interpreting the mechanism of leukemogenesis. Gene ontology (GO) annotation of the differentially regulated proteins reveals the functions and cellular localization of the de-

regulated proteins. Functional partnerships between proteins are at the core of complex cellular phenotypes. The interactome of the observed disease-regulated proteins obtained through bioinformatics could propose research avenues for addressing the leukemogenic B-cell biology. Furthermore, candidate proteins which exhibit opposite trends of de-regulations in myeloid and lymphoid leukemia might not only point out prospective biomarkers but also enhance our knowledge on regulation of commitment and differentiation of the HSC into myeloid or lymphoid lineages.

2-DE based proteomic identification of differentially regulated plasma proteins might serve in a less-invasive (than bone-marrow aspiration) diagnostic and prognostic monitoring of B-ALL as well as detection of minimal residual disease. As most of the de-regulated proteins are involved in multiple physiological processes, the proteomic studies of blood plasma might also elucidate the pathophysiology and/or clinical manifestation of the B-ALL malignancy.

Comparative study of the membrane and cytosol proteome of erythrocytes purified from peripheral blood of normal volunteers, B-ALL patients and patients suffering from a non-malignant hematological disorder like hereditary spherocytosis may add insights to our understanding of altered erythrocyte physiology in leukemia vs. erythroid disorders.

Through this work, we emphasize upon the assets of proteomic studies over single protein detection assays in revealing differential regulation of different classes of proteins, simultaneously in a disease, which might be a step ahead in cutting through the complexity of heterogeneous diseases and explaining their pathophysiology and clinical manifestation.

4. Description of the research work

4.1 Differentially regulated CD19⁺ cell proteome in B-ALL:

With a two-dimensional gel electrophoresis (2DGE) followed by MALDI ToF/ToF tandem mass spectrometry approach, we present here the comparative proteomic study of a homogeneous population of CD19⁺ cells from 27 B-ALL patients, that led to the identification of

60 differentially regulated proteins in the malignant CD19⁺ cells compared to normal primary CD19⁺ cells.

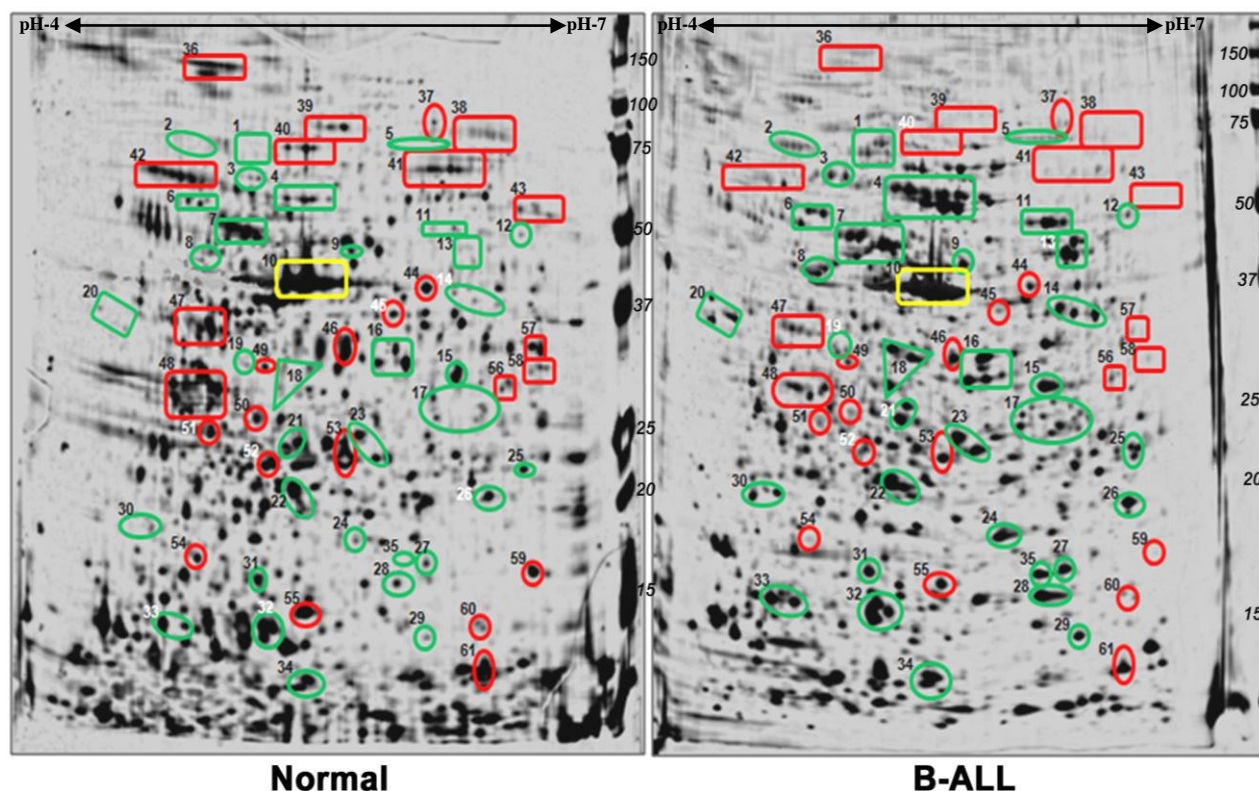


Figure 1: Representative B-cell proteome 2D-maps displaying proteins up-regulated (green) and down-regulated (red) in B-ALL compared to normal with β -actin as internal control (yellow).

Gene ontology (GO) annotation of the differentially regulated proteins revealed deregulation of several classes of proteins localized in almost all cellular compartments. Our study reveals that proteins participating in metabolism of proteins, nucleic acids or carbohydrates, stress response or cytoskeleton/movement, and cellular energy homeostasis, are significantly de-regulated in the malignant cells.

Our data implicate a number of novel proteins and pathways in the pathobiology of B-ALL. We discuss how the interactome of the observed de-regulations could propose research avenues for addressing the leukemogenic B-cell biology. Several of the proteins identified could be linked to specific signal transduction pathways relevant to lymphoid leukemogenesis. Furthermore, a multifunctional protein which exhibits opposite trends of de-regulations in myeloid and lymphoid leukemia was observed to exist in different polypeptide forms in myeloid

and lymphoid lineages. Depending on the expression levels and gene dosage, such candidates seem to function as either an oncogene or a tumour suppressor in myeloid and lymphoid lineages respectively.

Spot No.	Protein Name	Spot No.	Protein Name
1	DnaK-type molecular chaperone HSPA5 precursor (BiP protein)	32	TGFB- induced anti-apoptotic factor 1
2	Haematopoietic lineage cell specific protein HS1	33	SH3 domain binding protein SH3BP-1
3	Ubiquilin 1	34	Glutaredoxin-related protein C14 or f87
4	Heat shock protein 60	35	Enhancer of rudimentary homolog
5	Heat shock cognate 71 kDa protein (Heat shock 70 kDa protein 8)	36	Superoxide Dismutase (SOD)
6	Protein Disulfide isomerase	37	Endoplasmic precursor + HSP 90 beta
7	ATP synthase beta chain, mitochondrial precursor	38	Mitofilin
8	Tubulin b	39	Ezrin(Cytovillin)
9	Heterogeneous nuclear ribonucleoprotein F	40	Vinculin (Metavinculin)
10	Actin beta (<i>Internal Control</i>)	41	L-plastin(lymphocyte cytosolic protein 1)
11	Protein disulfide isomerase	42	Serum albumin precursor
12	D-3-phosphoglycerate dehydrogenase	43	UV excision repair protein RAD23 homolog
13	Phosphopyruvate hydratase (Alpha enolase)	44	T-complex protein 1 subunit beta (TCP-1- b)
14	Heterogeneous nuclear ribonucleoprotein H3	45	Stomatin like protein 2 SLP-2)
15	Growth factor receptor-bound protein 2 (SH2/SH3 adaptor GRB2)	46	F-actin capping protein alpha-1 subunit (CapZ alpha1)
16	Glutathione S-transferase	47	Inorganic pyrophosphatase
17	Prohibitin	48	Nucleophosmin
18	Peroxiredoxin 3 + peroxiredoxin 6	49	Tropomyosin 3 + Tropomyosin 2 (beta)
19	Alternative splicing factor ASF-1	50	Annexin A5
20	Heterogeneous nuclear ribonucleoprotein C1/C2	51	Proliferating cell nuclear antigen (PCNA)
21	Vimentin	52	Clathrin light polypeptide (Lca)
22	Fascin 2	53	Lactoylglutathione lyase (Methylglyoxalase, Aldoketomutase)
23	Rho GDP dissociation inhibitors Ly-GDI + Rho GDI 1+ Rho GDI 2	54	PACAP protein (Pituitary adenylate cyclase-activating polypeptide
24	Ubiquitin carboxyl terminal hydrolase	55	receptor)
25	Peroxiredoxin 2	56	Transcription elongation factor B polypeptide 2
26	HSP 27+ proteasome subunit b3+proteasome endopeptidase complex		Programmed cell death protein 5 (TFAR19 protein)
27	GrpE protein homolog 1, mitochondrial precursor	57	Translation initiation factor eIF-2B alpha subunit (eIF-2B GDP-GTP exchange factor)
28	Nucleoside Diphosphate Kinase A	58	Triosephosphate isomerase
29	Stathmin (phosphoprotein p19)	59	Cytochrome c oxidase subunit Va (COX5A protein)
30	Prefoldin subunit 2	60	Peptidylprolyl isomerase
31	Translationally controlled tumor protein (TCTP)	61	Fatty acid binding protein (FABP)

Table 1: List of differentially regulated proteins identified upon in-gel tryptic digestion and tandem mass spectrometry of the protein spots excised from 2D gels.

CyDye labeling of B-cell proteins from normal and B-ALL samples, Differential In Gel Electrophoresis (DIGE) and subsequent analysis using DeCyder software confirmed the results obtained in 2DGE, with identification of 19 new differentially regulated proteins.

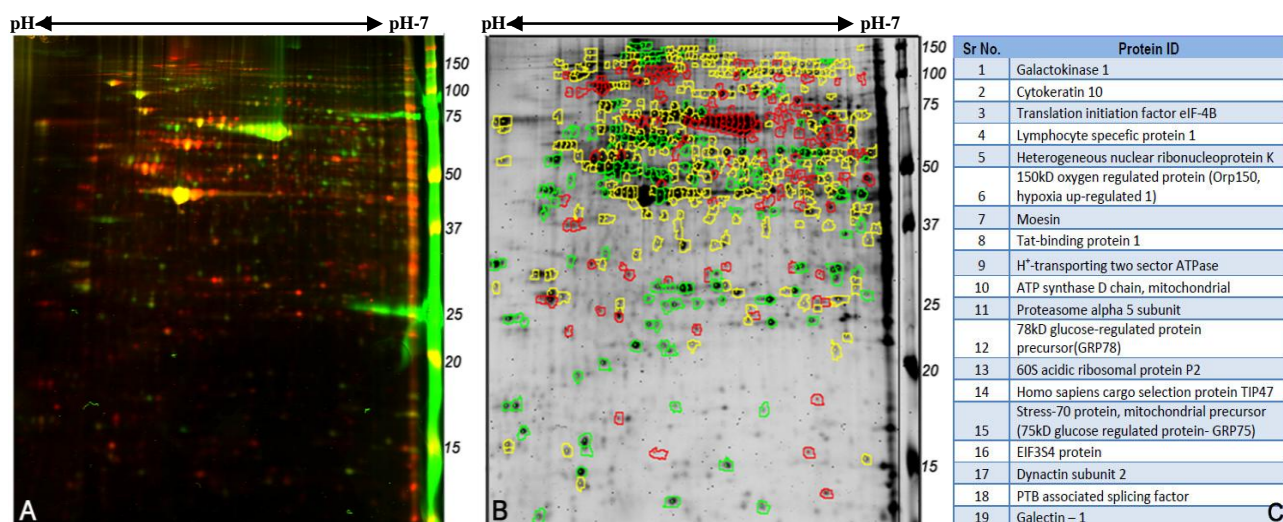


Figure 2: (A)- Scanned image of 2D-DIGE of B-cell proteome from normal (green, Cy3) and B-ALL (red, Cy5) samples, with β -actin (yellow) as internal control. (B)- Representative image obtained on image analysis using the Differential In gel Analysis (DIA) module of DeCyder software. Green spots → proteins up-regulated in B-ALL; red spots → down-regulated proteins; yellow spots → proteins with similar expression in normal and B-ALL B-lymphocytes. (C)- List of the 19 new proteins identified to be differentially regulated in DIGE experiments.

4.2 Altered plasma levels of proteolysis-modulating, carrier and acute phase proteins in B-cell Acute Lymphoblastic Leukemia:

Ammonium sulfate precipitation based pre-fractionation of plasma followed by two-dimensional gel electrophoresis (2DGE) of normal and B-ALL plasma samples & MALDI-ToF/ToF tandem mass spectrometry led to depletion of multiple high-abundance proteins and subsequent identification of 15 disease-regulated proteins. Functional annotation of the identified proteins revealed differential regulation of chiefly carrier proteins and proteolysis modulators along with several acute phase and tissue-leakage proteins. The fact that the simple inexpensive fractionation of plasma proteins with ammonium sulfate does not differentially deplete plasma proteins from sample to sample is validated through the 2DE profiles of ammonium sulfate precipitates from acute myeloid leukemia (AML) and E β -thalassemia patient plasmas that indicate opposite trend of differential regulation of most of the 15 proteins, pointing towards the specificity of the observations in B-ALL.

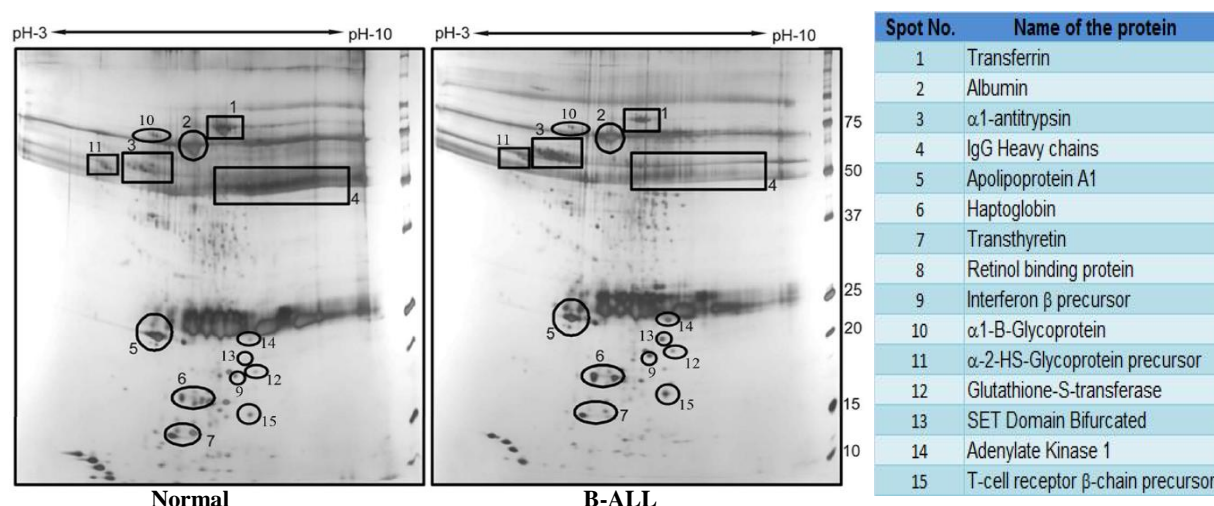


Figure 3: Representative 2D- proteome maps of ammonium sulfate precipitates from normal and B-ALL plasma samples displaying disease-regulated proteins as listed in the adjoining table.

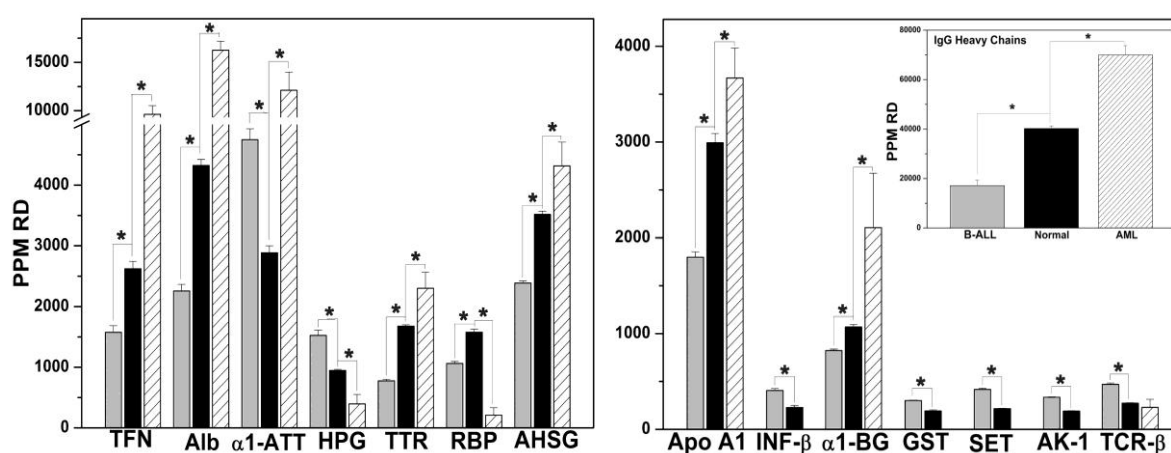


Figure 4: Histogram plot showing change in parts per million relative densities (PPM RD) of differentially regulated proteins. Grey bars: B-ALL; Black bars: Normal; Hatched bars: AML

4.3 Comparison of membrane and hemoglobin-depleted-cytosol proteomes of erythrocytes from normal, B-ALL and hereditary spherocytosis (HS) blood:

Hypotonic lysis of erythrocytes from peripheral blood followed by hemoglobin depletion, 2DGE, and MALDI-ToF/ToF tandem mass spectrometry led to the identification of several differences between the respective normal, B-ALL and HS proteomes. While Hb-depleted HS erythrocyte cytosol showed up-regulation of redox regulators and down-regulation of a co-chaperone and a nucleotide kinase; the hemoglobin-depleted erythrocyte cytosol proteome of B-ALL patients showed somewhat opposite trends with down-regulation of an oxidoreductase

(aldehyde dehydrogenase) and pI shift of a chaperone (HSP-70).

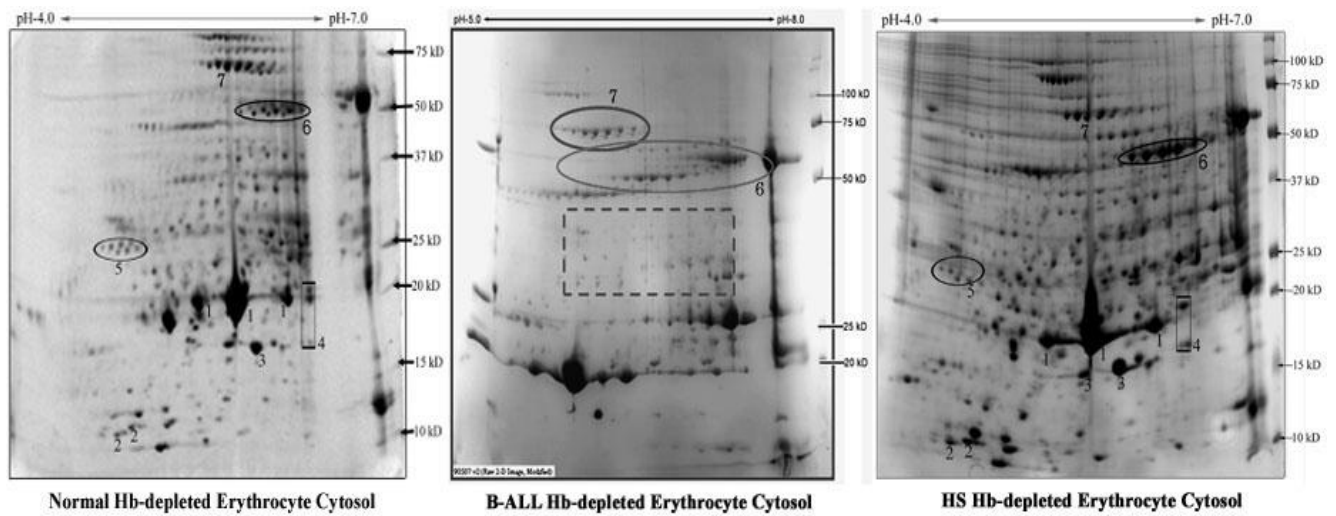


Figure 5: Representative 2DGE maps of hemoglobin-depleted erythrocyte cytosol from normal, B-ALL and HS individuals. 1- peroxiredoxin 2; 2- thioredoxin; 3- superoxide dismutase; 4- nucleoside diphosphate kinase; 5- suppressor of tumorigenicity 13; 6- aldehyde dehydrogenase; 7- heat shock protein 70.

The erythrocyte ghost membranes were prepared following protocols described earlier (10) with minor modifications and the membrane proteins were solubilized following published protocol (11). Comparison of the erythrocyte membrane proteomes on 2DGE led to the observation of elevated levels of membrane associated globin chains and reduced membrane association of glyceraldehydes-3-phosphate dehydrogenase (G3PD) in both B-ALL and HS patients. Increased levels of low molecular weight fragments of several major cytoskeletal proteins were observed in both B-ALL and HS erythrocyte membrane proteomes; HS samples displaying much higher levels of cytoskeletal protein fragments than B-ALL samples. While increased association of globin chains with the spherocyte membranes in HS directly indicate severe oxidative stress in the spherocytes, membrane-bound denatured/oxidized hemoglobin and defective erythrocyte cytoskeletal network in B-ALL may be implicated in the erythrocyte destruction in spleen, making the patients anaemic.

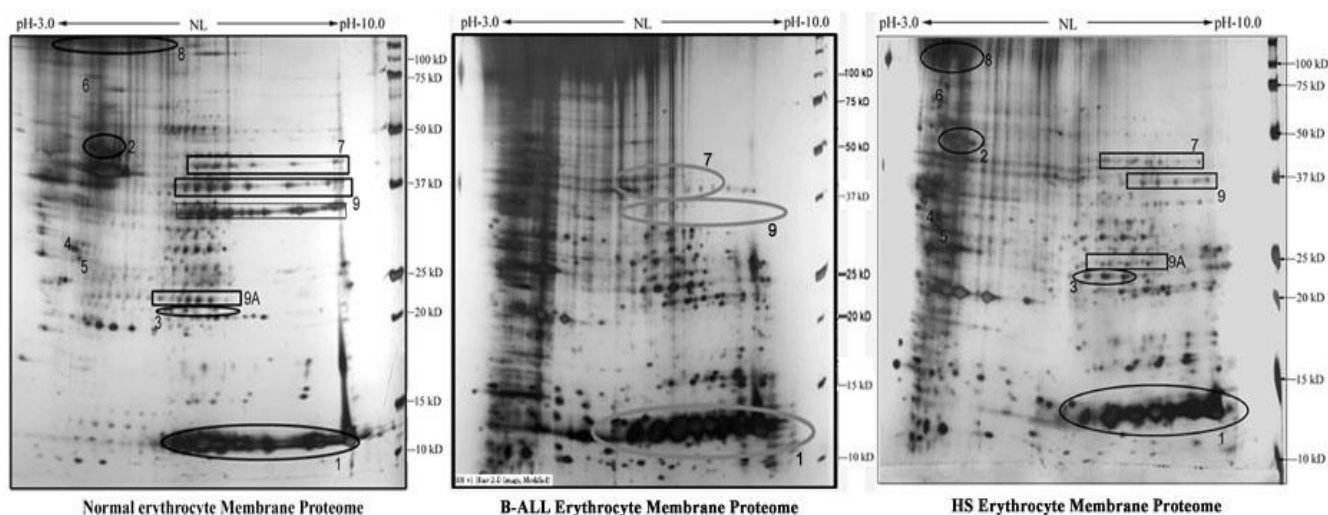


Figure 6: Representative erythrocyte membrane proteomes of normal, B-ALL and HS individuals. 1- Hemoglobin; 2- Band 4.1; 3-Ankyrin; 4- Tropomyosin 3; 5- Tropomyosin 1; 6- Calpastatine; 7- Dematin; 8- Spectrin; 9- Glyceraldehyde 3 phosphate dehydrogenase (G3PD); 9A- G3PD fragments

5. Conclusions

The success of proteomic studies on B-cell malignancies needs to be measured in terms of outcomes, such as identifying proteins that; a) contribute to our understanding of B-cell malignancies; b) can be used for diagnosis or prognosis and c) are potential therapeutic targets. In this respect our study adopting comparative proteomic strategies to identify de-regulations in CD19⁺ B-lymphocyte, plasma, and erythrocyte proteomes, delivered quantitative data on protein abundances and hence potentially identified novel deregulated proteins in B-ALL. Several of the de-regulated proteins identified could be linked to specific signal transduction pathways relevant to leukemogenesis. Our data also implicated a number of novel proteins and pathways in the pathobiology of B-ALL. Our study provided new insights in B-ALL pathogenesis and may help to form the basis for testing new target-specific therapeutics. However, current proteomics techniques are limited in their sensitivity for protein detection. In our study, no single 2DE image yielded > 3000 independent protein spots, which is far fewer than the total number of human proteins predicted from sequencing of the human genome (30 000–40 000 proteins without taking into account the products of alternative RNA splicing).

Any changes which are detected in proteomic studies either due to the disease or treatment are likely to be limited to relatively abundant proteins, albeit they may still be important or biologically significant proteins. Further improvements in proteomics tools and their application to the direct comparison of protein profiles among background-matched cell fractions prepared from fresh specimens should provide an insight into the intracellular events that underlie malignant transformation in human leukaemias. Our hope then is the translation of that knowledge into clinical applications. Proteomics yielding ever greater insights into ALL pathogenesis; one can expect an expanding repertoire of targeted therapies for clinical evaluation.

6. List of Publications

- Saha, S., Banerjee, S., Banerjee, D., Chandra, S., Chakrabarti, A. Differentially regulated CD19⁺ B-lymphocyte proteome in B-cell Acute Lymphoblastic Leukemia: Biological insights. (*Communicated*)
- Saha, S., Halder, S., Bhattacharya, D., Banerjee, D., Chakrabarti, A. Altered plasma levels of proteolysis-modulating, carrier and acute phase proteins in B-cell Acute Lymphoblastic Leukemia. (*Communicated*)
- Saha, S., Ramanathan, R., Basu, A., Banerjee, D., and Chakrabarti, A. (2011) Elevated levels of redox regulators, membrane bound globin chains and cytoskeletal protein fragments in hereditary spherocytosis erythrocyte proteome. *Eur J Haematol*. (In Press)
- Chakrabarti, A., Bhattacharya, D., Basu, A., Basu, S., Saha, S., and Halder, S. (2011) Differential expression of red cell proteins in hemoglobinopathy. *Proteomics Clin Appl* 5, 98-108.
- Bhattacharya, D., Saha, S., Basu, S., Chakravarty, S., Chakravarty, A., Banerjee, D., and Chakrabarti, A. (2010) Differential regulation of redox proteins and chaperones in HbEbeta-thalassemia erythrocyte proteome. *Proteomics Clin Appl* 4, 480-488.

- Chakrabarti, A., Datta, P., Bhattacharya, D., Basu, S., and Saha, S. (2008) Oxidative crosslinking, spectrin and membrane interactions of hemoglobin mixtures in HbEbeta-thalassemia. *Hematology* 13, 361-368.
- Banerjee, D., Saha, S., Basu, S., and Chakrabarti, A. (2008) Porous red cell ultrastructure and loss of membrane asymmetry in a novel case of hemolytic anemia. *Eur J Haematol* 81, 399-402.

7. List of seminars and workshops attended

- *Oral Presentation* at the **47th Annual Conference of the Indian Society of Haematology & Transfusion Medicine**, Guwahati Medical College, Guwahati, November 24-26, 2006, on *Proteomics in the study of hematological malignancies*.
- *Workshop* on **iTRAQ Technology for Quantitative Proteomics**, Centre for Cell and Molecular Biology, Hyderabad, August 27-29, 2007.
- *Oral Presentation* at **CME 2007 Scientific Meet on Haemato-Oncology**, Netaji Subhash Chandra Bose Cancer Research Institute, Taj Bengal, Kolkata, September 8-9, 2007, on *Proteomics in the study of hematological malignancies*.
- *Poster Presentation* at the **International Symposium on Complex Diseases: Approaches to Gene Identification and Therapeutic Management**, Saha Institute of Nuclear Physics, Kolkata, September 25-26, 2008, on *Clinical Proteomics in Blood Disorders*.
- *Presentation* at the **11th ISMAS Triennial International Conference on Mass Spectrometry**, 11th ISMAS-TRICON-2009, Ramoji Film City, Hyderabad, November 24-28, 2009, on **“Salting out” the hidden plasma proteome**.
- *Presentation* at the **National seminar on Proteomics: Advances, Applications and Challenges (PRAAC)**, Institute of Bioinformatics and Applied Biotechnology, Bangalore, February 19- 20, 2010, on *Salting out the hidden plasma proteins implicated in B-ALL*.

• *Poster Presentation and Oral Presentation at the 5th AOHUPO Congress, 14th ADNAT Convention & 1st PSI Conference of New Perspectives in Proteome Research*, February 21-25, 2010, Centre for Cellular & Molecular Biology, Hyderabad, on *Identification of disease regulated blood plasma proteins in B-ALL & Proteomics of CD19+ B cells implicated in acute lymphoblastic leukemia* respectively.

8. References

1. Cobaleda, C., and Sanchez-Garcia, I. (2009) B-cell acute lymphoblastic leukaemia: towards understanding its cellular origin. *Bioessays* 31, 600-609.
2. Pui, C. H., and Jeha, S. (2007) New therapeutic strategies for the treatment of acute lymphoblastic leukaemia. *Nat Rev Drug Discov* 6, 149-165.
3. Anderson, N. L., and Anderson, N. G. (2002) The human plasma proteome: history, character, and diagnostic prospects. *Mol Cell Proteomics* 1, 845-867.
4. Kumar, A., and Gupta, C. M. (1983) Red cell membrane abnormalities in chronic myeloid leukaemia. *Nature* 303, 632-633.
5. Ota, J., Yamashita, Y., Okawa, K., Kisanuki, H., Fujiwara, S., Ishikawa, M., Lim Choi, Y., Ueno, S., Ohki, R., Koinuma, K., Wada, T., Compton, D., Kadoya, T., and Mano, H. (2003) Proteomic analysis of hematopoietic stem cell-like fractions in leukemic disorders. *Oncogene* 22, 5720-5728.
6. Tirumalai, R. S., Chan, K. C., Prieto, D. A., Issaq, H. J., Conrads, T. P., and Veenstra, T. D. (2003) Characterization of the low molecular weight human serum proteome. *Mol Cell Proteomics* 2, 1096-1103.
7. Jiang, L., He, L., and Fountoulakis, M. (2004) Comparison of protein precipitation methods for sample preparation prior to proteomic analysis. *J Chromatogr A* 1023, 317-320.
8. Bhattacharya, D., Mukhopadhyay, D., and Chakrabarti, A. (2007) Hemoglobin

depletion from red blood cell cytosol reveals new proteins in 2-D gel-based proteomics study.

Proteomics Clin Appl 1, 561-564.

9. Boyd, R. S., Jukes-Jones, R., Walewska, R., Brown, D., Dyer, M. J., and Cain, K. (2009) Protein profiling of plasma membranes defines aberrant signaling pathways in mantle cell lymphoma. *Mol Cell Proteomics* 8, 1501-1515.
10. Bhattacharyya, M., Ray, S., Bhattacharya, S., and Chakrabarti, A. (2004) Chaperone activity and prodan binding at the self-associating domain of erythroid spectrin. *J Biol Chem* 279, 55080-55088.
11. Bhattacharya, D., Saha, S., Basu, S., Chakravarty, S., Chakravarty, A., Banerjee, D., and Chakrabarti, A. (2010) Differential regulation of redox proteins and chaperones in HbEbeta-thalassemia erythrocyte proteome. *Proteomics Clin Appl* 4, 480-488.

9. Proposed contents of the thesis

SYNOPSIS

LIST OF FIGURES

LIST OF TABLES

CHAPTER 1 An Introduction to Proteomic Study in a Hematological Malignancy viz.
B-cell Acute Lymphoblastic Leukemia (B-ALL)

CHAPTER 2 Differentially regulated CD19+ cell proteome in B-ALL

CHAPTER 3 Altered plasma levels of proteolysis-modulating, carrier and acute phase
proteins in B-ALL

CHAPTER 4 Comparison of membrane and hemoglobin-depleted-cytosol proteomes
of erythrocytes from normal, B-ALL and hereditary spherocytosis (HS)
blood.

REFERENCES

CONCLUDING REMARKS

LIST OF FIGURES

<u>Figure</u>	<u>Page No.</u>
<i>Figure 1.1: Stages of B-cell development</i>	3
<i>Figure 1.2: Role of transcription factors in lymphopoiesis</i>	7
<i>Figure 1.3: Signalling cascades in early B cell development</i>	11
<i>Figure 1.4: Characteristic B-ALL bone marrow smear</i>	16
<i>Figure 1.5: Estimated Frequency of Specific Genotypes of ALL in Children and Adults</i>	17
<i>Figure 1.6: Assignment of human B-ALL to their normal B-cell counterparts</i>	18
<i>Figure 1.7: Presumptive cellular origins of chromosomal translocations in human B-ALLs</i>	19
<i>Figure 1.8: Human B-cell acute lymphoblastic leukaemias form a hierarchy</i>	21
<i>Figure 1.9: A common pathway targeted by translocation-generated chimeric transcription factors, such as MLL fusion proteins, TEL-AML1, and E2A-PBX1: is the HOX gene-mediated transcriptional cascade</i>	23
<i>Figure 1.10: Mechanism of Transcriptional Repression by TEL-AML1.</i>	24
<i>Figure 1.11: The Retinoblastoma (RB) and p53 Tumor-Suppressor Network.</i>	27
<i>Figure 1.12: Immunophenotype of bone marrow specimen containing precursor B-cell acute lymphoblastic leukemia (ALL) cells and hematogones.</i>	29
<i>Figure 1.13: Correlation of genotype with immunophenotyping of B-ALL</i>	31
<i>Figure 1.14: Cell-cycle phases targeted by agents that are conventionally used in B-ALL</i>	32
<i>Figure 1.15: A simplified diagram of molecular target sites for potential new therapeutic agents</i>	33
<i>Figure 1.16: The 2D workflow</i>	38
<i>Figure 1.17 Iso-electric focusing on an IPG strip</i>	39

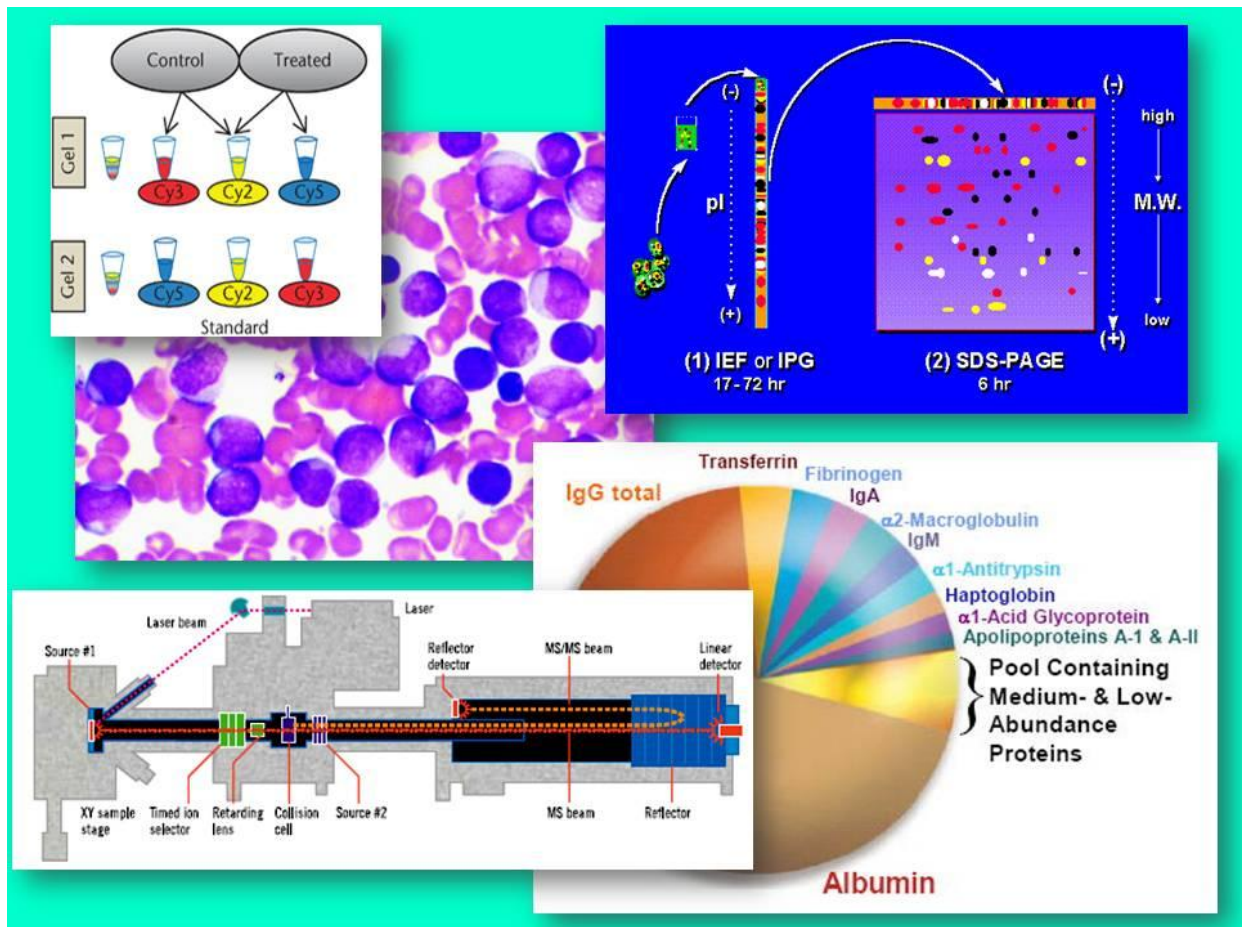
<i>Figure 1.18: Comparison of staining techniques</i>	42
<i>Figure 1.19: The DIGE technology</i>	44
<i>Figure 1.20: Ionization scheme in MALDI MS</i>	47
<i>Figure 1.21: Tandem mass spectrometry in a MALDI-TOF/TOF spectrometer.</i>	51
<i>Figure 1.22: MSMS fragmentation</i>	52
<i>Figure 1.23: A typical MASCOT search result</i>	54
<hr/>	
<i>Figure 2.1: Representative two dimensional proteome maps of CD19+ cells from normal controls and B-ALL patients</i>	82
<i>Figure 2.2: Heat map of the expression levels of differentially regulated proteins in normal and B-ALL samples; and cluster analysis of the expression profiles</i>	83
<i>Figure 2.3(A): Distribution of gel samples (blue) and protein spots (red) in a 2D PCA-biplot-space projection</i>	88
<i>Figure 2.3(B): Magnified projection of protein spots in a 2D PCA-space</i>	89
<i>Figure 2.4: DIGE and DIA analysis results for CD19+ proteomes from normal and B-ALL Samples</i>	90
<i>Figure 2.5: Western immunoblot result for nucleophosmin in B-ALL and AML cells</i>	92
<i>Figure 2.6: Gene Ontology (GO) functional annotation of the differentially regulated proteins in B-ALL CD19+ cell proteome</i>	93
<i>Figure 2.7: Histogram plot of the expression levels of the 60 differentially regulated proteins in B-ALL CD19+ cell proteome, with a color code on the basis of GO function.</i>	94
<i>Figure 2.8 Gene Ontology (GO) annotation of the differentially regulated proteins in B-ALL CD19+ cell proteome on the basis of cellular localization</i>	95
<i>Figure 2.9: Representative Immunophenotype patterns of the B-ALL patient samples</i>	95
<i>Figure 2.10: DIGE image of a lymphoma cell line (DG75) vs. a myeloid leukemia cell line</i>	

<i>(HL60) showing NPM down-regulation in the lymphoid cells</i>	100
<i>Figure 2.11: Crucial signalling cascades involved in precursor B-cell development</i>	103
<i>Figure 2.12: STRING interactome of the differentially regulated proteins and key kinases, adaptor proteins and epigenetic regulators involved in pre-B-cell fate decisions</i>	104
<hr/>	
<i>Figure 3.1: Comparison of 1D-SDS-PAGE profiles of 10-55% (NH₄)₂SO₄ precipitates from normal blood plasma</i>	124
<i>Figure 3.2: Coomassie stained 1D SDS-PAGE of raw plasma, its ammonium sulfate precipitate and supernatant.</i>	125
<i>Figure 3.3: (A) Silver stained 2DE profile of raw normal plasma. (B) Silver stained 2DE profile of 20% (NH₄)₂SO₄ precipitate from normal plasma. (C) Silver stained 2DE profile of supernatant left after 20% (NH₄)₂SO₄ precipitation. (D) 3D view of boxed regions in 1B and 1C</i>	125
<i>Figure 3.4: Protein annotations from 20% (NH₄)₂SO₄ precipitate obtained from normal plasma</i>	126
<i>Figure 3.5: Gene Ontology of the identified proteins according to the PANTHER classification system</i>	135
<i>Figure 3.6: Display of differentially regulated proteins in B-ALL blood plasma compared to normal</i>	137
<i>Figure 3.7 (A): Histogram plots of parts per million relative spot densities of individual proteins in 16 2D gel profiles for 8 normal and 8 B-ALL plasma samples</i>	140
<i>Figure 3.7 (B): Histogram plot showing change in ppm relative densities of the 15 differentially-regulated proteins.</i>	142
<i>Figure 3.8: Comparison of 20% (NH₄)₂SO₄ precipitation and Sigma Affi-Gel Blue based depletion of abundant plasma proteins</i>	143

<i>Figure 3.9: Functional classification of the differentially regulated proteins</i>	<i>144</i>
<i>Figure 3.10: (A) Western immunoblots of 5 differentially regulated proteins in normal and;</i> <i>(B) Histogram plot of the band intensities</i>	<i>145</i>
<i>Figure 3.11: Comparison of the 2DE profiles of 20% (NH₄)₂SO₄ precipitate from ALL,</i> <i>Normal, Eβ-Thalassemia, and AML patient plasma</i>	<i>147</i>
<i>Figure 3.12: Role of proteolysis modifiers in cancer progression</i>	<i>149</i>
<hr/>	
<i>Figure 4.1: Representative 2DGE maps of hemoglobin-depleted erythrocyte cytosol from</i> <i>normal, B-ALL and HS individuals</i>	<i>157</i>
<i>Figure 4.2: Representative erythrocyte membrane proteomes of normal, B-ALL and</i> <i>HS individuals</i>	<i>159</i>
<i>Figure 4.3: Transmission electron micrographs of RBC ghost preparations</i>	<i>161</i>
<i>Figure 4.4: Representative erythrocyte membrane proteomes of a non-HS hemolytic</i> <i>anemia case</i>	<i>163</i>

LIST OF TABLES

<u>Table</u>	<u>Page No.</u>
<i>Table 1.1: Other potential therapeutic targets for ALL treatment</i>	34
<i>Table 1.2: Comparison of lipid raft proteins identified in B-cell malignancies and primary Cells</i>	64
<i>Table 2.1: Clinical Details of Leukemia Patients</i>	76
<i>Table 2.2: Identification of differentially regulated proteins in B-ALL CD19+ proteome</i>	84
<i>Table 2.3: Identification of 19 new differentially expressed proteins in DIGE experiments</i>	91
<i>Table 2.4: Implications of the differentially regulated proteins in leukemogenesis according to available literature (references in parentheses)</i>	106
<i>Table 3.1: Mass spectrometry identification details of the 88 protein annotations from 20% (NH₄)₂SO₄ precipitate of normal plasma</i>	127
<i>Table 3.2: Clinical Details of Leukemia Patients</i>	136
<i>Table 3.3: Statistical evaluation of the spot densities of differentially-regulated proteins in plasma of B-ALL patients</i>	138
<i>Table 3.4: PDQuest raw pixel densities from 2DGE profiles, normalization, & statistics</i>	139
<i>Table 4.1: Identification of differentially regulated proteins by MALDI TOF/TOF mass spectrometry in Hemoglobin-depleted-erythrocyte cytosol proteome</i>	158
<i>Table 4.2: Identification of differentially regulated proteins by MALDI TOF/TOF mass spectrometry in erythrocyte membrane proteome</i>	159



CHAPTER 1

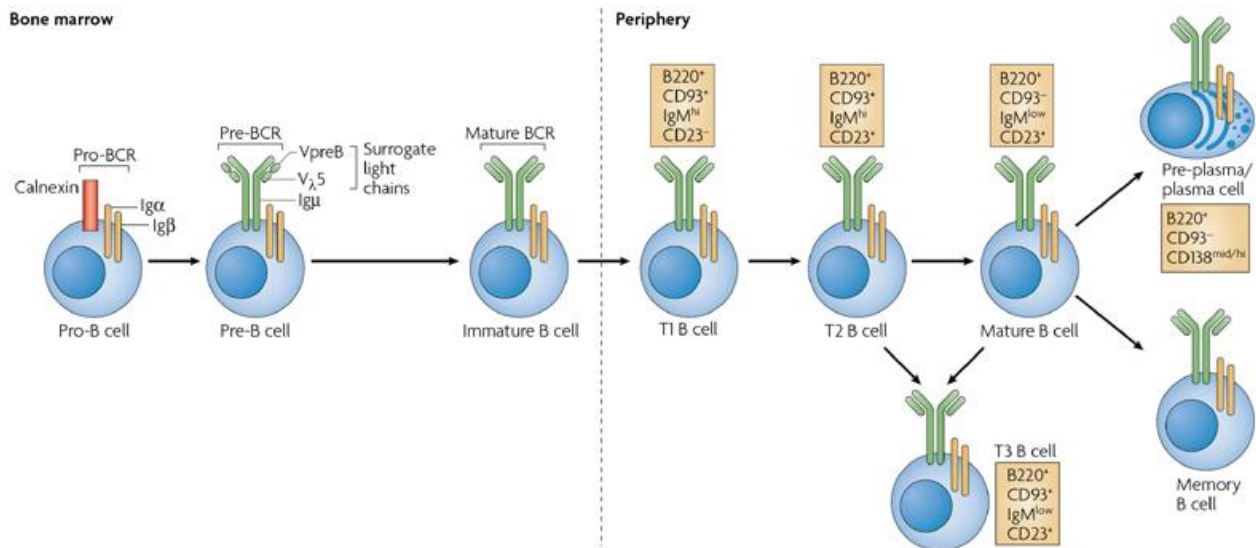
An Introduction to Proteomic Study in a Hematological Malignancy: B-cell Acute Lymphoblastic Leukemia (B-ALL)

1.1 Development of B Lymphocytes

B cells are a central component of the humoral arm of the immune system and are essential in protecting against infection and disease. They mediate their effector functions through the production of neutralizing antibody, induction of antibody-dependent cell-mediated cytotoxicity, and activation of the complement system. B cells are produced throughout the duration of our life, and the efficiency with which they are generated is affected by extrinsic and intrinsic factors including chemokines, cytokines, and transcription factors. Severe immunodeficiency is observed in cases where B cell development is reduced or absent and results in persistent infection. B lymphopoiesis occurs in a series of steps whereby progenitor cells undergo rearrangement of their immunoglobulin (Ig) loci, and this leads to the eventual expression of a functional B cell receptor (BCR) that is capable of responding to antigen (Figure 1.1). Expression of the pre-B cell receptor (pre-BCR) and the mature BCR are critical events during maturation and mediate transition through checkpoints that select for functional cells that are not self-reactive. Ig recombination is initiated at the heavy chain locus in committed B cell progenitors (pro-B cells) and results in the generation of the μ heavy chain proteins (μ HC). μ HCs associate with surrogate light chain (SLC) proteins VpreB and $\lambda 5$ to form the pre-BCR, which is expressed on the surface of newly formed pre-B cells. Pre-B cells express μ HCs on their cell surface with only one specificity, and further rearrangement at the HC locus is prevented by a process referred to as allelic exclusion. Successful pre-BCR expression and signalling activate survival, proliferation, and differentiation pathways that lead to the selection and expansion of large pre-B cells. Proliferating large pre-B cells exit the cell cycle and become resting small pre-B cells that begin rearrangement of the light chain (LC) proteins. LC proteins associate with μ HCs to form the BCR, which is first expressed on immature cells in the bone marrow (BM). Immature B cells are positively and negatively selected based on their antigen specificity and migrate from the BM to the spleen. Immature B

cells arriving in the spleen pass through a series of transitional stages prior to developing into mature follicular (Fo), marginal zone (MZ), and B-1 B cells.

Figure 1.1: Stages of B-cell development [1]



Mature B cells circulate throughout the periphery and localize in the BM, spleen, lymph nodes (LN), and peritoneal cavities. Antigen-activated mature B cells proliferate and differentiate into plasmablasts, which secrete high levels of antibodies. Antibodies can coat pathogens and cause them to agglutinate, which limits their mobility and replication, and prevents their entry into host cells. Antibody-bound pathogens can also be recognized by complement, which initiates the complement cascade. This cascade can result in both opsonization, whereby a pathogen is ingested and destroyed by phagocytes, and direct killing by means of the complement membrane attack complex. Antibody binding can also trigger antibody-dependent cell-mediated cytotoxicity (ADCC), a mechanism by which natural killer cells, monocytes, and/or eosinophils release compounds such as granzymes, IFN- γ , major basic protein, and perforin, all of which can lyse infected cells and kill invading pathogens. In addition to fighting off immediate infection, B cells also develop into long-lived memory cells that remain in the body to protect against future infections [2].

1.1.1 B cell Ontogeny

As with all hematopoietic lineages, B cells are derived from self-renewing hematopoietic stem cells (HSC). B lymphopoiesis can first be detected in the fetal liver of mice and humans on day 14 and week 8 of gestation, respectively. Development continues in the fetal BM, which is seeded with progenitor cells from the fetal liver. BM is also the predominant site of post-natal hematopoietic B lymphopoiesis, where developing cells are closely associated with stromal cells, a class of large adherent BM cells that include fibroblasts, reticular cells, preadipocytes, endothelial cells, and macrophages. This microenvironment provides essential support for hematopoiesis, and development is severely inhibited in cases where bone structure is abnormal. In the BM, progression from HSC to committed B cell follows a path in which a series of stochastic decisions result in cells that progressively develop B cell traits while repressing traits of other lineages. Cells are biased towards a certain lineage fate by the expression and interaction of transcription factors (TF) in a process referred to as specification. However, final commitment occurs only after all other lineage potentials are fully arrested. During murine development, HSCs are characterized by their lineage (lin^-), Sca-1^+ , $\text{c-Kit}^{\text{high}}$ (LSK) phenotype as well as self-renewing capacity and transition into non-self renewing multipotent progenitors (MPP). A subset of these LSK cells express high levels of Flt-3 and are designated lymphoid primed MPPs (LMPP). Expression of recombination of activation genes (*Rag*) as well as terminal deoxy-nucleotidyl-transferase (TdT) denotes the gradual transition to early lymphoid progenitors (ELP), which subsequently gives rise to common lymphoid progenitors (CLPs). CLPs are the first cells to express the interleukin-7 receptor (IL-7R) and possess B, T, natural killer (NK), and dendritic (DC) cell potential in vivo. B220^+ (CD45) pre-pro-B cells develop from CLPs and are the first cells specified to the B cell fate. Pro-B cells, identified by CD19 expression and increased levels of the TF Pax-5, are fully committed to the B lineage and are dependent on interleukin-7 (IL-7) for their proliferation and survival.

1.1.2 Markers of B cell Differentiation

B cell development has been described by various conventions that identify similar B cell populations but differ in nomenclature. Ig recombination is initiated by Rag proteins in c-Kit⁺ pro-B cells that subsequently develop into pre-BI cells, which are rearranging their HC genes and express SLC proteins. Large cycling Pre-BII cells express the pre-BCR, down-regulate c-Kit, and begin to express the IL-2 α receptor (CD25). Pre-BCR expression is difficult to detect on the cell surface and thus it is convenient to use CD25 in conjunction with other B cell markers to identify pre-B cells. Small pre-B cells re-express Rag proteins that allow LC rearrangement to begin. Detailed examination of the surface of small pre-B cells revealed that the pre-BCR is down-regulated and internalized during the large pre-B to small pre-B transition. The mature BCR is first expressed on the surface of CD25 negative immature B cells.

Human hematopoietic precursors can be identified by CD34 expression and, similar to mouse development, human HSCs pass through lineage restriction stages that bias them towards either myeloid or lymphoid fate. CD45RA⁺ CD10⁺ CD19⁻ IL-7R⁺ cells are specified B cell progenitors that possess DJ_H rearrangements and express components of the pre-BCR (Ig α/β , VpreB), events similarly observed in specified murine B cell progenitors. CD34⁺ CD10⁺ human pro-B cells expressing CD19 are committed to the B lineage. Subsequent stages of human B cell development closely follow those characterized in mice, with pro-B cells developing into large cycling pre-B cells (CD34⁻ CD10⁺ CD19⁺), small pre-B cells (also CD34⁻ CD10⁺ CD19⁺), and immature B cells (CD34⁻ CD10⁺ CD19⁺ CD40⁺ sIgM⁺). In mice and humans, immature B cells exiting the BM go through a series of transitional stages before becoming mature functional B cells. These cells all express AA4.1 and low/intermediate levels of CD21/CD35. Transitional cells can be further subdivided into recent splenic emigrants, termed T1 cells (IgM^{high} IgD^{low} CD23⁻), which give rise to T2 cells (IgM^{high} IgD^{high} CD23⁺)

that subsequently develop either directly into Fo and MZ cells or go through a T3 (IgM^{lo} IgD^{hi} CD23⁺) intermediate stage. Mature B cells lose expression of AA4.1 and can be distinguished by their IgM^{lo} IgD^{hi} CD21^{int} CD23^{hi} (Fo) or IgM^{hi} IgD^{lo} CD21^{hi} CD23^{lo/-} (MZ) phenotypes.

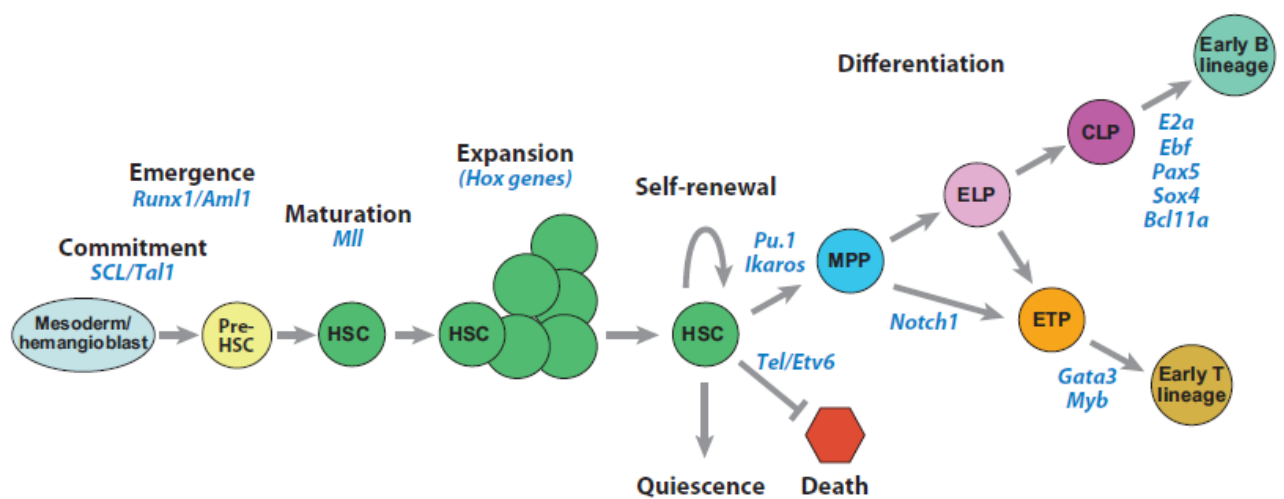
1.1.3 Factors Regulating B cell Development

The development of non-committed progenitor cells is influenced by both environmental conditions and cell-intrinsic factors. Transcription factors (TFs) are DNA-binding proteins, which, by induction or repression of target genes, control many of the events leading to lineage specification and commitment. These factors can be shared or lineage-specific and, typically, no single factor leads to lineage commitment. Instead it is the quantity, combination, and cross competition between them that regulate the gene expression patterns that activate lineage-directed programs. TFs in turn are regulated by growth factors, cytokines, and chemokines, which are produced by supportive cells in developmental niches such as the fetal liver, BM, spleen, and thymus. It is the combination of these factors in the appropriate environmental context that provides the necessary cues for B cell development to occur (Figure 1.2).

MPPs express a variety of TFs that prime cells for lineage commitment, including the zinc-fingered domain proteins Ikaros and Bcl11a, as well as the ETS family member PU.1. Mice deficient for any of these factors display a defect at the CLP stage, likely due to failed expression of Flt3 and/or IL-7R α . However, ectopic expression of IL-7R α in PU.1^{-/-} progenitors does not fully rescue B lymphopoiesis as PU.1 has alternative roles during B cell development, including the repression of T-cell and NK-cell development. In addition to directing the early stages of lymphoid specification, Ikaros and PU.1 also influence later B lineage development. In contrast to fully deficient animals, mice exhibiting reduced levels of Ikaros develop normally past the CLP stage but are impaired at the pro-B to pre-B transition. Ikaros also acts in conjunction with related family member Aiolos to suppress *Igll1* (λ 5) expression. Studies in which levels of PU.1 were manipulated showed that high level PU.1 expression correlates with the development of myeloid cells at the expense of B cells, while

low levels failed to support myeloid development and led to increased generation of B cells. However, lymphoid versus myeloid cell fate does not appear to be this straightforward. Subsequent studies have shown that PU.1 levels are similar in precursor populations and that high levels of PU.1 required for both myeloid and B cell development. Further commitment or differentiation of B cells is not dependent on PU.1, as conditional knockout of PU.1 at the pro-B stage does not alter subsequent B cell development.

Figure 1.2: Role of transcription factors in lymphopoiesis [3]



Activation of the helix-loop-helix domain family members E2A and early B cell factor-1 (EBF) is a critical step in B cell specification. Defects in either E2A or EBF block development prior to B cell commitment, with cells having yet to begin Ig recombination. E2A is composed of E-protein splice variants E12 and E47 that homo- or heterodimerize prior to binding of the consensus DNA sequence CANNTG, denoted the E-box motif. E proteins regulate the expression of several important factors during B cell development including the IgH enhancer and EBF. The other E-box proteins (E2-2 and HEB) have both redundant and independent functions during B cell development. Deletion of either decreases pro-B cells by about half, and mice heterozygous for any two E-protein family members also display B cell defects. E-proteins can also bind inhibitors of DNA-binding proteins (ID 1–4), which are

structurally similar to E-proteins but lack the DNA-binding domain. Dimerization of ID and E-proteins abolishes E-protein DNA-binding potential and inactivates its function. Experimentally, over-expression of ID1 leads to a block at the pro-B stage of development. This suggests that ID proteins work to regulate the levels of E-proteins during development. The ability of EBF to control B cell specification has been demonstrated in studies where ectopic expression skewed the differentiation of HSCs towards the B lineage. EBF expression can also partially or fully rescue B cell development in mice deficient for PU.1, E2A, IL-7, or the IL-7R α . EBF partners with E2A to specify cells to the B cell lineage through the induction of Ig rearrangement and the regulation of Ig α , Ig β , VpreB, and λ 5. Another critical target of EBF is Pax-5, a paired homeodomain TF necessary for B-lineage commitment. Numerous factors regulate EBF expression, including PU.1, E2A, IL-7, Pax-5 and even EBF itself [4]. This multileveled regulation allows for the control of EBF expression and provides positive feedback loops to maintain its expression. Pax-5 functions not only to induce gene expression patterns leading to B cell commitment, but also to repress other lineage options. The N-terminal paired domain motif of Pax-5 binds DNA and positively regulates gene transcription. Pax-5 targets include *mb-1* (Ig α), BLNK, CD19, *Igll1* (λ 5), as well as numerous TFs such as interferon regulatory factors 4 and 8 (IRF-4/8) and Aiolos [5]. Pax-5 also represses non-B lineage genes myeloperoxidase (*MPO*), *Notch-1*, *M-CSFR*, and *Flt3*. This gene repression is essential in maintaining B cell commitment as Pax-5^{-/-} cells retain the ability to differentiate into other hematopoietic lineages when cultured under permissive conditions. Additionally, injection of Pax-5^{-/-} pro-B cells into Rag-2^{-/-} mice leads to reconstitution of the thymus and generation of T cells. This T-cell development is likely due to the failure to repress Notch-1, a critical T-cell transcription factor. Continual expression of Pax-5 is necessary throughout B cell development, as conditional deletion of Pax-5 in pro-B or later stage mature cells leads to the reactivation of many repressed genes and reversion to other lineage types. However, recent work has identified novel roles for EBF in B cell commitment independent of Pax-5. Sustained

expression of EBF in Pax-5^{-/-} hematopoietic progenitor cells restricted their ability to differentiate into myeloid or T cells *in vivo* and, *in vitro*, EBF repressed myeloid and T-cell genes in Pax-5^{-/-} pro-B cells [6]. The authors proposed that the lack of lineage commitment observed in Pax-5^{-/-} cells is actually the result of a failure of these cells to maintain EBF expression. A variety of abnormalities in the Pax-5 locus have been identified in numerous cases of B cell progenitor acute lymphoblastic leukemia (BCP-ALL). In one such case, the t(9;12)(q11;p13) translocation generated a fusion protein composed of Pax-5 and the Ets transcription factor TEL [7]. This hybrid molecule possessed the DNA-binding potential of Pax-5 and the transcriptional repressor function of TEL. When tested *in vitro*, the Pax-5/TEL fusion protein down-regulated Pax-5 targets CD19, BLNK, *mb-1*, and Flt3, led to increased CXCL12-induced migration, and improved survival after IL-7 withdrawal or TGF- β treatment. The apparent contribution of genomic alterations of B lineage transcription factors in BCP-ALL is becoming increasingly recognized. Characterization of single nucleotide polymorphism (SNP) arrays from over 200 BCP-ALL samples showed that 40% of them contained such defects [8]. While Pax-5 cases were the most prevalent (>30%), aberrations were also observed for other B cell transcription factors, including E2A, EBF, Ikaros, and Aiolos.

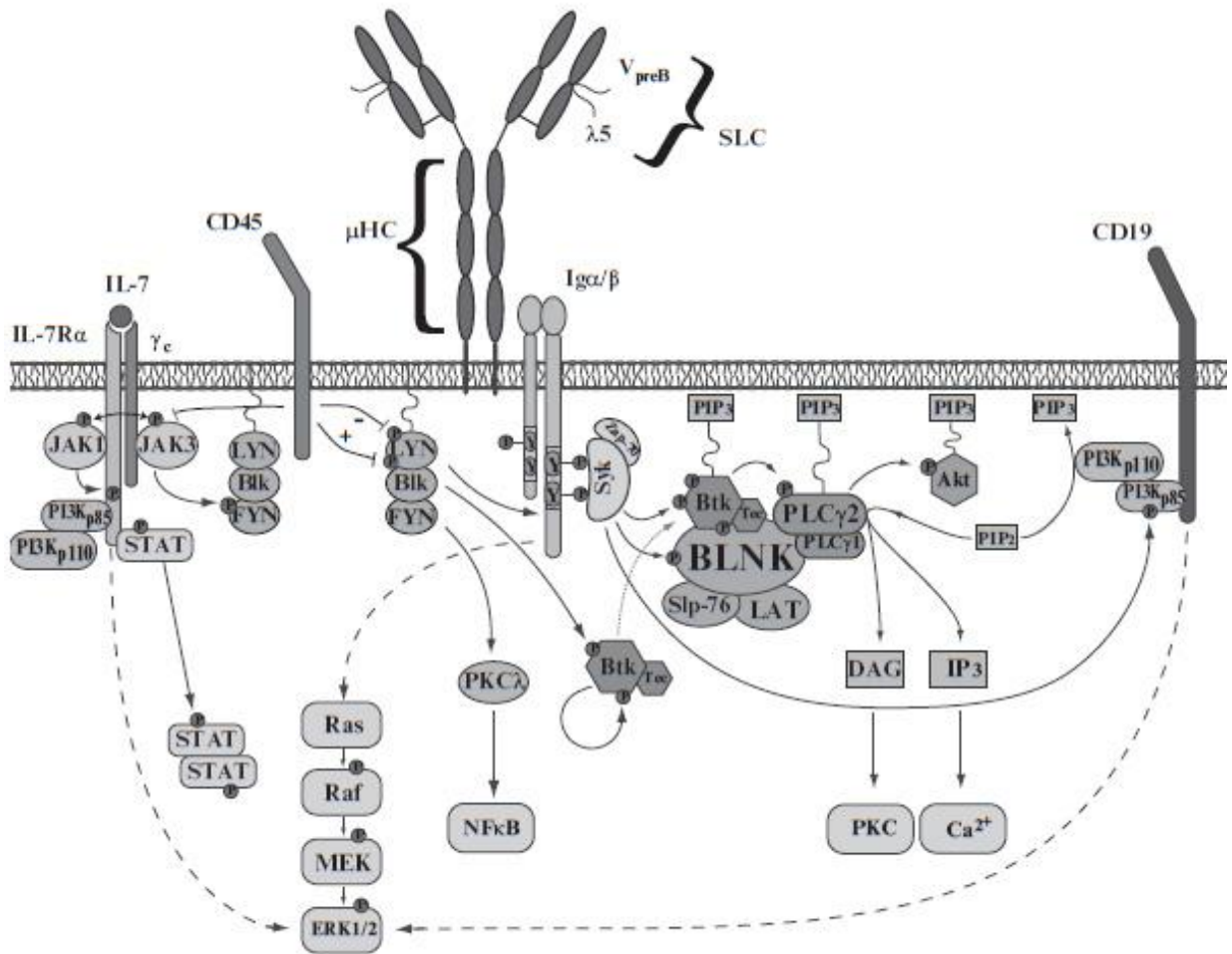
Stem cell factor (SCF, c-Kit-Ligand), which exists in either soluble or membrane bound form, binds the surface-expressed tyrosine kinase receptor KIT (c-Kit). SCF is required in the earliest stages of hematopoietic development and SCF^{-/-} or c-Kit^{-/-} mice die within a week of birth due to anaemia. SCF also has specific influences on developing B cells. In Vicked mice (viable c-kit deficient) or Wepo mice (rescued by erythropoietin over-expression), B cell development is normal during fetal life but numbers of pro-B and pre-B cells greatly diminished as mice age. *In vitro*, SCF can act synergistically with IL-7 to increase the numbers of pro-B cells in cultures. This explains the decreased number of B cells observed in knockout mice. However, the increase in B cell populations *in vitro* is more likely due to the fact that SCF promotes the survival and proliferation of B cell progenitors in culture and thus increases

the input of IL-7-responsive pro-B cells. Flt-3 and its receptor Flt-3L also play critical roles in enhancing the survival and proliferation of early progenitors. In Flt-3^{-/-} mice, pre-pro-B and pro-B cell numbers are significantly reduced while subsequent pre-B and immature populations are relatively normal. When Flt-3 is added to *in vitro* cultures, it synergizes with IL-7 and led to an increase in the survival and proliferation of pre-pro-B cells.

The growth factor IL-7 is produced by cells in the BM, spleen, thymus, and fetal liver and provides signals required for the survival, proliferation, and differentiation of developing B cells. Mice with targeted deletions of IL-7 or the IL-7R display a severe block at the early pro-B cell stage of development. Transgenic expression of IL-7 in mice results in increased immature and mature B cell populations in the BM as well as the appearance of pro-B and pre-B populations in the spleen, blood, and lymph nodes that ultimately lead to lymphoproliferative disorders in these mice. Regulated IL-7 signalling is also important during B cell commitment as high-level expression of the IL-7R on multipotent stem cells leads to a block in B cell development prior to expression of CD19, and blocked cells express decreased levels of EBF and Pax-5.

The IL-7R is a heterodimer composed of α chain and the common (γ) chain (γ_c) utilized by the IL-7 and thymic stromal lymphopoietin (TSLP) receptors, and the γ_c chain is a shared component of the receptors for IL-2, IL-4, IL-7, the IL-9, IL-15, and IL-21. IL-7 receptor binding leads to the heterodimerization of the α and γ_c chains, which in turn allows for the trans-phosphorylation of constitutively associated JAK1 and JAK3 proteins and subsequent IL-7 α chain phosphorylation (Figure 1.3). Receptor phosphorylation leads to activation of Src kinases (LYN/FYN/Blk) and also creates docking sites for SH2 containing proteins PI3K and STAT. PI3K is recruited to the IL-7R α chain and activates the anti-apoptotic molecule AKT. Inhibition of PI3K activation led to the observation that it is important for cell proliferation and survival but dispensable for IL-7-mediated differentiation events.

Figure 1.3: Signalling cascades in early B cell development [9]



Recruitment of STATs to the IL-7R α chain results in their hetero- and homodimerization prior to nuclear translocation. Deletion of STAT5 leads to a block in development at the pro-B stage, similar to that observed in IL-7R^{-/-} mice, and is a result of failed expression of EBF and Pax-5 [10]. Conversely, STAT5 over-expression can overcome IL-7R deficiency and demonstrates STAT5s essential role in mediating IL-7-induced events. STAT3 is also critical during B cell development: the impaired differentiation and survival displayed by STAT3^{-/-} B cells leads to a decrease in pro-, pre-, and immature B cell populations [11]. Finally, it has been shown that stimulation with IL-7 leads to the activation of the MAP kinase ERK, and inhibition of this pathway prevents proliferation and survival of pro- and pre-B cells.

1.1.4 Regulation of B cell Development by the Pre-BCR and BCR

Following receptor activation, signal transduction is dependent on receptor aggregation and leads to the formation of the surface signalling complex. The complex includes the pre-BCR

and co-activators, such as CD19, but excludes CD45 (Figure 1.3). Signalling intermediates are recruited to the complex through their interaction with ITAMs and immunoreceptor tyrosine inhibition motifs (ITIMs), which are contained within the cytoplasmic tails of surface molecules. Signal transduction is mediated by kinases and phosphatases, which function to phosphorylate and dephosphorylate proteins, and by adaptors that lack intrinsic kinase activity but instead operate to bring molecules together and allow for their interaction. Pre-BCR signals are initiated by Src kinase phosphorylation of the ITAM regions of Ig α / β (Figure 1.3). Src kinases also induce NF- κ B signalling via PKC λ , and phosphorylate the tyrosine kinase Btk, which leads to its subsequent autophosphorylation and activation. The Src family of kinases contain members including Src, Lyn, Blk, and Fyn with Blk being the only B cell exclusive member. Due to the redundant nature of these molecules, mice deficient for any one of the members show no defect in signalling. However, Lyn/Fyn/Blk triple-deficient mice display a dramatic decrease in pre-B cell numbers but normal numbers of pro-B cells. This observation demonstrates the important role this family plays in transducing signals downstream of the pre-BCR. Phosphorylated Ig α / β ITAMs serve as docking sites for the SH2-containing Syk kinase, which is subsequently able to activate several downstream pathways through signalling mediators PI3K, Btk, and BLNK. Deletion of Syk revealed that it is not the only family member that mediates transduction in developing B cells and that Zap-70 can compensate for its loss. A full block was observed when both of these family members were deleted. This was a surprising discovery since it had previously been reported that Zap-70 can only expressed in T and NK cells. Similar redundancy is observed for BLNK, Btk, and PLC γ 2 as LAT and SLP-76 can compensate for BLNK, Tec can partially compensate for Btk, and PLC γ 1 performs similar function as PLC γ 2 (Figure 1.3). Signalling intermediates are recruited to the receptor complex by way of receptor motifs and adaptors. They can also be targeted to the complex by interaction of their pleckstrin homology (PH) domains with phosphatidylinositol lipids present in biological membranes. Phosphatidylinositol 3,4,5-triphosphate (PIP3) is a key mediator of

membrane localization and is generated by PI3K, which converts phosphatidylinositol 4,5-bisphosphate (PIP₂) to PIP₃. PI3K is a dimer composed of a p110 subunit that possesses catalytic activity, and a SH2-containing p85 subunit that is important in targeting the kinase to the signalling complex. This B cell defect is due to the ineffective targeting of signalling molecules Btk, PLC γ 2, and protein kinase B (PKB, also referred to as AKT) to the receptor complex. PIP₂ also functions as a substrate for PLC γ 2, which converts PIP₂ into diacylglycerol (DAG) and inositol triphosphate (IP₃). DAG and IP₃ are secondary messengers that lead to protein kinase C (PKC) activation and calcium (Ca²⁺) mobilization, respectively. PLC γ 2 and Btk are both recruited to the receptor complex by the adaptor protein BLNK. This protein assembly allows Btk to phosphorylate PLC γ 2, and leads to its full activation. BLNK has also been shown to be a binding partner for Syk in mature B cells. This association results in a positive feedback loop that is necessary for ERK, NF- κ B, and Ca²⁺ responses but not for Akt activation [12].

Pre-BCR regulation of apoptotic factors is mediated through downstream pathways including, the PI3K/AKT pathway and the Ras/Raf/MEK/ERK pathway. Mice deficient for or over-expressing the anti-apoptotic protein Bcl-XL display reduced or elevated numbers of pre-B cells, respectively. While Bcl-XL provides survival signals to pre-B cells, Bcl-2, another anti-apoptotic molecule, exerts its effect on immature cells, and Bcl-2 transgenic mice have increased IgM⁺ cell numbers. Cell proliferation, another outcome of pre-BCR signalling, is mediated in large part through the activation of the Ras-ERK pathway. The importance of this pathway in B cell development has been highlighted in ERK1/2^{-/-} mice, which exhibit diminished pre-BCR-mediated expansion and a block at the pro-B to pre-B stage of development [13]. Engagement of the pre-BCR or IL-7R results in downstream phosphorylation of ERK, and these pathways synergistically activate ERK to allow for the proliferation of large pre-BCR⁺ cells in picogram concentrations of IL-7. Pre-BCR activation of BLNK and Btk limits the proliferation of large pre-B cells and allows for further maturation.

BLNK^{-/-} or Btk^{-/-} mice show a partial block in development at the large pre-B stage with increased expression of SLC components, increased surface pre-BCR expression, and enhanced proliferative capacity. Transcriptional down-regulation of SLC expression via BLNK, Btk, and IRF-4/8 is believed to diminish individual cell surface pre-BCR expression and thus limit large pre-B cell signalling and proliferation. However, over-expression studies have demonstrated that SLC silencing is not absolutely required to limit the expansion of pre-B cells but is necessary to prevent constitutive B cell activation. BLNK^{-/-} or Btk^{-/-} pre-B cells also exhibit normal allelic exclusion and reduction of Rag and TdT expression, which suggests that these effects are mediated by Btk- and BLNK-independent mechanisms and possibly are not even pre-BCR-dependent events. This theory is strengthened by the observation that allelic exclusion is observed in SLC^{-/-} mice. However, studies using m MT mice have shown that insertion of the m HC into the lipid bilayer is essential. The signalling mechanisms that result in allelic exclusion have not been fully elucidated, but it has been demonstrated that Syk^{-/-}/Zap-70^{-/-} and PLCγ1^{+/-}/PLCγ2^{-/-} mice do not display allelic exclusion while BLNK^{-/-} mice retain this ability. Consequently, allelic exclusion at the HC locus is initiated only after membrane expression of a productively rearranged m HC protein initiates downstream signals through Syk and PLCγ family members.

1.1.5 Signalling Defects and Clinical Disease

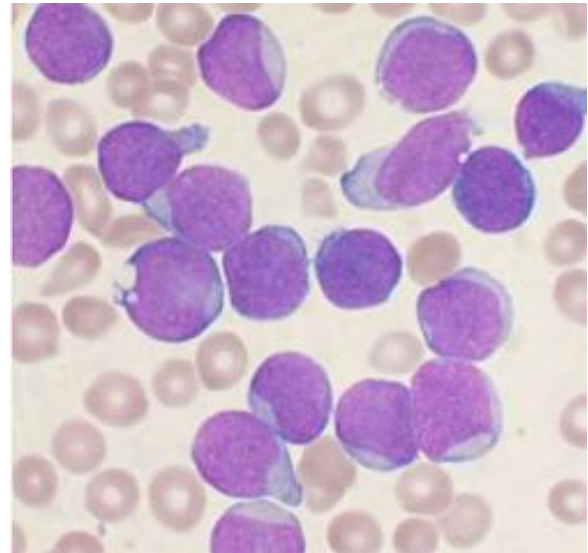
Bruton's tyrosine kinase (Btk) deficiency in humans results in X-linked agammaglobulinemia (XLA), the most common genetic defect observed in patients with early B cell defects. Patients with XLA or defects in BLNK exhibit low levels of serum Ig of all classes and are typically diagnosed within the first few years of life after exhibiting susceptibility to recurrent bacterial infections. Btk and BLNK deficiencies have also been observed in approximately 50% of childhood pre-B acute lymphoblastic leukemias (ALL). Unlike mice deficient in Btk or BLNK, which exhibit an expansion in pre-B cells, humans deficient in these molecules exhibit a reduction in pre-B cells. Defective pro-B to pre-B cell development corresponds with the

agammaglobulinemia phenotype but it does not fit with the leukemic nature of these cells. In such cases it is believed that oncogenesis is the result of BCR-ABL truncation of BLNK and/or Btk, which results in constitutively activated signalling pathways. BCR-ABL is a common translocation observed in ALL patients. It results from the fusion of the break cluster region (BCR), not to be confused with the B cell receptor, and the c-abl proto-oncogene. Cells exhibiting this translocation display increased survival and proliferation, independent of pre-B cell receptor expression, and are immortalized with either an unresponsive or a non-productive/non-functional pre-BCR.

1.2 B- cell Acute Lymphoblastic Leukemia

B-cell acute lymphoblastic leukaemia (B-ALL) is a clonal malignant disease originated in a single cell and characterized by the accumulation of blast cells that are phenotypically reminiscent of normal stages of B-cell differentiation. B-ALL origin has been a subject of continuing discussion, given the fact that human disease is diagnosed at late stages and cannot be monitored during its natural evolution from its cell of origin, although most B-ALLs probably start off with chromosomal changes in haematopoietic stem cells [14]. However, the cells responsible for maintaining the disease appear to differ between the different types of B-ALLs and this remains an intriguing and exciting topic of research, since these cells have been posited to be responsible for resistance to conventional therapies, recurrence and dissemination. During the last years this problem has been addressed primarily by transplantation of purified subpopulations of human B-ALL cells into immunodeficient mice. ALL is one of the four main categories of human leukaemia and the majority of ALLs are of the B-cell type. Since immunophenotyping enables the determination of the differentiation stages of normal lymphoid cells, it has also been used for the identification and classification of ALLs. In this way it has been found that B-lineage leukaemias dominate within the lymphoid leukaemia groups in both children (where >80% ALLs are B-ALLs) and adults (>75%).

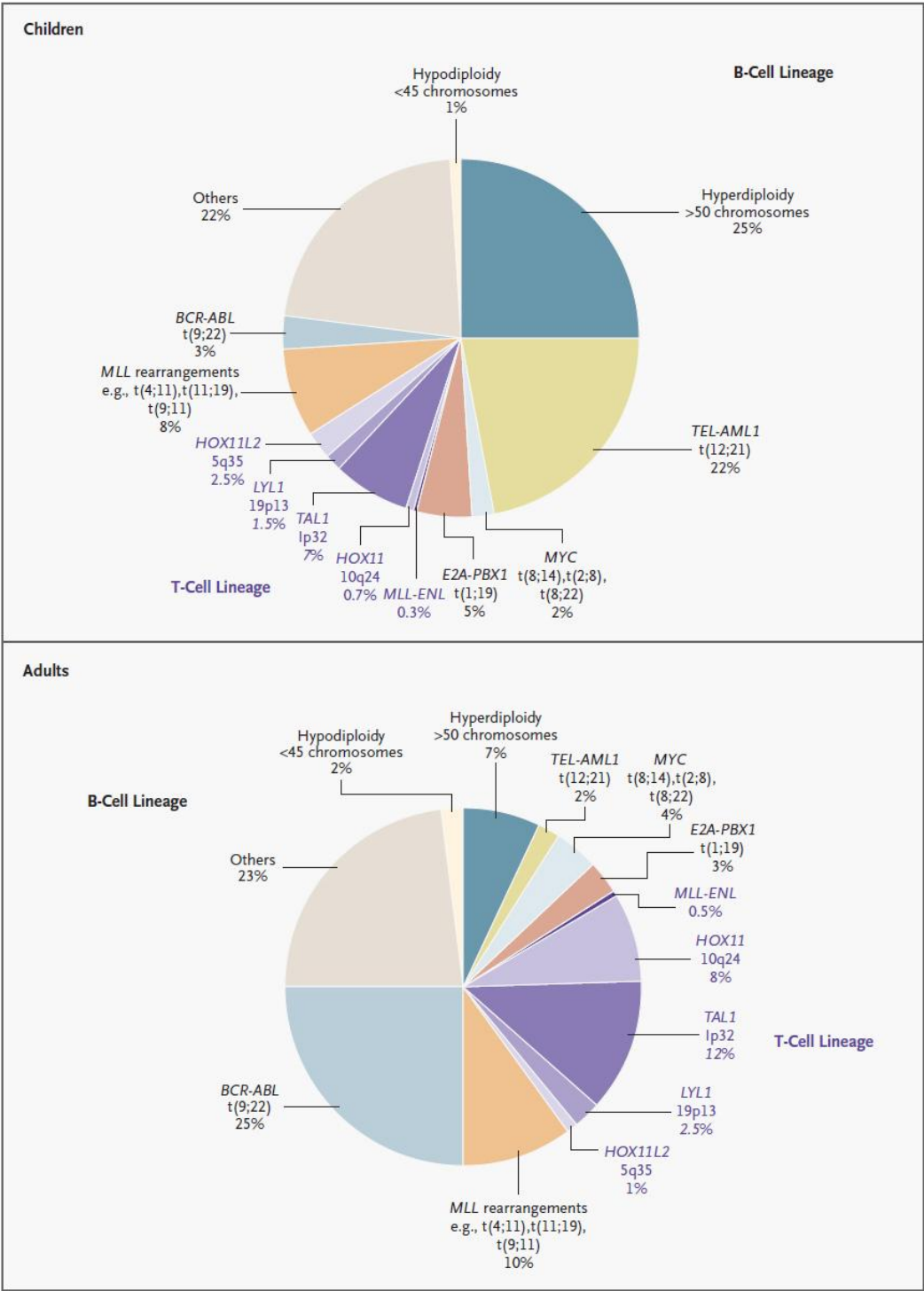
Figure 1.4: Characteristic B-ALL bone marrow smear showing clonal expansion of B-lymphoblasts



An improved understanding of B-ALL pathophysiology has been gained in the process of identification of the genetic abnormalities consistently present in B-cell blasts. A relatively reduced set of gene fusions created by chromosomal translocations are involved in the genesis of B-ALL: TELAML1, MLL rearrangements, BCR-ABL and E2A-PBX1. However, the frequency of genetically defined leukaemia subtypes differs between children and adults: for example, TEL-AML⁺ leukaemias are almost exclusively present in children (22% of ALLs vs. 2% in adults) while BCR-ABL⁺ ALLs are much more frequent in adults (25% vs. 3% in children). These primary oncogenic events seem, however, to require secondary cooperative changes to generate a fully transformed cell (Figure 1.5). Nevertheless, the mechanisms responsible for this B-cell developmental arrest in B-ALL are unknown, although several possible explanations could account for it. First, the oncogenic alterations associated with B-ALL could interfere with the networks controlling B-cell differentiation. Second, the B-cell blasts might lose responsiveness to external cues that regulate normal B-cell differentiation or, alternatively, the proliferating clone may outgrow the limited supply of external differentiation-inducing cues while staying potentially responsive to them (given the right microenvironment); this may be especially relevant in a foreign environment like that of the mice used for xenotransplantation. Third, it is also conceivable that the oncogenic events associated with B-

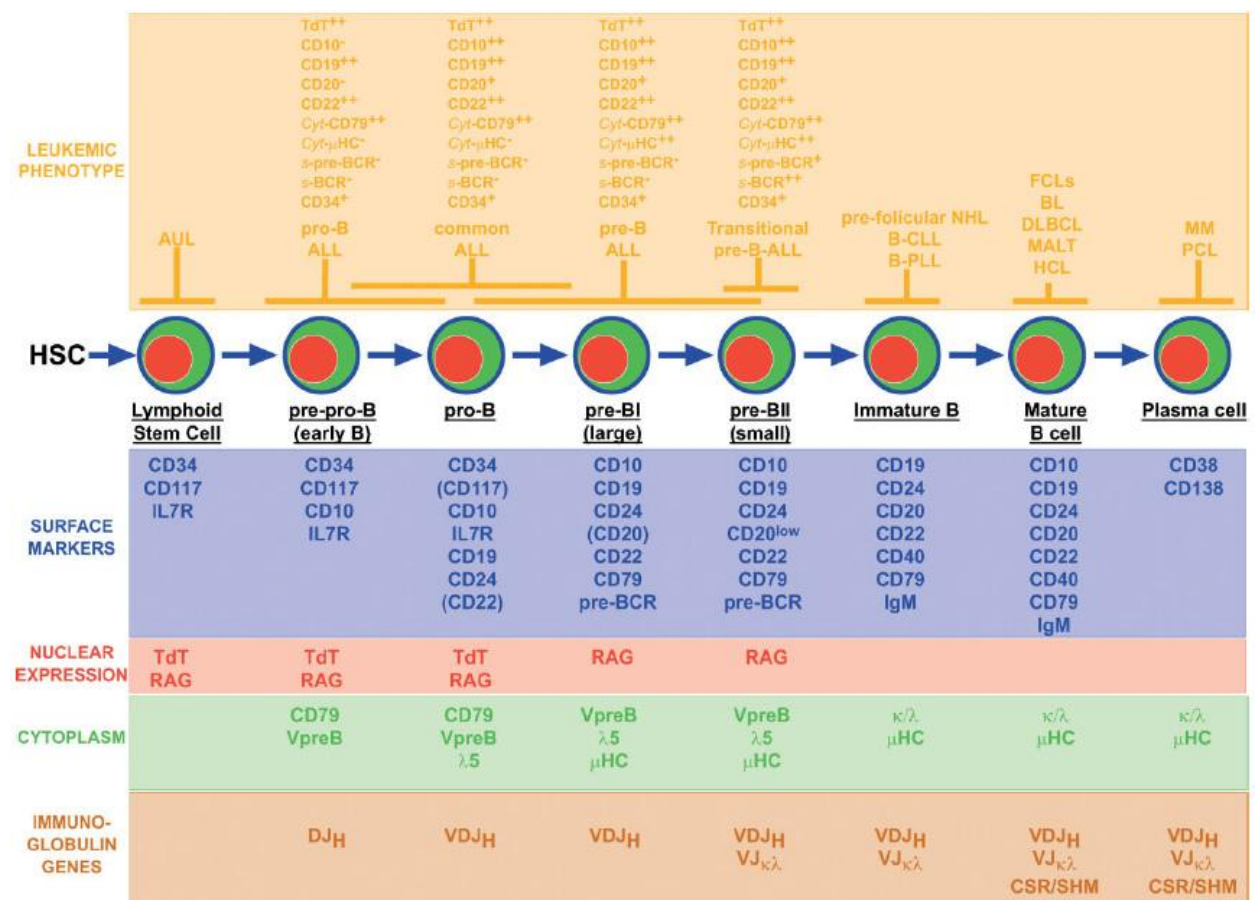
ALL might dictate the B-cell phenotype by activating pathways that mimic a particular stage of normal B-cell differentiation.

Figure 1.5: Estimated Frequency of Specific Genotypes of ALL in Children and Adults [15]



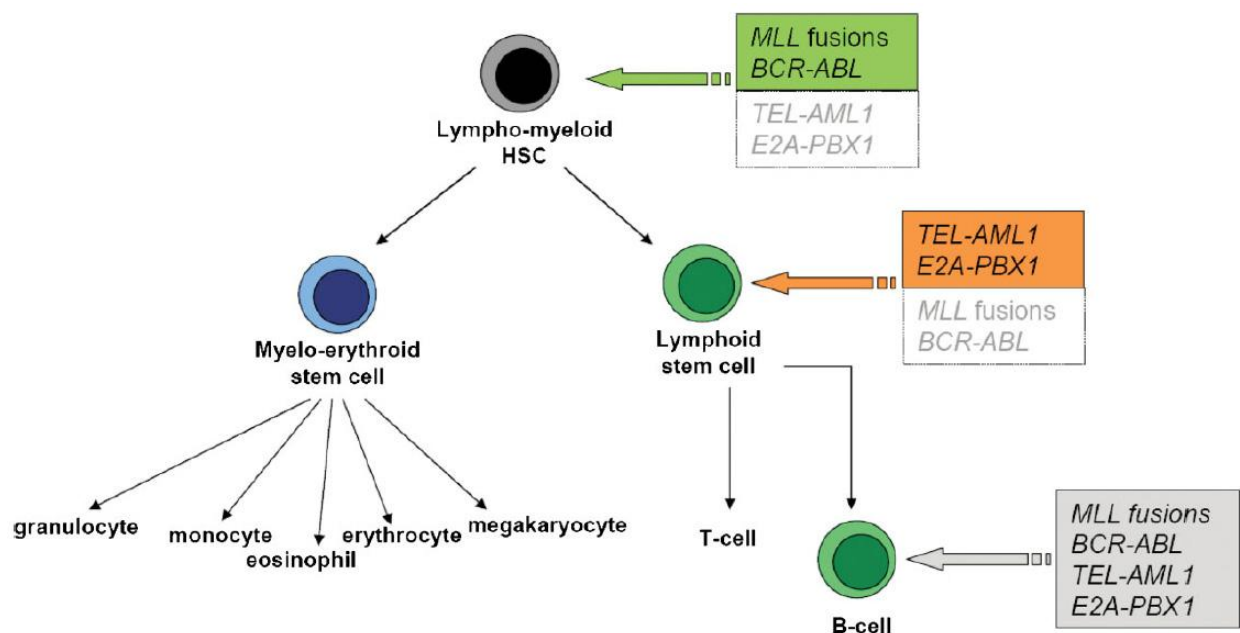
Traditionally, the correlation between the different types of normal B-cell developmental stages and the types of B-ALL has been determined by the combined evaluation of microscopic

appearance and immunophenotype. By these criteria, B-cell malignancies can be related in most cases to the different stages of normal B-cell differentiation. The maturation of bone marrow progenitor cells to mature B-cells proceeds through stages that can be identified by the status of the immunoglobulin gene rearrangements, the pattern of expression of cellular immunoglobulin proteins and the expression of cell surface antigens (Figure 1.6).



differentiation. Furthermore, there is now compelling evidence that several of the common chromosome translocations that are seen in childhood B-ALL often originate prenatally *in utero* during fetal haematopoiesis. These studies have confirmed the prenatal origin of MLL fusion genes in infant B-ALL, and show that many TEL-AML1 fusions in B-ALL also originate prenatally. These observations suggest that childhood BALLs might originate prenatally through gene fusions created by chromosomal translocations, implying that these chromosomal changes can take place either in haematopoietic stem cells or even in earlier stages in the fetal liver or bone marrow (Figure 1.7).

Figure 1.7: Presumptive cellular origins of chromosomal translocations in human B-ALLs [14]

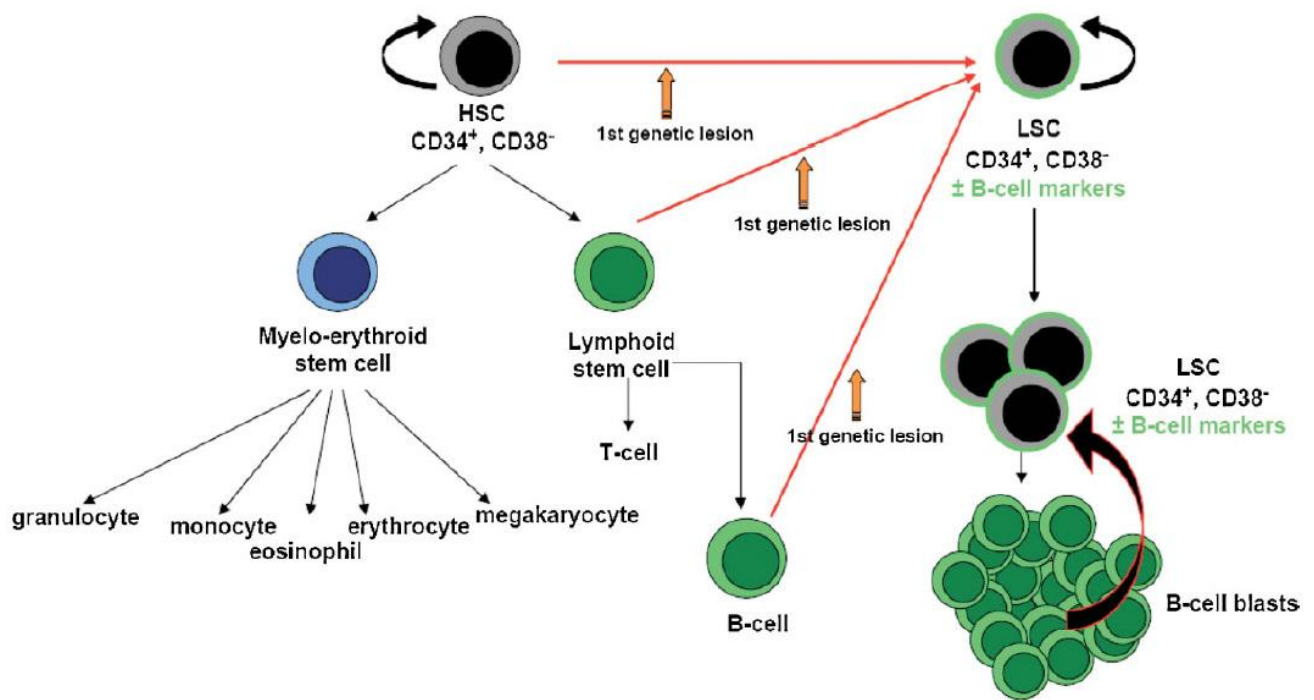


However, the precise cellular origin of the translocations within the progenitor hierarchy in the haematopoietic system is difficult to ascertain, especially since the functional impact of the translocation (i.e. the resulting clonal expansion) can manifest in the form of cellular types whose markers of differentiation place them either down- or upstream of the point of origin of the translocation. Thus, cells at later stages of B-cell development cannot be formally excluded as B-ALL cells-of-origin. This fact is of special relevance for adult ALLs and for childhood leukaemias where the origin has been proven to be mainly postnatal, e.g. E2A-PBX1⁺ ALLs.

It has long been proposed that stem cells are the main target for key initiating genetic events both in B-ALL and other cancers. In this context, however, we should also take into account a special property of B-cells: their unusually high degree of plasticity. This plasticity has recently been shown in the mouse for mature $\text{IgM}^+ \text{IgD}^+$ peripheral B-cells that can dedifferentiate all the way back to early multipotent progenitors just in response to the complete loss of the B-cell commitment factor Pax5. In this context, a complete loss of Pax5 in mature B-cells also leads to the appearance of tumours of an early pro-B-cell phenotype which, however, have their origin in much later B cell developmental stages. Due to their long life span and their particular developmental characteristics, B-cells (and also T cells) have sometimes been postulated as being single lineage stem cells. In line with this, it is not unconceivable that, given the right conditions (e.g. oncogene activation by chromosomal translocations), they can acquire all the properties of a stem cell, as we have mentioned above with the loss of Pax5 in mouse lymphomas [16]. The cancer stem cell (CSC) hypothesis proposes that cancer is organized as a heterogeneous tissue where CSCs (=‘cancer-propagating cells’=‘cancer-maintaining cells’) are defined as cells that retain broad self-renewal potential and have the ability to regenerate all the cellular diversities of the original tumour [17]. In human B-ALLs, demonstration of the existence and definition of the identity of CSCs come from experiments utilizing serial transplantation of FACS-sorted cell populations into immunocompromised mice. The CSC containing population should recapitulate the cellular heterogeneity present in the primary human B-ALL and must have the capacity for self-renewal on serial passaging (Figure 1.8). However, there are many technical issues concerning the isolation and determination of CSC capabilities from human B-ALL samples, ranging from the methods of selection of the cells themselves to the choice of the recipient animals in which the cells can reveal their potential. In spite of all the technical caveats, evidence has accumulated over the last years supporting the existence of CSCs in B-ALLs. These CSCs have frequently been isolated using markers specific for normal haematopoietic stem cells, especially CD34

and CD38. Another important aspect to remember is the heterogeneous nature of B-ALLs from many points of view, from the molecular abnormalities to the presentation (childhood vs. adults) and the different prognoses and responses to treatment. In the context of the debate about the existence of CSCs, the nature of ALL cells-of-origin and their potential phenotypes, this variability is of special relevance. It is for example, well accepted now that there are differences in the capacity that oncogenes have for activating a stem cell program in target cells.

Figure 1.8: Human B-cell acute lymphoblastic leukaemias form a hierarchy [14]



This implies that different oncogenes must use different means to finally give rise to CSCs: in some cases the oncogene itself will be able to activate a stem cell-specific program in non-stem target cells. In other cases, the stem cell characteristics will be conferred by the target cell-of-origin itself or by additional mutation(s) that can allow the cell to revert to early developmental stages with stem characteristics. The dependence of the final tumorigenic phenotype on the initiating oncogenic lesion will be different depending on the cases, and this will have a clear impact on any therapeutic approach.

1.2.1 Molecular genetic alterations in B-ALL

Molecular analysis of the common genetic alterations in leukemic cells has contributed greatly to our understanding of the pathogenesis and prognosis of B-ALL. Although the frequency of particular genetic subtypes differs in children and adults, the general mechanisms underlying the induction of ALL are similar. They include the aberrant expression of proto-oncogenes, chromosomal translocations that create fusion genes encoding active kinases and altered transcription factors, and hyperdiploidy involving more than 50 chromosomes [3]. These genetic alterations contribute to the leukemic transformation of hematopoietic stem cells or their committed progenitors by changing cellular functions. They alter key regulatory processes by maintaining or enhancing an unlimited capacity for self-renewal, subverting the controls of normal proliferation, blocking differentiation, and promoting resistance to death signals (apoptosis).

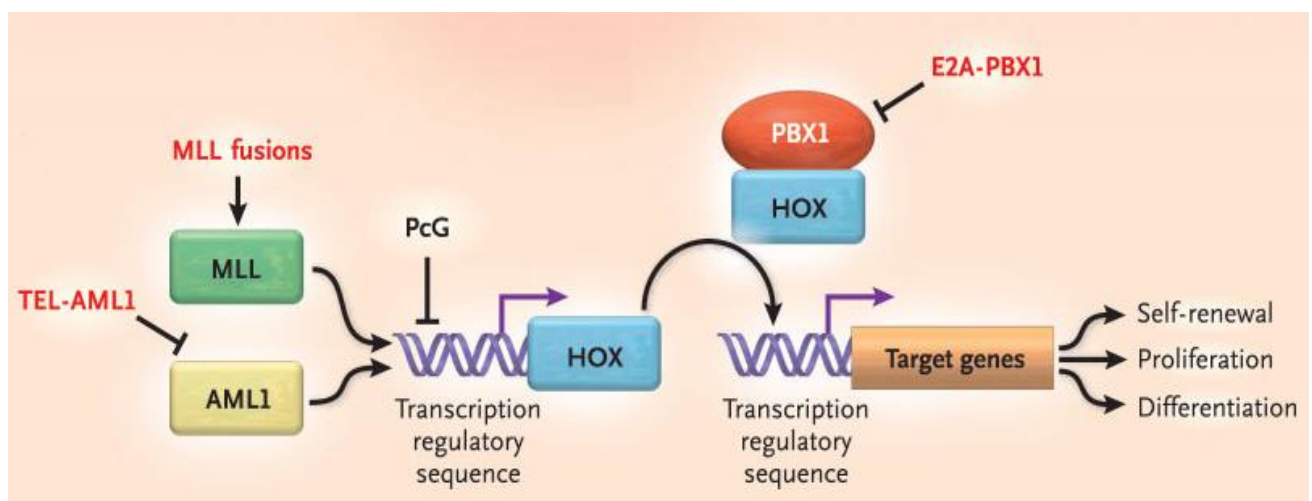
Genetic lesion	Associated clinical features	Presumed mechanism of action
B-ALL		
Hyperdiploidy (>50)	20% with FLT3 activation; good prognosis	
<i>BCR-ABL</i> t(9;22)	Poor prognosis; associated <i>IKZF1</i> or <i>CDKN2A</i> deletions; imatinib resistance develops rapidly	Constitutive tyrosine kinase; interacts with RAS, AKT, JAK/STAT pathways
<i>MLL</i> rearrangements	Improved outcome with high-dose cytarabine for some rearrangements; <i>MLL-AF4</i> poor outcome	Chimeric TF; some upregulate hENT1 cytarabine transporter
<i>TEL-AML1</i> t(12;21)	Good prognosis with intensive chemotherapy that includes asparaginase	Prenatal translocation, chimeric TF, represses AML1 target genes
<i>PAX5</i>	Most frequent target of somatic mutation	Translocated (rare) or deleted TF
<i>E2A-PBX1</i> t(1;19)	Intensified chemotherapy improves prognosis	Chimeric TF
<i>E2A-HLF</i>	Aggressive disease; adolescents; hypercalcemia; disseminated intravascular coagulation	Chimeric TF with anti-apoptotic SLUG induction; dimerize E2A proteins

Altered self-renewal and differentiation of hematopoietic stem cells can result from chimeric transcription factors, which arise from genetic translocations that fuse portions of two different transcription factors, for example TEL-AML1 fusion gene, translocations involving the MLL gene, *etc.* These chimeric transcription factors activate diverse transcriptional cascades that, at least in part, converge to modify the normal pattern of expression of members of the important family of HOX genes, which encode the HOX transcription factors (Figure 1.9). The HOX transcription factors bind to DNA and regulate genes involved in the differentiation of both the

embryo and the hematopoietic stem cell; they are also important in the self-renewal and proliferation of hematopoietic stem cells [15].

The t(12;21) translocation creates a fusion gene that includes the 5' portion of *TEL*, a member of the *ETS* family of transcription factor genes, and almost the entire coding region of another transcription factor gene, *AML1*, which encodes the α subunit of core binding factor, a master regulator of the formation of definitive hematopoietic stem cells. The chimeric TEL-AML1 transcription factor retains an essential protein–protein interaction domain of TEL and the DNA-binding and transcriptional regulatory sequences of AML1 (also called CBF α).

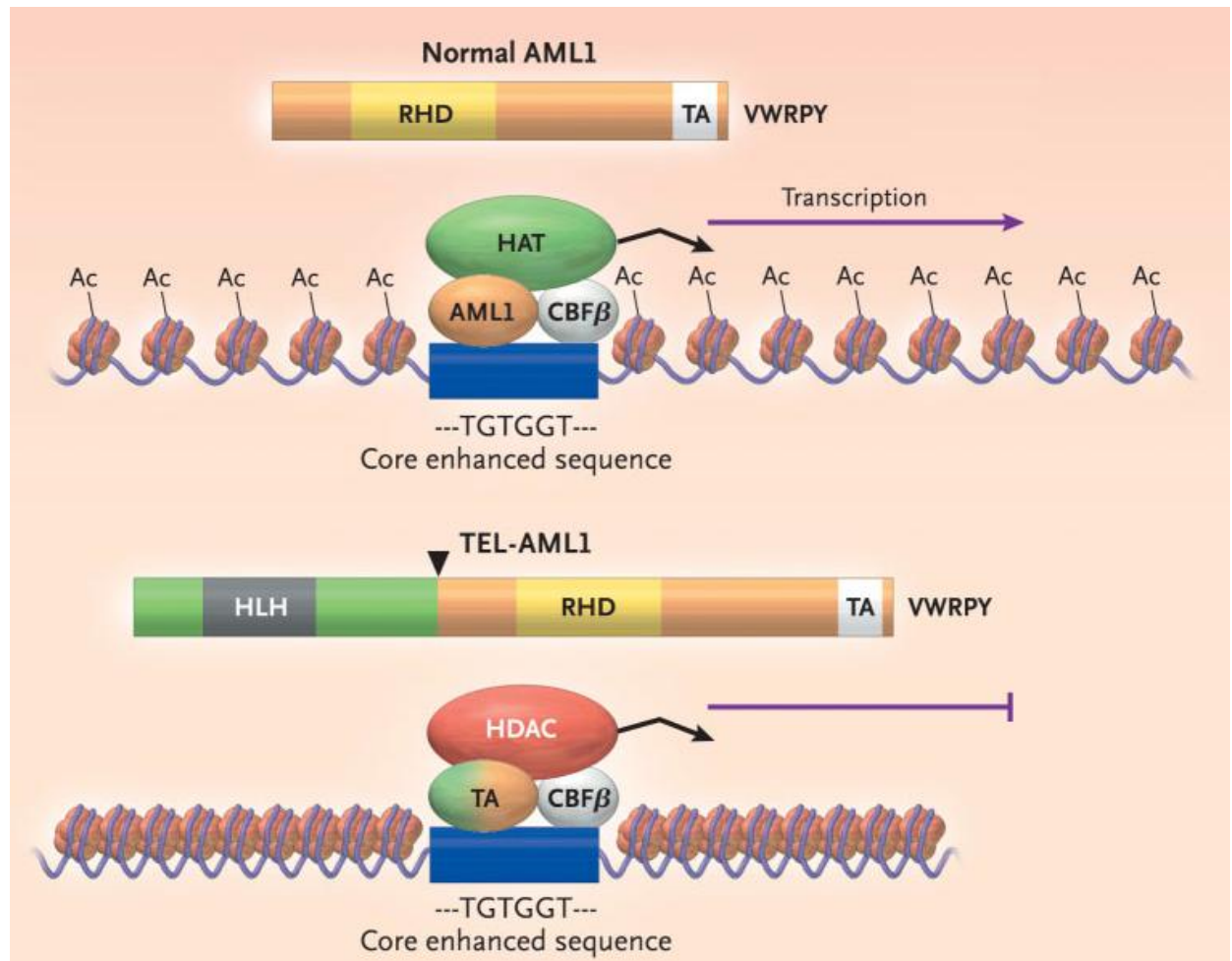
Figure 1.9: A common pathway targeted by translocation-generated chimeric transcription factors, such as MLL fusion proteins, TEL-AML1, and E2A-PBX1, is the HOX gene-mediated transcriptional cascade [15]



TEL is required for the homing of hematopoietic progenitor cells to the bone marrow, whereas AML1 is the DNA-binding component of the heterodimeric transcription factor (CBF α plus CBF β) called core-binding factor, which has a central role in hematopoiesis. The *HOX* genes probably operate downstream of the transcriptional cascade initiated by core-binding factor. A prominent effect of the TEL-AML1 fusion protein is inhibition of the transcriptional activity that is normally initiated when AML1 binds to a DNA region termed the core enhanced sequence. The binding of AML1 to the core enhanced sequence recruits other transcription

factors and co-activators to this region, and the resulting protein complex regulates transcription. This complex includes histone acetylases, which add acetyl groups to DNA-bound histones, thereby causing conformational changes in chromatin that enhance the transcription of target genes. Like AML1, the abnormal TEL-AML1 fusion protein can bind to the core enhanced sequence, but instead of activating transcription, it recruits histone deacetylase, which induce closure of the chromatin structure and, hence, inhibition of transcription (Figure 1.10). These changes in the normal AML1-mediated transcriptional cascade alter both the self-renewal capacity and the differentiation capacity of hematopoietic stem cells.

Figure 1.10: Mechanism of Transcriptional Repression by TEL-AML1 [15]



The conversion by chromosomal translocation of a transcription factor from an activator to a repressor of genes is a recurrent pathogenic mechanism not only in ALL, but also in acute

myeloid leukaemias that form fusion proteins containing AML1 or the retinoic acid α receptor. Recently developed small-molecule inhibitors of the histone deacetylase enzymes can reverse transcriptional repression by chimeric transcription factors, thereby abolishing their oncogenic activity. Indeed, histone deacetylase inhibitors have shown activity in preclinical studies and are now in clinical trials. These inhibitors appear to possess only limited activity when used alone, but in combination with other agents they could be beneficial.

A second component of the *HOX* regulatory pathway is the mixed-lineage leukaemia (MLL) protein, a nuclear protein that maintains the expression of particular members of the *HOX* family. Leukemia-associated translocations of *MLL* result in chimeric proteins consisting of the N-terminal portion of MLL fused to the C-terminal portion of 1 of more than 40 partners. This genetic alteration occurs in more than 80 percent of infants with ALL and in most therapy-induced leukaemias caused by topoisomerase II inhibitors. The MLL fusion proteins have a dominant gain-of-function effect that enhances their transcriptional activity. This alteration disrupts the normal pattern of expression of *HOX* genes, causing a change in the self-renewal and growth of hematopoietic stem cells and committed progenitors. In mice, overexpression of an MLL fusion protein in hematopoietic cells enhances the self-renewal of early hematopoietic progenitors and eventually leads to leukemia. These effects depend on the presence of *HOXA7* and *HOXA9*, suggesting that altered expression of these specific *HOX* family members is necessary for leukemogenesis.

Support for a critical role of altered *HOX* gene expression in leukemogenesis comes from other lines of investigation. In adult mice, forced expression of *HOXB4* induced the proliferation of hematopoietic stem cells, whereas enforced expression of *HOXA10* induced leukemia directly. In humans, increased expression of certain *HOX* genes and their DNA-binding cofactor MEIS1 is a consistent finding in leukemias with *MLL* rearrangements, in a subgroup of T-cell ALL, and in specific subtypes of acute myeloid leukemia. Another *HOX* DNA binding cofactor, PBX1, is targeted by the t(1;19) translocation, which occurs in

approximately 25 percent of cases of pre-B-cell ALL. This translocation forms a fusion gene that encodes a chimeric transcription factor, E2A-PBX1, which disrupts both the expression of *HOX* genes and the targets of the E2A transcription factor. All these findings make components of the HOX regulatory pathway attractive targets for the development of novel therapeutic agents. Identification of the specific molecules best suited to serve as drug targets is likely to be a high priority in the coming years [3].

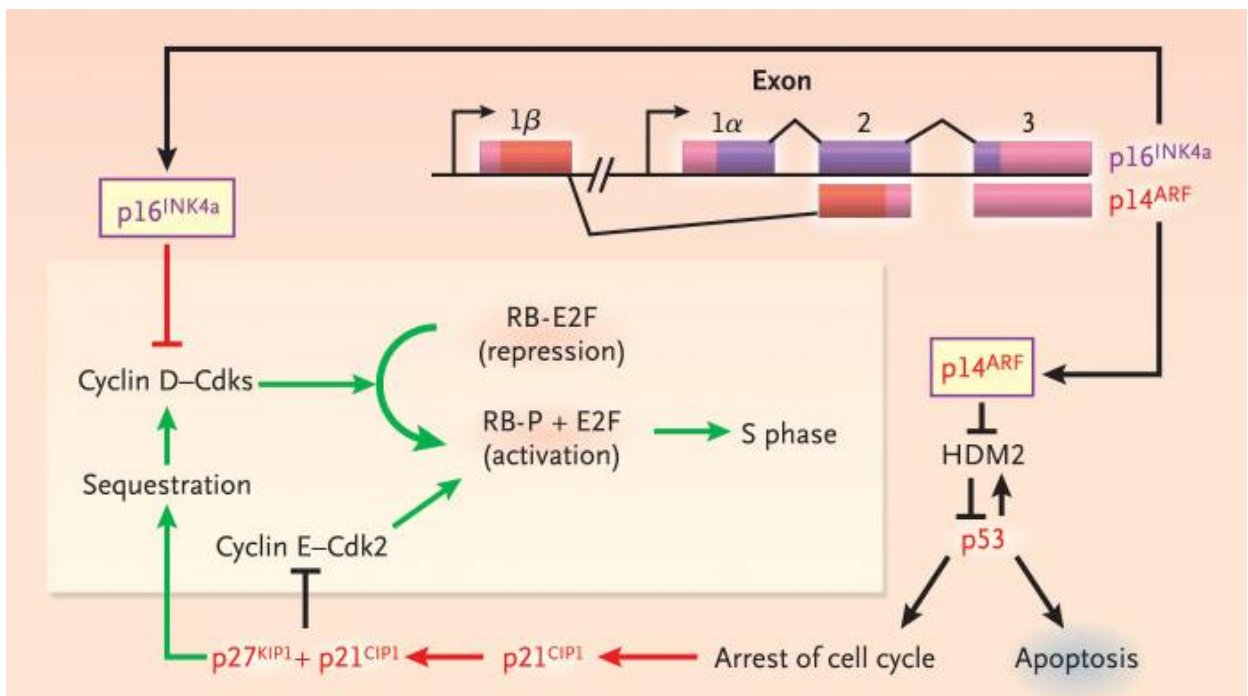
The oncogenic events triggered by chromosomal rearrangements are probably insufficient by themselves to cause leukemia. Instead, genetic alterations that impair differentiation, such as those described above, probably cooperate with a second class of mutations that alter the proliferation and survival of hematopoietic progenitors. Although this scheme is an oversimplification, it provides a framework for investigating other genes in the pathogenesis of B-ALL. We turn now to several genes involved in the second type of mutations.

Overexpression of FLT-3, a receptor tyrosine kinase important for the development of hematopoietic stem cells, occurs in cases of ALL with either *MLL* rearrangements or hyperdiploidy involving more than 50 chromosomes. Normally, the FLT-3 ligand triggers the tyrosine kinase activity of FLT-3, but in these subtypes of leukemia, the kinase is constitutively turned on by activating mutations, autocrine secretion of the FLT-3 ligand, or self-activation induced by the overexpression of FLT-3. Continuous signaling by the receptor contributes to the abnormal growth of leukemic cells, as demonstrated by the ability of small-molecule inhibitors of FLT-3 to block the in vitro growth of primary leukemic cells containing *MLL* rearrangements. These findings, and the remarkable success of a related tyrosine kinase inhibitor, imatinib mesylate, in the treatment of chronic myeloid leukemia, provide the impetus for clinical testing of inhibitors of the FLT-3 receptor kinase.

Another frequently altered regulatory network in ALL consists of the interrelated pathways controlled by the tumor suppressor retinoblastoma protein (RB), the related proteins

p130 and p107, and p53 (Figure 1.11). The principal role of RB is to control entry into the cell cycle. In its hypophosphorylated state, RB inhibits the ability of the E2F family of transcription factors to transcribe the genes necessary for entry into the S phase. Mitogenic signals induce the formation of active cyclin D–dependent kinase complexes that together with cyclin E–Cdk2 phosphorylate RB, thereby abrogating its ability to inhibit cell proliferation. The activity of cyclin D–dependent kinases is in turn inhibited by the INK4 proteins (p16^{INK4a}, p15^{INK4b}, p18^{INK4c}, and p19^{INK4d}), thereby preventing the phosphorylation of RB. Despite the rarity of inactivating mutations or deletions of *RB* in ALL, functional inactivation of the RB pathway through the deletion or epigenetic silencing of *P16*^{INK4a} and *P15*^{INK4b} occurs in nearly all cases of childhood T-cell ALL and in a small proportion of cases of B-cell–lineage ALL. Alterations of these inhibitors of cyclin D–dependent kinase occur to a lesser extent in adult T-cell ALL.

Figure 1.11: The Retinoblastoma (RB) and p53 Tumor-Suppressor Network [15]



Like *RB*, the *TP53* gene, which encodes the p53 transcription factor, is itself rarely altered in ALL; however, components of the p53 pathway are frequently mutated in ALL. As a tumor suppressor, p53 becomes activated in response to aberrant cellular proliferation, DNA damage, or hypoxia. The activated p53 triggers the arrest of the cell cycle or apoptosis, depending on the cellular context. The activity of p53 is harnessed by HDM2, a protein that

binds to p53 and induces its degradation; HDM2, in turn, is inhibited by the p14^{ARF} tumor suppressor. Deletion or transcriptional silencing of *P14^{ARF}* is a frequent event in ALL, whereas overexpression of *HDM2* or silencing of the p53 transcriptional target p21^{CIP1} occurs in approximately 50 percent of cases of ALL. *P16^{INK4a}* and *P14^{ARF}* are encoded by alternative reading frames in the same genetic locus. The high frequency of disabling homozygous deletions in *P16^{INK4a}* and *P14^{ARF}* thus suggests that alterations of the RB and p53 pathways collaborate in the pathogenesis of ALL. The central role of these pathways in both tumor suppression and the response of tumor cells to chemotherapy suggest that some components of these pathways are rational drug targets.

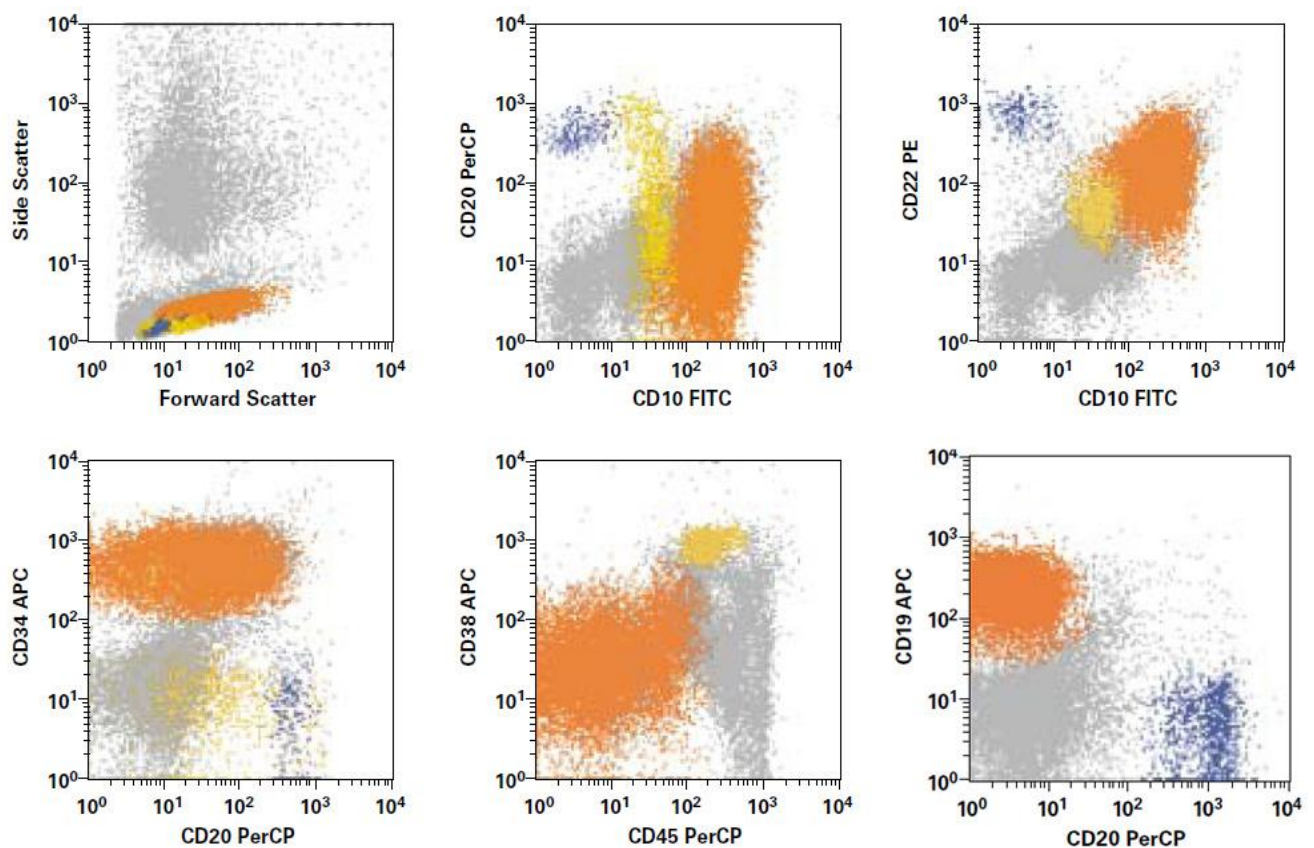
1.2.2 Immunophenotypic characterization of B-ALL

Multiparametric flow cytometry is a useful tool for characterizing hematolymphoid populations in B-ALL. The power of this method comes from the ability to analyze the expression of multiple antigens simultaneously on each analyzed cell. In current clinical practice, this typically entails the use of 3 or 4 fluorescently labelled antibodies to various surface or intracellular antigens within a single reaction mixture (3-color and 4-color flow cytometry, respectively). In addition, one typically also records 2 light scatter parameters for each event, so-called forward and side (or orthogonal) light scatter.

The term *hematogone* describes a population of lymphoid cells seen in sternal bone marrow aspirates. Although originally of unknown nature, they are now known to represent a population of normal maturing B-cell precursors, ie, the normal counterpart of precursor B-ALL cells [18]. Hematogones are detectable in approximately 80% of bone marrow aspirates from patients with a variety of clinical conditions. In addition, small numbers of these cells also are detectable in the peripheral blood of about two thirds of adult patients and most children. In our experience with a large number of unselected bone marrow samples, they constituted a mean of 1.6% and a median of 0.3% of total bone marrow events. On average, they decrease in number with age, but a wide variation in number is seen at any given age. Because they

resemble neoplastic lymphoblasts, the risk of confusing florid hematogone proliferations with ALL is very real. Finally, hematogones share some immunophenotypic features with B-ALL, such as expression of CD10 and low levels of CD20 and CD22. Fortunately, it has been demonstrated that multicolour flow cytometry with the appropriate antibody combinations can distinguish hematogones from B-ALL in essentially all cases. The foundation for this distinction is the observation that hematogones display a characteristic qualitative maturation pattern that is essentially invariant across patients. Two 4-color tubes that are useful to demonstrate this pattern are CD10/CD22/CD20/CD34 and CD10/CD19/CD20/CD38, as illustrated in Figure 1.12. The majority of hematogones have light scatter properties of small lymphocytes. However, when they are present in large numbers, a medium-sized subpopulation generally is evident.

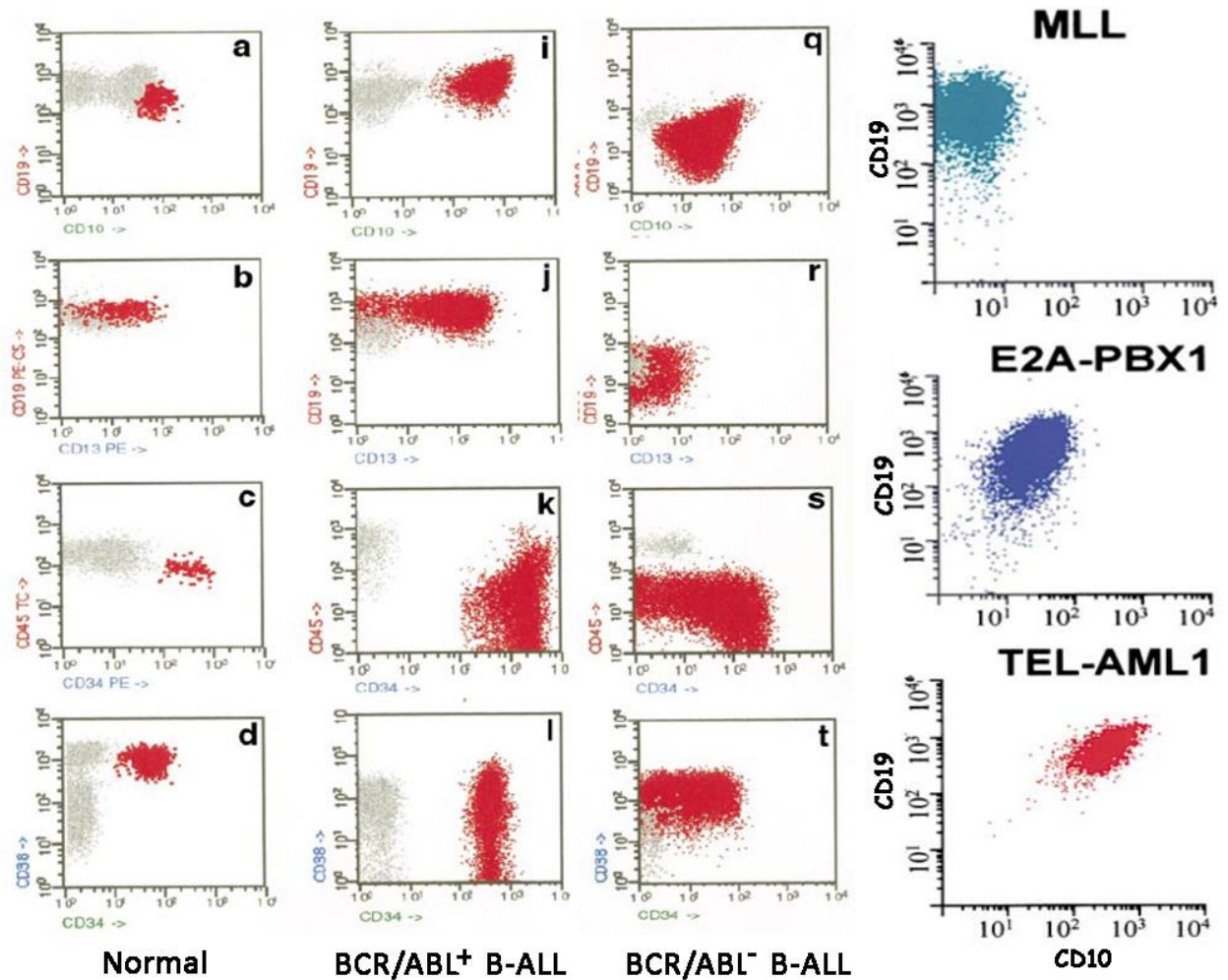
Figure 1.12: Bone marrow specimen containing precursor B-cell acute lymphoblastic leukemia (ALL) (orange) and hematogones (yellow) [18]



The least mature hematogones express CD34, bright CD38, relatively bright CD10, moderate levels of CD22, and slightly dim CD19 (compared with mature B cells). As they mature, they decrease their expression of CD10, stop expressing CD34, slightly up-regulate CD19, and begin gaining CD20. They continue to gain CD20 until this antigen is expressed at the same level as in mature B cells. At this time, they stop expressing CD10 and up-regulate CD22, at which time they are considered mature B cells. Among antigens normally expressed on hematogones, the vast majority of B-ALL cases express TdT on the entire neoplastic population, and most also express CD34 on the entire population or show a continuous spectrum of CD34 expression, distinct from the pattern seen in hematogones. These features are particularly helpful when distinguishing hematogones from neoplastic lymphoblasts.

An additional application of flow cytometry in the initial workup of acute leukemia is in guiding the evaluation for translocations (Figure 1.13). While generally evident on karyotypic analysis, at times this study is not available or is technically unsuccessful. In addition, these translocations also might be karyotypically occult, requiring molecular methods for their detection. Among B-ALLs, a CD10⁻/CD15⁺/CD19⁺/CD24^{-/+} immunophenotype is specific for ALL with 11q23 rearrangements involving the *MLL* (mixed lineage leukemia) gene. These *MLL*-rearranged cases also have been found to lack CD13 despite expression of other myeloid markers such as CD65, CD15, and CD33. Homogeneous expression of CD19, CD10, and CD9 and lack of or partial expression of CD20 is 100% sensitive with a positive predictive value of 50% for the *E2A/PBX1* (E2A/pre-B-cell leukemia transcription factor) rearrangement seen in ALL carrying the t(1;19)(q23;p13). B-ALLs carrying the t(12;21)(p13;q22) usually are CD10 bright⁺, and almost half are CD13⁺ and/or CD33⁺. Conversely, about two thirds of childhood ALLs expressing CD13 and/or CD33 contain the t(12;21),⁴⁶. These studies used a 20% cut-off for calling an antigen positive.

Figure 1.13: Correlation of genotype with immunophenotyping of B-ALL [19, 20]



1.2.3 Therapeutic strategies for the treatment of B-ALL

Although contemporary treatments cure more than 80% of children with acute lymphoblastic leukaemia (ALL), some patients require intensive treatment and many patients still develop serious acute and late complications owing to the side effects of the treatments. Furthermore, the survival rate for adults with ALL remains below 40%. Therefore, new treatment strategies are needed to improve not only the cure rate but also the quality of life of these patients. Here, we discuss emerging new treatments that might improve the clinical outcome of patients with ALL. These include new formulations of existing chemotherapeutic agents, new antimetabolites and nucleoside analogues, monoclonal antibodies against leukaemia-associated antigens, and molecular therapies that target genetic abnormalities of the leukemic cells and their affected signalling pathways [21].

Conventional chemotherapeutic agents interfere with different stages of DNA and protein synthesis. Thiopurines block *de novo* purine synthesis and the conversion of inosine monophosphate to adenosine and guanine. Also, they incorporate into DNA and RNA, triggering apoptosis. Methotrexate inhibits dihydrofolate reductase, leading to the depletion of the intracellular tetrahydrofolate coenzymes that are required for thymidylate and purine biosynthesis, and thereby block DNA synthesis. It also inhibits *de novo* purine synthesis by blocking other folate dependent enzymes, including thymidylate synthase. Cytarabine inhibits DNA polymerase and incorporates into DNA, where it terminates strand elongation. Anthracyclines complex with DNA and topoisomerase II, leading to double stranded DNA breaks. Epipodophyllotoxins induce double-stranded DNA breaks through their sequence specific binding to DNA that is in complex with topoisomerase II. Alkylating agents function by crosslinking with DNA and thereby inducing the fragmentation of DNA strands. Asparaginase deprives leukemic cells of asparagine, which is required for protein synthesis. Vinca alkaloids inhibit mitosis by binding to tubulin (Figure 1.14)

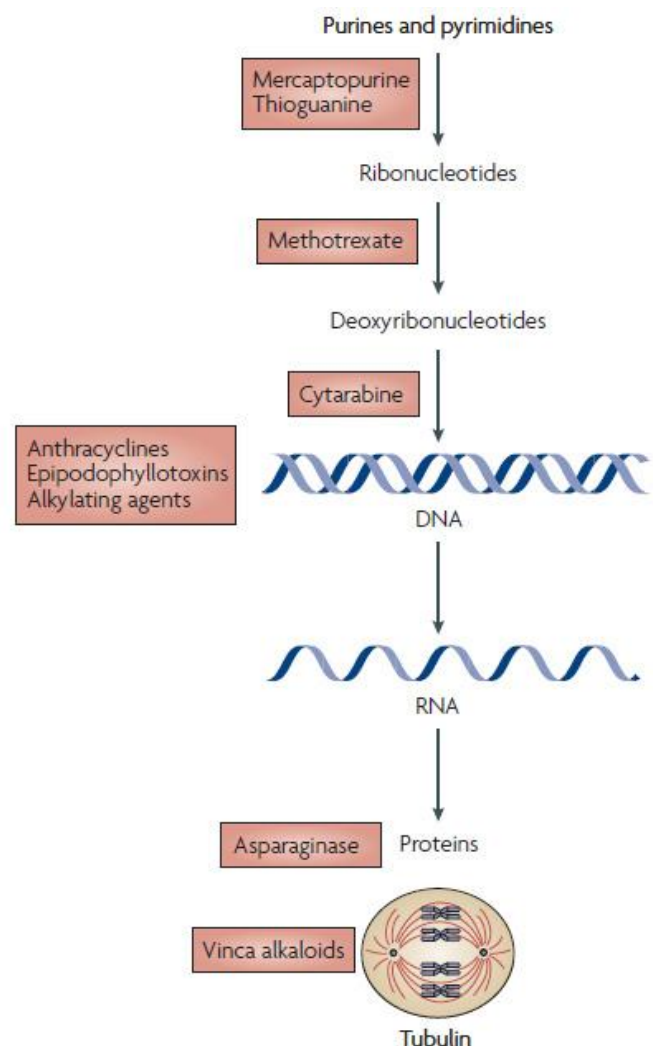


Figure 1.14: Cell-cycle phases targeted by agents that are conventionally used in B-ALL [21]

Lineage-associated antigens expressed by leukemic cells are increasingly becoming targets for treatment with mAbs that are administered in the unconjugated form or conjugated to anti-leukemic drugs, immunotoxins or radioactive molecules. The development of antigen-specific cytotoxic T lymphocytes has expanded the role of lineage associated antigens to targeted cellular immunotherapy. Monoclonal antibodies have been successfully used alone and in combinations as enlisted in Table 1.1. Target antigens are often not expressed exclusively by leukemic blasts but can also be expressed by normal haematopoietic cells, reducing the cytotoxic selectivity of mAbs. Strategies to analyse the molecular genetic and epigenetic aberrations in cancer cells are rapidly maturing. As these approaches, commonly referred to as genomics, transcriptional profiling and proteomics, yield ever greater insights into ALL pathogenesis, one can expect an expanding repertoire of targeted therapies for clinical evaluation. Ultimately, these emerging technologies should lead to a new era of individualized molecular medicine, which results in more effective and less toxic regimens.

The list of targeted molecular treatments for ALL remains modest (Table 1.1), although collectively the treatments demonstrate the feasibility of directing drugs to signalling pathways that control cell-cycle progression, gene transcription, cell motility, apoptosis and cell metabolism (Figure 1.15).

Figure 1.15: Molecular target sites for potential new therapeutic agents [21]

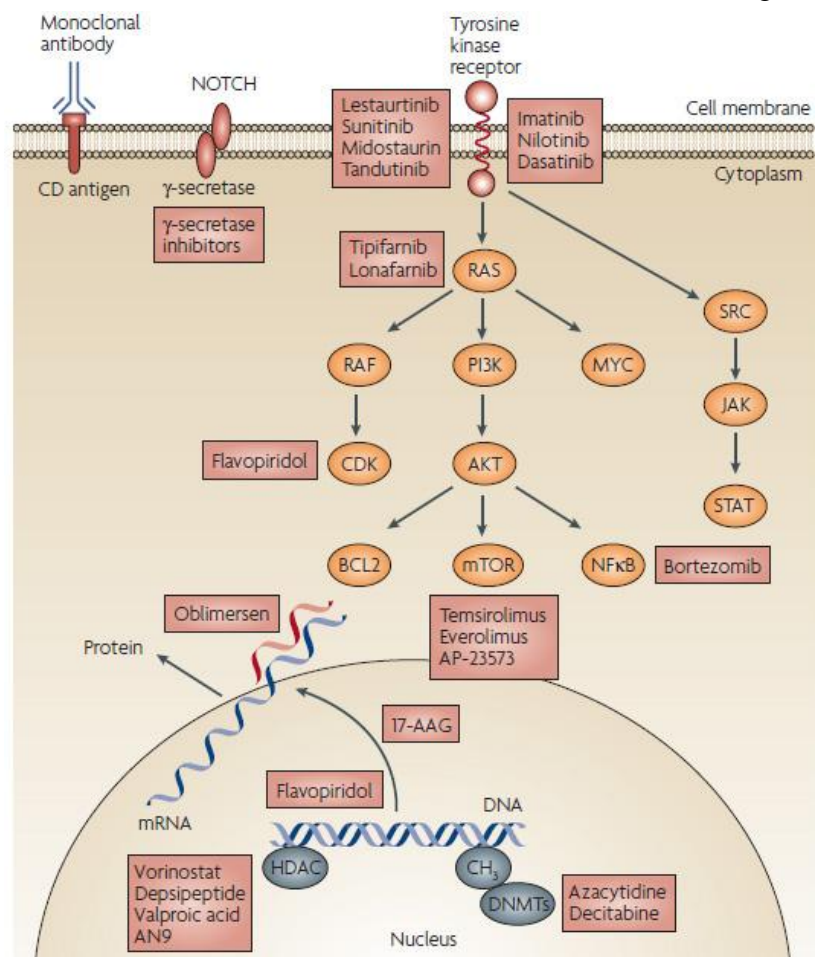


Table 1.1: Other potential therapeutic targets for ALL treatment [21]

Drug	Target	Type of ALL	Potential combinations
Rituximab (Rituxan, Mabthera; Biogen Idec)	CD20	CD20 ⁺ ALL/NHL	Chemotherapy; conjugated to radioactive molecules
Epratuzumab	CD22	CD22 ⁺ ALL	Chemotherapy; conjugated to radioactive molecules
Anti-CD19	CD19	CD19 ⁺ ALL	Chemotherapy; conjugated to immunotoxins
Alemtuzumab (Campath, MabCampath; Genzyme Corp)	CD52	CD52 ⁺ ALL	Chemotherapy
Gemtuzumab ozogamycin (Mylotarg; Wyeth)	CD33	CD33 ⁺ ALL	Chemotherapy
Imatinib mesylate (Gleevec; Novartis)	ABL, KIT, PDGFR	BCR-ABL ⁺ ALL; NUP214-ABL1 ⁺ T-cell ALL	Chemotherapy; transplantation
Nilotinib	ABL, KIT, PDGFR	Imatinib-resistant BCR-ABL ⁺ ALL (except T315l)	Chemotherapy
Dasatinib (Sprycel; Bristol-Myers Squibb)	SRC/ABL	Imatinib- and nilotinib-resistant BCR-ABL ⁺ ALL (except T315l)	Chemotherapy; imatinib
MK-0457	Aurora kinase	Imatinib-, nilotinib- and dasatinib resistant BCR-ABL ⁺ ALL (including T315l)	Chemotherapy
Lestaurtinib Midostaurin Tandutinib Sunitinib malate (Sutent; Pfizer) IMC-EB10	FLT3	MLL ⁺ ALL; CD117/KIT ⁺ T-cell ALL; hyperdiploid ALL; FLT3 ⁺ ALL	Chemotherapy
Tipifarnib Lonafarnib	Farnesyl transferase	BCR-ABL ⁺ ALL	Imatinib
Azacytidine (Vidaza; Pfizer) Decitabine (Dacogen; SuperGen) Temozolomide (Temodal, Temodar; Schering-Plough)	DNA methyltransferase	MLL ⁺ ALL	Vorinostat; depsipeptide; valproic acid
Romidepsin Valproic acid Vorinostat (Zolinza; Merck) MD-27-275 AN-9	Histone deacetylase	ALL; T-cell ALL; MLL ⁺ ALL BCR-ABL ⁺ ALL	Imatinib; TRAIL; anthracyclines; favopiridol
Sirolimus (Cypher, Rapamune; Wyeth) Temsirolimus Everolimus (Certican, Promus; Novartis) AP-23573	mTOR	ALL; BCR-ABL ⁺ ALL	Doxorubicin; imatinib
γ-secretase inhibitors	NOTCH1	T-cell ALL	Chemotherapy
Bortezomib (Velcade; Millenium Pharmaceuticals)	NFκB	ALL; BCR-ABL ⁺ ALL	Dexamethasone; cytarabine; doxorubicin; asparaginase; vincristine; HDACIs
Flavopiridol	CDK	ALL; BCR-ABL ⁺ ALL	HDACIs; TRAIL; cytarabine; imatinib
Oblimersen	BCL2	BCR-ABL ⁺ ALL	Chemotherapy; radiotherapy; imatinib
17-AAG	HSP90	BCR-ABL ⁺ ALL; ZAP-70 ⁺ ALL	HDACIs; imatinib; FLT3 inhibitors; arsenic trioxide; chemotherapy

ABL, v-abl Abelson murine leukemia viral oncogene homolog-1; BCL2, B-cell CLL/lymphoma-2; CDK, cyclin-dependent kinase; FLT3, fms-related tyrosine kinase-3; HDACIs, histone deacetylase inhibitors; HSP90, heat shock protein-90; KIT, v-kit Hardy-Zuckerman-4 feline sarcoma viral oncogene homolog; MLL, mixed lineage leukaemia; mTOR, mammalian target of rapamycin; NFκB, nuclear factor κB; NHL, non-Hodgkin's lymphoma; NOTCH1, Notch homolog-1, translocation-associated (*Drosophila*); PDGFR, platelet-derived growth-factor receptor; SRC, v-src sarcoma (Schmidt-Ruppin A-2) viral oncogene homolog (avian); TRAIL, tumour necrosis factor-related apoptosis-inducing ligand.

With the exception of imatinib mesylate and the second-generation ABL kinase inhibitors, which target a primary genetic abnormality (the BCR-ABL tyrosine kinase), the targeted therapies now in development for ALL are almost all directed to secondary cooperative

mutations or pathways regulating growth or apoptosis. The failure of tyrosine kinase inhibitors to have a curative effect makes it unlikely that any of the current forms of molecularly targeted therapies will be curative by themselves.

Even so, recent success in defining the cellular biochemical responses to DNA-damaging agents and drug-resistance pathways might allow a more rational combination of conventional anti-leukemic drugs, mAbs and molecularly targeted drugs in ways that disrupt the DNA-repair response or restore the apoptotic response, leading to maximum leukemic cell kill. The initial excitement generated by the responsiveness of CML to imatinib mesylate led to the expectation that other targeted therapeutics would be equally successful. Subsequent results indicated that although molecularly targeted agents might possess anti-leukemic activity, the responses they induce are seldom durable and certainly do not extend to all patients. This sobering fact emphasizes the need to link targeted therapeutics to effective molecular diagnostic methods that will determine whether the signalling pathway that drives a particular case of ALL is targeted by the drug or the drugs under consideration for that leukaemia. In the meantime, it is important to broaden the potential of targeted therapeutics by carefully analysing the pharmacogenetics of leukemic and normal host cells, therefore enabling the selection of optimal drugs and dosages to avoid over- or under-treatment of individual patients.

1.3 Proteomics based on Two-Dimensional Gel Electrophoresis (2DGE), Differential In-Gel Electrophoresis (DIGE) and Mass Spectrometry

Proteomics is global profiling of proteins, as in healthy vs. pathological states to discover specific marked expression changes for early diagnosis, disease progression, treatment response and early detection for novel therapeutic targets. This comparative strategy has come up over the last decade. The idea of making an inventory of the total proteins in a specific tissue or cell in normal and abnormal physiology had been initiated in the mid-1990's with the initiation of

the proteome project [22]. Since then many technological advancements have made possible the progress of this specialized field to where it stands today.

1.3.1. Gel Based Proteomics

The perfect technical marriage that made the proteome project feasible was between high resolution two-dimensional gel electrophoresis to separate large number of proteins and mass spectrometry to identify and characterize the proteins displayed by the 2D gels. However, before this could be made possible, the protein studies have evolved manifold until these two unrelated fields combined together [23]. It started in 1959 when protein electrophoresis on a gel platform formed by cross linking of acrylamide and N, N1-methylene-bis-acrylamide was demonstrated by Raymond and Weintraub [24] and was termed polyacrylamide gel electrophoresis (PAGE).

The adaptation of polyacrylamide gel to make a stable pH gradient by which a protein mixture could be separated along their isoelectric points (called isoelectric focusing or IEF) were first introduced by Svensson in 1962 and was available by the end of the 1960's and early 1970's in combination with PAGE. In 1975, a breakthrough was achieved by combining the IEF in denaturing conditions with denaturing SDS-PAGE to complete the modern 2D PAGE by three independent groups; the most powerful one was by O'Farrell where he showed over a thousand protein spots by his method in 2D gels of *E.Coli* extract. O'Farrell's method has become the method of choice for the next 20 years where many systems were investigated using his method.

The introduction of computer generated gel analysis software from the late 1970's [25] have made the analysis and comparison of 2D gel images simpler resulting in improved quantitative analysis of the complex and minor changes in the expression level detectable in the 2D gels.

However, the identification of proteins from the 2D gels spots has been a challenge to the initial workers as one and only available method those days was the Edman sequencing of

proteins [26] which would have required much higher quantity of proteins that could be separated by the 2D gels. That problem hindered the advancements of this field for another decade when the emerging DNA based technologies like recombinant DNA technology using PCR and DNA sequencing took centre stage.

The surge in proteomics was again emerged from the early nineties with the introduction of simpler IPG (Isoelectric pH Gradient) strips supported by plastic backing instead of cumbersome tube gels with conventional carrier ampholytes [27] and followed up with much improvement by Angelica Görg [28]. The introduction of IPG resulted in superior resolution, high reproducibility and much higher loading applications.

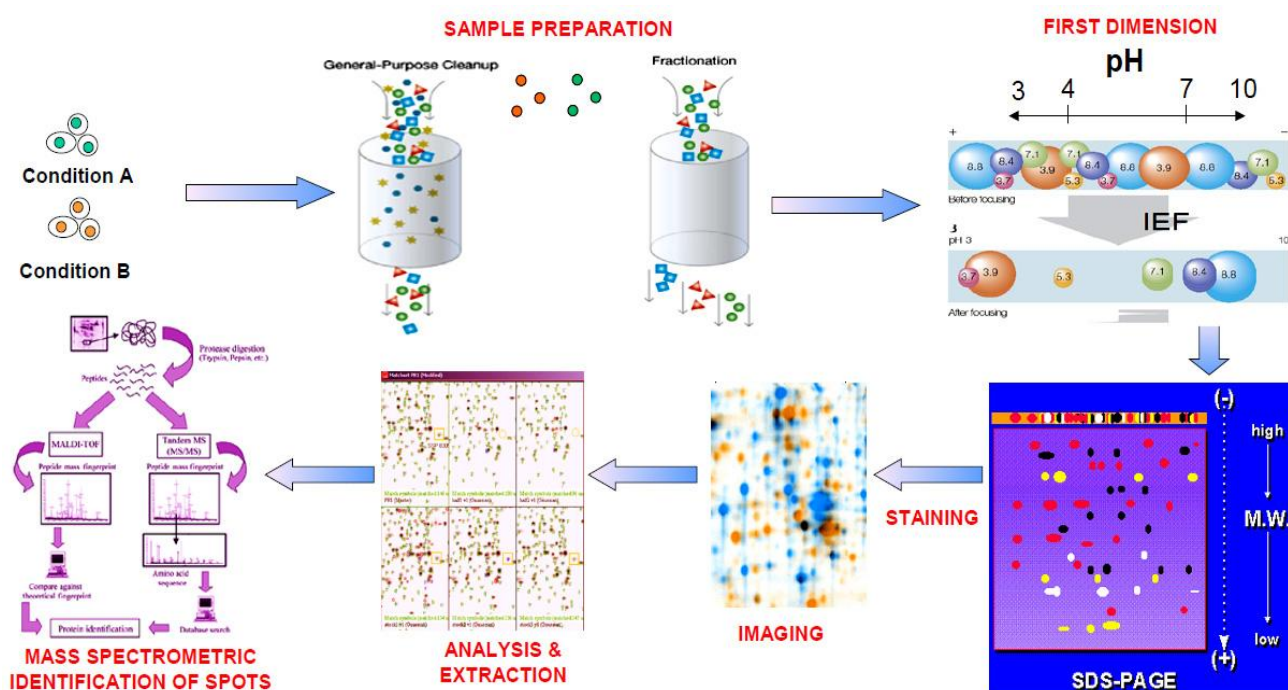
The biggest boost to 2DGE came when information about each protein spot became available by the means of digesting the protein spot bound to the gel using specific endoproteases like trypsin to generate peptide fingerprints known as ‘In-gel tryptic digestion’ followed by the identification of the digested peptides using mass spectrometry. The peptide analysis using ‘soft ionization techniques’ were first applied in MALDI (Matrix assisted Laser Desorption Ionization) developed by Karas and Hilcamp [29] and ESI-MS (Electro Spray Ionization Mass Spectrometry) developed by Fenn and co workers [30]. The mass spectrometric peptide map which is better known as ‘Peptide Mass Fingerprint’ (PMF) could be identified by comparing with a theoretical peptide map in a database. The door to building up several extensively annotated 2D gel databases came up using the concept of database searching using PMF and MS/MS spectra (short partial sequence tag obtained from an individual peptide in a PMF) associated with newer developments in the technical, computational and instrumentation has now rendered proteomics an essential tool for today’s investigative biology.

The 2D gel technique has now been widely used, thanks to its capacity to present a global view of the sample by resolving hundreds and in some cases thousands of proteins simultaneously on a single gel. The advancements like commercial availability of IPG strips of

various broad and low range pH ranges, the latest gel running modules where up to 12 gels can be run at a time and development of newer mass spectrometry compatible high sensitive stains like SYPRO RUBY, SYPRO ORANGE, FLAMINGO and Blue Silver have made detection of sub nanogram levels of protein possible not to mention silver staining which, possibly has the highest sensitivity but not very mass spectroscopy compatible.

In 2DGE, the proteins are separated in the first dimension during IEF according to their isoelectric point and in the second dimension during SDS-PAGE by their molecular mass. However, as shown in Figure 1.16, the process involves six steps (i) sample preparation, (ii) first dimension (IEF), (iii) second dimension (SDS-PAGE), (iv) 2DGE protein pattern visualization, (v) 2DGE pattern analysis and (vi) selection and digestion of protein spots for MS identification [31].

Fig 1.16: The 2DGE workflow



1.3.1.1 Sample Preparation: The sample preparation involves cell rupture, removal of interfering substances like nucleic acids, sugars, charged lipids and excess salts and the solubilization of most of the proteins using combinations of chaotropic agents like urea and

thiourea, non-ionic or zwitterionic detergents like CHAPS and sulphobetaine derivatives like SB 3-10 or ASB 14; non-charged reducing agents like DTT or TBP and finally carrier ampholytes of suitable pH range for efficient IEF of proteins. For complex samples, often pre fractionation becomes necessary.

1.3.1.2 Isoelectric focusing using IPG: There have been commercially available IPG strips of different lengths from 7-24 cms and varying pH ranges ranging from pH 3 to pH 11 including ultra narrow range (≤ 1 pH unit) and overlapping pH ranges. In some of these strips, >1 mg of protein could be loaded. The IEF cells have also been devised where stepwise voltage gradients could be applied. For a typical 18 cm long IPG strip, a final voltage of 10000V is often required. Before the second dimension it is essential to equilibrate the IPG strips so that the proteins interact fully with SDS. Glycerol and urea are added in equilibrium buffer for efficient liberation of proteins from strip to gel. It is often done in 2 steps where in the first step a reducing agent like DTT is added for disulfide bond reduction and in the second step, the free sulphhydryl ends are deactivated by iodoacetamide. Iodoacetamide also alkylates any free DTT left; otherwise the free DTT migrates with the protein in SDS-PAGE resulting protein streaking (Figure 1.17).

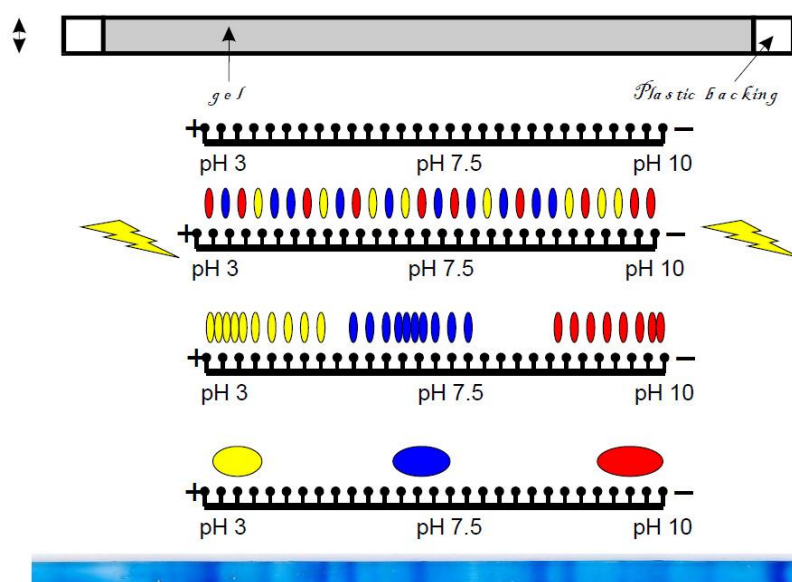


Figure 1.17 Isoelectric focusing on an IPG strip

1.3.1.3 SDS-PAGE: The second dimension is usually run according to the Laemmli's buffer system and is stained in different ways. The staining is important as in most cell or tissue

system the protein concentrations vary by 5-6 orders of magnitude and for body fluids like serum or erythrocytes this goes up to 10 orders of magnitude. As a result, the optimized staining system should have high detection sensitivity (low detection limit), high linear dynamic range (for quantitative accuracy), reproducibility and compatibility with downstream protein identification methodology like MS. Unfortunately, no current staining protocol matches all the qualifications.

1.3.1.4 Protein Detection Methods: Universal detection methods of proteins on 2D gels include staining with anionic dyes (*e.g.* Coomassie Blue), negative staining with metal cations (*e.g.* zinc imidazole), Silver-staining, fluorescence staining or labeling, and radioactive isotopes, using autoradiography, fluorography, or Phosphor-imaging. For most of these staining procedures, the resolved polypeptides have to be fixed in solutions such as in ethanol/acetic acid/ H₂O for at least several hours (but usually overnight) before staining to remove any compounds (*e.g.* detergents) that might interfere with detection. Specific staining methods for detection of PTM (glycosylation, phosphorylation *etc.*) are employed either directly in the 2D gel or, more frequently, after transfer (blotting) onto an immobilizing membrane. The blotted proteins can be probed with specific antibodies (*e.g.* against phosphotyrosine residues) or with lectins (against carbohydrate moieties). The initial method of choice was coomassie brilliant blue (CBB) which was easy to use, cheap, mass compatible but lacked sensitivity below 500-600 ng. CBB in colloidal dispersions and further modifications using phosphoric acid [32] have increased the sensitivity.

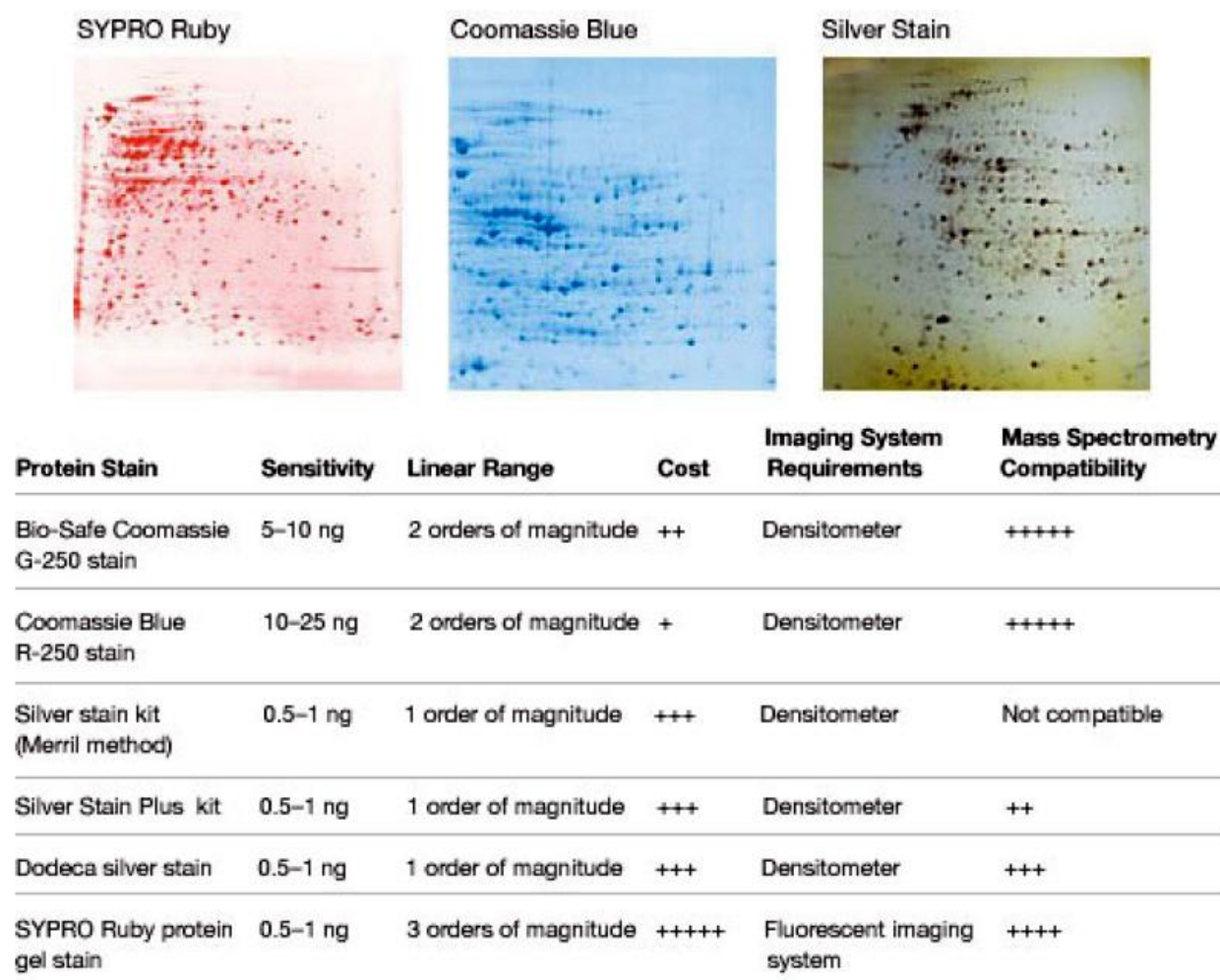
Reverse staining exploits the fact that protein-bound metal cations (*e.g.* potassium, copper or zinc) are usually less reactive than the free salt in the gel. Thus, the speed of precipitation of free or only weakly bound ions to form an insoluble salt is slower on the sites occupied by proteins than in the protein-free background. This generates transparent protein zones or spots, while the gel background becomes opaque due to the precipitated, insoluble salt. Compared to the other reverse staining methods, but also CBB, the zinc stain offers some

distinct advantages as it can be completed in 15 min for most applications, and is more sensitive than CBB, KCl or copper stains. Hence, zinc or imidazole-zinc stains [33, 34] currently the most sensitive reverse (or negative) staining methods applied in 2DGE. Zinc-imidazole staining is rapid, simple, and sensitive, and has a detection limit of roughly 20–50 ng of protein *per* spot. Moreover, it is compatible with subsequent protein identification by MS, making the stain quite popular for detection of proteins separated on micro preparative 2D gels. The major disadvantage of zinc-staining is its rather restricted linear dynamic range, which makes this staining procedure unsuitable for detecting quantitative differences on 2D gels. Silver staining [35] more sensitive (<1 ng) than CBB and zinc stain but the major handicap with silver staining is that it is not stoichiometric and as a result lacks the reproducibility of CBB. Also the aldehyde based sensitizers result in protein cross-linking resulting poor availability for subsequent MS based analysis. Some non-aldehyde based methods have now been developed [36] but with compromise in sensitivity.

Better and more sensitive results are now obtained with the help of fluorescent based dyes. Two major approaches have currently been practiced. These are: (i) covalent derivatization of proteins with fluorophores prior to IEF, and (ii) post-electrophoretic protein staining by intercalation of fluorophores into the SDS micelles coating the proteins, or by direct electrostatic interaction with the proteins [37]. The best known examples for pre-electrophoretic fluorescent labels are monobromobimane [38] and the cyanine-based dyes [39] that react with cysteinyl residues and lysyl residues, respectively. The latter dyes are commercially available as CyDyes (Amersham Biosciences/ GE Healthcare), and their properties will be discussed in more detail in section on DIGE. The major problem of pre-electrophoretic labeling is the occurrence of protein size and/or protein charge modifications which may result in altered protein mobilities alongside the M_r and/or pI axis. Alternatively, proteins can be stained with a fluorescent dye molecule after the electrophoretic separation has been completed. The most prominent example is the ruthenium-based dye SYPRO Ruby [40].

Staining is accomplished within a few hours in a single step procedure which may be easily adapted for use with automated instrumentation. The detection limit is approximately 1–2 ng protein/spot, and the linear dynamic range of quantitation is about three orders of magnitude.

Figure 1.18: Comparison of staining techniques



1.3.1.5 Image Acquisition and Analysis: One of the key objectives of proteomics is to identify the differential expression between control and experimental samples run on a series of 2D gels. That is, the protein spots that have been inhibited (disappeared), induced (appeared) or have changed abundance (increased or decreased in size and intensity). Once these gel features have been found, the proteins of interest can be identified using MS. This goal is usually accomplished with the help of computerized image analysis systems [41]. The first step in computerized image analysis of 2DGE protein patterns is capture of the gel images in a digital

format. A range of devices, including modified document scanners, laser densitometers, CCD cameras, and fluorescent and phosphor imagers are available for the acquisition of 2D gel images. The saved images are then subjected to computer assisted image analysis. The traditional workflow for a 2DGE software package is (i) preprocessing of the gel images, *i.e.* image normalization, cropping and background subtraction; (ii) spot segmentation, detection and expression quantification; this includes creation of Gaussian images to segregate between overlapped spots and a spot and a false positive. (iii) landmarking, *i.e.* an initial user guided pairing of a few spots between the reference and sample gels. The sample gel is then warped to align the landmarks; (iv) matching, *i.e.* automatic pairing of the rest of the spots; (v) identification of differentially expressed spots; (vi) data presentation and interpretation; and (vii) creation of 2D gel databases [41, 42]. Currently, several 2DGE image analysis software packages are commercially available. These programs have been continuously improved and enhanced over the years in terms of faster matching algorithms with lesser manual intervention, and with focus on automation and better integration of data from various sources. New 2DGE software packages have also emerged which offer completely new approaches to image analysis and novel algorithms for more reliable spot detection, quantitation and matching. Several programs include options such as control of a spot cutting robot, automated import of protein identification results from MS, superior annotation flexibility (*e.g.* protein identity, mass spectrum, intensity/quantity, links to the Internet), and/or multichannel image merging of different images to independent color channels for fast image comparison. However, despite these improvements, we are still a long way from totally automatic image analysis systems that do not require user intervention [43].

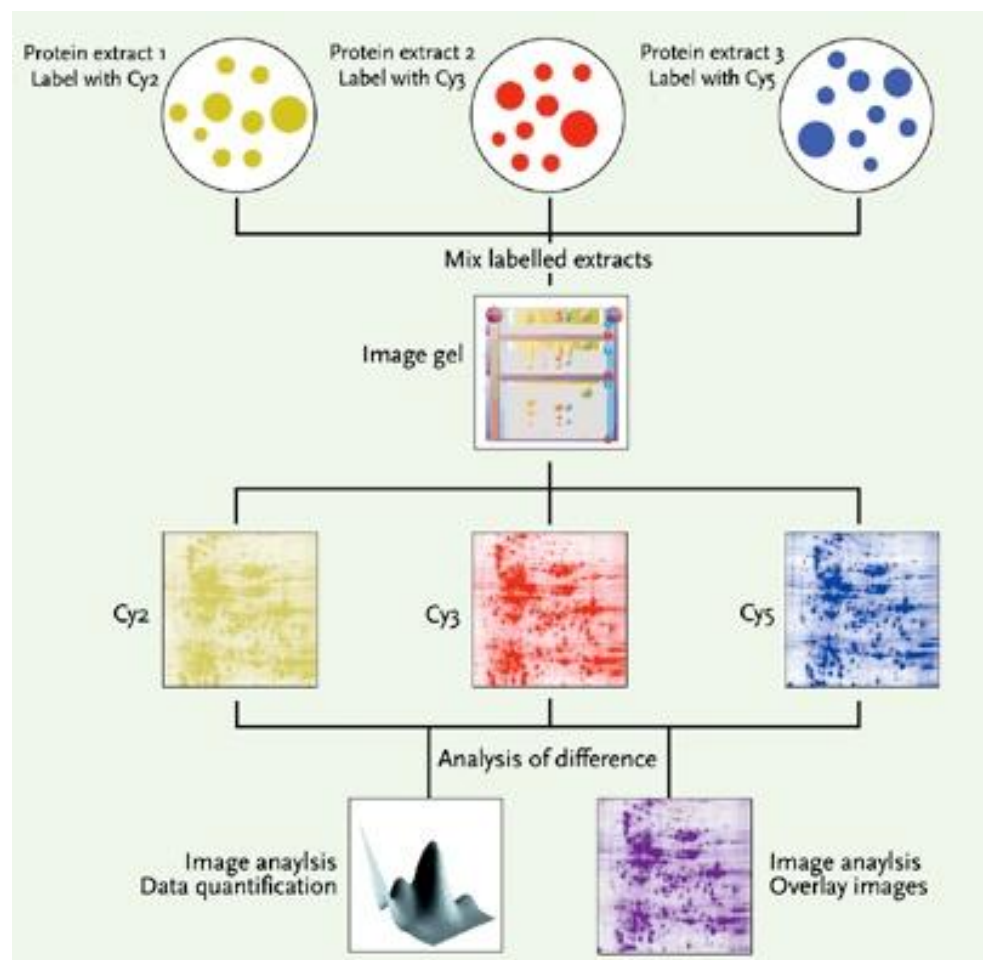
1.3.2 Differential In-Gel Electrophoresis (DIGE)

To account for the perennial problem of gel to gel variations of 2DGE, different 2D gels of the same sample often does not remain perfectly super imposable creating errors in gel analysis. DIGE, introduced by Unlu *et al.* 1997 [39] and further modified over the years [44] is a

modification of 2DGE in which controls and disease samples are labeled pre-electrophoresis using different fluorescent CyDyes. After labeling, equal amounts of disease and control samples are mixed and analyzed on a single 2D gel. The respective 2DGE patterns on the gel are visualized and discriminated from each other by their own unique excitation and emission wavelength signals, detected using a fluorescence imaging scanner. Comigrating samples on the same gel enable a perfect match of pairs of spots and thus the accurate analysis of differences in protein abundance between samples (Figure 1.19).

Two DIGE procedures are commercially available, known as minimal and saturation labeling. In the minimal labeling procedure, all three CyDyes are used; the individual disease or control sample is usually labeled with Cy3 or Cy5, while Cy2 is used to label an internal standard consisting of a pooled mixture of all samples (*i.e.* disease samples plus controls) in the experiment.

Figure 1.19: The DIGE technology



In the saturation-labeling procedure, two different CyDye-labeled samples, typically a sample and the internal standard are co-run on the same gel. Although the number of gels is higher using saturation labeling, the amount of protein needed is ten times lower, giving the advantage that more proteins are detectable than with the minimal-labeling procedure. Whatever labeling procedure is used, the analysis of one or two different samples on a single gel together with an internal standard, which is used in all gels within a series of experiments, reduces experimental variation and the need of gel replicates [45].

DIGE is a sensitive technique, capable of detecting as little as 0.5 fmol of protein and this detection system is linear over a 400000-fold concentration range. Data reproducibility and normalization among gels, as well as confidence in matching and quantifying different samples are also dramatically improved [46]. Although the CyDyes are very expensive, the advantages of DIGE over standard 2DGE has made their increasing use as recommended method for disease biomarker discovery in proteomics [31].

1.3.3 Spot Picking and In-Gel Digestion for Mass Spectrometry

The next step involves picking of spots of interest and preparing them for mass spectrometric identification. The spot picking is usually done by robotic devices controlled by the same image acquisition and analysis software platform. The picked up spots are then destained, dried and digested using an endopeptidase. The universal choice for digestion enzyme has been trypsin, since it is highly specific (digests exclusively at the C-terminus of Lysine/Arginine residues), can be obtained in highly pure form, is commercially available, and requires a low enzyme-substrate ratio (1:20-1:200). Also trypsin is active at slightly alkaline pH (~pH 8.0-9.0) which is easily achieved by using 25 mM ammonium bicarbonate. The digestion is usually done overnight at 37°C and the resultant peptides are eluted with an acetonitrile/water mixture with pH<3.0 which is achieved by using a volatile organic acid like formic acid or trichloroacetic acid (TCA). Although the main advantage of 2DGE technology is its capacity to provide a global view of a sample proteome at a given time by resolving hundreds to thousands

of proteins simultaneously on a single gel, there have been some limitations to this method as well. The limitations are associated with the inability of 2DGE to resolve all proteins present in a sample because of: (i) extreme differences in their solubility (highly hydrophobic proteins), (ii) a wide range in their expression levels (low abundance proteins), (iii) the presence of extremely basic or acidic pI values that exceed the gel IPG range capacity or (iv) upper or lower molecular size gel limits which limits visualization of proteins with MW > 250 kDa and <10 kDa extremely difficult. In addition, the 2D gel is a laborious procedure and gel to gel variations are difficult to overcome.

1.3.4 Biological Mass Spectrometry

The success of proteomics was possible due to the emergence of protein identification by the help of mass spectrometry which increased the through-put and sensitivity of detection by a giant leap. Mass spectrometry or MS deals with the study of systems by the formation of gaseous ions, with or without fragmentation, which are then characterized by their mass-to-charge ratios and relative abundances. The primary function of a mass spectrometer is to separate charge bearing molecules according to molecular mass and to measure their mass numbers. The species studied must be ions rather than molecules because mass separation relies on the properties of charged particles moving under the influence of electric and magnetic fields, usually in high vacuum where the mean free path is sufficient to ensure that they mostly travel without collisions. Ions may be positively or negatively charged, although most mass spectrometric experiments are performed on positive ions. Positive ions can be formed either by removal of one or more electrons from each molecule or by the addition of one or more cations. A charged species that is formed by the removal or attachment of an electron is referred to as a molecular ion, whereas ionization that is achieved by addition or removal of a charged atom or molecule such as H⁺ or NH₄⁺ gives a species that is termed a quasi-molecular ion. However, in common usage, they, too, tend to be referred to as molecular ions. Ions are separated either spatially, as by a magnetic field, or temporally, as in TOF. A mass

spectrometer therefore has three essential components, the ion source, the mass analyzer and an ion detector.

Mass spectrometric analysis of organic molecules were there since 30 years but the ionization technique used that time was called ‘Electron Impact’ (EI) ionization where analytes in vapor phase was bombarded with fast moving electrons resulting in an electron stripping from the analyte to produce mainly unipositive radical cations. However, this method was handicapped by low efficiency, high heat generation often resulting in decomposition of molecules. These posed major difficulty in analyzing complex molecules like peptides or proteins.

The biological mass spectrometry got revolutionized in the late 1980’s when two soft ionization methods were discovered. Those were MALDI and ESI, as mentioned earlier. However, later on different types of mass analyzers came up with higher resolution and sensitivity. Some of the important ones used today will be discussed here.

1.3.4.1 MALDI TOF and MALDI TOF/TOF : MALDI mass spectrometer was developed by Karas & Hillenkamp in 1988 [29]. MALDI is a solid state sputtering/desorption method that produces ions by laser bombardment on crystals containing a small amount of analyte dispersed in a large amount of matrix (Figure 1.20). When carried out in high vacuum and at high accelerating voltage, the pulsed nature of laser radiation produces ions in pulses.

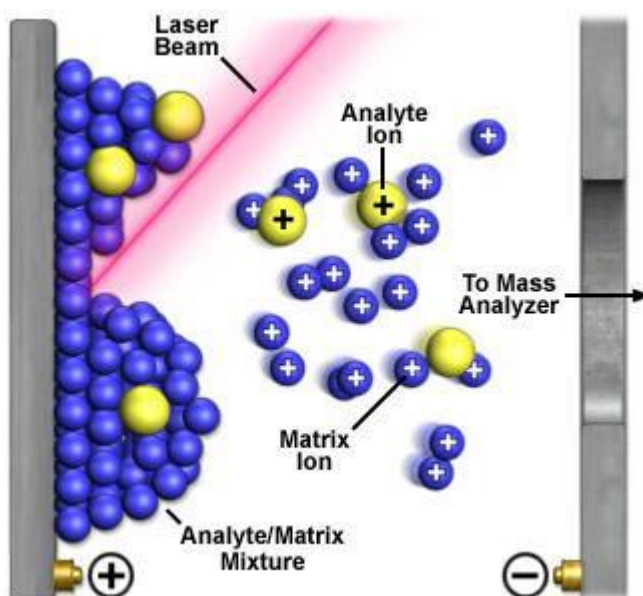


Figure 1.20: Ionization scheme in MALDI MS

Because the samples are solid, MALDI samples are co-crystallized with a very large molar excess of a matrix that acts as a chromophore for the laser radiation and protects even thermally sensitive analyte molecules from the direct effect of the laser irradiation. Effective matrix compounds in MALDI have been developed on a largely empirical basis, but the commonly used matrices such as 2,5-dihydroxybenzoic acid (DHB) and α -cyano-4-hydroxycinnamic acid (CHCA). Both can readily form co-crystal with peptides, absorb laser energy and get volatilized along with the peptide and in the vapor state one proton transfer takes place from the matrix to the analyte molecule resulting into primarily unipositive peptide ions [47]. The transfer of vibronic energy to the analyte ions is dependent on the nature of the matrix, allowing some “fine-tuning” of the spectra, for example, DHB imparts less internal energy than α -CHCA and gives molecular ions that are less prone to undergo unimolecular dissociation reactions [48].

MALDI forms predominantly singly charged ions, so for the analysis of large molecules it requires a mass separation method having a high m/z range, such as a TOF analyzer. Samples are dissolved in water and mixed with a matrix dissolved in water alone or water mixed with an organic solvent such as methanol or acetonitrile, and sometimes acidified with formic acid or trifluoroacetic acid. A small drop of 1 μ l or less is deposited on a multiposition sample plate and allowed to dry. Each sample spot will contain 1–5 μ g of matrix, and for a typical unseparated digest of a protein, something between a femtomole and a picomole per peptide (i.e., a molar range of peptide: matrix in the region of 1:10⁴–10⁷). The sample plate is loaded into the instrument through a vacuum lock without breaking vacuum. This can be viewed inside the vacuum chamber via a video camera, and its position can be manipulated as each sample is irradiated. The sample spot is normally larger than the focused laser beam and different regions of the spot can be selected. Protocols are available that give relatively homogeneous sample preparations [49, 50] that are preferable for automated data collection, in which the laser is moved around the surface, either systematically or randomly.

Two developments led to enhanced performance, namely delayed extraction (DE), described by a number of authors in 1995 [51, 52] and the general adoption for MALDI-TOF instruments of the reflectron or electrostatic ion mirror that had been described many years earlier.

However, in spite of all improvements when MALDI ionization of tryptic peptides is used, protein sequence coverage of 30–40% is obtained. The limited sequence coverage can be explained by the competition for the protons in the matrix plume and limited mass range of the mass spectrometer. The more basic Arg-containing peptides have higher affinity for the protons than the Lys-containing peptide. The higher proton affinity and the higher stability of the Arg-containing peptides are therefore more frequently observed in MALDI-MS spectra. In addition, some peptides may not be able to co-crystallize with the used matrix [53].

1.3.4.2 TOF Ion Optics: In TOF-MS a population of ions, for example derived by MALDI, is accelerated by an electrical potential. After acceleration, the ions pass through a field-free region where each ion is traveling with a speed characteristic of their m/z value. At the end of the field-free region a detector measures the TOF. The recorded TOF spectrum is a sum of the following times: $\text{TOF} = t_a + t_D + t_d$, where t_a is the flight time in the acceleration region, t_D is the flight time in the field-free region, and t_d is the detection time. Because the acceleration region is much smaller than the field-free region, the flight time can be approximated by the drift time,

$$t_D = D \sqrt{\frac{m}{2zeV_{ac}}}$$

where, D is the drift distance, z is the number of charges of the ion, e is the elementary charge, V_{ac} is the acceleration voltage, and m the mass of the ion. Therefore, t_D for an ion will be proportional to $(m/z)^{1/2}$ [54] for ions with different initial velocities, as does the reflectron or ion mirror. In a linear TOF, ions of a single mass accelerated through the same potential should all have the same flight time and should arrive at the detector simultaneously. In practice, the kinetic energy imparted by the accelerating voltage is superimposed upon a range of energies arising from the laser desorption process. Consequently, ions of a single mass have a

distribution of arrival times at the detector. A reflectron situated at the far end of the flight tube provides a linear potential gradient from ground to just above the accelerating voltage. This slows the ions and then reverses their direction of flight, accelerating them back toward a detector situated at a slightly offset angle. The fastest ions penetrate further into the reflectron and travel a longer distance before reaching the detector than the slowest ions. Through a suitable choice of geometry, it is possible to have all ions of each unique mass arriving at the detector simultaneously, even though they have slightly different velocities. With the combination of the DE source and the reflectron, modern high-performance MALDI-TOF instruments easily attain an RP of 10,000 or more, which with suitable calibration allows mass measurements to be made with an accuracy of better than 10 ppm [55]. In 1993, several groups independently demonstrated that a MALDI mass map of the peptides in an unseparated protein digest could correctly identify a protein that was present in a database, even when only a subset of the peptides was ionized and detected. Because every protein can potentially give a unique pattern of peptides, this technique is often referred to as peptide mass fingerprinting (PMF).

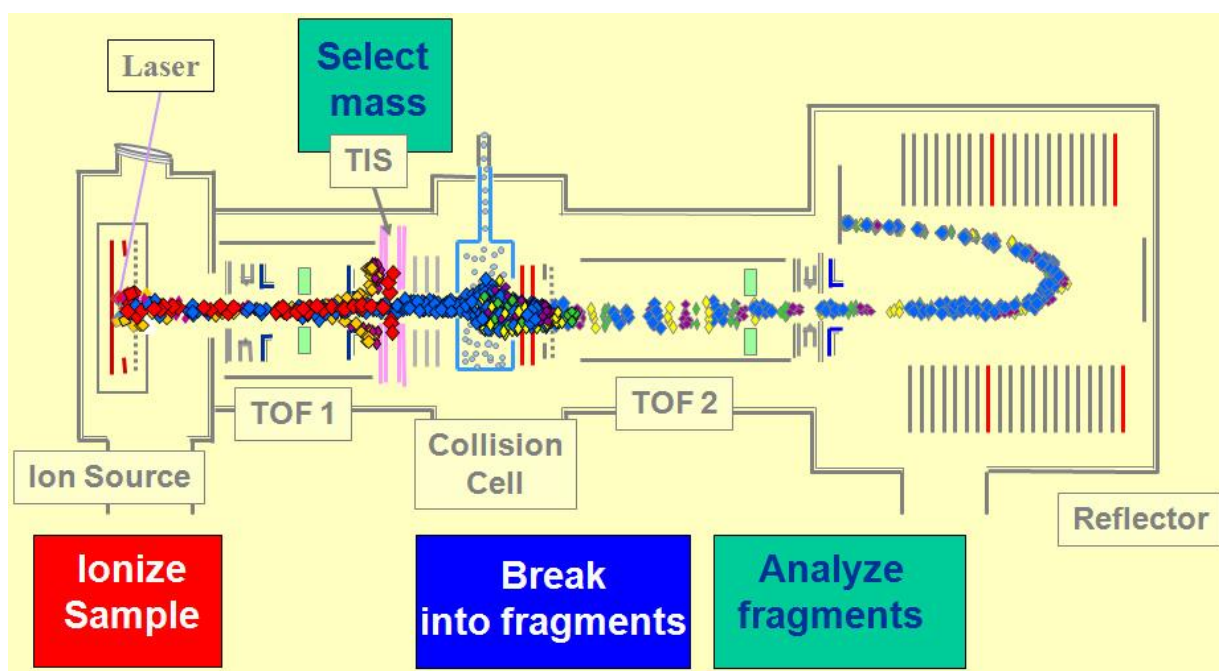
Since in-gel tryptic digestions generally precede MALDI MS, Using TOF ion optics a peptide mass fingerprint (PMF) is obtained with the peptides ending in lysine or arginine. It is called fingerprint because of the difference in amino acid sequence between two proteins, no two PMF's, in theory could show a 100% identity.

However, in practice, often some mass peaks in a spectrum cannot be matched with a theoretical mass of a tryptic peptide from a single protein. Typical reasons are tryptic miscleavage, modifications of tryptic peptides, tryptic peptides from other proteins, ions from matrix clusters, and fragmentation of ions during MALDI-TOF MS. The observed miscleavages are mainly because of pseudotrypsin, which is generated by autolysis of trypsin, which has a broader specificity than trypsin.

1.3.4.3 Tandem Mass Spectrometry - MALDI TOF/TOF: Since MALDI could normally cover only 30-70% of peptides from a particular protein, often it becomes necessary to verify or

see the amino acid sequence of one or more peptides in a particular PMF. Also, because of the high level of activity in genomic sequencing and the completion of several genomes, databases have grown dramatically larger, enforcing a requirement for more accurate mass measurement to increase the selectivity and specificity of mass mapping. So now PMF is rarely adequate and peptide sequence determination is virtually essential. This is certainly the case for protein identification in complex mixtures when there are too many peptide signals and PMF returns an unacceptably high number of candidates; to obtain protein sequence when no match is found in a database; or to identify and localize posttranslational modifications. Sequence information can be obtained readily by tandem MS, frequently known as MS/MS (Figure 1.21).

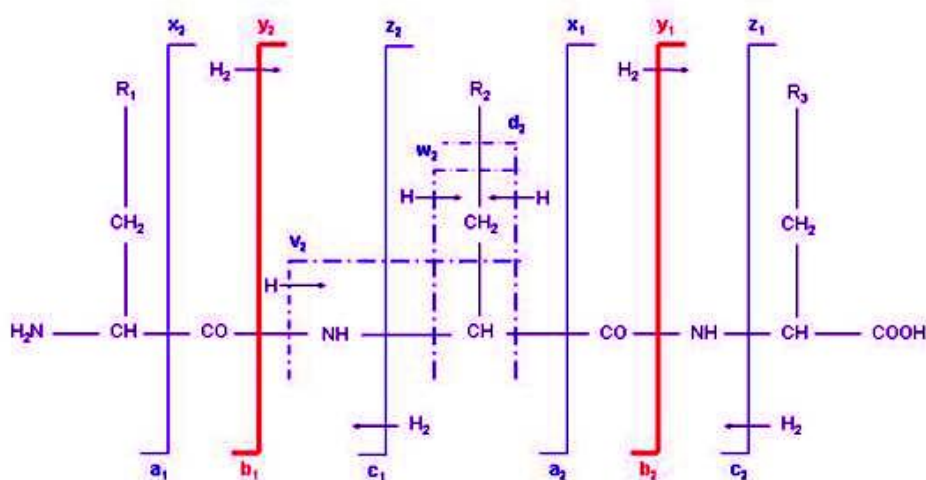
Figure 1.21: Tandem mass spectrometry in a MALDI-TOF/TOF spectrometer.



Conventional MS produces ions that are separated by m/z and analyzed directly. If a soft ionization method is used (i.e., one that causes minimal fragmentation), the mass spectrum will yield the molecular weight values of compounds present in the analyte but little or no structural information. In a tandem mass spectrometer, ions of a particular mass number selected by the first mass analyzer (MS1) can be subjected to collisions with neutral gas atoms or molecules that cause excitation of the ions, resulting in unimolecular decomposition. This process is

known as Collision Induced Dissociation (CID). The ionic fragments are then separated in a second analyzer (MS2), yielding structural information such as the amino acid sequence of a peptide. The high-velocity ions typical of MALDI-TOF mostly undergo a single collision that converts sufficient kinetic energy into internal energy to decompose the peptide into constituent ions. This was achieved in a MALDI mass spectrometer with a CID cell [56]. Collisions between ions and neutrals cause excitation of the ions with a distribution of elevated internal energies. The higher the average internal energy, the greater the number of channels that will be available for dissociation reactions; many possible reactions being accessible only to ions that are activated by high velocity collisions. Fragmentation at an amide (or “peptide”) bond giving a b ion (N-terminal fragment) or a y ion (C-terminal fragment) is a relatively low-energy process (Figure 1.22)

Figure 1.22: MSMS fragmentation



Higher energy processes lead to cleavage elsewhere along the backbone, for example, between an α -C and a carbonyl-C to give an a ion or simultaneous backbone and side-chain cleavage to give d or w ions that can distinguish leucine from isoleucine, or formation of the low mass immonium ions that can characterize the amino acids present. Thus, metastable ion spectra and typical low-energy CID spectra show sequence information in the form of b and y series ions, but they are devoid of some of the more structurally informative ions. Also, any

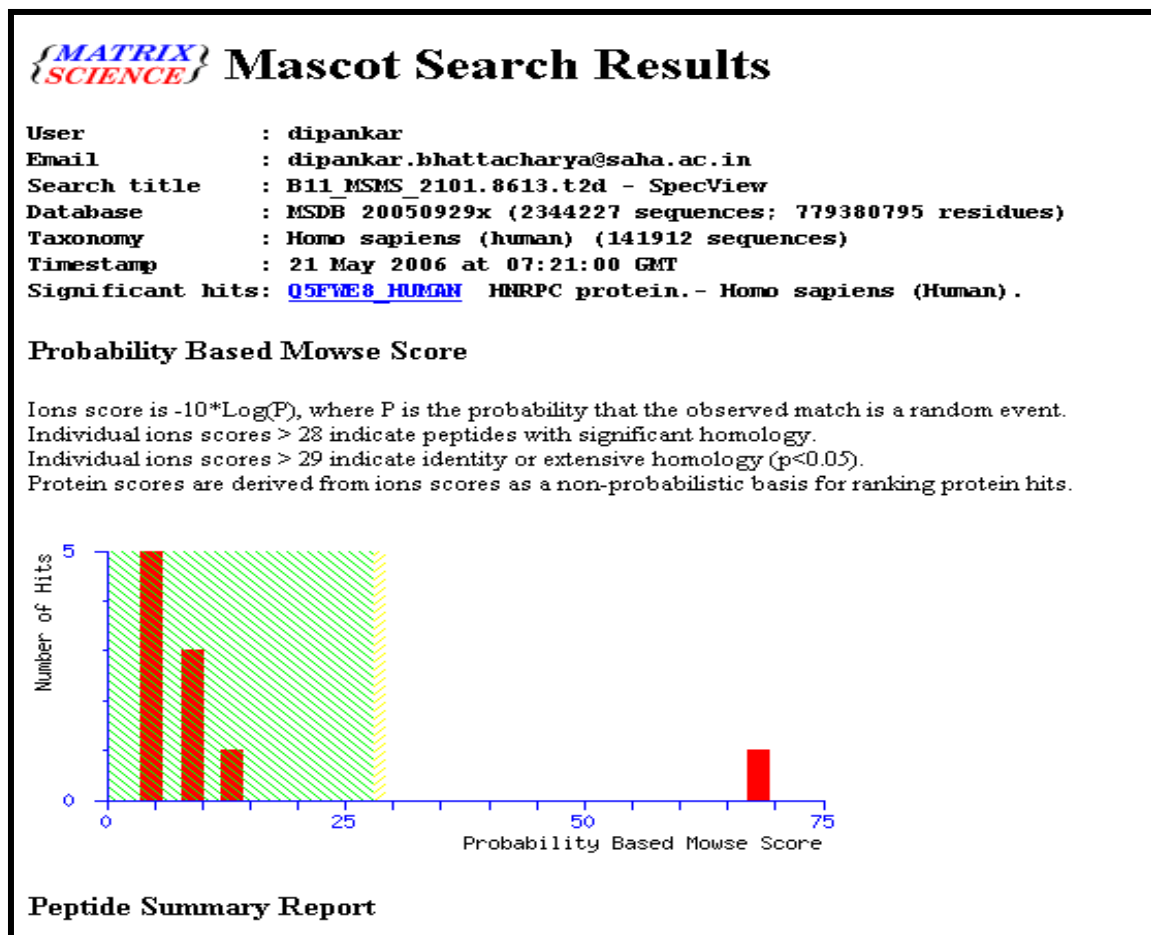
particularly favorable amide cleavage such as at the N-terminus of a proline residue, where the secondary amino nitrogen can stabilize the positive charge, may dominate the unimolecular spectrum at the expense of other sequence ions. Consequently, if sufficient fragmentation is desired to derive the sequence from first principles, high-energy CID may be essential. On the other hand, if fragment ions are being used to search the database for a peptide sequence “tag” [50] which is a series of fragment peaks that defines a sequence of amino acids within a peptide, low-energy CID will often suffice. The present MALDI TOF/TOF instrument was first modified by Vestal *et al* [57, 58].

The TOF compartment could be used twice, first as the normal PMF TOF, and secondly, after the activation of the CID chamber, the fragmented peptides could be identified after the timed ion selection using the same TOF tube. The whole system is kept under high vacuum using turbo pumps so that high sensitivity ($S/N > 10000$) and high accuracy (≤ 10 ppm) could be achieved.

1.3.4.4 Data Analysis Softwares: The advancements and automation in mass spectrometric data acquisition has resulted into generation of huge bulk of mass spectrometric data in a short time, as a result robust bioinformatics tools have been employed to analyze the bulk data. Peptide identification algorithms fall into two broad classes: database search and *de novo* search. The former search takes place against a database containing all amino acid sequences assumed to be present in the analyzed sample, whereas the latter infers peptide sequences without knowledge of genomic data. At present, database search is more popular and considered to produce higher quality results for most uses. With increasing instrument precision, however, *de novo* search may become increasingly attractive. MASCOT [59] is a proprietary identification program available from Matrix Science. It performs mass spectrometry data analysis through a statistical evaluation of matches between observed and projected peptide fragments rather than cross correlation. As of version 2.2, support for peptide quantitation methods compatible to ICAT or ITRAQ methods are provided in addition to the

identification features. Figure 1.23 presents a MASCOT result for a combined PMF plus MSMS search.

Figure 1.23: A typical MASCOT search result



1.4 Proteomics of B cell malignancies

The identification of proteins aberrantly expressed in malignant B-cells can potentially be used to develop new diagnostic, prognostic or therapeutic targets. Proteomic studies of B-cell malignancies have made significant progress, but further studies are needed to increase our coverage of the B-cell malignant proteome [60]. The belief is that by applying this information along with gene expression data and knowledge of metabolic and signalling pathways, deductions can be made as to the mechanisms underlying the initiation and development of neoplasia. The knowledge that mRNA microarray data produces on genome wide expression

does not necessarily translate through to protein expression. Thus, proteins are subject to numerous post-translation modifications (PTMS), such as phosphorylation, glycosylation, methylation and proteolytic cleavage which can vary according to different stages in the life of a cell and are affected by metabolism, cell cycle, differentiation and cell death. Proteomics can now be used to identify changes in not only whole cells but also identify more insightful and informative changes in discrete organelles and the various sub-cellular compartments of the cell, which may be related to the cause and/or onset of neoplasia.

The human genome consists of approximately 30,000 genes, which with alternate splicing, sequence deletion and posttranslational modifications can translate to in excess of 10^6 distinct protein species. The exact number of proteins will depend on cell type, metabolic or disease status, but signalling proteins or those acting at key signalling or metabolic control points will be in low abundance, while housekeeping/constitutive, metabolic enzymes and cytoskeletal proteins will often be in very high abundance. Protein levels are also highly dynamic and subject to rapid changes, according to the physiological status of the cell. Proteomic analyses of tumour cells are inherently problematic, as it is often difficult to get appropriate quantities of tumour samples. In this respect, B-cell malignancies are more amenable to proteomic analysis as white blood cells can be obtained from patients relatively easily, affinity purified and in sufficient quantity for meaningful analysis. This, however, does carry the assumption that the proteome of peripheral malignant B-cells reflects their point of origin in the germinal centre within the lymph node or bone marrow environments. For many proteins this may be true but some proteins may show significant differences. Thus, for example B-CLL cells from lymph nodes express higher Zap-70 levels than B-CLL cells from peripheral blood [61]. Also, a recent microarray study, focussing on 34 apoptosis-linked genes, found similar levels of expression for most of these genes in peripheral and lymph node B-CLL cells [62]. However, Noxa a pro-apoptotic protein was up-regulated at both the mRNA and protein levels in peripheral B-CLL as compared to lymph node cells. Treatment of peripheral

B-cells with a proteasome inhibitor up-regulates Noxa and induces apoptosis. Thus, if possible, proteomic studies obtained from peripheral cells need to be compared to lymph node analyses. Be that as it may, the circulating lymphocytes are good candidates, suitable for antibody (cell surface) targeted diagnostic and therapeutic purposes. Consequently, there is considerable interest in selectively characterising the proteome of the plasma membrane. However, it is also clear that many B-cell lymphomas invariably involve a defect in Bcl-2 and associated family members, so the expression, organelle localisation and protein interactions of such proteins may also provide important clues for putative therapeutic targets.

A variety of proteomics approaches have been used to investigate B-cell malignancies, including protein antibody microarrays, 2DGE coupled to MALDI-TOF, and ‘shotgun proteomics’ using 2D-HPLC and 1D SDS-PAGE gel separations coupled to LC-MS/MS. Protein antibody microarray studies offer high sensitivity and throughput but are limited to the availability of high quality antibodies and cannot identify unknown proteins, but potentially it should be possible to tailor antibody arrays to selectively identify a particular disease or a set of markers which could be used in prognostic decision and or therapeutic rationales.

1.4.1 2DGE studies of B-cell malignancies

Attempts to produce Federated Databases have resulted in the compilation of comparatively few examples of lymphoid proteomic 2DGE databases (Swiss-2D PAGE Prot 2D world wide database, <http://www.expasy.org/ch2d/>). Earlier attempts to produce an online database of B-lymphoid proteins have not remained durable and the open database for example created for lymphoma cells [63] is not maintained. A number of studies have been carried out on B-cell lymphomas, and 2DGE maps for reactive lymph node (control) and mantle cell lymphoma (MCL) lymph nodes were obtained and approximately 750 spots visualised with MS compatible colloidal Coomassie blue staining. PDQuest 2DGE analysis software identified 145 differences (up and down-regulated) and 20 proteins were identified by MALDI-TOF that

exhibited 3-10 fold up-regulation (8 proteins) and 2-12-fold down-regulation (12 proteins). Thus, the percentage of actual spots identified by MS was only 2-3% of the proteins visualised on the 2D gel and many of the proteins identified were highly abundant species (eg. glutathione S-transferase, succinate dehydrogenase, catalase, and peroxiredoxin). Low-copy number proteins were not identified, although the fact that highly abundant proteins displayed marked changes is in itself an interesting finding. For example, the latter study also identified stathmin 1 and highlighted an apparent increase in the phosphorylated form of the protein. Stathmin 1 (STMN1), a 19 kDa cytosolic protein is the first member of a family of phylogenetically related microtubule-destabilizing phosphoproteins, critically involved in the construction and function of the mitotic spindle. STMN1 is required for orderly progression through mitosis in a variety of cell types and is over-expressed across a broad range of human malignancies. It is up-regulated in normally proliferating cells but only rarely up-regulated in non-proliferating cells. STMN1 was identified by 2DGE as an up-regulated protein in acute lymphoblastic leukemia (ALL) and acute myeloid leukemia (AML), but was also up-regulated in normal proliferating lymphoid cells [64]. The presence of STMN1 in proliferating cells suggests that it is a proliferation marker rather than a specific biomarker for lymphoma.

In other studies, 2DGE identified approximately 930-960 proteins in cell lysates obtained from Burkitt lymphoma cells treated with 5-azacytidine (AZC) a DNA demethylase inhibitor. Compared to control cell lysates, 21 (15 identified) proteins were down-regulated and 14 proteins (8 identified, including STMN1) were up-regulated. 2D-DIGE and large format gels (IEF range pH 4-7 range) have been used to construct a protein expression map for lymphoid neoplasms (using 42 cell lines). Out of 1500 proteins which were visualised, 389 proteins were identified by MALDI-TOF mass spectrometry [65]. Proteins were classified according to the Amigo gene ontology system (<http://amigo.geneontology.org>) and seven major GO terms (nucleotide binding, hydrolase activity, structural molecules, metal ion binding,

hydrolase, protein binding, transferases, and obsolete molecular function (i.e., defined as not assigned to any other recognizable GO term) accounted for ~50% of the identified proteins. Whilst, the identification rate in this study was much better than other studies, rather surprisingly this study failed to identify a single CD (cluster of differentiation) protein. This is somewhat surprising given the fact that membrane-associated CD proteins are particularly abundant in B-cell plasma membranes but highlights the difficulties of using 2DGE to separate hydrophobic (membrane) proteins. It is clear from this and other examples that global 2DGE analysis of entire cells can only visualise a very small % of the cellular proteome. Any changes which are detected in these studies either due to the disease or treatment are likely to be limited to relatively abundant proteins, albeit they may still be important or biologically significant proteins (e.g. STMN1 is an emerging anti-cancer target, reviewed in [66]). More specifically, cell lysates from prognostic subtypes of CLL distinguished by the absence (UM-CLL) or presence (M-CLL) of somatic hypermutation of immunoglobulin heavy chain gene have been analysed by 2DGE and mass spectrometry [67]. Consistent differences in protein expression were observed between the two forms of CLL. Nucleophosmin 1 was identified by MALDI-TOF and is a protein which is associated with ribosomal proteins and appears to be highly expressed in the nucleoli and nucleoplasm of all cells. However, immunocytochemistry showed that in some cells, nucleophosmin 1 was also present in the cytoplasm and appeared to be more frequent in cells isolated from CLL patients without somatic hypermutation. This study also highlights that changes in protein expression detected by a proteomics approach contrasts with microarray studies on UM-CLL and M-CLL which did not detect not any significant changes in transcribed mRNA. This difference between the protein and mRNA results may be due to the influence of microRNAs (miR) which are known to play an important role in the expression of proteins. In summary, a small number of 2DGE studies have analysed both primary tissues and cell lines derived from lymphoid neoplasms with some success. These

studies have produced interesting results, but suffer from the inherent limitations of 2DGE, particularly, with regard to the analysis of plasma membrane proteins.

1.4.2 Shotgun proteomic studies on B-cell malignancies

Hydrophobic membrane and basic proteins are difficult to resolve with 2DGE and an alternative approach to analysing membrane proteins is to use 1D SDS-PAGE and ‘shotgun proteomics’, which has emerged as a powerful technique for analysing membrane proteomes. Shotgun proteomics basically exploits the power of modern LC–MS/MS tandem mass spectrometers to discriminate between thousands of peptides, which can be individually separated and then sequenced by fragmentation using CID. Coupled with the available expanding protein databases and sophisticated bioinformatics techniques it is now possible to identify many different proteins in one sample. One of two techniques is usually employed: a) MudPIT (multi-dimensional LC–MS/MS) in which the protein mixture is digested using proteases (usually trypsin) and then the peptides are separated by cation exchange chromatography followed by reverse phase chromatography to yield the signature peptides which are identified in the tandem mass spectrometer; b) gel-based shotgun proteomics, where the proteins are separated by molecular weight on 1-D SDS-PAGE gels which are sequentially sliced and subjected to in-gel trypsinolysis to yield the peptides which are identified by LC–MS/MS mass spectrometry. Both shotgun approaches are equally efficient at identifying large numbers of proteins, and the only major difference between the two approaches is that the gel-based approach gives extra information on the protein, in that detection of the protein with an anomalous molecular weight can be indicative of proteolytic cleavage or degradation (e.g. during caspase-dependent cell death) or PTM (e.g., glycosylation). Shotgun proteomics is a powerful tool and coupled with appropriate quantitative strategies can deliver important information on protein changes in B-cell malignancies and a number of methodologies have been developed to provide quantitative data (reviewed in [68]). Invariably, these techniques involve either pre- or post-labelling of proteins with stable isotope tags, which can be detected

and quantitated by mass spectrometry. Stable isotope labelling of amino acids in culture (SILAC) is a relatively non-invasive technique in which cells are pre-labelled in media containing appropriately ^{13}C and/or ^{15}N labelled amino acids. Two cell cultures are produced incorporating a 'light' or 'heavy' form of the amino acid into the proteins; after a number of cell divisions (minimum of 5 doublings) the natural amino acid is replaced by its isotope-labelled analogue. There is little chemical difference between the labelled and natural amino acids and cells behave exactly like their normally cultured counterparts. Control and test cells are lysed and combined before being analysed by LC-MS/MS, which identifies the natural and labelled peptides by the defined mass shift (e.g. with lysine this is 6 Da). The relative peak heights for a given peptide is thus a measure of the relative amounts of that protein. Importantly while this technique is readily applied to cell lines, it is not readily applicable to the analysis of primary leukemic cells and tissue, which normally do not proliferate in culture. However, it is possible to culture primary cells, using feeder cell co-culture techniques (e.g. CLL cells proliferate on CD154/CD40L expressing mouse fibroblast cells [69]), which may be amenable to SILAC approaches.

An alternative approach for primary leukemic cells is to post-label the protein with ICAT or the peptides using iTRAQ (isobaric tagging for relative and absolute quantification). The iTRAQ technique uses 4 or 8 isobaric reagents (each isobaric reagent consists of reporter, balance and reactive groups to give the same mass) to TAG peptides which are then identified by MS/MS [70]. The reactive group attaches the tag to N-terminal amines and lysines with reporter groups (masses of 114, 115, 116, and 117 Da) and complementary balance groups (masses of 31, 30, 29, and 28 Da). The compensating masses of reporter and balance groups have the same mass (145 Da) and a particular peptide tagged by any of the iTRAQ reagents, has the same mass to charge ratio in the MS spectrum. As both control and test samples are combined, this increases the sensitivity of peptide detection and during MS/MS, fragmentation

releases a distinctive reporter ion that can be used for relative quantitation of the peptide. As iTRAQ tags react with free amine groups they can be used to relatively quantitate all the peptides in a complex mixture. Post-labelling with ICAT or iTRAQ can be used with primary leukemic cells, and cICAT (cleavable form of ICAT) has been used to analyse M-CLL and UM-CLL sub-groups. Membrane and cytosol fractions were labelled with cICAT and in the M-CLL sub-group, 13 proteins showed greater than 3-fold difference in expression and one protein in particular, cytochrome c oxidase subunit, COX G was shown by Western blotting to be significantly up-regulated in 6 M-CLL patients. The UM-CLL sub-group was associated with a more aggressive disease progression and thus, COX G could be a prognostic marker for predicting disease outcome in CLL. Currently, iTRAQ has not been used to study B-cell lymphomas, but it has been used in Ba/F3 cells to identify quantitative changes in six leukemogenic (myeloid) protein tyrosine kinases (PTKs), including BCR-ABL [70]. The Ba/F3 cells were retrovirally transfected with various vectors containing the six PTKs and the transfected cells analysed with specific iTRAQ isobaric tags allowing relative quantitation of the effects of the PTKs in a single tandem mass spectrometry experiment. This approach identified disparate effects on the proteomes of the transfected cells with only a few common targets. BCR-ABL produced the greatest effect on the proteome, although a common feature of this study was the lack of any correlation between the proteomic and transcriptome data.

Methods of label-free quantitation have been developed, based on the number of peptides (protein abundance index- PAI) or spectra (spectral abundance factor-SAF) detected [71]. Relative quantitation is achieved by comparing the number of peptides or MS/MS spectra for a given protein in each sample. Spectral counting has gained acceptance as a straightforward label-free, semi-quantitative measure of protein abundance in proteomic studies. Other improvements have been suggested such as selective reaction monitoring (SRM) measurements of a limited set of internal reference standards which were used to determine the absolute protein concentrations of more than a thousand proteins [72]. Thus, for example in a

recent study on MCL spectral counts were used to assess the abundance of the detected proteins and then selected a number of proteins for further validation with RT-PCR, including CD20, CD79b, CD22, CD31, CD11a, CD50, CD82, CD44, 5-LO (5-lipoxygenase), Cbp (Csk-binding protein) and raftlin (raft linking protein) [73]. Appropriate antibodies and Western blotting were used to profile primary MCL cells against normal age-matched samples and for example were correlated with spectral count data for CD70, 5-LO and raftlin. Thus, spectral counting can be a powerful and reliable method for determining expression data in primary leukemic samples. Whilst label-free expression profiling is not a perfect method for absolute quantitation, it can identify potential changes in normal and malignant cells, which can then be validated with other methods.

1.4.3 Subcellular proteomic studies of B-cell malignancies

To overcome the limited protein coverage of current proteomic strategies, a more targeted approach can be used to increase discovery rate, by fractionating the cell into component fractions, such as nuclei, plasma membranes, mitochondria and cell cytosol which have a reduced number of proteins. Potentially, these approaches can markedly increase coverage and discovery rates.

The ability to target an antibody to an external cell surface protein is a potentially powerful therapeutic tool and serves to drive the intense interest in identifying the proteins associated with the plasma membrane of malignant B-cells. 2DGE can be used to analyse plasma membrane fractions and for example crude membrane preparations isolated from a DG75 lymphoma cell line were sequentially extracted with a urea/thiourea/CHAPS buffer before separating on IPG strips (pH 5-8) and SDS-PAGE. In this study the effect of 5-azacytidine (AZC) treatment was investigated and approximately 960 spots were visualised, with 7 proteins down-regulated and 42 proteins up-regulated. Approximately, 70% of these proteins were identified by MALDI-TOF and/or LC-MS/MS. However, only 5 proteins were identified with transmembrane regions or membrane anchorage, and only TNFSF member 12

(also known as TWEAK) is a recognizable plasma membrane protein. Purified plasma membrane preparations are solubilised in SDS and separated on 1-D SDS-PAGE gels which are sliced into 1-3 mm sections for trypsinolysis and identification by LC-MS/MS. Plasma membranes from CLL and MCL have been analysed by this method and ~500 (CLL) and 423 (MCL) proteins identified, including many CD cell surface proteins [60]. In the case of MCL plasma membranes, 111 transmembrane proteins, including 49 CD antigens, 40 known (in B-cells) and 13 unknown (in B-cells) proteins were identified along with many BCR-associated proteins and HLA proteins.

Extraction of hydrophobic and proteo-lipid micro-domains of the membrane offers additional mechanisms for reducing the number of proteins to be detected and thereby increasing the discovery rate. Lipid rafts have been implicated in a variety of cell signalling and trafficking pathways. In B-cells, antigen cross-linked BCR associates with lipid rafts in a rapid time-dependent manner. Thus, in resting B-cells, the BCR is excluded from the rafts, which contain the Src-family kinase LYN. Many other proteins, including the B-cell regulators CD22 and CD45 are absent from the raft and the BCR monomer has weak affinity for lipid rafts. However, antigen cross-linked BCR has a much higher affinity for lipid rafts and associates with LYN, which phosphorylates immunoreceptor tyrosine-based activation motifs (ITAMS) that in turn recruit SYK and other proteins such as, CD45, Btk, VAV and SHIP. Analysing the lipid raft before and after BCR stimulation has been investigated with the Ramos B-cell line using mass spectrometry and ICAT. Proteins identified in B-cell lipid rafts, were grouped into various functional categories, including receptors/surface glycoproteins, structural, protein kinases, protein phosphatases, small G proteins, heterotrimeric G proteins, motor proteins and vesicle fusion or trafficking proteins. BCR ligation induces threonine dephosphorylation and transient dissociation of ezrin from the actin cytoskeleton and lipid rafts. This allows the lipid rafts to coalesce or cluster into large more stable complexes, which promote more efficient and long lasting signal transduction.

Table 1.2: Comparison of lipid raft proteins identified in B-cell malignancies and primary cells [60]

Protein	Ramos	Raji	CH27 B-cells	MCL	MCL cell lines
<i>Cytoskeletal or structural proteins</i>					
	Actin β tubulin Ezrin Flotillin 1 and 2	Actin β tubulin Ezrin F actin capping protein subunit β	Actin β tubulin Ezrin Flotillin 1 and 2	Actin β tubulin Ezrin Flotillin 1 and 2	Actin β tubulin Ezrin Flotillin 1 and 2
	Talin		Vimentin		PAG
	Raftlin	Raftlin			Raftlin
<i>Receptors/surface glycoproteins</i>					
	CD20 CD22 CD37 CD48 CD81 CD108 CD147 CD180	CD10 CD22 CD48	CD37	CD20 CD48 CD74 CD98	CD20 CD48 CD74 CD98
	HLA-A	HLA-DR α chain	Igμ H chain	CD317 Igμ H chain	CD47 CD317 Igμ H chain
	β2-microglobulin HLA-DRAB CXCR4 TM9S2 TM9S4			HLA-DW2.2 β chain HLA-DR α chain HLA-β-K	HLA-DR α chain Igκ chain C
			MHCII A α-K chain MHCII E β-K chain	Transmembrane protein 43	
<i>Kinases</i>					
	JAK1 Lck	Casein kinase 1 Fgr		Hck	Hck
<i>Protein phosphatases</i>					
	PP2A (PR65) regulatory subnit	Lyn		Lyn	Lyn
<i>Small G proteins</i>					
	Rap1A,B,C Rap2B C Rac2,3	Protein phosphatase-1γ		Protein phosphatase-1γ	
		Ral-A		Rras1 Rras2 Rab7a	Rras1 Rab7a Rab 35 Rab-5a,b,c'

Table 1.2: contd.

Protein	Ramos	Raji	CH27 B-cells	MCL	MCL cell lines
<i>Heterotrimeric G proteins</i>					
	Gia1 Gia 2,3 Gb1,2	Gia 2,3 Gb1,2	Gb2	Gia 2,3 Gb2,3 Gia23 Gia13	Gia 2,3 Gia2,3 Gia23 Gsa
<i>Motor protein</i>					
	Myh9 Myo1D	Myh9 Myosin 1 β Myosin 1G			
	Myosin light chain akali Myosin regulatory light chain				Tropomyosin α 3 Myosin regulatory light chain 2
<i>Vesicle fusion/trafficking proteins</i>					
	Clathrin heavy chain			Clathrin heavy chain SNAP23 Syntaxin 7	Clathrin heavy chain SNAP23

1.4.4 Phosphoproteomics studies of B-cell malignancies

One key issue in phosphoproteomics is the relatively high amount of cellular material required to identify a phosphorylated peptide from a signalling protein; given that phosphorylation is a transient modification, a phosphorylated peptide is often less abundant than its non-phosphorylated form. Consequently, phosphoproteome analysis requires highly sensitive and specific strategies. Today, most phosphoproteomic studies are conducted by mass spectrometric strategies in combination with phosphor specific enrichment methods. Methods for enrichment of phosphopeptides usually employ immunoprecipitation with a specific anti-phospho antibody or IMAC using immobilized metal ions (Fe^{3+} or Ga^{3+}) or titanium dioxide.

So far most phosphoproteomic studies have focused on myeloid malignancies. To date very few phosphoproteomics studies have been carried out on B-cell malignancies. With regard to B-cell malignancies, studies investigating the role of protein phosphorylation in the pathology of leukemic cells can be divided into: 1) studies that have surveyed the phosphoproteins in a given cell type or after a drug treatment; 2) studies that have taken a more

targeted approach analysing the phosphorylation of a specific protein or complex. Thus, a recent study used IMAC and LC-MS/MS to indentify 76 unique abundant phosphoproteins in MCL cell lines [74]. A targeted study in primary CLL cells was recently reported with the chemokine receptor, CXCR4 (CXC motif receptor 4), which is involved in CLL survival. Stimulation of the CXCR4 receptor in primary CLL cells resulted in the identification of 251 unique phosphoproteins from only 2 mg of cell lysate. In conclusion relatively few phosphoproteomics studies have been done in primary leukemic cells or tissue. Cell lines, due to the ease of generating cellular material and experimental manipulation have been most intensively used. The studies with CML show that the most effective approach is to target a specific protein/complex, but even this approach demands complex and challenging methodology. However, the analysis of phosphoproteins in primary leukemic cells or tissue is still a valid aim and no doubt improvements in phosphoprotein or peptide enrichment, mass spectrometer sensitivity and quantitative methodology will aid the pursuit of this aim.

1.4.5 Identification of potential biomarkers in B-cell malignancies

A major aim in treating lymphoid malignancies is the development of high-throughput cost-effector biomarker technologies, which can be used for diagnosis and/or prognosis. One such approach is the antibody array, which is an alternate method of profiling for a selected set of proteins present in cells or tissue. Recently a protein microarray containing 512 highly specific monoclonal antibodies (MAbs, BD Clontech) was used to compare protein profiles of B-cells derived from malignant MCL lymph node/spleen biopsies and normal tonsillar B-cells [75]. This study identified 77 differentially expressed proteins in MCL, although only a few of these were transmembrane proteins. A subset of 13 proteins exhibited a higher than 2-fold difference expression in 4/6 MCL patients, and some of these results were confirmed with Western blotting and histochemistry. This study also highlighted the fact that expression data from the MCL cell line MO2058 failed to correlate with primary MCL patient samples. This lack of correlation between primary cells and cell lines was also highlighted in a recent study on MCL

and emphasizes the importance of obtaining protein profiling data from primary malignant B-cells, rather than immortalised cell lines [73].

An alternative biomarker approach to using antibody arrays is Surface Enhanced Laser Desorption Ionization TOF-MS (SELDI-TOF-MS), which can be used to detect serum markers. In general SELDI-TOF-MS identifies biomarkers in terms of mass ranges. So, in serum derived from normal and leukemic patients, biomarkers were identified with $m/z=13000$; $m/z=9000$ and $m/z<2000$ [76]. The differential masses detected with SELDI-TOF-MS were subsequently identified by chromatographic extraction tandem mass spectrometry and included a sulphite form of transthyretin (13,841 Da) was shown to be increased in the leukemic patients and a second set of markers (8.6 and 8.9 kDa) were identified as complement related fragment proteins C3 and C4 (known as anaphylatoxins) were also significantly up-regulated in patient serum. SELDI-TOF-MS has also been used to screen the serum of healthy adults and patients with DLBCL. In this study serum samples were analysed and 9 potential biomarkers identified with m/z ranging from 2821 to 7975 Da, which were higher in tumour samples and therefore potential biomarkers for discriminating DLBCL patients from healthy individuals. Additional biomarkers were also identified as being good indicators of prognosis. SELDI-TOF-MS can be used to assay for specific proteins and an example is BAFF, which along with APRIL is involved in B-cell survival and proliferation. These ligands bind to BAFF-R, TAC1 and BMCA receptors and have been detected at the mRNA and protein level in normal B-cells and CLL cells. Interestingly, in contrast to normal B-cells, BAFF and APRIL are expressed at the membranes of the leukemic cells. Moreover, a soluble form of BAFF (28-kDa) was detected by SELDI-TOF-MS in the sera of CLL patients but not in healthy donors [60].

Proteomics approaches have identified a number of proteins involved in B-cell neoplasms and are potential targets for therapy but clearly there is still considerable scope for new discoveries. In conclusion proteomics using advanced mass spectrometry methods offers the opportunity to identify many new therapeutic targets and biological mechanisms in B-cell

malignancies. The challenge is to develop appropriate targeted, mechanistic and functional approaches which allow the identification of both novel and known protein species, which are present and functioning in unexpected cells, cellular compartments and protein complexes. However, successful proteomic studies on B-cell malignancies must be integrated and validated with biological and clinical studies.

1.5 Motivation and aim of the present study

Although contemporary treatments cure more than 80% of children with B-ALL, some patients fall in high risk and/or poor prognosis classes requiring intensive treatment, others exhibit drug resistance and many patients still develop serious acute and late complications owing to the side effects of the treatments. Furthermore, the survival rate for adults with B-ALL remains below 40% despite the use of transplantation, and treatment outcome is poor among patients who relapse on current front-line ALL regimens [21]. Although molecularly targeted agents might possess anti-leukemic activity, the responses they induce are seldom durable and certainly do not extend to all patients. Although identification of the genetic abnormalities has led to an improved understanding of B-ALL pathophysiology, the mechanisms responsible for the B-cell developmental arrest are unknown. Nevertheless, the primary oncogenic events seem to require secondary cooperative changes to generate a fully transformed cell.

The primary objective of this study was to identify differentially regulated proteins in B-ALL that; a) may contribute to our understanding of B-cell malignancies; b) can be used for diagnosis or prognosis and c) can be potential therapeutic targets. Several transcriptomic studies of mononuclear cell populations from lymphoid malignancies have been carried out in past, but the transcriptome data on genome-wide expression does not necessarily translate through to protein expression patterns. Unlike the static genome, the proteome of a cell is dynamic, as it shows characteristic perturbations in response to disease and physiological state of the cell. A thorough comparison of the proteomic profiles of normal and malignant cells can not only point out candidate diagnostic markers and/or therapeutic targets of the malignancy, but also throw

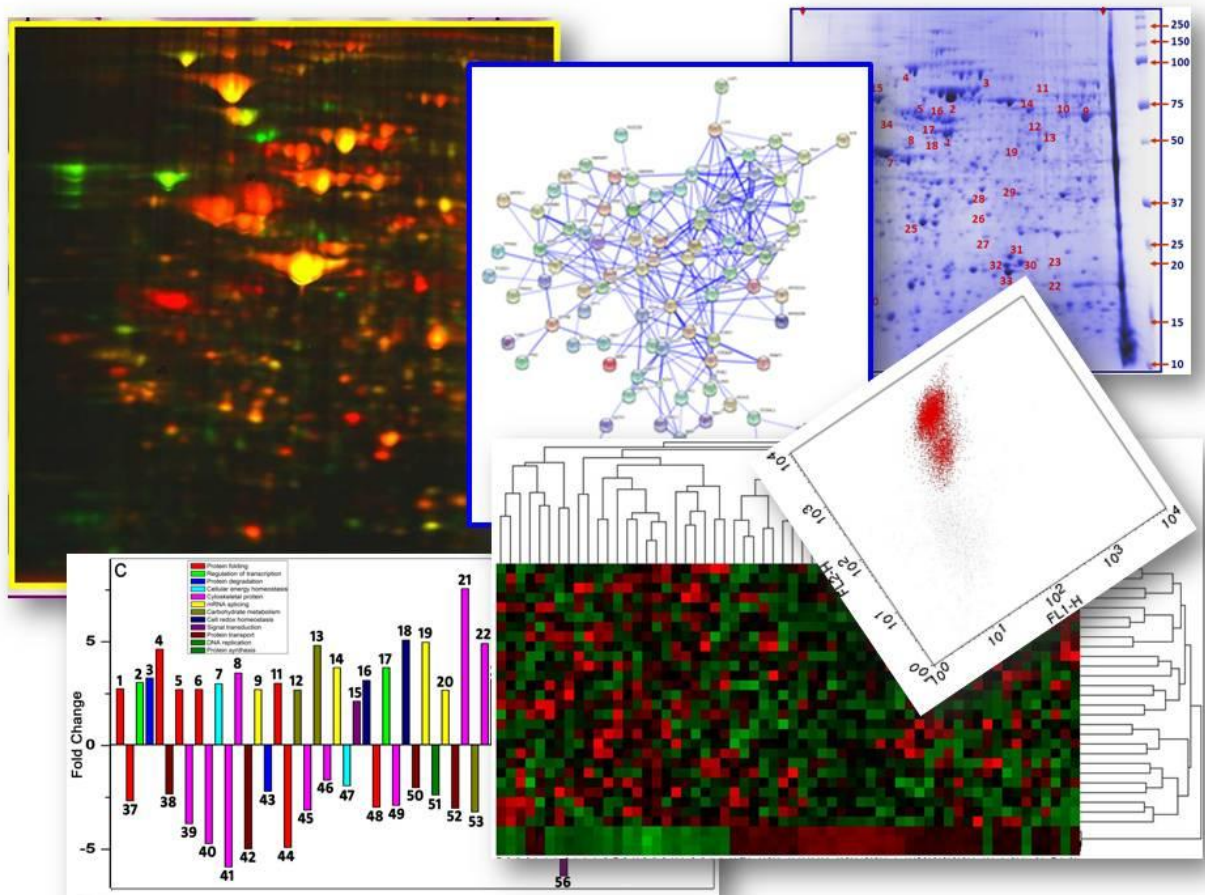
light on the mechanism of transformation of the cells from normal to malignant state. Identification of disease specific markers helps in diagnostic and prognostic monitoring of the malignancy and the associated minimal residual disease, but, disease regulated proteins in B-ALL are still unclear.

Since the proteome is strongly influenced by cell differentiation, a simple comparison of MNCs from different patients is likely to result in the identification of proteins whose apparent change in expression actually reflects a difference in the cellular composition of the specimens. Significant differences between primary tumour cells and immortalised cell lines, emphasizes the importance of obtaining protein profiling data from primary malignant B-cells, rather than immortalised cell lines. **CHAPTER 2** presents a comparative proteomic study of a homogeneous population of CD19⁺ cells from B-ALL patient samples and background-matched primary normal control cells using two-dimensional gel electrophoresis and MALDI-TOF/TOF tandem mass spectrometry. The study led to the identification of many proteins differentially regulated in B-ALL compared to normal controls. For a comprehensive analysis of the large proteome dataset and proper selection of significantly altered protein, a combination of univariate and multivariate statistics is employed. Multifactorial statistical analysis enlightens on the variation of each of the differentially regulated proteins with respect to that in others in a holistic perspective and might be helpful in interpreting the mechanism of leukemogenesis. Gene ontology (GO) annotation of the differentially regulated proteins reveals the functions and cellular localization of the de-regulated proteins. Functional partnerships between proteins are at the core of complex cellular phenotypes. The interactome of the observed de-regulations obtained through bioinformatics could propose research avenues for addressing the leukemogenic B-cell biology. Furthermore, candidate proteins which exhibit opposite trends of de-regulations in myeloid and lymphoid leukemia might not only point out prospective biomarkers but also enhance our knowledge on regulation of commitment and differentiation of the HSC into myeloid or lymphoid lineages.

2DGE based proteomic identification of differentially regulated plasma proteins might serve in a less-invasive (than bone-marrow aspiration) diagnostic and prognostic monitoring of B-ALL as well as detection of minimal residual disease. However, the protein content of blood plasma is dominated by a handful of proteins such as albumin, immunoglobulins, and lipoproteins present across an extraordinary dynamic range of concentration. This exceeds the analytical capabilities of traditional proteomic methods, making detection of lower abundance serum proteins extremely challenging. Reduction of sample complexity is thus an essential first step in the analysis of plasma proteome. As presented in **CHAPTER 3**, we used pre-fractionation of plasma proteins with ammonium sulphate, to reduce concentrations of high-abundance components and enrich lower abundant components in plasma 2DGE profiles, thereby facilitating the identification of disease markers. As most of the de-regulated proteins are involved in multiple physiological processes, the proteomic studies of blood plasma might also elucidate the pathophysiology and/or clinical manifestation of the B-ALL malignancy.

Like most of the other leukemic subtypes, B-ALL malignancies are presented with mild to severe anaemia. Moreover, several studies have reported abnormalities of the membrane cytoskeleton and enzyme activities of erythrocytes in myeloid as well as lymphoid leukaemias. These facts inspired us for a comparative study of the membrane and cytosol proteome of erythrocytes purified from peripheral blood of normal volunteers, B-ALL patients and patients suffering from a non-malignant haematological disorder like hereditary spherocytosis (HS) that may add insights to our understanding of altered erythrocyte physiology in leukaemia vs. erythroid disorders. **CHAPTER 4** presents a comparative study of the erythrocyte membrane and cytosol proteomes of normal, B-ALL and HS. However, proteomic analysis of erythrocyte cytosol had been handicapped by the large abundance of hemoglobin, masking majority of the other cytosolic proteins. We have used cation exchange chromatography to deplete hemoglobin very efficiently and specifically, and subsequently studied the hemoglobin depleted erythrocyte cytosol proteome.

Through this work, we emphasize upon the assets of proteomic studies over single protein detection assays in revealing differential regulation of different classes of proteins, simultaneously in a disease, which might be a step ahead in cutting through the complexity of heterogeneous diseases and explaining their pathophysiology and clinical manifestation.



CHAPTER 2

*Differentially regulated CD19⁺ B-cell
proteome in B-cell Acute Lymphoblastic Leukemia*

2.1 Introduction

B-ALL is the most common cancer in children and constitutes the major class of lymphoid leukemia. It is a clonal malignant disease that originates from genetic changes in the hematopoietic stem cell (HSC) and is characterized by an accumulation of blast B-cells that fail to differentiate, resulting in suppression of normal haematopoiesis. The cells in B-ALL are generally regarded as malignant counterparts of normal B-cell precursors. Immunophenotyping results establish that B-lineage leukaemias dominate within the lymphoid leukaemia groups in both children (where >80% ALLs are B-ALLs) and adults (>75%). Gene fusions like TEL-AML1, BCR-ABL, E2A-PBX1 and MLL rearrangements, created by chromosomal translocations are involved in the genesis of B-ALL. In human B-ALLs, BCR-ABL and MLL-involving translocations presumably originate in early progenitor (HSC or lymphoid-myeloid progenitor), while TEL-AML1- and E2A-PBX1-harbouring leukemic cells seem to represent more differentiated, lymphoid-committed precursors [14]. Although identification of the genetic abnormalities has led to an improved understanding of B-ALL pathophysiology, the mechanisms responsible for the B-cell developmental arrest are unknown. Nevertheless, the primary oncogenic events seem to require secondary cooperative changes to generate a fully transformed cell.

The treatment strategies for B-ALL include conventional chemotherapeutic anti-metabolites and nucleoside analogues that interfere with either different stages of DNA and protein synthesis or the integrity of mitotic spindle apparatus; monoclonal antibodies against leukaemia-associated antigens; and molecular therapies that target genetic abnormalities of the leukemic cells and their affected signalling pathways. Although contemporary treatments cure more than 80% of children with B-ALL, some patients fall in high risk and/or poor prognosis classes requiring intensive treatment, others exhibit drug resistance and many patients still develop serious acute and late complications like pancytopenia, CNS and extramedullary relapses, etc. owing to the side effects of the treatments. Furthermore, the survival rate for

adults with B-ALL remains below 40% despite the use of transplantation, and treatment outcome is poor among patients who relapse on current front-line ALL regimens [21]. The majority of relapse cases have a clear relationship to the diagnosis leukemic clone, either arising through the acquisition of additional genetic lesions or, more commonly, arising from an ancestral (pre-diagnosis) clone [77]. The initial excitement generated by the phenomenal success of a kinase inhibitor - imatinib, led to the expectation that other targeted therapeutics would be equally successful. Subsequent results indicated that although molecularly targeted agents might possess anti-leukemic activity, the responses they induce are seldom durable and certainly do not extend to all patients [78]. This sobering fact emphasizes the need to link targeted therapeutics to effective molecular diagnostic methods that will determine whether the signalling pathway that drives a particular case of ALL is targeted by the drug or the drugs under consideration for that leukaemia.

Proteomic studies for the identification of proteins aberrantly expressed in malignant B-cells can potentially be used to develop new diagnostic, prognostic or therapeutic targets. The knowledge that transcriptome data produces on genome-wide expression does not necessarily translate through to protein expression. The relatively low correlation between the abundance of a given mRNA and that of the encoded protein makes it important to characterize the protein profile or ‘proteome,’ of malignant cells directly. The difference between the protein and mRNA abundances may result from the influence of micro RNAs which are known to play an important role in the expression of proteins. Besides, the activities of many proteins are influenced by PTMs such as phosphorylation, glycosylation, methylation and proteolytic cleavage which can vary according to different physiological stages of a cell and are affected by metabolism, cell cycle, differentiation and cell death. Gene expression profiling has the disadvantage of being one step away from the targets of most drugs, namely proteins. But genetic studies facilitate formulation of rational hypotheses about the candidate “drivers” of neoplastic transformation. Proteomic studies of B-cell malignancies have made significant progress, but further studies are needed to increase our coverage of the B-cell malignant

proteome and to uncover new insights in B-cell biology [60]. 2DGE offers in essence a 2-step approach to separating complex protein mixtures in exquisite detail. Fluorescent labeling techniques with fluorescent cyanide (Cy) dyes can be used to label proteins prior to 2DGE. 2D-DIGE is then used to identify differences between normal (control) and aberrant (test) cells.

Given that the proteome is strongly influenced by cell differentiation, a simple comparison of mononuclear cells (MNCs) from different patients is likely to result in the identification of proteins whose apparent change in expression actually reflects a difference in the cellular composition of the specimens. Polypeptide differences between abnormally proliferating cells could be lineage related or could reflect, in part, the selective activation of genes that are not expressed in normal cells. To prevent such a complication and eliminate such population-shift effects, we isolated B-lymphoblasts on the basis of their surface expression of CD19 (and CD10). Comparison of such background-matched fractions should eliminate pseudopositive data that might result from different proportions of leukemic blasts or from differences in cell lineage to which the leukemic blasts are committed [79]. Our choice of CD antigen(s) was based on the information that early precursor-B cells express CD10 and CD19, and as the precursor-B stage ends, CD10 is no longer expressed.

With a 2DGE followed by MALDI TOF/TOF tandem mass spectrometry approach, we present here the comparative proteomic study of a homogeneous population of CD19⁺ cells from 27 B-ALL patients, that led to the identification of 60 differentially regulated proteins in the malignant CD19⁺ cells compared to normal primary CD19⁺ cells. Gene ontology (GO) annotation of the differentially regulated proteins revealed deregulation of several classes of proteins localized in almost all cellular compartments. Our study reveals that proteins participating in metabolism, folding and transport of proteins; regulation of transcription; cellular energy and redox homeostasis; cytoskeletal organization; RNA splicing; carbohydrate metabolism; signal transduction; and DNA replication are significantly de-regulated in the malignant cells. Multivariate statistics and principal component analysis (PCA) revealed age and genetic anomaly dependent variations in the malignant cell proteome. We have discussed

how the interactome of the observed de-regulations could propose research avenues for addressing the altered B-cell biology. Furthermore, candidate proteins which exhibit opposite trends of de-regulations in myeloid and lymphoid leukemia might not only point out prospective biomarkers but also enhance our knowledge on the regulation of differentiation of the HSC into myeloid or lymphoid lineages.

2.2 Materials and Methods

2.2.1 B-ALL patient samples and enrichment of CD19⁺ cells

Bone marrow and peripheral blood samples were obtained from B-ALL patients after informed consent and following institutional ethical guidelines. Characteristics of individual patient samples are provided in Table 2.1.

Table 2.1: Clinical Details of Leukemia Patients

Patient Identity	Age	Sex	Clinical Details	Immunophenotype / Classification
B-ALL 1	33 yrs	F	Hb-6.0 g/dL, TLC-3,900 cells/mm ³	87% CD10 ⁺ high/CD19 ⁺ high cells. CD34 ⁺ het, CD13 ⁻ , CD38 ⁺ high Pre-B-ALL
B-ALL 2 *	13 yrs	M	Hb-7.9 g/dL, TLC-15,000 cells/mm ³	70.6% CD10 ⁺ int/CD19 ⁺ high cells. CD34 ⁺ het, CD13 ⁻ , CD38 ⁺ int Pre-B-ALL
B-ALL 3	7 yrs	M	Hb-5.9 g/dL, TLC-95,000 cells/mm ³	79% CD10 ⁺ high/CD19 ⁺ high cells. CD34 ⁺ het, CD13 ⁻ , CD38 ⁺ high Pre-B-ALL
B-ALL 4	14 yrs	F	Hb-8.6 g/dL, TLC-57,000 cells/mm ³	76.5% CD10 ⁺ high/CD19 ⁺ high cells. CD34 ⁺ het, CD13 ⁻ , CD38 ⁺ high Pre-B-ALL
B-ALL 5	16 yrs	M	Hb-10.1g/dL, TLC-8,500 cells/mm ³	94.6% CD10 ⁺ high/CD19 ⁺ high cells. CD34 ⁺ het, CD13 ⁻ , CD38 ⁺ high Pre-B-ALL
B-ALL 6	8 yrs	F	Hb-6.3 g/dL, TLC-1,22,000 cells/mm ³	81% CD10 ⁺ low/CD19 ⁺ high cells. CD13 ⁺ , CD34 ⁺ low, CD38 ⁺ het Pre-B-ALL
B-ALL 7 *	25 yrs	F	Hb-5.5 g/dL, TLC-89,000 cells/mm ³	64.4% CD10 ⁺ high/CD19 ⁺ high cells. CD34 ⁺ het, CD13 ⁻ , CD38 ⁺ high Pre-B-ALL
B-ALL 8	56 yrs	F	TLC-80,600 cells/ mm ³	79.0% CD10 ⁺ high/CD19 ⁺ high cells. CD13 ⁺ , CD34 ⁺ , CD38 ⁺ het Pre-B-ALL
B-ALL 9	9 months	M	Hb-8.2 g/dL, TLC-66,000 cells/mm ³	85% CD10 ⁺ high/CD19 ⁺ high cells. CD34 ⁺ het, CD13 ⁻ , CD38 ⁺ high Pre-B-ALL

Table 2.1:contd.

Patient Identity	Age	Sex	Clinical Details	Immunophenotype / Classification
B-ALL 10	13 yrs	F	Hb-6.6 g/dL, TLC-72,000 cells/mm ³	71% CD10 ⁺ low/CD19 ⁺ high cells. CD13 ⁺ , CD34 ⁺ low, CD38 ⁺ het Pre-B-ALL
B-ALL 11 *	16 yrs	F	Hb-4.7 g/dL, TLC-1,20,000 cells/mm ³	80.8% CD10 ⁺ high/CD19 ⁺ high cells. CD34 ⁺ het, CD13 ⁻ , CD38 ⁺ high Pre-B-ALL
B-ALL 12	2&1/2 months	M	Hb-3.6 g/dL, TLC-2,70,000 cells/mm ³	91.1% CD10 ⁺ high/CD19 ⁺ high cells. CD13 ⁺ , CD34 ⁺ , CD38 ⁺ het Pre-B-ALL
B-ALL 13	13 yrs	F	Hb-7.4 g/dL, TLC-89,000 cells/mm ³	82.6% CD10 ⁺ low/CD19 ⁺ high cells. CD13 ⁺ , CD34 ⁺ low, CD38 ⁺ het Pre-B-ALL
B-ALL 14	12 yrs	M	Hb-5.9 g/dL, TLC-94,000 cells/mm ³	89% CD10 ⁺ high/CD19 ⁺ high cells. CD34 ⁺ het, CD13 ⁻ , CD38 ⁺ high Pre-B-ALL
B-ALL 15	5 yrs	M	Hb-7.5 g/dL, TLC-57,600 cells/ mm ³	78.3% CD10 ⁺ high/CD19 ⁺ high cells. CD34 ⁺ het, CD13 ⁻ , CD38 ⁺ high Pre-B-ALL
B-ALL 16	29 yrs	F	Hb-4.0g/dL, TLC-3,14,000 cells/ mm ³	92.6% CD10 ⁺ low/CD19 ⁺ high cells. CD13 ⁺ low, CD34 ⁺ low, CD38 ⁺ het Pre-B-ALL
B-ALL 17	11 yrs	F	Hb-3.9 g/dL, TLC-42,000 cells/mm ³	90.5% CD10 ⁺ high/CD19 ⁺ high cells. CD34 ⁺ het, CD13 ⁻ , CD38 ⁺ high Pre-B-ALL
B-ALL 18	9 yrs	M	Hb-4.8 g/dL, TLC-77,000 cells/mm ³	83% CD10 ⁺ high/CD19 ⁺ high cells. CD34 ⁺ het, CD13 ⁻ , CD38 ⁺ high Pre-B-ALL
B-ALL 19	7 yrs	F	Hb-3.7 g/dL, TLC-45,000 cells/mm ³	76.2% CD10 ⁺ int/CD19 ⁺ high cells. CD34 ⁺ het, CD13 ⁻ , CD38 ⁺ int Pre-B-ALL
B-ALL 20	6 yrs	F	Hb-7.4 g/dL, TLC-1,35,000 cells/mm ³	77.4% CD10 ⁺ high/CD19 ⁺ high cells. CD34 ⁺ het, CD13 ⁻ , CD38 ⁺ high Pre-B-ALL
B-ALL 21	28 yrs	M	Hb-6.8 g/dL, TLC-1,63,000 cells/mm ³	95.0% CD10 ⁺ low/CD19 ⁺ high cells. CD13 ⁺ , CD34 ⁺ low, CD38 ⁺ het Pre-B-ALL
B-ALL 22	24 yrs	M	Hb-5.7 g/dL, TLC-87,000 cells/mm ³	69.7% CD10 ⁺ high/CD19 ⁺ high cells. CD34 ⁺ het, CD13 ⁻ , CD38 ⁺ high Pre-B-ALL
B-ALL 23	13 yrs	F	Hb-4.4 g/dL, TLC-39,000 cells/mm ³	77% CD10 ⁺ int/CD19 ⁺ high cells. CD34 ⁺ het, CD13 ⁻ , CD38 ⁺ int Pre-B-ALL
B-ALL 24	36 yrs	M	Hb-8.1 g/dL, TLC-55,000 cells/mm ³	84.3% CD10 ⁺ high/CD19 ⁺ high cells. CD34 ⁺ het, CD13 ⁻ , CD38 ⁺ high Pre-B-ALL
B-ALL 25	27 yrs	F	Hb-3.7 g/dL, TLC-1,19,000 cells/mm ³	67% CD10 ⁺ low/CD19 ⁺ high cells. CD13 ⁺ , CD34 ⁺ , CD38 ⁺ het Pre-B-ALL
B-ALL 26	15 yrs	M	Hb-7.9 g/dL, TLC-22,000 cells/mm ³	72% CD10 ⁺ high/CD19 ⁺ high cells. CD34 ⁺ het, CD13 ⁻ , CD38 ⁺ high Pre-B-ALL

Table 2.1:contd.

Patient Identity	Age	Sex	Clinical Details	Immunophenotype / Classification
B-ALL 27	8 yrs	F	Hb-7.9 g/dL, TLC-74,000 cells/mm ³	88.3% CD10 ⁺ high/CD19 ⁺ high cells. CD34 ⁺ het, CD13 ⁻ , CD38 ⁺ high Pre-B-ALL
B-ALL 28 [#]	12 yrs	F	Hb-9.5 g/dL, TLC-68,000 cells/mm ³	86.7% CD10 ⁺ high/CD19 ⁺ high cells. CD34 ⁺ het, CD13 ⁻ , CD38 ⁺ high Pre-B-ALL
B-ALL 29 [#]	19 yrs	F	Hb-5.2 g/dL, TLC-93,000 cells/mm ³	78.6% CD10 ⁺ low/CD19 ⁺ high cells. CD13 ⁺ , CD34 ⁺ low, CD38 ⁺ het Pre-B-ALL
B-ALL 30 [#]	11 yrs	M	Hb-6.7 g/dL, TLC-74,000 cells/mm ³	79.9% CD10 ⁺ high/CD19 ⁺ high cells. CD34 ⁺ het, CD13 ⁻ , CD38 ⁺ high Pre-B-ALL
AML 1 *	9 yrs	M	Hb- 7.8 g/dL, TLC-1, 69,000 cells/mm ³	18% CD19 ⁺ , 6% CD2 ⁺ , 82% CD13 ⁺ , 69% CD33 ⁺ cells. AML
AML 2 *	15 yrs	F	Hb-2.9 g/dL, TLC- 2, 67,000 cells/mm ³	15% CD19 ⁺ , 2% CD2 ⁺ , 82% CD13 ⁺ , 31% CD33 ⁺ cells. AML (FAB M1)
AML 3 *	18 yrs	M	Hb-6.3 g/dL, TLC-1,89,000 cells/mm ³	19% CD19 ⁺ , 3.5% CD2 ⁺ , 80% CD13 ⁺ , 51% CD33 ⁺ cells. AML (FAB M1)

*# Patient samples used in 2D-DIGE experiments; * Patient samples used in western immunoblots analysis*

Leukemic blasts were isolated by Ficoll-Paque (1.077, Sigma, St Louis, MO, USA), and CD19⁺ progenitors were then enriched by immunomagnetic separation (Miltenyi Biotec, Bergisch, Gladbach, Germany). CD19⁺ populations were > 95% pure as determined by flow cytometry. Purified CD19⁺ B cells from normal individuals were purchased from Lonza-Poietics (Walkersville, MD USA), and also sorted from Peripheral Blood Mononuclear Cells (PBMCs) using FACS.

2.2.2 Two dimensional gel electrophoresis, staining and image analysis

CD19⁺ cells were lysed in lysis buffer {1M HEPES, 1M NaCl, 20% (v/v) Glycerol, 1% (v/v) NP-40, 0.1M MgCl₂, 0.5M EDTA, 0.1M EGTA, 1M PMSF} and proteins precipitated using chilled acetone. Protein lysates prepared from 10⁶ pure CD19⁺ cells were re-suspended in 350 µl of 2D rehydration buffer {7M urea, 2M Thiourea, 2% (w/v) CHAPS, 0.05% Bio-lyte 3-10 ampholyte, 20 mM DTT (Bio-Rad, Hercules, CA), Protease inhibitor (Roche Diagnostics, Basel, Switzerland)}. The protein concentrations of the samples were estimated using RC DC

protein estimation kit (Bio-Rad), and an absolute amount of 1.8 mg for Coomassie staining, or 600 µg for silver staining, or 1.2 mg for SYPRO RUBY staining, was taken to 2DGE. 17 cm pH 3-10 IPG strips (Bio-Rad) were passively rehydrated or cup-loaded with the protein samples. IEF was carried out in a Protean IEF cell (Bio-Rad), stepwise up to 120000 Volt-Hours. Equilibration of the strips post IEF was performed following published protocol [80]. The second dimension was run on 8-16% polyacrylamide gradient gels in a Protean II XL electrophoresis module (Bio-Rad). Gels were stained either with Blue Silver Coomassie [32] or SYPRO-RUBY (Sigma-Aldrich, Seelze, Germany) according to manufacturer's instructions, or Silver stain according to the method used earlier [80]. Image captures and analyses were done on Versa Doc series 3000 imaging system using PDQuest software version 7.1 (Bio-Rad). Densitometry analysis of the gel spots of interest was performed using the density tool of PDQuest. Spot volume (intensity) of the desired spot(s) was normalized as parts per million (ppm) of the total spot volume using the spots that were present in all gels, to calculate the relative abundance of a spot in a sample.

2.2.3 Data Analysis

For statistical evaluation of the differences observed in 2DGE for each of the 60 proteins, densitometry data were subjected to both parametric student's t-test and non-parametric Wilcoxon-Mann-Whitney test. For multivariate Principal Component Analysis (PCA), the densitometry data served as the source for the initial matrix with 60 columns (protein spots/spot clusters as 'variables') and 30 rows (27+3 sample gels as 'observations'). A column vector of binary values (zeroes and ones) indicated the group membership (normal or B-ALL) of the samples. Group scaling of the data was done prior to PCA in order to deal with the heterogeneous variation in the spot volumes [81]. The statistical calculations of the principal components were calculated by finding the eigenvalues and eigenvectors of the covariance matrix. These calculations were performed using XLSTAT software, version 2011. The quantitative differences of selected candidate proteins were verified in two independent experimental series. The contribution of the differences in protein abundance of the

differentially expressed proteins to distinguish between normal and B-ALL populations was assessed from the squared cosines of the variables (protein spots/spot clusters).

2.2.4 CyDye labelling, 2D-DIGE and image analysis

Total protein was extracted from CD19⁺ cells using sample lysis buffer (7 M urea, 2 M Thiourea, 30 mM Tris, 4% (w/v) CHAPS, 1 mM PMSF and 1% protease inhibitor cocktail. After estimation of protein concentration, equal amounts of protein sample from normal and B-ALL CD19⁺ cells were used for subsequent DIGE analysis. The pH values of the desalted samples were adjusted to 8.5 with 100 mM sodium hydroxide before labeling. Proteins were labelled with CyDye Fluor minimal dyes (GE Healthcare) according to the manufacturer's recommended protocols. The internal standard (IS) was comprised of a pooled equal amount from normal and B-ALL experimental samples. A total of 80 µg of protein from the normal and B-ALL samples were labelled with 400 pmol of either Cy3, Cy5, or Cy2 (Cy2 was used to label the IS). The labelled mixtures were combined, cleaned up using 2D CleanUp kit, Bio-Rad, and then re-suspended in 2D rehydration buffer (7 M urea, 2 M Thiourea, 2% CHAPS, 0.05% Bio-lyte 3-10 ampholyte, 20 mM DTT, and Protease inhibitor) prior to IEF and subsequent SDS-PAGE. All electrophoresis procedures were performed in the dark. Gels were scanned using a Typhoon™ Trio Series Variable Mode Image (GE Healthcare) at 100 µm resolution, followed by SYPRO-RUBY staining. The resulting gel images generated from triplicate gels were analyzed using Differential In gel Analysis (DIA) module of DeCyder software (GE Healthcare).

2.2.5 In-Gel tryptic digestion and mass spectrometry

Sequencing grade trypsin was purchased from Promega (Madison, WI). All other reagents were purchased from Pierce (Rockford, USA). The protein spots from Coomassie and SYPRO-RUBY stained 2D gels were excised using a robotic spot-cutter (Bio-Rad). The gel pieces were de-stained with 50% acetonitrile, 25mM ammonium bicarbonate. Subsequent in-gel tryptic digestion, peptide elution, acquisition of MS and MS/MS spectra and database searches were done following our published protocol [80]. Recrystallized CHCA and 2, 5-DHB (Sigma) were

used as matrices. MS of the digested peptides was done in positive reflector mode in a MALDI-TOF/TOF tandem mass spectrometer (Applied Biosystems, AB 4700). Autolytic and common keratin peaks were validated and subsequently excluded from MS/MS analysis. Twelve most intense peptides from each spot were subjected to MS/MS analysis. Peak lists were prepared from MS and MS/MS data using GPS explorer V3.6 (Applied Biosystems) software and noise reduction and de-isotoping were performed using default settings. Resulting PMF and MS/MS data were searched against human MSDB and Swiss-Prot databases using in-house MASCOT V2.1 (Matrix Science, UK) server and MOWSE score (with $p < 0.05$) was considered to determine significant hits. For homologous proteins having similar MOWSE scores, preference was given to the protein with best match between theoretical and experimental molecular weight and pI. All MS experiments were repeated at least thrice, with spots excised from three separate gels. The database search parameters included one missed cleavage, error tolerance of ± 100 ppm for PMF and ± 1.2 Da for MS/MS ion search and variable modifications like carbamidomethyl cysteine, methionine oxidation, and N-terminal acetylation.

2.2.6 Western immunoblotting

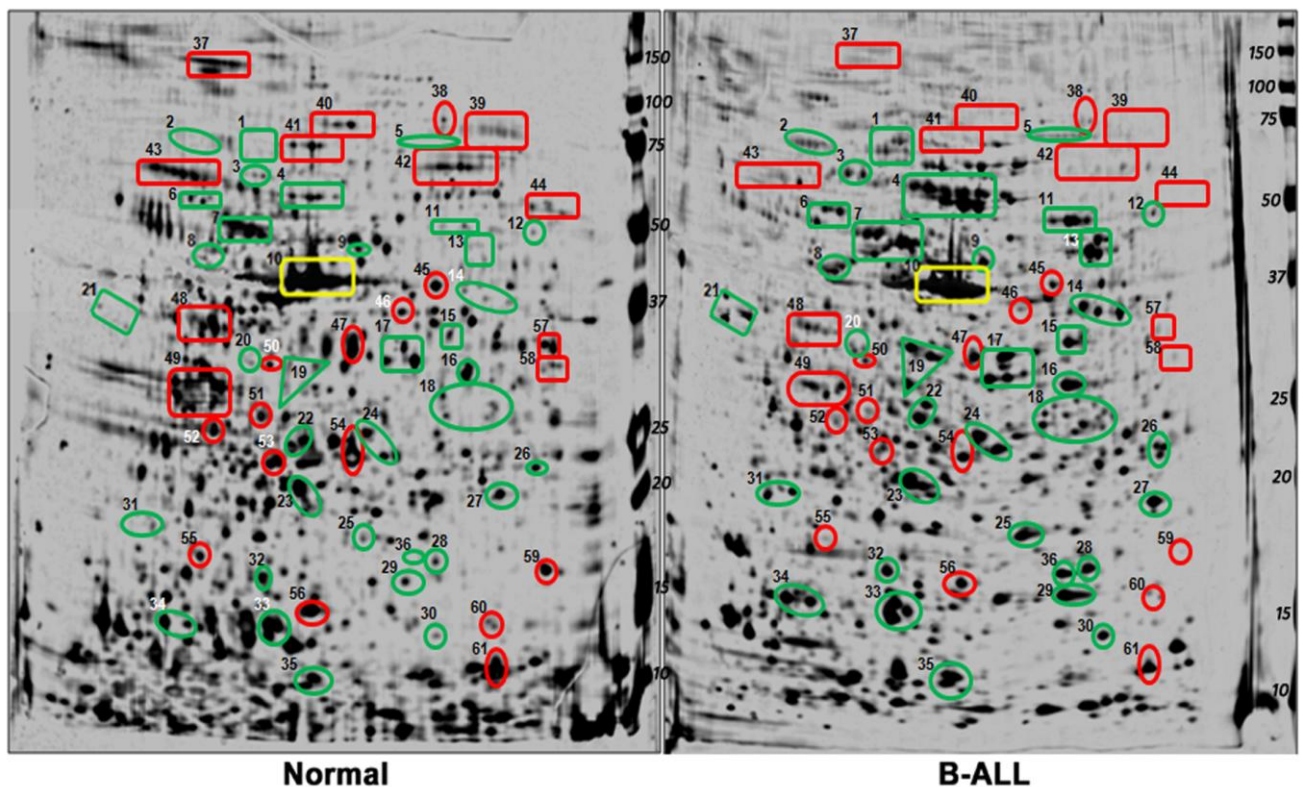
Protein samples (25 μ g) were re-suspended in 30 μ L SDS-PAGE buffer (2% mercaptoethanol, 1% SDS, 12% glycerol, 50mM Tris-HCl and trace amount bromophenol blue), heated at 95 °C for 5 min, cooled and loaded directly onto 12% gel. 1D-SDS-PAGE was performed in a Mini Protean III-cell (Bio-Rad) using Tris-glycine with 0.1% SDS, following manufacturer's instructions. Proteins separated on gel were blotted onto PVDF membranes and subsequently blocked with Tris-buffer-saline (TBS), 5% non fat dry milk for 2h at room temperature. Primary antibodies for nucleophosmin and β -actin (Abcam) were diluted in TBS/0.1% Tween (TBST) following manufacturer's protocol. β -actin was used as loading control. Anti-rabbit or anti-mouse HRP-conjugated IgGs were used as secondary antibodies (Abcam). Blots were probed with respective primary and HRP-conjugated secondary antibodies, washed with TBST and detected by ECL (Pierce).

2.3 Results

2.3.1 Identification of differentially expressed proteins in B-ALL CD19⁺ cells

Figure 2.1 shows representative filtered/gaussian images of silver-stained 2D gels for CD19⁺ cells from B-ALL patients and normal controls. Most polypeptides in two-dimensional gels occurred as part of recognizable constellations of spots. These constellations were uniformly identifiable in gel patterns of different cell types and served as landmarks. For any patient, there was no recognizable difference between the patterns of blasts derived from bone marrow and from peripheral blood. PDQuest based densitometric comparison of the 27 B-ALL and 3 normal proteome profiles, followed by parametric and non-parametric statistical evaluation of observed differences (student's t-test, Wilcoxon-Mann-Whitney test) identified >100 spots/spot-clusters that showed a significant difference in abundance between B-ALL and normal proteomes.

Figure 2.1: Representative two dimensional proteome maps of CD19⁺ cells from normal controls and B-ALL patients. Red and green boxes respectively represent proteins down-regulated and up-regulated in B-ALL; Yellow box indicates the internal control (β -actin)



Peptide mass fingerprinting and tandem mass spectrometry by MALDI-TOF/TOF of these spots/spot-clusters resulted in the identification of the corresponding 60 proteins differentially regulated in the leukemic B-lymphocytes, of which 35 were up-regulated and 25 were down-regulated. The spot for β -actin did not show any significant difference in expression between B-ALL and normal B-cell proteomes, and hence chosen to serve as the internal control. Figure 2.2 shows a heat map generated from the B-cell expression profiles for the 61 proteins in each of the 30 individuals (27 B-ALL and 3 normal). Table 2.2 provides a list of the differentially regulated proteins together with the fold changes, p-values and summary of mass spectrometry identification. The mass spectrometry data have been submitted to the PRIDE proteomics identifications database and are available at <http://tinyurl.com/3wq7m49>.

Figure 2.2: Heat map of the expression levels of differentially regulated proteins in normal and B-ALL samples; and cluster analysis of the expression profiles

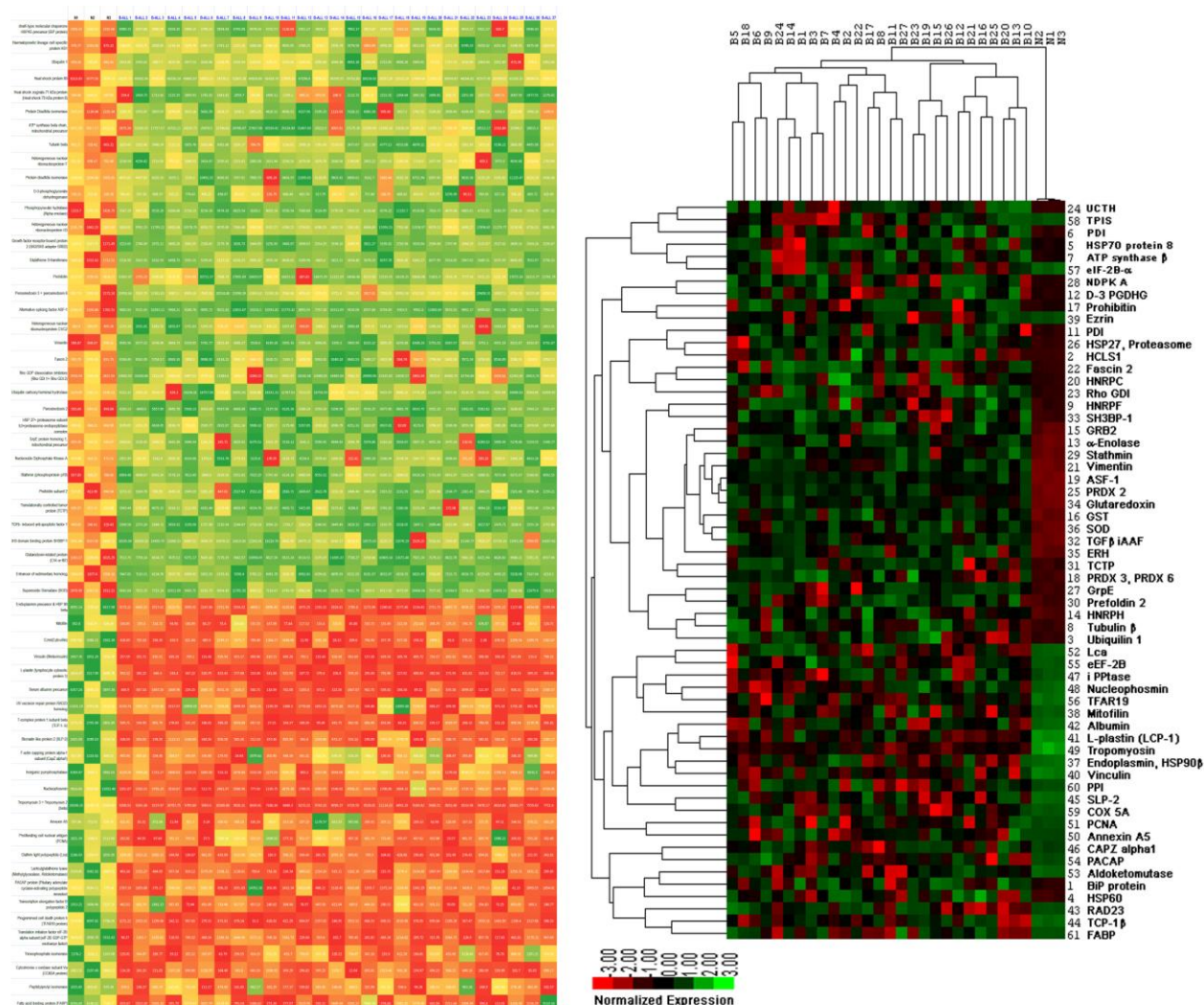


Table 2.2: Identification of differentially regulated proteins in B-ALL CD19⁺ proteome

Spot No.	Protein Name	Fold Change	p-value		Mascot score	MW (kD)	pI	Sequence Coverage	MS/MS matches
			t-test	WMW test					
1	DnaK-type molecular chaperone HSPA5 precursor (BiP protein)	2.74	0.028	0.015	503	72	5.03	58%	6
2	Haematopoietic lineage cell specific protein HS1	3.04	0.0265	<0.001	108	54	4.74	48%	4
3	Ubiquitin 1	3.26	0.0367	0.003	191	62.5	5.02	37%	6
4	Heat shock protein 60	4.64	0.0296	<0.001	312	61	5.7	61%	6
5	Heat shock cognate 71 kDa protein (Heat shock 70 kDa protein 8)	2.7	0.0388	0.046	215	71	5.37	31%	4
6	Protein Disulfide isomerase	2.71	0.0138	0.015	245	57	4.76	62%	7
7	ATP synthase beta chain, mitochondrial precursor	2.98	0.0454	0.033	563	56.5	5.26	73%	11
8	Tubulin b	3.49	0.0344	0.002	436	49.6	4.78	57%	10
9	Heterogeneous nuclear ribonucleoprotein F	2.7	0.0149	0.003	171	46	5.38	51%	3
10	Actin beta (<i>Internal Control</i>)	-	-	-	275	40.98	5.56	67%	4
11	Protein disulfide isomerase	3	0.0092	0.011	120	57	6.1	58%	7
12	D-3-phosphoglycerate dehydrogenase	2.68	0.034	0.026	215	56.5	6.31	36%	6
13	Phosphopyruvate hydratase (Alpha enolase)	4.82	<0.0001	<0.001	227	47	6.99	38%	7
14	Heterogeneous nuclear ribonucleoprotein H3	3.75	0.0034	<0.001	219	49	5.89	65%	3
15	Growth factor receptor-bound protein 2 (SH2/SH3 adaptor GRB2)	2.14	0.0392	0.041	109	25.19	5.89	34%	3

Table 2.2: contd.

Spot No.	Protein Name	Fold Change	p-value		Mascot score	MW (kD)	pI	Sequence Coverage	MS/MS matches
			t-test	WMW test					
16	Glutathione S-transferase	3.14	< 0.0001	< 0.001	296	23.2	5.44	46%	3
17	Prohibitin	3.75	0.0243	0.020	192	30	5.57	55%	5
18	Peroxioredoxin 3 + peroxioredoxin 6	5.08	0.0405	0.002	94 129	27.6 24.9	7.67 6.02	27% 65%	3 6
19	Alternative splicing factor ASF-1	4.98	< 0.0001	< 0.001	108	22.5	7.72	48%	4
20	Heterogeneous nuclear ribonucleoprotein C1/C2	2.67	0.0332	0.011	329	32	5.1	65%	5
21	Vimentin	7.56	< 0.0001	< 0.001	50	53.5	5.06	38%	-
22	Fascin 2	4.92	0.0281	0.008	59	55	7.95	20%	1
23	Rho GDP dissociation inhibitors Ly-GDI + Rho GDI 1+ Rho GDI 2	3.2	0.0315	0.015	179 167	23.2 22.97	5.02 5.1	34% 74%	3 3
24	Ubiquitin carboxyl terminal hydrolase	6.6	0.0216	0.003	85	26.2	4.84	53%	3
25	Peroxioredoxin 2	8.25	< 0.0001	< 0.001	255	21.75	5.67	49%	2
26	HSP 27+ proteasome subunit b3+proteasome endopeptidase complex	5.6	0.0049	0.003	123 112 72	22.77 22.93 25.88	5.98 6.14 6.92	40% 49% 58%	3 3 3
27	GrpE protein homolog 1, mitochondrial precursor	7.36	0.0026	0.011	89	24.26	8.24	52%	2
28	Nucleoside Diphosphate Kinase A	5.69	0.0385	0.041	186	17.14	5.83	76%	3
29	Stathmin (phosphoprotein p19)	7.29	< 0.0001	< 0.001	211	17.16	5.77	62%	3
30	Prefoldin subunit 2	3.54	0.0035	0.002	145	16.64	6.2	53%	4
31	Translationally controlled tumor protein (TCTP)	4.12	0.0034	0.003	70	19.58	4.84	50%	4

Table 2.2: contd.

Spot No.	Protein Name	Fold Change	p-value		Mascot score	MW (kD)	pI	Sequence Coverage	MS/MS matches
			t-test	WMW test					
32	TGFb- induced anti-apoptotic factor 1	6.22	< 0.0001	< 0.001	57	12.41	8.35	80%	1
33	SH3 domain binding protein SH3BP-1	3.34	0.0114	0.011	66	10.43	4.82	47%	1
34	Glutaredoxin-related protein C14 or f87	6.78	< 0.0001	< 0.001	93	16.62	6.28	35%	2
35	Enhancer of rudimentary homolog	3.61	< 0.0001	< 0.001	91	12.25	5.63	46%	1
36	Superoxide Dismutase (SOD)	3.82	< 0.0001	< 0.001	93	15.8	5.7	30%	2
37	Endoplasmin precursor + HSP 90 beta	-2.66	< 0.0001	< 0.001	50 220	92.41 83.08	4.76 4.97	20% 36%	2 5
38	Mitofilin	-2.33	0.0004	0.005	61	83.63	6.08	32%	1
39	Ezrin(Cytovillin)	-3.76	< 0.0001	< 0.001	139	69.23	5.95	35%	3
40	Vinculin (Metavinculin)	-4.72	< 0.0001	0.006	56	123.59	5.51	21%	2
41	L-plastin(lymphocyte cytosolic protein 1)	-5.85	< 0.0001	< 0.001	98	70.25	5.2	50%	1
42	Serum albumin precursor	-4.98	< 0.0001	< 0.001	124	69.32	5.92	32%	3
43	UV excision repair protein RAD23 homolog	-2.2	0.0107	0.011	179	43.15	4.79	23%	4
44	T-complex protein 1 subunit beta (TCP-1-b)	-4.91	< 0.0001	< 0.001	134	57.32	6.02	71%	5
45	Stomatin like protein 2 SLP-2)	-3.11	< 0.0001	< 0.001	168	38.52	6.88	51%	5
46	F-actin capping protein alpha-1 subunit (CapZ alpha1)	-1.67	0.0421	0.041	90	32.9	5.45	52%	5
47	Inorganic pyrophosphatase	-1.94	0.0025	0.003	242	32.64	5.54	49%	6
48	Nucleophosmin	-2.97	< 0.0001	0.001	261	32.44	4.67	45%	5

Table 2.2: contd.

Spot No.	Protein Name	Fold Change	p-value		Mascot score	MW (kD)	pI	Sequence Coverage	MS/MS matches
			t-test	WMW test					
49	Tropomyosin 3 + Tropomyosin 2 (beta)	-2.88	< 0.0001	< 0.001	218	28.91	4.72	47%	4
					160	32.76	4.64	44%	3
50	Annexin A5	-2.03	0.0448	0.049	61	35.78	4.94	46%	1
51	Proliferating cell nuclear antigen (PCNA)	-2.38	0.0045	0.008	83	28.75	4.57	46%	2
52	Clathrin light polypeptide (Lca)	-3.02	< 0.0001	< 0.001	119	23.65	4.45	35%	2
53	Lactoylglytathione lyase (Methylglyoxalase, Aldoketomutase)	-3.2	< 0.0001	< 0.001	134	20.58	5.25	36%	4
54	PACAP protein (Pituitary adenylate cyclase-activating polypeptide receptor)	-2.56	0.0105	0.003	102	20.68	5.37	70%	2
55	Transcription elongation factor B polypeptide 2	-2.72	< 0.0001	0.002	57	13.13	4.73	19%	2
56	Programmed cell death protein 5 (TFAR19 protein)	-6.28	< 0.0001	< 0.001	101	14.15	5.78	67%	1
57	Translation initiation factor eIF-2B alpha subunit (eIF-2B GDP-GTP exchange factor)	-3.78	< 0.0001	< 0.001	54	33.69	6.9	29%	3
58	Triosephosphate isomerase	-2.42	0.0017	0.003	340	26.52	6.51	64%	9
59	Cytochrome c oxidase subunit Va (COX5A protein)	-3.32	< 0.0001	< 0.001	117	16.75	6.3	54%	5
60	Peptidylprolyl isomerase	-1.93	0.0096	0.005	85	17.87	7.82	73%	1
61	Fatty acid binding protein (FABP)	-2.84	0.0015	0.005	157	15.02	6.84	76%	3

2.3.2 PCA analysis

For optimum analysis of proteome data, a proper approach for selection of significant spots is a combination of univariate and multivariate analysis that also enlightens on the variation of each of the differentially regulated proteins with respect to that in others in a holistic perspective. Hence, for a comprehensive analysis of the large dataset, we employed multifactorial PCA to evaluate the quantitative changes in protein expression obtained on analysing 2DGE data. PCA is a classification procedure using numeric taxonomy in which the taxonomic distance is given by a relative hyperdimensional distance in the chosen projection planes. The principal components are measures of truly different ‘dimensions’ in the data set with lack of abundant correlations [82]. On PCA of our densitometry data, the first two principal components (PC 1&2) covered 61.13% of the total variance. The scores of the first principal component in the PCA models based on the 61-spot subset showed a consistent grouping in that the group of normal and B-ALL had scores of opposite signs, and only a small within-group scattering. Figure 2.3 illustrates the spatial distribution of gel samples and protein spots using a 2D PCA-biplot-space projection.

Figure 2.3(A): Distribution of gel samples (blue) and protein spots (red) in a 2D PCA-biplot-space projection

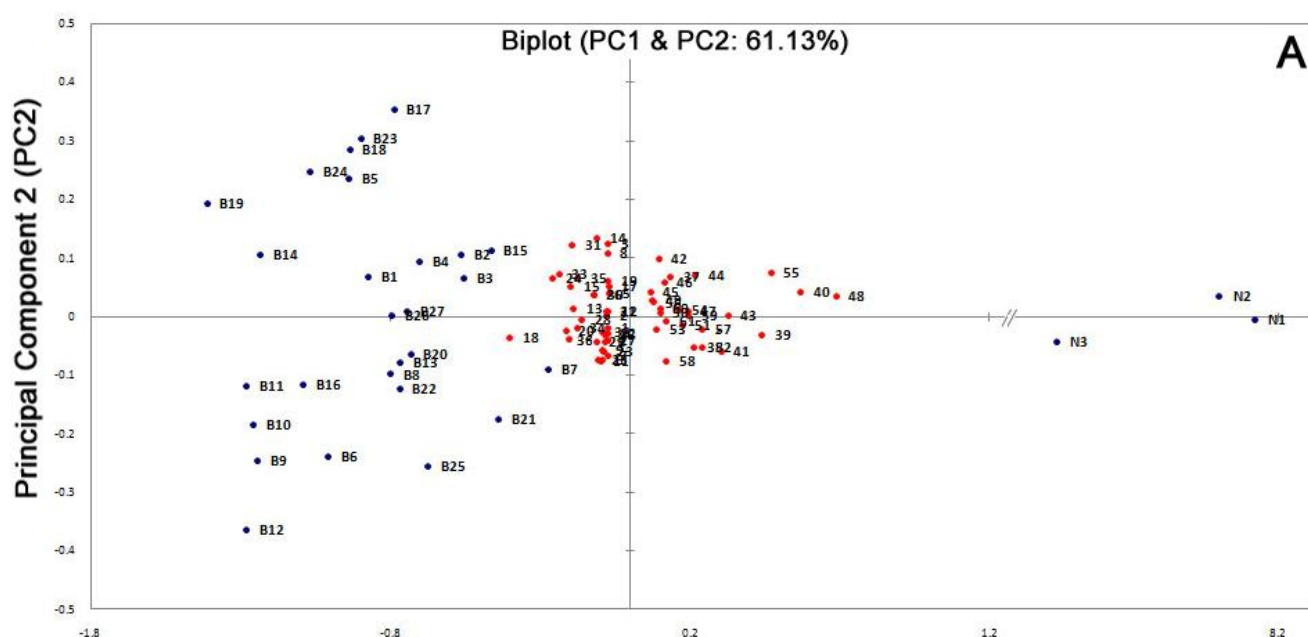
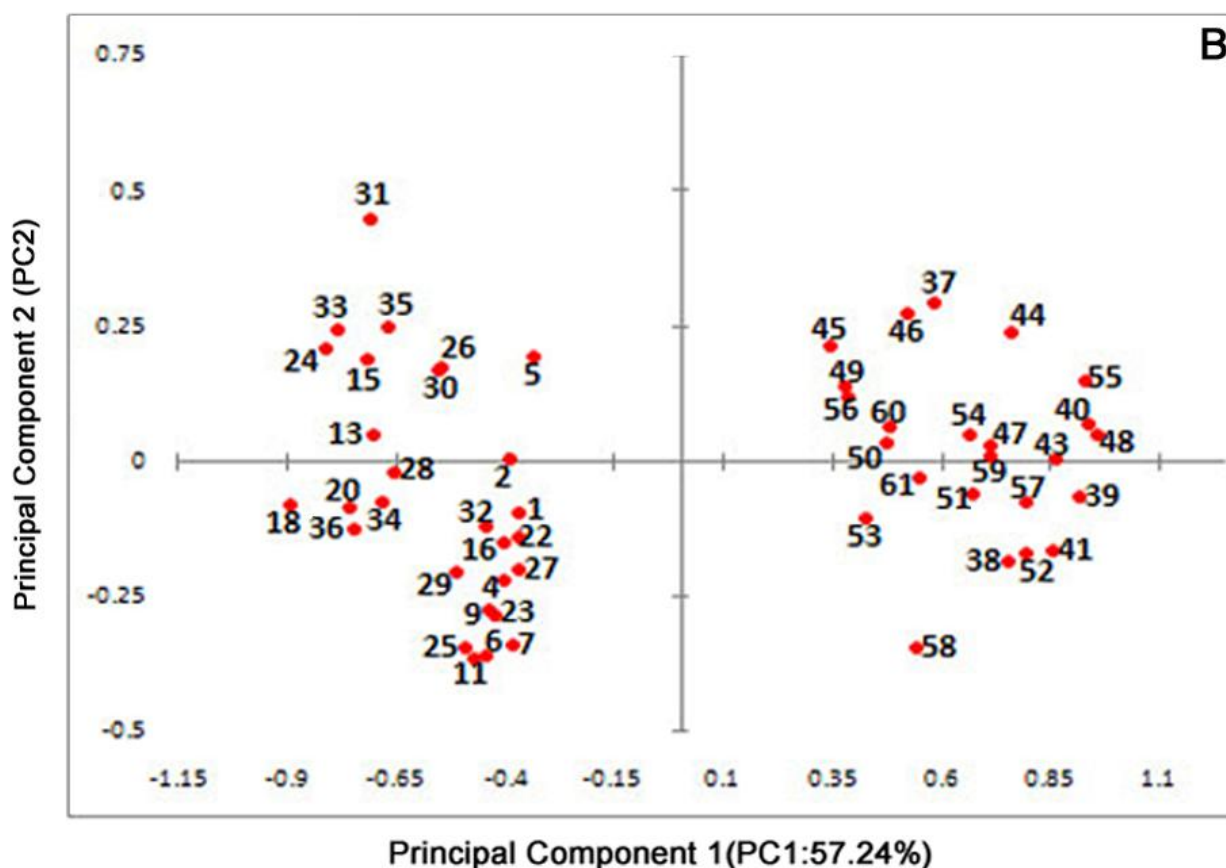


Figure 2.3(B): Magnified projection of protein spots in a 2D PCA-space

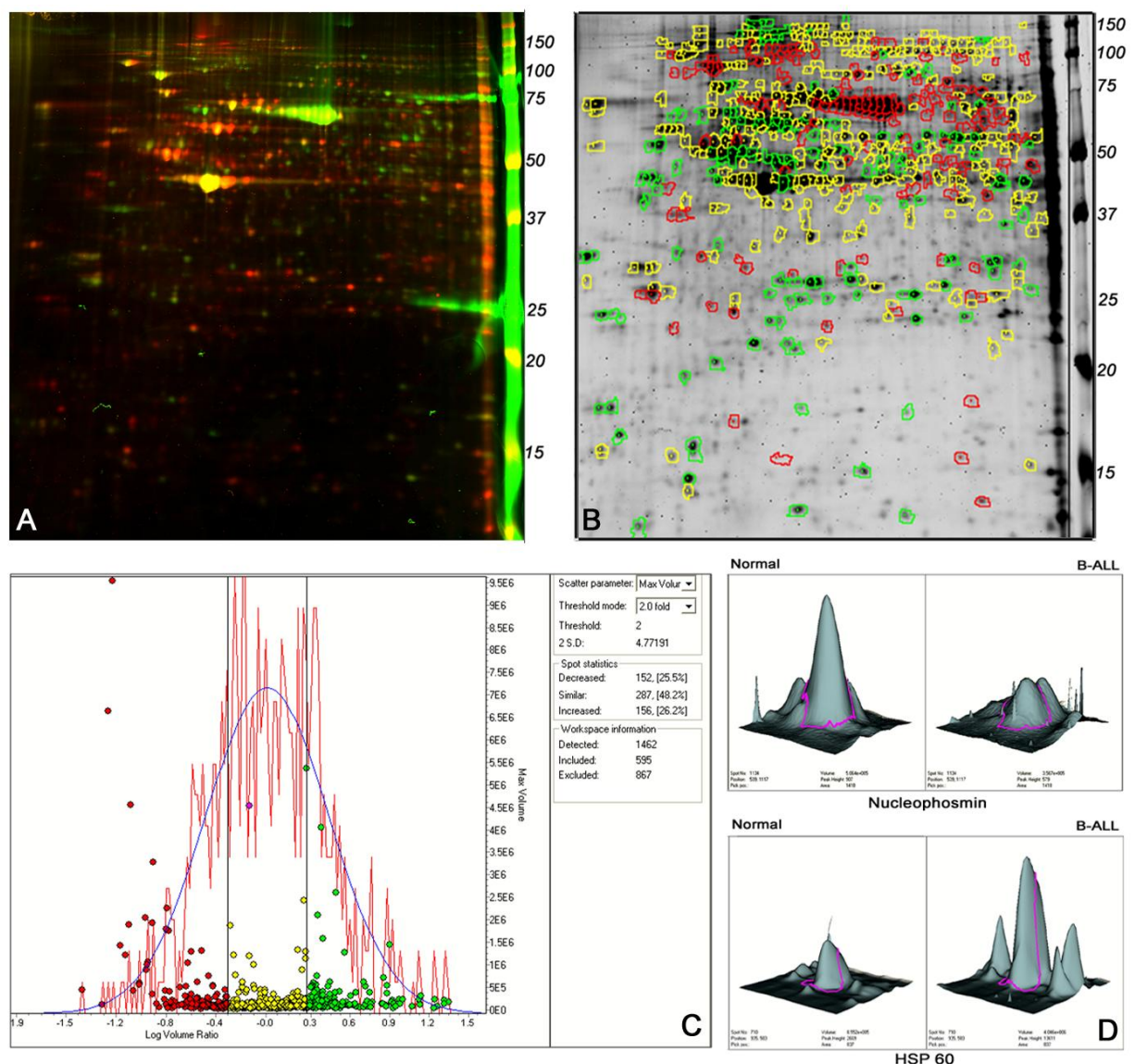


It is possible to recognize two main groups of protein patterns in Figure 2.3(B). The group on the left side of the first principal component consists of the proteins with higher abundance in B-ALL samples compared to normal samples i.e., up-regulated in B-ALL CD19⁺ cells; while the group on the right side is represented by proteins showing higher abundance in normal samples i.e., down-regulated in B-ALL CD19⁺ cells. The relative nearness for each gel in PCA space illustrates a similarity. The larger distance between the analysed samples indicates dissimilarity in protein abundance. PCA is not only suitable for grouping the gels according to a relationship in their protein patterns but also for the determination of typical polypeptide spots in the analysed gels. This mathematical procedure allows the projection of eigenvectors for the most distinct proteins present in the same space defined by the first two principal components with the largest eigenvalues (Figure 2.3B). The positions of the proteins with significant eigenvector values for the first principal component are shown and only protein spots which showed reproducible positions in two independent experiments are numbered.

2.3.3 2D-DIGE analysis of differentially expressed proteins

The use of fluorescent dyes resolves the limitations of 2D-PAGE in terms of reproducibility and dynamic range. Hence we confirmed the results obtained in 2DGE by 2D-DIGE. Figure 2.4 shows the reference 2D maps of CyDye-labelled B-ALL and normal B-cell proteomes along on DIA analysis using DeCyder.

Figure 2.4: DIGE and DIA analysis results for CD19⁺ proteomes from normal and B-ALL samples. (A) Representative scanned image for DIGE of B-ALL (red) vs. normal (green) B-cell proteome. (B) Reference 2D map of CyDye-labelled B-ALL and normal B-cell proteomes obtained on DIA analysis showing de-regulated proteins (green: up-regulated, red: down-regulated in B-ALL) and those with similar abundances (yellow). (C) Histogram plot for log volume ratios in the DIA workspace. (D) 3D view of individual spots of a down-regulated protein (nucleophosmin) and an up-regulated protein (HSP 60).



The DIA analysis results enlisted more than 300 spots that showed a significant difference in expression level of more than two-fold, between the B-ALL and normal B-cell proteomes. MALDI-TOF/TOF tandem mass spectrometry led to the identification of corresponding 79 proteins, which included the 60 proteins that were identified to be differentially expressed in 2DGE experiments with comparable fold changes. Table 2.3 enlists the 19 new proteins identified to be differentially regulated in DIGE experiments, along with the respective average volume ratio obtained on DIA analysis. The mass spectrometry data have been submitted to the PRIDE proteomics identifications database and are available at <http://tinyurl.com/3wq7m49>.

Table 2.3: Identification of 19 new differentially expressed proteins in DIGE experiments

Sr No.	Protein ID	Volume Ratio	Mascot Score	Sequence Coverage	Number of MS/MS Matches
1	Galactokinase 1	+2.64	76	39%	4
2	Cytokeratin 10	+2.2	74	28%	2
3	Translation initiation factor eIF-4B	+2.4	141	46%	5
4	Lymphocyte specific protein 1	+2.35	71	53%	3
5	Heterogeneous nuclear ribonucleoprotein K	+4.75	129	54%	3
6	150kD oxygen regulated protein (Orp150, hypoxia up-regulated 1)	-3.17	49	24%	2
7	Moesin	-2.24	69	30%	3
8	Tat-binding protein 1	-3.4	251	65%	4
9	H ⁺ -transporting two sector ATPase	+2.03	188	52%	8
10	ATP synthase D chain, mitochondrial	+20.75	117	76%	1
11	Proteasome alpha 5 subunit	+20.44	86	39%	3
12	78kD glucose-regulated protein precursor (GRP78)	+3.34	271	47%	5
13	60S acidic ribosomal protein P2	+2.65	52	86%	1
14	Homo sapiens cargo selection protein TIP47	-10.69	302	66%	5
15	Stress-70 protein, mitochondrial precursor (75kD glucose regulated protein- GRP75)	+2.59	376	46%	9
16	EIF3S4 protein	+2.34	61	60%	3
17	Dynactin subunit 2	-2.83	260	62%	6
18	PTB associated splicing factor	+3.16	140	39%	3
19	Galectin – 1	+8.11	86	76%	2

2.3.4 Multifunctional nucleophosmin showed interesting expression pattern in B-ALL CD19⁺ cells

As mentioned in Tables 2.2 and shown in Figures 2.1 & 2.4, the multifunctional nucleolar phosphoprotein ‘nucleophosmin’ (NPM) was observed to be significantly down-regulated in B-ALL compared to normal B-cells. Review of literature revealed that NPM has been repeatedly implicated in acute myeloid leukemia. Contrary to the down-regulation observed in our B-ALL samples, NPM is known to be frequently over-expressed in actively proliferating cells [83]; and is often mutated in AML [84]. The expression level of this multifunctional protein has been seldom investigated in lymphoid leukaemia. We used western immunoblotting to compare the NPM expression in B-ALL and AML. Figure 2.5 shows the result. With β -actin serving as the loading control, NPM exhibits expression of distinctly different forms in B-ALL cells vs. AML cells. While a 37 kD form exists in the lymphoid lineage malignancy, the myeloid lineage shows expression of an 20 kD polypeptide. B-ALL cells also show a 25 kD protein that might be a cleaved product of the 37 kD NPM [85]. However the abundances of the different forms were comparable leading to the conclusion that the 37 kD NPM predominates in B-lymphoblasts while the malignant myeloid cells exclusively express a 20 kD NPM.

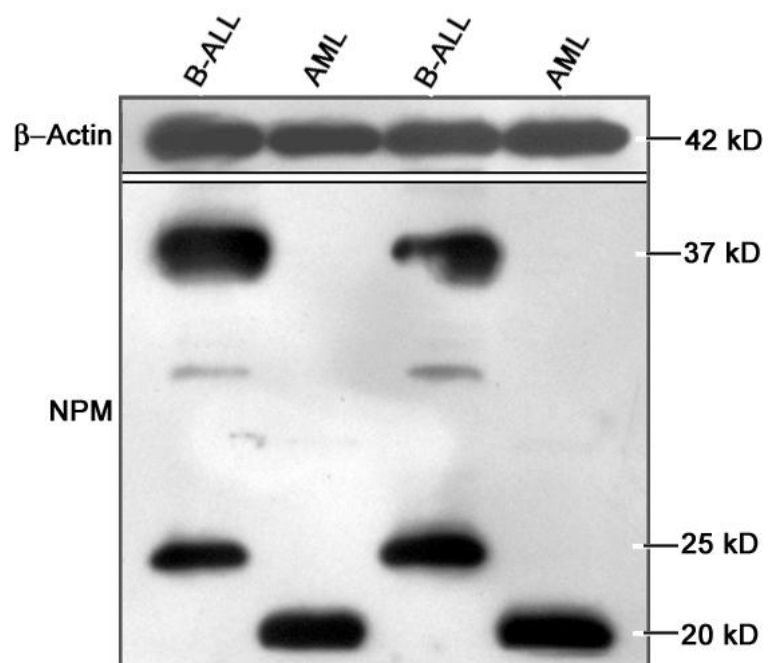


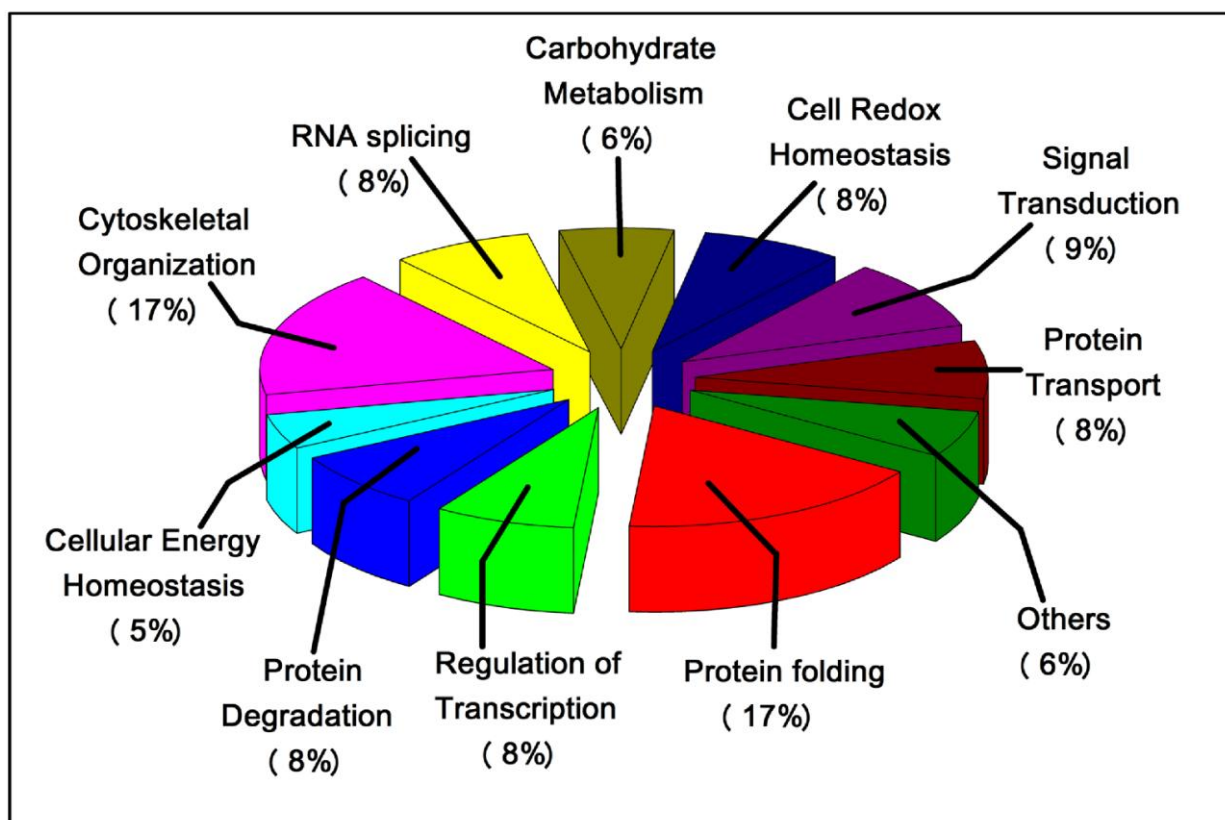
Figure 2.5: Western immunoblot result for nucleophosmin in B-ALL and AML cells

2.3.5 Gene Ontology Annotation

The functional classification of the identified proteins was achieved according to the ontology

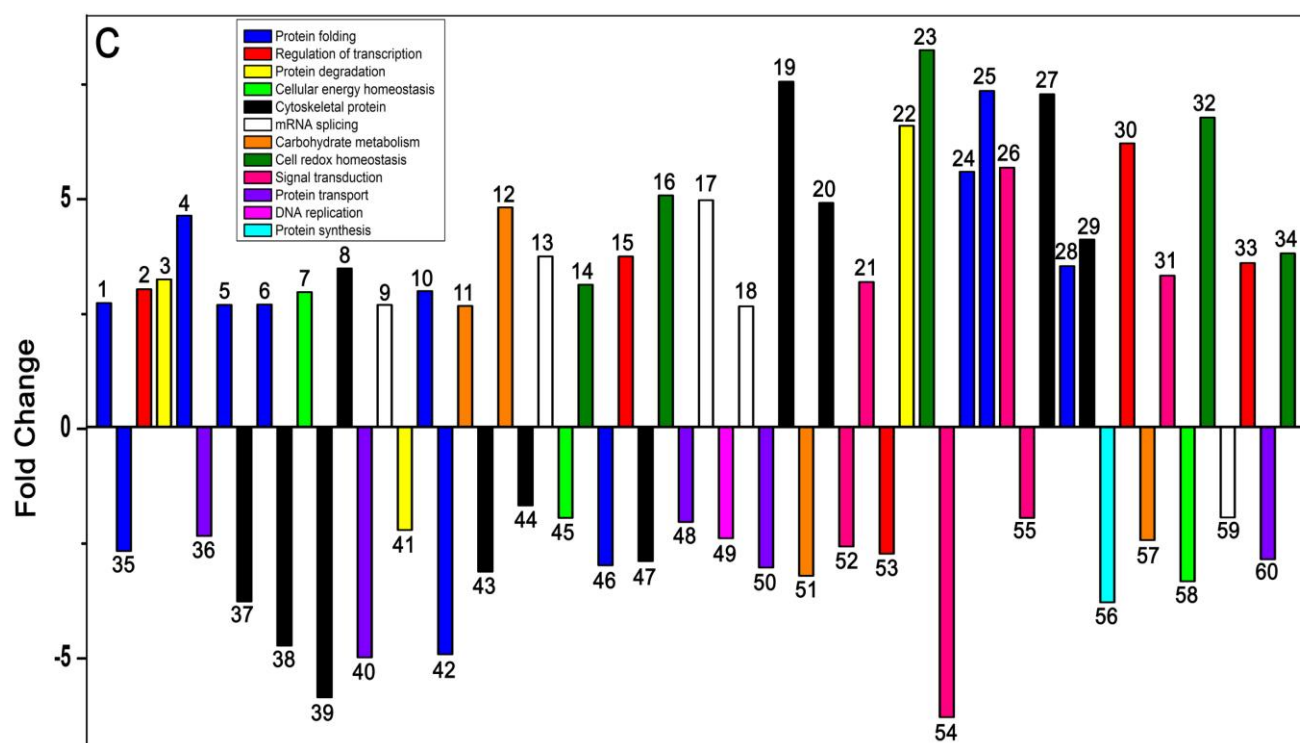
in the UniProt and PANTHER databases and is summarized in Figure 2.6. Each identified known protein was classified according to its GO functional annotation. These differentially expressed proteins were essentially those involved in metabolism of proteins, nucleic acids or carbohydrates, or in stress response or cytoskeleton/movement, or in cellular energy homeostasis. Most of the differentially expressed proteins were involved in important biological functions. As evident from Figure 2.6, most of the differentially regulated proteins (32%) are associated with cellular metabolism (8% with each of protein degradation, RNA splicing, carbohydrate metabolism and protein transport/translocation). The next majority (25%) participates in stress response (chaperones-17% and redox regulators-8%) followed by those involved in cytoskeletal organization. Rests are involved in signal transduction, cellular energy homeostasis and others.

Figure 2.6: Gene Ontology (GO) functional annotation of the differentially regulated proteins in B-ALL CD19⁺ cell proteome



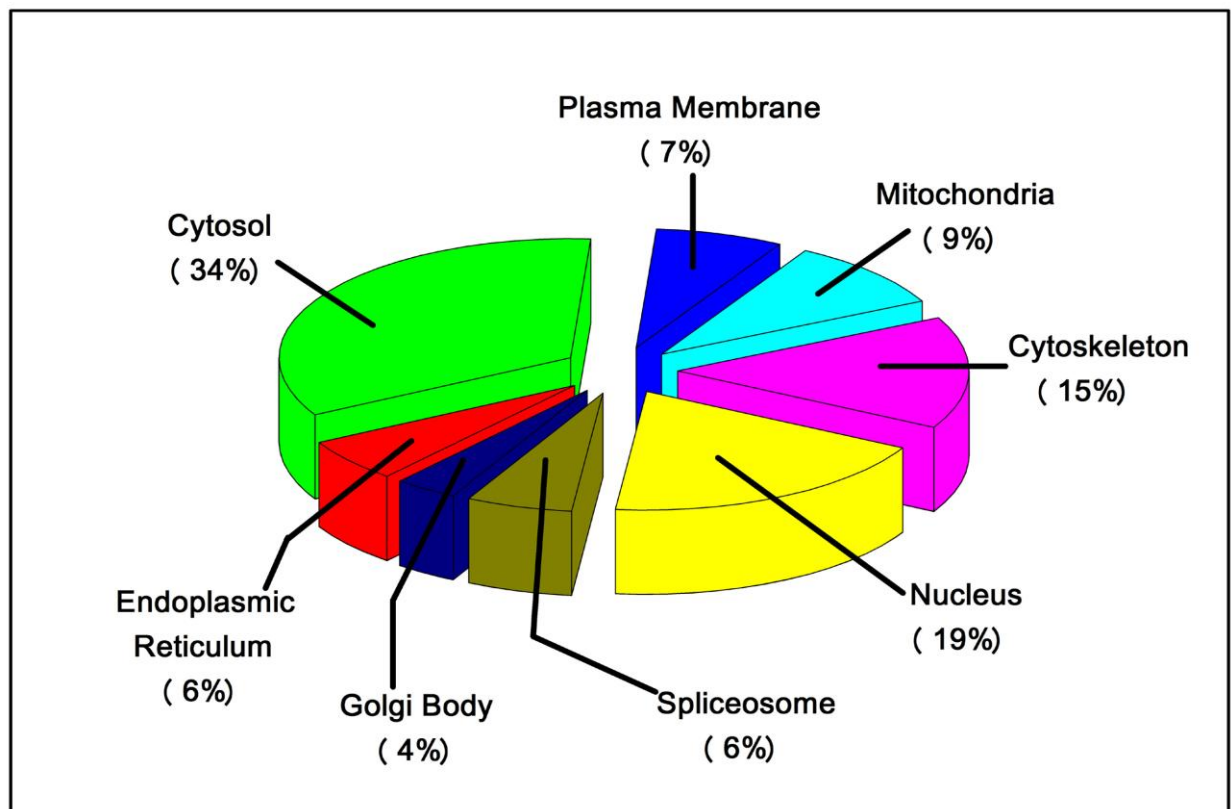
As can be extrapolated from Figure 2.7, a huge proportion of the stress response proteins including the redox regulators, chaperones and those associated with proteasomal degradation, are up-regulated in B-ALL CD19⁺ cells; all of the proteins associated with protein transport/translocation are down-regulated; cytoskeletal and signal transduction proteins show both up- and down-regulation trends; and most of the de-regulated proteins associated with macromolecular metabolism and energy homeostasis show higher abundance in B-ALL.

Figure 2.7: Histogram plot of the expression levels of the 60 differentially regulated proteins in B-ALL CD19⁺ cell proteome, with a color code on the basis of GO function.



The differentially regulated proteins were also classified according to their cellular localization as detailed in Figure 2.8. This classification shows that our protein identifications were not confined to any particular cellular compartment and somewhat represents normal localizome (the subcellular distribution of total cellular proteins) with cytosolic proteins occupying the majority followed by nuclear/nucleolar proteins and mitochondrial and exocytic proteins including those of the endoplasmic reticulum and secretory vesicles proteins respectively [86].

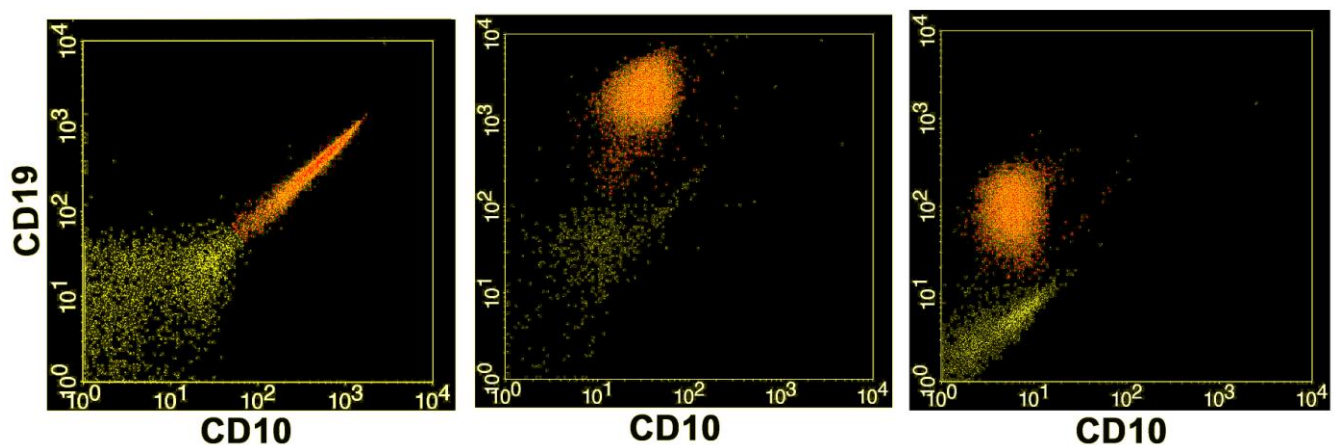
Figure 2.8 Gene Ontology (GO) annotation of the differentially regulated proteins in B-ALL CD19⁺ cell proteome on the basis of cellular localization



2.4 Discussion

Leukemic cells obtained from bone marrow or peripheral blood samples of many of the B-ALL patients showed CD19-CD10 co-expression immunophenotype (Figure 2.9), and thereby revealed the malignant clone to be of precursor B-cells.

Figure 2.9: Representative Immunophenotype patterns of the B-ALL patient samples



Although the clinical details of many B-ALL patients lacked cytogenetic data, the latter could be predicted from multiparametric immunophenotyping [19, 20, 87, 88]. The immunophenotypes of about 60% patients were indicative of TEL-AML1 chromosomal translocation, while rest indicated presence of MLL gene fusions, and BCR-ABL or E2A-PBX1 translocations. However, irrespective of the cytogenetic subtypes, the general mechanisms underlying the induction of ALL appear similar, encompassing aberrant expression of proto-oncogenes, chromosomal translocations that create fusion genes encoding active kinases and altered transcription factors, and hyperdiploidy. These genetic alterations in turn, alter key regulatory processes by maintaining or enhancing an unlimited capacity for self-renewal, subverting the controls of normal proliferation, blocking differentiation, and promoting resistance to apoptosis [15]. In our study, random sampling of B-ALL patients irrespective of their genetic subtypes left us with a scope of delineating the relationship between various chromosomal translocations and the differentially regulated B-cell proteome in a 'bottom-up' approach as discussed later.

Although 2DGE protein profiling based studies have reported few differentially expressed proteins in ALL, but these studies either compared the protein profiles of leukemic cells with normal white blood cells, or comprised of observations in leukemic cell lines [65, 89]. Significant differences between primary tumour cells and immortalised cell lines [73], emphasizes the importance of obtaining protein profiling data from primary malignant B-cells, rather than immortalised cell lines. Our results demonstrate the potential of proteome analysis with background-matched cell fractions obtained from fresh clinical specimens to provide insight into the mechanism of human leukemogenesis.

To evaluate the quantitative alterations of protein spots, and to search for co-regulated proteins that might be helpful in interpreting the mechanism of leukemogenesis, we utilized the multifactorial method known as PCA in addition to parametric/non-parametric statistical assessments. Instead of multidimensional space we restricted ourselves to the first two components that reflect the relevant differences in the protein patterns analysed. The vector

values of the positions of sample ‘observations’ and protein ‘variables’ in the biplot indicate their relative ‘weight’ for the principal component. These values are especially important in the proposal and resolution of the possible mechanism related to the differences in the studied samples. However in variable selection, it is crucial to allow spots with small absolute volumes showing a relevant variation to influence the model, whereas spots with large volumes that do not vary according to the design should be weighted low to avoid that they dominate the model components due to their high numerical values. This aspect was strictly taken care of by ‘group-scaling’ of the data before submission to PCA. Nevertheless, univariate analysis is also important because the nonparametric univariate method does not make use of the within-group variation directly but is based on ‘extreme outcomes’. In the (parametric) *t*-test, the mean of the two groups (normal or B-ALL) is compared and the criterion for significance is based on the variation within each group and the absolute difference between the group means with data assumed to be normally distributed. The use of a univariate method as a way of reducing the data set prior to the multivariate modelling entails a potential risk of false positives and/or false negatives. In the present study, the inclusion of false positives was not initially considered to be a big problem as the multivariate variable selection would sort out these spots as being non-significant. The risk of not including a relevant spot in the subset is, on the other hand, a more severe problem, as an excluded spot will never appear again in the following variable selection. Inclusion of replicate gels reduced the probability of analytical uncertainties and biological variation, and getting false positives or negatives. With substantial analytical error, the risk of spot selection errors is increased due to possible problems with spot identification and quantification that result in wrong rankings. PCA has been used to extract the systematic variation in spot volumes and to specify the protein spots responsible for the sample grouping of interest. Multivariate statistics and principal component analysis (PCA) revealed interesting age- and genetic anomaly- dependent variations in the malignant cell proteome. The group on the upper side of the second principal component in the biplot consisted of 14 B-ALL samples with immunophenotypes indicative of either TEL-AML1 or E2A-PBX1 translocation and

78.5% of these patients were below 15 years of age; while the group on the lower side was comprised of 13 B-ALL patients belonging to various age groups (child and adult) and with immunophenotypes indicative of all sorts of chromosomal translocations. Hence, proteins above PC2 may be the downstream targets of TEL-AML1 and E2A-PBX1 mediated cellular transformation. Such PCA mediated delineation of genotype dependent proteome changes may be useful in assessing the prognosis of B-ALL.

The separation of proteins in 2D gels is associated with a substantial analytical variability in addition to which comes the variation between samples (individuals) within a group that in a study like the present might easily be even more pronounced. Inclusion of technical replicates of the samples counteracted the analytical variability, and the use of DIGE technology with internal standard minimized the consequences of inter-gel variations. Also an increased number of samples were studied to minimize effects of biological variation. Many of the observed deregulations (27 of 60) were either absent or presented opposite trends in acute myeloid and T-lymphoid leukaemia (data not shown), and thus were specific to B-ALL. Comparison of our data with microarray based gene expression profiles of B-ALL cells, available in ArrayExpress, NCBI [90], revealed ~75% agreement between proteomic and transcriptomic trends. The 25% deviation presumably arises from substantial variation in post-translational processing.

GO analysis applied to predict the possible function of differentially expressed proteins revealed that some of these proteins might possess important biologic functions affecting the living status of the B-cells and many were essential for their survival. The distinctive expressions of some of these molecules possibly influence the survival of the CD19⁺ cells in B-ALL, by direct/indirect regulation of self-renewal, proliferation and differentiation of the leukemic cells. Mitochondria play important roles in cellular energy metabolism, free radical generation, and apoptosis. Deregulation of major mitochondrial proteins like ATP synthase, mitofilin, HSP60, cytochrome oxidase, glutaredoxin, prohibitin, etc. observed in this study indicate that defects in mitochondrial function contribute to the development and progression of

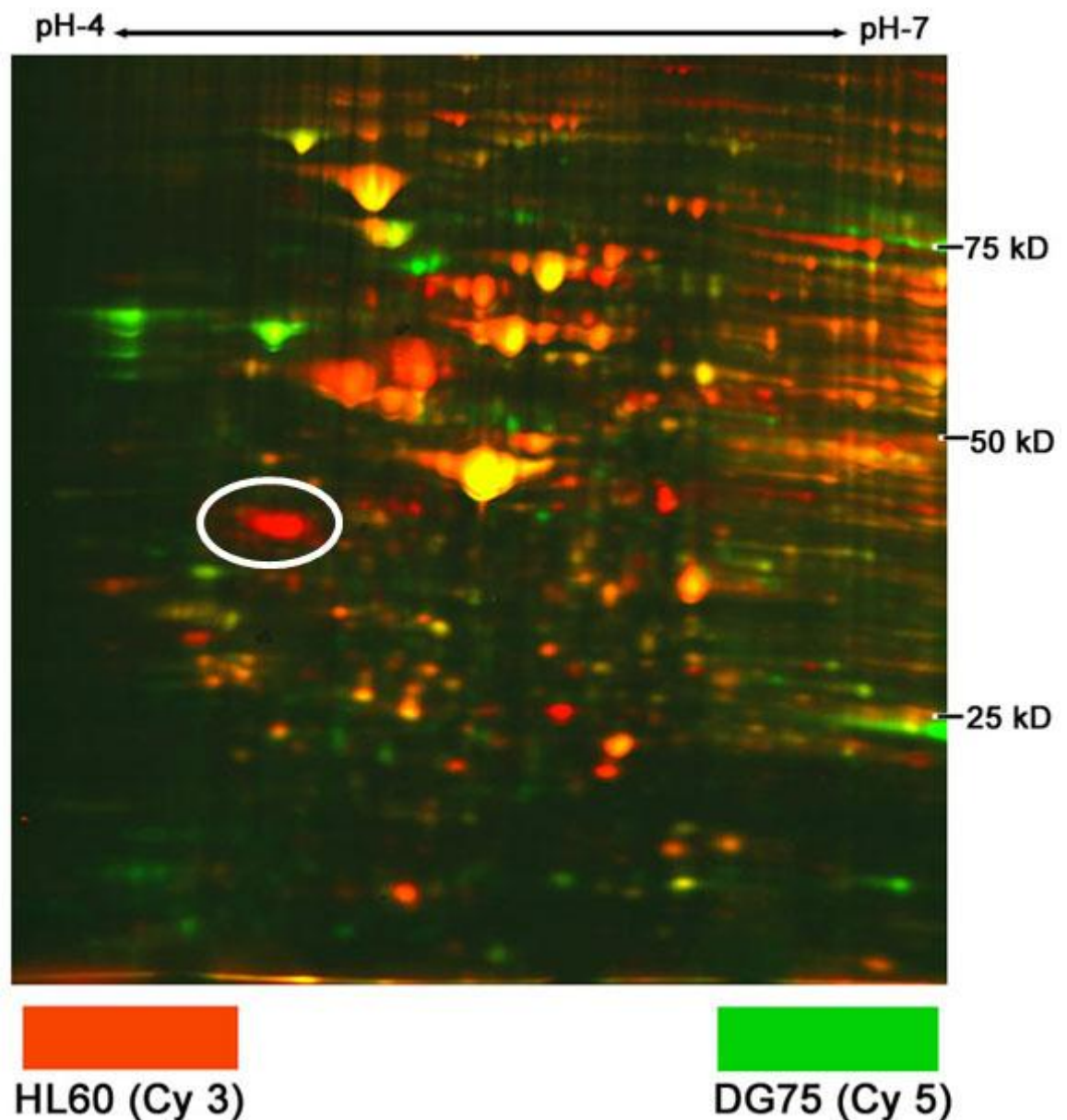
cancer. Up-regulation of several cytoskeletal proteins suggest a common effect on cell shape or cell motility.

We found that several proteasome subunits and ubiquitin are highly expressed in B-ALL cells. Our results are consistent with a new therapeutic strategy based on proteasome inhibition, recently approved by the FDA [74].

Eukaryotic translation initiation factor 2 is involved in the induction of PI3K that activates mTOR signalling that in turn also regulates the translation elongation process through eEF2 phosphorylation [91]. We observed down-regulation of both these translation factors that not only supports their afore-mentioned dependence but also points out deregulation of the translation machinery in B-ALL cells.

Nucleophosmin (NPM, also known as B23) is a ubiquitously expressed nucleolar phosphoprotein that constantly shuttles between the nucleus and cytoplasm. NPM contains distinct functional domains through which it has many functions in the cell related to both proliferation and growth suppression pathways. It participates in the process of ribosome biogenesis, and it controls genetic stability through the regulation of centrosome duplication. As a result, NPM overexpression correlates with uncontrolled cell growth and cellular transformation, whereas the disruption of NPM expression can cause genomic instability and centrosome amplification, which increases the risk of cellular transformation. Loss of NPM function leads to the destabilization and functional impairment of the ARF tumour-suppressor pathways, as NPM functions as a positive regulator of ARF protein stability. NPM is implicated in human tumorigenesis. It is frequently overexpressed in AML [92]. In our study, we observed down-regulation of NPM in B-ALL cells. Transcriptome data available in ArrayExpress, NCBI [90] also advocate NPM down-regulation in ALL as opposed to its up-regulation in AML. Additionally, we observed NPM down-regulation in lymphoma cell line DG75 in contrast to NPM up-regulation in promyelocytic leukemia cell line HL60, using DIGE (Figure 2.10).

Figure 2.10: DIGE image of a lymphoma cell line (DG75) vs. a myeloid leukemia cell line (HL60) showing NPM down-regulation in the lymphoid cells



NPM function can potentially be impaired both by the presence of antagonizing mutated products hetero-dimerizing with the wild-type protein, and by the reduction in the dosage of the gene to a single functional allele. Depending on its expression levels and gene dosage, NPM seems to function as either an oncogene or a tumour suppressor in myeloid and lymphoid lineages respectively. Either partial functional loss or aberrant overexpression could lead to neoplastic transformation through distinct mechanisms [92]. Additionally, like the NPM form observed in our B-ALL cells, Nakamura and colleagues observed a 37 kD NPM in T-lymphoblasts [93]. This advocates the fact that the 37 kD NPM predominates in lymphoid cells

and may have pronounced tumour suppressor functions. Nevertheless, this makes NPM a prospective marker for B-ALL. Delineation of the polypeptide constituents of leukemic cells using two-dimensional electrophoresis has provided additional markers that expand the phenotype based on cell-surface analysis such as with monoclonal antibodies. The two approaches are not mutually exclusive. In fact, the characterization of the polypeptide markers detected in two-dimensional gels will be facilitated by the development of corresponding antisera or monoclonal antibodies. These probes will help elucidate the distribution of the polypeptide markers in individual cells, such as in normal bone marrow or in immature lymphoid tissues.

The heat shock proteins (HSPs) are molecular chaperones whose expression is induced by a variety of cellular stressors and they are thought to facilitate protein folding and oligomerization. Although it is not known how HSPs induce malignant transformation, the stress-induced tyrosine phosphorylation of these proteins suggests that they function downstream of protein tyrosine kinases. Many molecular chaperones have also been shown to possess antiapoptotic activity. An increased expression of HSP family proteins in leukemic blasts might thus be directly linked to leukemogenesis. HSPA5 70 kDa that showed increased abundance in B-ALL cells prevents activation of Bax and thereby suppresses mitochondria mediated apoptosis. Recently, it has been demonstrated that HSPA5 also prevents apoptosis by inhibiting cytochrome *c* release from mitochondria [94]. Leukemic cells are exposed to chronic metabolic stress that triggers ER stress by accumulation of misfolded proteins. The cells adapt to this stress by reducing protein synthesis, facilitating ER-associated protein degradation (ERAD) using the ubiquitin-proteasome and autophagy-lysosome systems, expanding the size of the ER through augmented lipid biosynthesis, and increasing production of chaperones that help proteins in the ER lumen to fold [95].

The redox state of cells reflects a precise balance between the production of reactive oxygen species and the activity of reducing agents, the latter of which include thiol-based buffers and SOD. GST functions in cellular detoxification by catalysing the conjugation of

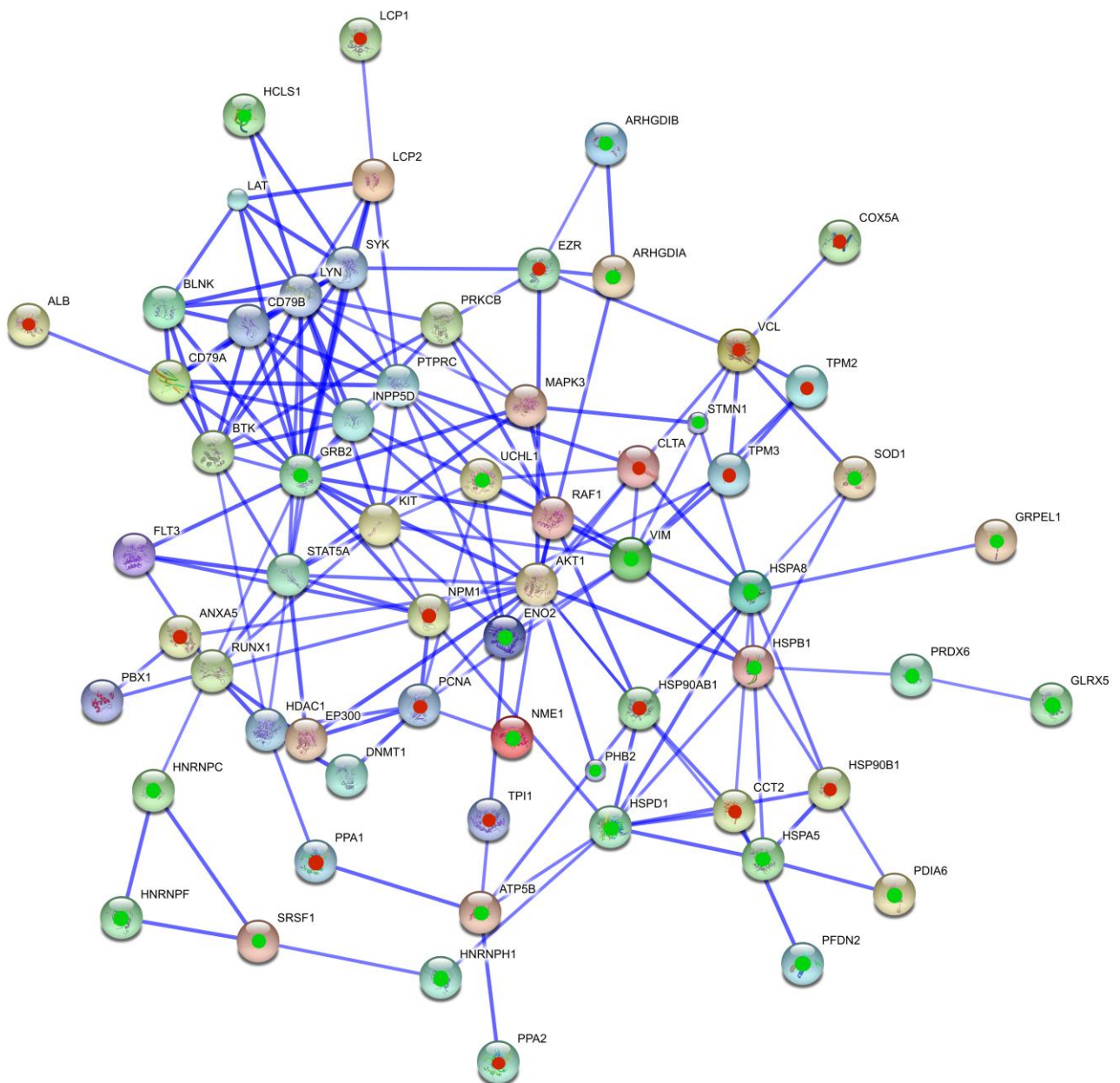
reduced glutathione (GSH) to target molecules. In addition, GST isoforms have been shown to be directly regulated by c-Jun NH₂- terminal kinase (JNK). SOD catalyses dismutation of the superoxide anion into O₂ and H₂O₂. Overexpression of this enzyme has been detected in cancer cells. It remains to be determined how an increased expression of GST or SOD contributes to leukemogenesis.

Stathmin is identified by 2DGE as an up-regulated protein in acute lymphoblastic leukaemia (ALL) and acute myeloid leukaemia (AML), but is also up-regulated in normal proliferating lymphoid cells [64]. The presence of stathmin in proliferating cells suggests that it is a proliferation marker rather than a specific biomarker.

There are approximately 518 kinases in the human genome, and virtually every signalling pathway will involve phosphorylation and kinase activity. Not surprisingly, deregulation of protein phosphorylation is a major mechanism by which leukemic cells evade normal physiological control of survival and growth [70]. 60% of the differentially regulated proteins identified in our study were phosphoproteins in contrast to very few amongst the similarly expressed proteins, as stated in the PTM ontology terms of the identified proteins in UniProt database. Hence phosphoproteomic studies might help define a “core phosphoproteome” in order to improve knowledge of the signal transduction pathways involved in leukemogenesis. But, one key issue in phosphoproteomics is the relatively high amount of cellular material required to identify a phosphorylated peptide from a signalling protein; given that phosphorylation is a transient modification, a phosphorylated peptide is often less abundant than its non-phosphorylated form. To date very few phosphoproteomics studies have been done in primary leukemic cells or tissue. The analysis of phosphoproteins in primary leukemic cells or tissue is thus a valid aim and no doubt improvements in phosphoprotein or peptide enrichment, mass spectrometer sensitivity and quantitative methodology will aid the pursuit of this aim. 75% of the differentially regulated proteins identified in our study were prone to acetylation as observed in UniProt database. This

regulated proteins identified in our study with key kinases, adaptor proteins and epigenetic regulators involved in pre-B-cell fate decisions [101], as shown in Figure 2.12. Node names are gene IDs of the respective proteins.

Figure 2.12: STRING interactome of the differentially regulated proteins (green: up-regulated, red: down-regulated) and key kinases, adaptor proteins and epigenetic regulators involved in pre-B-cell fate decisions



B-cell linker protein (BLNK/SLP-65) down-regulation has been crucially linked to pre-B-ALL. The SLP-65 gene contains alternative exons and deregulation of the splicing machinery is

implicated in regulation of SLP-65 expression [100]. Our data shows deregulation of several spliceosome proteins that provides one mechanism to explain the differentiation block involved in B-ALL pathogenesis. STRING derived interactome indicates functional links of NPM, GRB2, α -enolase, vimentin and ubiquitin carboxyl terminal hydrolase (UCTH) with FLT3, c-KIT, and STAT5A that participate in three indispensable pathways of early B-cell development [98]. GRB2, lymphocyte cytosolic protein 1 (LCP1/L-plastin), ezrin, haematopoietic lineage cell specific protein HS1 (HCLS1), albumin, clathrin light chain (Lca), vimentin, α -enolase, and UCTH interact with Bruton's tyrosine kinase (BTK), BLNK, lymphocyte cytosolic protein 2 (LCP2/SLP76), tyrosine-protein kinase SYK, Linker for activation of T-cells family member 1 (LAT), CD79A, CD79B, tyrosine-protein kinase Lyn, receptor-type tyrosine-protein phosphatase C (PTPRC), protein kinase C β (PKC- β), and phosphatidylinositol-3,4,5-trisphosphate 5-phosphatase 1 (SHIP) that are integral mediators of signals regulating proliferation, survival, differentiation and apoptosis of developing B cells [100, 102]. Several evidences suggest interaction of NPM, annexin A5, proliferating cell nuclear antigen (PCNA), and inorganic pyrophosphatase (iPPtase) with acute myeloid leukemia 1 protein (AML1), pre-B-cell leukemia transcription factor 1 (Homeobox protein PBX1), histone acetyltransferase p300, histone deacetylase 1 and, DNA (cytosine-5)-methyltransferase 1 that are known to be key components of the transcriptional and epigenetic networks implicated in ALL [3, 101]. DNA-K-type molecular chaperone HSPA5 (BiP protein), HSP 27, prohibitin, nucleoside di-phosphate kinase, annexin A5, PCNA, NPM, GRB2, ezrin, vinculin, rho-GDP dissociation inhibitor, stathmin, vimentin, HSP 70, and HSP 90 show functional links with RAC- α serine/threonine-protein kinase (AKT1), mitogen-activated protein kinase 3 (ERK-1), and RAF proto-oncogene serine/threonine-protein kinase (RAF1) that mediate pre-B-cell receptor (pre-BCR) induced cell death, survival and proliferation as shown in Figure 2.11 [99]. Table 2.3 summarizes implications of the differentially regulated proteins in leukemogenesis.

Table 2.3: Implications of the differentially regulated proteins in leukemogenesis according to available literature (references in parentheses)

Spot No.	Name of the Protein	Probable Implications in B-ALL & Previous Reports in Other Malignancies (Relevant References)
1	DnaK-type molecular chaperone HSPA5 precursor (BiP protein)	serves as a pivotal component of the pro-survival axis of the unfolded protein response (UPR) signalling network; activates the anti-apoptotic PI3-K/AKT and NFkB pathways; is abundantly expressed in relapsed B-lineage acute lymphoblastic leukaemia (ALL) and contributes to chemotherapy resistance of leukaemic B-cell precursors. (<i>Br J Haematol.</i> 2011 Jun, 153(6),741-52)
2	Haematopoietic lineage cell specific protein HS1	a prominent substrate of intracellular protein tyrosine kinases in haematopoietic cells; promotes actin-related protein (Arp) 2/3 complex-mediated actin polymerization which is of importance for the major role of HS1 in apoptosis and cell migration. (<i>BMC Genomics.</i> 2005 Feb 14,6,15; <i>Biochem J.</i> 2003 Apr 15,371(Pt 2),485-93)
3	Ubiquitin 1	participates in protein aggregation/degradation and cellular protein quality control; binds cyclins; interacts with tumor suppressor proteins; modulates DNA synthesis and cell cycle progression; Ubiquitin 1 mRNA and protein levels are both significantly increased in lung adenocarcinoma samples. (<i>Discov Med.</i> 2009 Jun,8(40),18-22)
4	Heat shock protein 60	cytosolic Hsp60 prevents translocation of the pro-apoptotic protein Bax into mitochondria and thus promotes cell survival; significantly higher Hsp60 gene expression in the peripheral blood of patients at the time of leukemia diagnosis compared with healthy controls; elevated mRNA expression of Hsps may reflect the disease severity and/or have a relationship to the prognosis. (<i>Tumour Biol.</i> 2011 Feb,32(1),33-44.)
5	Heat shock cognate 71 kDa protein (Heat shock 70 kDa protein 8)	over-expression of intracellular Hsp70 protects cells from apoptosis and constitutively expressed Hsp70 interacts with an anti-apoptotic protein that binds to Bcl-2; roles in immune surveillance when expressed on the cell surface; primary association with childhood ALL development. (<i>Cell Stress Chaperones.</i> 2010 Sep,15(5),475-85; <i>Tumour Biol.</i> 2011 Feb,32(1),33-44.)
6	Protein Disulfide isomerase	increased expression of PDI may play a crucial role in SH-mediated protection and drug resistance in malignant B lymphocytes; up-regulated during the unfolded protein response in AML. (<i>Blood.</i> 2011 Jun 2;117(22),5931-40; <i>Cancer Res.</i> 2003 Jan 1,63(1),100-6)
7	ATP synthase beta chain, mitochondrial precursor	up-regulation observed amongst the high-risk B-ALL patients may have implications in glucocorticoid drug-resistance of malignant cells; ATP synthase down-regulation forms the basis for dexamethasone triggered apoptosis of B-ALL cells. (<i>Biochim Biophys Acta.</i> 2011 Jun,1807(6),719-25)
8	Tubulin beta	role in microtubule drug resistance. (<i>Mol Cancer Ther.</i> 2008 Oct,7(10),3150-9)
9	Heterogeneous nuclear ribonucleoprotein F	implicated in all-trans-retinoic acid (ATRA) induced apoptosis in acute promyelocytic leukemia (APL); role in microtubule drug resistance. (<i>Blood.</i> 2004 Sep 1,104(5),1314-23; <i>J Biol Chem.</i> 2003 Nov 14,278(46),45082-93)

Spot No.	Name of the Protein	Probable Implications in B-ALL & Previous Reports in Other Malignancies (Relevant References)
10	Beta actin	internal control with similar expression levels
11	Protein disulfide isomerase	increased expression of PDI may play a crucial role in SH-mediated protection and drug resistance in malignant B lymphocytes; up-regulated during the unfolded protein response in AML. <i>(Blood. 2011 Jun 2;117(22),5931-40; Cancer Res. 2003 Jan 1,63(1),100-6)</i>
12	D-3-phosphoglycerate dehydrogenase	diverts glycolytic carbon to serine and glycine metabolism and contributes to oncogenesis; pathways downstream of serine metabolism contribute to biosynthesis and metabolic signaling functions associated with the folate pool, amino acid and lipid intermediates, and redox regulation; diverting fluxes from 3PG out of glycolysis leads to limiting ATP production, oxidation of 3PG to influence redox status and the generation of αKG from glutamate, all of which benefit cell growth through multiple mechanisms. <i>(Nat Genet. 2011 Jul 31. doi: 10.1038/ng.890)</i>
13	Phosphopyruvate hydratase (Alpha enolase)	has 97% homology with Myc-binding protein-1 s involved in regulation of cell growth and apoptosis; γ-Enolase found at higher abundance in ALL cells; leukemic lymphocytes are positive only for alpha-enolase while lymphoma cells are positive for beta-enolase indicating isoenzyme switches accompanying differentiation. <i>(Biochim Biophys Acta. 2007 Sep, 1774(9), 1173-83; Lab Invest. 1989 Jan,60(1),38-44)</i>
14	Heterogeneous nuclear ribonucleoprotein H3	interacts with a zinc-finger protein associated with DNA repair and implicated in an atypical myeloproliferative disease <i>(Exp Cell Res. 2005 Sep 10,309(1),78-85)</i>
15	Growth factor receptor-bound protein 2 (SH2/SH3 adaptor GRB2)	major mediator in Ras-MAPK and PI3K/AKT proliferation and/or survival pathways in B-cell precursors; critical in BCR-ABL signaling in adult ALL; is an essential signal integrator of activating as well as inhibitory signalosomes in B-lymphocytes. <i>(Mol Cell Biol. 2000 Oct,20(19),7109-20; J Clin Oncol. 2007 Apr 10,25(11), 1341-9; Immunol Rev. 2009 Nov,232(1),135-49)</i>
16	Glutathione S-transferase	inhibits apoptosis and causes dexamethasone resistance by suppression of Bim through dual mechanisms of both downregulation of p38-MAPK and upregulation of NF-kappaB p50 in ALL cells; implicated in multidrug resistance in ALL in India <i>(Cancer Sci. 2010 Mar, 101(3), 767-73; Ann Hematol. 1998 May,76(5),195-200)</i>
17	Prohibitin	up-regulated in the nucleoli of pre-B-ALL cells; functions in regulation of transcription in the nucleolus and as mitochondrial chaperone. <i>(Leuk Res. 2011 Jul 21, doi:10.1016/j.leukres.2011.06.038)</i>
18	Peroxisome 3 + peroxiredoxin 6	c-Myc that is required for pro-B expansion to pre-B is an activator of PRDX3 expression; PRDX3 is required for Myc-mediated proliferation and transformation; PRDX6 up-regulation is implicated in the mechanisms of RB oncogenesis. <i>(Genes Cancer. 2010 Jun, 1(6), 605-16; Int J Cancer. 2009 Jul 15, 125(2),264-75; Proc Natl Acad Sci U S A. 2002 May 14,99(10),6649-54; Proteomics Clin Appl. 2010 Apr,4(4), 449-63)</i>
19	Alternative splicing factor ASF-1	switches utilization of alternative 5' splice sites; deregulation of the splicing machinery is implicated in regulation of SLP-65 expression. <i>(Annu Rev Immunol. 2005,23,415-45)</i>

Spot No.	Name of the Protein	Probable Implications in B-ALL & Previous Reports in Other Malignancies (Relevant References)
20	Heterogeneous nuclear ribonucleoprotein C1/C2	binds and enhances translation at the internal ribosomal entry site element (IRES) of c-myc; posttranscriptional down-regulation of HNRNP C1/C2 mediates all-trans-retinoic acid-induced growth inhibition processes in acute promyelocytic leukemia. (<i>Blood</i> . 2004 Sep 1;104(5):1314-23)
21	Vimentin	contributes to the survival of chronic lymphocytic leukaemia cells; is a direct downstream target of PU.1 in leukemia cells; up-regulated in response to leukemogenic PTKs like BCR/ABL, TEL/PDGFR, FIP1/PDGFR, D816V KIT, NPM/ALK, and FLT3ITD. (<i>Br J Haematol</i> . 2010 Nov;151(3):252-64; <i>PLoS One</i> . 2010 Dec 30;5(12):e15992; <i>J Biol Chem</i> . 2010 Apr 2;285(14):10300-9; <i>Mol Cell Proteomics</i> . 2008 May;7(5):853-63)
22	Fascin 2	actin-bundling cytoskeletal protein implicated in B-cell lymphoma. (<i>Leuk Lymphoma</i> . 2009 Jun;50(6):937-43)
23	Rho GDP dissociation inhibitors Ly-GDI + Rho GDI 1 + Rho GDI 2	accelerate cancer invasion via regulation of cytoskeletal machinery and augmentation of cell motility and adhesion; increase in RhoGDI2 might prolong the GTP bound state of Rho-GTPases and thereby prolong signals involved in numerous Rho GTPase-dependent processes, ranging from integrin activation, cytoskeletal dynamics and motility to NADPH oxidase activity to gene expression. (<i>Exp Hematol</i> . 2008 Jan;36(1):37-50; <i>J Proteome Res</i> . 2009 Aug;8(8):3824-33; <i>Trends Cell Biol</i> . 2005 Jul;15(7):356-63)
24	Ubiquitin carboxyl terminal hydrolase	has oncogenic potential e.g. in regulating cell proliferation, growth factor signaling, etc; UCH-L1 levels are high in acute lymphoblastic leukemia; studies of relation between UCH enzymes and oncogenesis are at a preliminary stage. (<i>Biochim Biophys Acta</i> . 2010 Aug;1806(1):1-6)
25	Peroxioredoxin 2	thioredoxin-dependent cytosolic enzyme that protects against apoptosis by scavenging hydrogen peroxide. (<i>Cell Death Differ</i> . 2005 Aug;12 Suppl 1,991-8)
26	HSP 27+ proteasome subunit b3+proteasome endopeptidase complex	hsp27 expression increases in B-cell precursors from c-ALL patients; hsp27 mediates anti-apoptotic signaling and has previously been linked to chemotherapeutic resistance; ALL patients have significantly higher proteasome levels than AML and MDS patients; increased levels of proteasomal proteins lead to constitutive NF-kB activity in acute leukemia cells via regulation of both canonical and non-canonical NF-kB pathways. (<i>Blood</i> . 1995 Jan 15;85(2):510-21; <i>PLoS One</i> . 2010 Jul 22;5(7):e11716; <i>Leuk Res</i> . 2011 Apr;35(4):526-33; <i>Br J Haematol</i> . 2011 Apr;153(2):222-35)
27	GrpE protein homolog 1, mitochondrial precursor	functions as nucleotide exchange factor of mitochondrial Hsp70 and accelerates the release of ADP from Hsp70 that stimulates the ATP turnover rate. (<i>J Biol Chem</i> . 2010 Jun 18;285(25):19472-82)
28	Nucleoside Diphosphate Kinase A	considered as a differentiation inhibitory factor in various hematological cancers and as a marker of poor prognosis and relapse. (<i>Anticancer Res</i> . 2001 Jan-Feb;21(1B):819-23)
29	Stathmin (phosphoprotein p19)/Oncoprotein 18 (Op18)	Altered expression implicated in vincristine resistance of childhood ALL cells; phosphorylated stathmin is essential for cell cycle progression. (<i>Proteomics</i> . 2006 Mar;6(5):1681-94; <i>Leukemia</i> . 1997 Oct;11(10):1690-5)

Spot No.	Name of the Protein	Probable Implications in B-ALL & Previous Reports in Other Malignancies (Relevant References)
30	Prefoldin subunit 2	involved in inhibiting mitochondrial cell death pathway in response to cell stress via phosphorylation of BAD; component of the NF-kappaB transcriptional enhanceosome; delivers unfolded target proteins (newly synthesized or denatured, for example, by heat) to cytosolic chaperonin, thus preventing them from following competing pathways for nonnative proteins within the cell. Such pathways include aggregation, degradation, or interaction with chaperones involved in protein sorting or alternate folding pathways. (<i>Sci Signal</i> . 2008 Feb 19, 1(7),pe9; <i>J Cell Biol</i> . 2007 Jul 16, 178(2),231-44; <i>Cell</i> . 1998 May 29,93(5),863-73)
31	Translationally controlled tumor protein (TCTP)	its down-regulation is a major contributor in cellular reprogramming and rare events of tumour reversion and hence TCTP constitutes a therapeutic target of tumour reversion; enhances stability and antiapoptotic activity of Mcl-1, a Bcl-2 family member that is a critical determinant in various cell survival pathways. (<i>Nat Rev Cancer</i> . 2009 Mar,9(3),206-16; <i>Mol Cell Biol</i> . 2005 Apr,25(8), 3117-26)
32	TGFb- induced anti-apoptotic factor 1	is a downstream effector of the TGFb-mediated growth regulation; interacts with several mitochondrial proteins <i>in vivo</i> ; inhibits tumor necrosis factor cytotoxicity; up-regulated and plays a protective role against apoptosis during allograft rejection. (<i>Ann N Y Acad Sci</i> . 2003 May,995, 11-21; <i>Biochem Biophys Res Commun</i> . 1998 Dec 30,253(3),743-9; <i>Transplantation</i> . 2003 Jun 27,75(12),2076-82)
33	SH3 domain binding protein SH3BP-1	a member of the rhoGAP family of proteins that are GTPase-activating proteins for rho-related small GTPases required for the ras-mediated signals; binds to the SH3 domain of Abl tyrosine kinase; links tyrosine kinases to Ras-related proteins. (<i>J Biol Chem</i> . 1994 Jan 14,269(2), 1137-42; <i>Cell</i> . 1993 Oct 8,75(1),25-36; <i>Science</i> . 1992 Aug 7,257(5071):803-6; <i>EMBO J</i> . 1995 Jul 3, 14(13),3127-35)
34	Glutaredoxin-related protein C14 or f87	Thioredoxin (Trx) system including NADPH, TrxR, and Trx coupled with peroxiredoxins and the GSH system composed of NADPH, GR, GSH coupled with Glutaredoxins (Grxs), GPxs, GSTs are the two main electron donor systems that mediate the cellular activity including DNA synthesis, protection against oxidative stress, and thus control cellular proliferation, viability, and apoptosis. Therapeutic disruption of both systems is necessary to block electron supply for DNA synthesis and enhance oxidative stress and thus induce apoptosis of leukemic cells, since down-regulation of certain anti-oxidant mechanisms can be compensated for by the up- and down-regulation of the other anti-oxidant mechanisms. (<i>Proc Natl Acad Sci U S A</i> . 2007 Jul 24, 104(30), 12288-93)
35	Enhancer of rudimentary homolog	Involved in fundamental processes like regulation of pyrimidine metabolism, cell cycle progression, transcription and cell growth control; increased levels of the ERH transcript observed in rapidly dividing mammalian cell lines. (<i>FEBS J</i> . 2008 Jan,275(2), 332-40)
36	Superoxide Dismutase (SOD)	antioxidant enzyme up-regulated in ALL compared to normal and AML; PI3K/Akt pathway protects cells against oxidative stress by NFkB-mediated upregulation of Cu/Zn-SOD gene expression. (<i>Hematol Oncol</i> . 2003 Mar,21(1),11-6; <i>Cell Death Differ</i> . 2006 May, 13(5),852-60)

Spot No.	Name of the Protein	Probable Implications in B-ALL & Previous Reports in Other Malignancies (Relevant References)
37	Endoplasmin precursor + HSP 90 beta	ER counterpart of the cytoplasmic heat shock protein 90 (HSP90) and is an ER calcium binding protein; has pro-survival properties with implicated function in cancer progression; critical role in MAPK-mediated signaling, maintenance of calcium homeostasis and ER stress signaling; optimizes early B-cell lymphopoiesis serving as chaperones for integrin and TLR. (<i>PLoS One</i> . 2010 May 26;5(5),e10852; <i>Nat Methods</i> . 2010 Oct,7(10),801-5; <i>Blood</i> . 2010 Mar 25,115(12),2380-90)
38	Mitofilin	mitochondrial protein that controls cristae formation and thus indispensable for normal mitochondrial function; loss of mitofilin leads to increased membrane potential and ROS production as well as defective oxidative phosphorylation; role in mitochondrial protein import. (<i>Mol Biol Cell</i> . 2005 Mar, 16(3), 1543-54; <i>FEBS Lett</i> . 2007 Jul 24,581(18),3545-9)
39	Ezrin(Cytovillin)	acts as linker between plasma membrane and cytoskeleton and is key component in tumor metastasis playing important roles in the polarization and invasive behaviour of T-ALL cells; downstream substrate of phosphorylation by oncogenic tyrosine kinases KIT/FLT3 in leukemic blasts; is a signal transducer in functions as diverse as cell morphogenesis, adhesion, motility, proliferation, and survival depending on the cell stimuli and cell type; altered expression associated with vincristin resistance in childhood ALL. (<i>Leuk Res</i> . 2010 Jun,34(6), 769-76; <i>Blood</i> . 2008 Mar 15;111(6):3163-72; <i>Proteomics</i> . 2006 Mar,6(5), 1681-94)
40	Vinculin (Metavinculin)	focal adhesion protein known to link integrins with the actin cytoskeleton and participate in integrin-mediated signaling; participate in assembling signalling complexes that are important for cell motility and cell proliferation; mediates Bcr-Abl induced cytoskeleton remodeling contributing to the pathogenesis of Bcr-Abl-positive leukemia; is up-regulated during the differentiation of HL-60 leukemia cells. (<i>Proc Natl Acad Sci U S A</i> . 2008 Nov 11,105(45), 17238-44; <i>Curr Opin Cell Biol</i> . 2000 Feb, 12(1), 133-9; <i>J Cell Sci</i> . 2007 Apr 15, 120(Pt 8), 1436-46; <i>Cancer Res</i> . 1992 Jun 1,52(11),3063-6)
41	L-plastin(lymphocyte cytosolic protein 1)	actin filament bundling protein which regulates actin turn-over and contributes to cancer cell invasion in a phosphorylation-dependent manner. (<i>PLoS One</i> . 2010 Feb 15,5(2),e9210)
42	Serum albumin precursor	Cytoprotective antioxidant activity of serum albumin inhibits spontaneous and reactive oxidant induced apoptosis in B-CLL cells that lack the intracellular antioxidant defences; proliferating lymphocytes bind, endocytose and secrete albumin that is known to support the proliferation of activated lymphocytes. (<i>Br J Haematol</i> . 2002 Feb, 116(2), 316-28)
43	UV excision repair protein RAD23 homolog	regulates protein turnover at a postubiquitylation step; involved in regulation of cell cycle progression; down-regulated in human Burkitt lymphoma cells. (<i>Mol Biol Cell</i> . 2010 Jan 1,21(1), 177-85; <i>J Biol Chem</i> . 1999 Jun 25,274(26), 18785-92; <i>J Biol Chem</i> . 1998 Oct 23,273(43),28057-64)

Spot No.	Name of the Protein	Probable Implications in B-ALL & Previous Reports in Other Malignancies (Relevant References)
44	T-complex protein 1 subunit beta (TCP-1-b)	a.k.a chaperonin containing TCP-1 (CCT) is part of a chaperone network linked to protein synthesis; participates in the folding of newly synthesized polypeptides, including actin, tubulin, and several cell cycle regulators; plays an important role in cytoskeletal organization and cell division; altered expression in vincristine resistant childhood ALL. (<i>J Biol Chem.</i> 2009 May 29;284(22),14939-48; <i>Proteomics.</i> 2006 Mar;6(5), 1681-94)
45	Stomatin like protein 2 (SLP-2)	modulates mitochondrial calcium extrusion, thereby altering the ability of mitochondria to buffer Ca^{2+} and to shape cytosolic Ca^{2+} signals; mitochondrial inner membrane protein required in stress-induced mitochondrial hyperfusion. (<i>Cell Calcium.</i> 2010 Jan;47(1), 11-8; <i>EMBO J.</i> 2009 Jun 3;28(11), 1589-600)
46	F-actin capping protein alpha-1 subunit (CapZ alpha1)	has high affinity for barbed actin filament ends and plays an important role in the calcium-independent regulation of actin filament assembly; participates in CKIP-1 (casein kinase interacting protein / c-Jun-binding protein) induced alterations of the actin cytoskeleton and cell morphology. (<i>PLoS Biol.</i> 2010 Jul 6;8(7), e1000416; <i>Biochemistry.</i> 1996 Mar 19;35(11), 3518-24; <i>J Biol Chem.</i> 2006 Nov 24;281(47), 36347-59)
47	Inorganic pyrophosphatase	important in cellular phosphate metabolism and is therefore of strategic importance in cell growth and proliferation; down-regulated in drug resistant human breast cancer cells. (<i>Cancer Res.</i> 2006 Mar 15;66(6), 3248-55)
48	Nucleophosmin	is a haploinsufficient suppressor of myeloid and lymphoid malignancies in the mouse; NPM gene alterations has an enormous impact in the diagnosis, prognostic stratification, monitoring of minimal residual disease and therapeutic intervention of various lymphomas and leukemias; NPM inactivation leads to unrestricted centrosome duplication and genomic instability. (<i>Blood.</i> 2008 Apr 1, 111(7), 3859-62; <i>Haematologica.</i> 2007 Apr;92(4), 519-32; <i>Cancer Sci.</i> 2006 Oct;97(10), 963-9)
49	Tropomyosin 3 + Tropomyosin 2 (beta)	coiled-coil domain of TPM3 contributes with its dimerization/activation moiety to building tyrosine kinase fusion proteins implicated in leukemia/lymphoma; TPM2 mRNA levels in CLL cells are lower than normal hematopoietic subsets. (<i>Leukemia.</i> 2006 Sep;20(9), 1623-4; <i>Haematologica.</i> 2006 Jan;91(1), 56-63)
50	Annexin A5	belongs to a super-family of closely related calcium and membrane-binding proteins that have a diverse range of cellular functions like vesicle trafficking, cell division, apoptosis, calcium signalling and growth regulation; used as a probe for apoptosis; interaction with Protein kinase C (PKC) is required in PKC activation and signaling that participates in a variety of signal transduction pathways such as apoptosis, cell proliferation, and tumor suppression. (<i>J Pathol.</i> 2008 Oct;216(2), 131-40; <i>J Biol Chem.</i> 2006 Aug 11;281(32), 23218-26)

Spot No.	Name of the Protein	Probable Implications in B-ALL & Previous Reports in Other Malignancies (Relevant References)
51	Proliferating cell nuclear antigen (PCNA)	orchestrates faithful transmission of genetic information to progeny; couples DNA replication/repair processes with other cellular functions such as chromatin remodeling and epigenetic modifications, cell cycle control/cell survival, transcription etc; prognostic protein biomarker in childhood ALL; lower expression levels in pre-B-ALL than T-ALL. (<i>Cell</i> . 2007 May 18; 129(4):665-79; <i>Cell Mol Life Sci</i> . 2008 Nov; 65(23):3789-808; <i>J Proteomics</i> . 2011 May 16; 74(6):843-57; <i>Blood</i> . 1990 Sep 1; 76(5):985-90)
52	Clathrin light polypeptide (Lca)	plays key roles in membrane trafficking during interphase and in stabilizing spindle fibers during mitosis; are critical for clathrin-mediated intracellular membrane trafficking between the TGN and the endosomal system by facilitating actin assembly on clathrin-coated structures. (<i>PLoS One</i> . 2010 Nov 30; 5(11):e15128; <i>Proc Natl Acad Sci U S A</i> . 2008 Jan 8; 105(1):168-73)
53	Lactoylglutathione lyase (Methylglyoxalase, Aldoketomutase)	is a novel target against Bcr-Abl ⁺ leukemic cells; is involved in resistance of human leukemia cells to antitumor agents. (<i>Cell Death Differ</i> . 2010 Jul; 17(7):1211-20; <i>Blood</i> . 2000 May 15; 95(10):3214-8)
54	PACAP protein (Pituitary adenylate cyclase-activating polypeptide receptor)	VIP/PACAP secreted by nerve ends in the bone marrow (BM) microenvironment inhibits the proliferation of BM CD34 ⁺ progenitors through the VPAC/PACAP receptor; its upregulation results in decreased proliferation and enhanced differentiation of human megakaryoblastic leukemia cells; with cAMP as secondary messenger, mediates VIP/PACAP induced inhibition of expression and/or DNA-binding activity of several transcriptional factors including c-myc and NF-kappaB in T-lymphocytes. (<i>Exp Hematol</i> . 2002 Sep; 30(9):1001-9; <i>J Mol Neurosci</i> . 2009 Feb; 37(2):160-7; <i>J Immunol</i> . 2001 Jan 15; 166(2):1028-40)
55	Transcription elongation factor B polypeptide 2	interacts with suppressors of cytokine signaling (SOCS) box family proteins, which function as negative regulators of Jak/STAT signaling; mediates flavopiridol (cyclin-dependent kinase inhibitor) induced transcription-halt and apoptosis in imatinib resistant CML cells and various human myeloid and lymphoid leukemia cells. (<i>J Biol Chem</i> . 2008 Aug 1; 283(31):21334-46; <i>Blood</i> . 2004 Jul 15; 104(2):509-18)
56	Programmed cell death protein 5 (TFAR19 protein)	involved in cell death and down-regulated in different forms of human tumors; accelerates DNA damage-induced apoptosis; TFAR19 gene loss involved in TEL-AML1 acute lymphoblastic leukemia and may partly account for the development of leukemia. (<i>Apoptosis</i> . 2009 Sep; 14(9):1086-94; <i>Neoplasia</i> . 2009 Apr; 11(4):345-54; <i>Cancer Sci</i> . 2007 May; 98(5):698-706)
57	Translation initiation factor eIF-2B alpha subunit (eIF-2B GDP-GTP exchange factor)	is essential for optimal activity of the eIF-2B complex; mediates eIF-2A phosphorylation induced inhibition of the guanine nucleotide exchange activity of eIF2B leading to impairment in eIF2 recycling and protein synthesis; eIF2A phosphorylation and subsequent eIF2B inhibition is involved in protein phosphatase mediated BCL2 dephosphorylation in human ALL-derived REH cells that are known to exhibit robust BCL2 phosphatase activity; eIF2A phosphorylation down-regulates cyclin D1 and activates PI3K/AKT signaling and cell survival. (<i>J Biol Chem</i> . 1998 May 22; 273(21):12841-5; <i>J Biol Chem</i> . 2008 Dec 19; 283(51):35474-85; <i>Mol Biol Cell</i> . 2007 Sep; 18(9):3635-44)

Spot No.	Name of the Protein	Probable Implications in B-ALL & Previous Reports in Other Malignancies (Relevant References)
58	Triosephosphate isomerase	interacts with the tumor suppressor ARF; down-regulated in human non-Hodgkin's lymphoma experimental model system; up-regulated during differentiation of myeloid leukemia cells in vitro. (<i>Cell Cycle</i> . 2006 Mar;5(6), 641-6; <i>Clin Cancer Res</i> . 2007 Apr 15;13(8),2496-503; <i>Cell Biochem Funct</i> . 1991 Jan;9(1),39-47)
59	Cytochrome c oxidase subunit Va (COX5A protein)	down-regulation of nucleus-encoded COX5A subunit decreases the quantity of cytochrome oxidase holoenzyme and affects the organization of respiratory supercomplexes; interacts with Bcl-2 and contributes to the homeostatic role of Bcl-2 in the redox biology and metabolism of cancer cells, signaling the Warburg effect . (<i>Biochem J</i> . 2010 May 27;428(3), 363-74; <i>Cell Death Differ</i> . 2010 Mar, 17(3), 408-20)
60	Peptidylprolyl isomerase	binds to and isomerizes the peptidyl-prolyl bond in serine or threonine phosphorylated Ser/Thr-Pro motifs; is a negative regulator of the tumor-suppressor protein PML; catalyzes the isomerization of peptidyl-prolyl-imide bonds in subunit α of the IKK kinase complex, and is required for IKK function and NF- κ B inhibition in lymphoid cells; potentiates binding of MLL to HDAC and transcriptional repression of MLL-fused proteins that are implicated in leukemogenesis. (<i>J Biol Chem</i> . 2010 Mar 26;285(13),9485-92; <i>Blood</i> . 2005 Aug 15,106(4), 1400-6; <i>Proc Natl Acad Sci U S A</i> . 2003 Jul 8, 100(14), 8342-7)
61	Fatty acid binding protein (FABP)	is a participant in leukotriene biosynthesis that confers a survival advantage to B-cells in mantle cell lymphoma; FABP and its ligands, fatty acids, play an important role in the process of lymphocyte apoptosis and the immune modulation induced by dexamethasone; has role in modulating nuclear receptors and gene transcription. (<i>Mol Cell Proteomics</i> . 2009 Jul;8(7), 1501-15; <i>J Biol Chem</i> . 2004 Feb 27;279(9):7420-6; <i>Mol Cell Biochem</i> . 2007 May,299(1-2),99-107; <i>Lipids</i> . 2008 Jan,43(1), 1-17)
Identification of 19 new differential regulations in addition to the above-mentioned 60 in DIGE experiments		
1	Galactokinase 1	the galactokinase gene is closely linked to the thymidine kinase gene whose expression is increased in AML and CLL patients. (<i>Photochem Photobiol</i> . 1993 Aug;58(2),259-64; <i>Proc Natl Acad Sci U S A</i> . 1988 Nov;85(22):8563-7; <i>Cancer Lett</i> . 2001 Apr 26,165(2), 195-200)
2	Cytokeratin 10	aberrant expression of cytokeratins is known to occasionally occur in malignant lymphomas and leukemias; loss of keratin 10 leads to MAPK activation and decreased tumor formation in mice; keratin intermediate filaments are expressed by K562 leukemic cell line. (<i>Pathol Res Pract</i> . 2008;204(8),569-73; <i>J Invest Dermatol</i> . 2004 Nov, 123(5),973-81; <i>Leuk Res</i> . 1986, 10(1),29-33)
3	Translation initiation factor eIF-4B	PI3K/Akt/mTOR and Ras/MAPK signaling cascades stimulate translation by controlling eIF-4B phosphorylation and activity; overexpression of eIF4B in <i>Drosophila</i> promotes cell survival and proliferation. (<i>EMBO J</i> . 2006 Jun 21;25(12),2781-91; <i>Eur J Biochem</i> . 2004 Jul,271(14),2923-36)

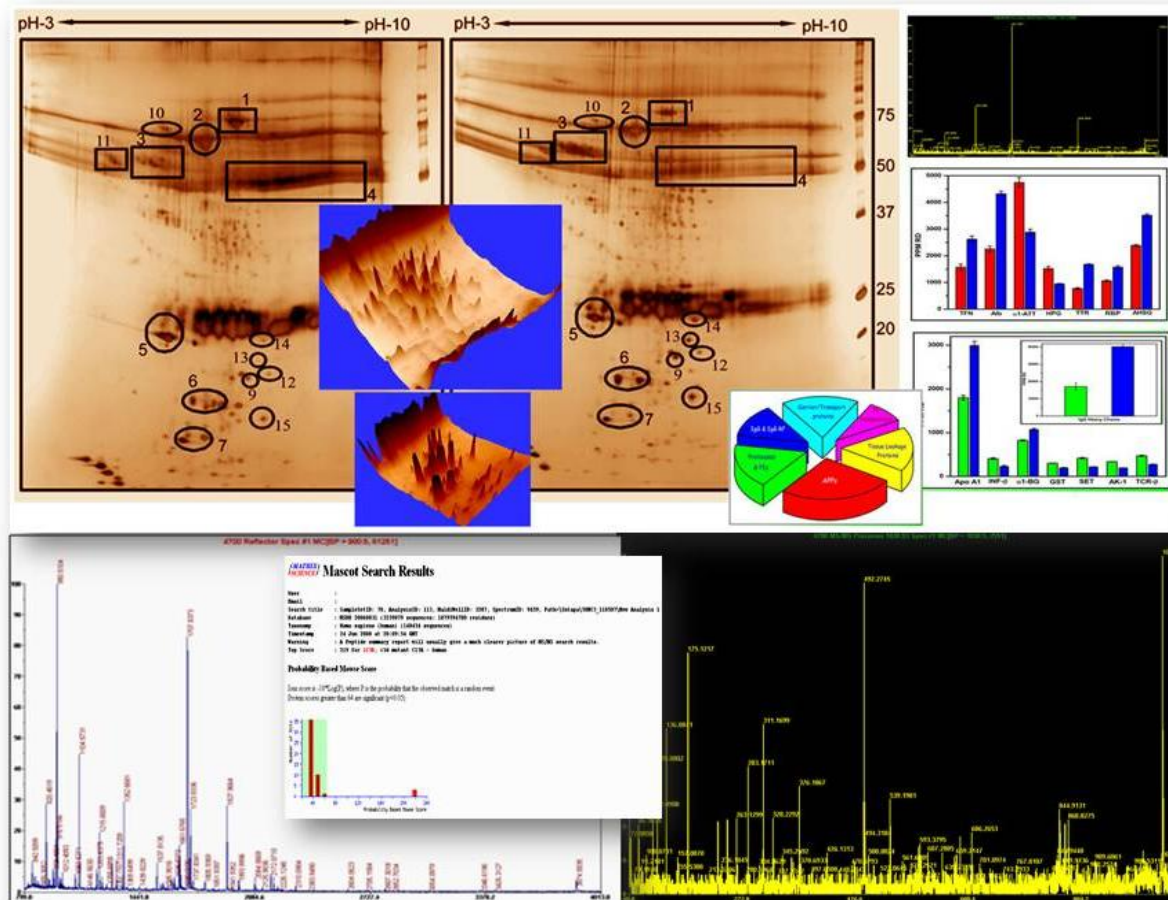
Spot No.	Name of the Protein	Probable Implications in B-ALL & Previous Reports in Other Malignancies (Relevant References)
4	Lymphocyte specific protein 1	differentially regulated in TEL/AML1-positive and -negative B-lineage ALL; major cellular substrate for protein kinase C in B cells, an enzyme that plays a key role in B cell signalling and development; widely expressed in leukaemias and lymphomas of B-cell origin; binds Ca^{2+} and actin cytoskeleton. (<i>BMC Genomics</i> . 2007 Oct 23;8,385; <i>Immunology</i> . 1999 Feb,96(2),262-71)
5	Heterogeneous nuclear ribonucleoprotein K	regulated by BCR-ABL and Ras-MAPK signaling pathways and overexpressed in CML; BCR/ABL-dependent enhancement of HNRPK translation-regulation is important for BCR/ABL leukemogenesis and contributes to blast crisis transformation of CML cells; PKC-delta down-regulates HNRNPk protein in a proteasome-dependent manner, which plays an important role in apoptosis induction in AML cells. (<i>Med Oncol</i> . 2010 Sep,27(3),673-9; <i>Blood</i> . 2006 Mar 15, 107(6),2507-16; <i>Exp Cell Res</i> . 2009 Nov 15,315(19),3250-8)
6	150kD oxygen regulated protein (Orp150, hypoxia up-regulated 1)	its up-regulation mediates purine analog-induced ER stress and unfolded protein response and apoptosis in human Raji B-cell lymphoma cells. (<i>J Proteome Res</i> . 2011 Mar 4,10(3),1030-42)
7	Moesin	acts as linker between the plasma membrane and the cytoskeleton and is key component in tumor metastasis; inactive cytoplasmic moesin associates with the membrane on activation and interacts with SYK and can trigger the ERK signal pathway; reciprocally regulates Rho GTPases; its altered expression is associated with vincristine resistance in childhood leukemia. (<i>Leuk Res</i> . 2010 Jun,34(6),769-76; <i>Int Immunol</i> . 2009 Aug,21(8),913-23; <i>Immunology</i> . 2004 Jun, 112(2),165-76; <i>Proteomics</i> . 2006 Mar,6(5),1681-94)
8	Tat-binding protein 1	exhibits tumor suppressor-like functions; its overexpression diminishes cell proliferation and almost completely inhibits transforming efficiency when stably expressed in human cancer cells; is a partner of p14ARF tumor suppressor and its overexpression results both in an increase in p14ARF half-life and activation of Mdm2/p53 pathway. (<i>Proc Natl Acad Sci U S A</i> . 1999 May 25,96(11),6434-8; <i>Oncogene</i> . 2007 Aug 2,26(35),5154-62)
9	H+-transporting two sector ATPase	up-regulation observed amongst the high-risk B-ALL patients may have implications in glucocorticoid drug-resistance of malignant cells; ATP synthase down-regulation forms the basis for dexamethasone triggered apoptosis of B-ALL cells; down-regulation by hypermethylation mechanism in CML cells is associated with multidrug resistance. (<i>Biochim Biophys Acta</i> . 2011 Jun, 1807(6),719-25; <i>Ann Oncol</i> . 2010 Jul,21(7),1506-14)
10	ATP synthase D chain, mitochondrial	is up-regulated in X-ray irradiated human erythroleukemia cells. (<i>Biochim Biophys Acta</i> . 2008 Apr, 1784(4),611-20)
11	Proteasome alpha 5 subunit	inhibition causes induction of leukemic cell death. (<i>Int J Cancer</i> . 2009 May 15, 124(10),2450-9)

Spot No.	Name of the Protein	Probable Implications in B-ALL & Previous Reports in Other Malignancies (Relevant References)
12	78kD glucose-regulated protein precursor(GRP78)	is a potent anti-apoptotic protein and plays a critical role in tumour cell survival, tumour progression and angiogenesis, metastasis and resistance to therapy. (<i>Biochem J.</i> 2011 Mar 1,434(2),181-8)
13	60S acidic ribosomal protein P2	modulates cytoplasmic translation by influencing the interaction between ribosomal subunits, thereby regulating the rate of cell proliferation; loss of function decreases cellular growth rate; is a potential molecular target for antisense therapy of human malignancies. (<i>Biochem J.</i> 2008 Aug 1,413(3),527-34; <i>Anticancer Res.</i> 2003 Nov-Dec,23(6C),4549-60)
14	Homo sapiens cargo selection protein TIP47	plays an important role in tumour cell development, differentiation and apoptosis; is involved in lipid droplet formation and in rearrangement of lipid membranes that are important in cell differentiation and division. (<i>Eur J Biochem.</i> 2003 Mar,270(6),1176-88; <i>J Cell Biol.</i> 2009 May 18, 185(4),641-55)
15	Stress-70 protein, mitochondrial precursor (75kD glucose regulated protein- GRP75)	its knockdown alters the hematopoietic progenitor pool in mice and contributes to abnormal hematopoiesis resulting in significant reduction of erythroid precursors and B lymphocytes; is a chaperone identified to be highly abundant on the cell surface of a wide variety of cancer cell types including B-ALL cells; is frequently deleted in myeloid leukemias and myelodysplasia, making it a candidate tumor suppressor gene in myeloid cells. (<i>Blood.</i> 2011 Feb 3,117(5),1530-9; <i>J Biol Chem.</i> 2003 Feb 28,278(9), 7607-16; <i>Leukemia.</i> 2000 Dec, 14(12),2128-34)
16	EIF3S4 protein	interacts with the cytoskeletal network and pelota, an evolutionary conserved protein reported to be involved in the regulation of cell proliferation and stem cell self-renewal; interacts with apoptosis-inducing factor (AIF) and mediates AIF's cellular functions of the inhibition of protein synthesis during apoptosis. (<i>BMC Cell Biol.</i> 2010 Apr 20, 11,28; <i>FEBS Lett.</i> 2006 Nov 27,580(27),6375-83)
17	Dynactin subunit 2	localizes at the centrosome and is involved in anchoring microtubules to centrosomes; the dynactin complex contribute to mitotic progression and maintains the integrity of metaphasic centrosomes to ensure transition to anaphase. (<i>Cell Motil Cytoskeleton.</i> 2004 May,58(1),53-66; <i>J Biol Chem.</i> 2011 Feb 18,286(7),5589-98)
18	PTB associated splicing factor (PSF)	RNA/DNA-binding nuclear protein involved in pre-mRNA processing, transcriptional repression, DNA repair, replication, and recombination; expression of ALK fusion proteins induces delocalization of PSF from the nucleus to the cytoplasm and forces overexpression of PSF; identified to be a fusion partners for ABL tyrosine kinase in B-ALL. (<i>Blood.</i> 2007 Oct 1,110(7),2600-9; <i>Eur J Haematol.</i> 2011 May,86(5),361-71)
19	Galectin – 1	is overexpressed in MLL-rearranged B-ALLs; inhibits host antitumor immune responses and modulates tumor angiogenesis and adhesion; induces apoptosis of activated T cells; is a stromal cell ligand of the pre-B cell receptor (BCR) implicated in synapse formation between pre-B and stromal cells and in pre-BCR triggering. (<i>Clin Cancer Res.</i> 2010 Apr 1,16(7),2122-30; <i>J Biol Chem.</i> 2010 Jan 22,285(4),2232-44; <i>Proc Natl Acad Sci U S A.</i> 2002 Oct 1,99(20),13014-9)

All the evidences in support of functional links between the differentially regulated proteins identified in our study and key mediators of B-cell signalling and tumorigenesis advocate that our findings, albeit requiring further validation, define novel molecular markers mediating ‘fine-tuning’ of B-cell signalling, and show prospects of adding insights to the mechanism of leukemogenesis in B-ALL. It is to be noted that the downstream signalling interactome is a resultant of several possible alternate crosstalk/overlap of pathways together with the cellular background that ultimately brings about the diverse functional changes/cellular effects required along the path of leukemic transformation. Changes in protein expression may be either causative or as consequence of the disease process. The identification of such changes in our study will provide important advances in understanding B-cell biology and malignancy. Ultimately, success of proteomic studies on B-cell malignancies needs to be measured in terms of outcomes, such as identifying proteins that; a) contribute to our understanding of B-cell malignancies; b) can be used for diagnosis or prognosis and c) are potential therapeutic targets. In this respect our study adopted proteomic strategies that delivered quantitative data on protein abundances or changes in protein expression and hence potentially identified novel deregulated proteins in B-ALL. Although the importance of all of these candidate proteins will require further validation *in vitro* and *in vivo*; nevertheless, they show promise to form the basis for testing new target-specific therapeutics for B-ALL. Also, proteins exhibiting opposite trends of de-regulation in B-ALL as compared to acute myeloid and/ or T-lymphoid leukaemias may explain high survival rates in the former, and thereby warrant investigations in the latter.

We propose that 2DGE maps could be used to at least produce unique fingerprints for various cell types or disease states and by building up a database of proteome maps they could be used to characterise distinct cellular proteomes. However, current proteomics techniques are limited in their sensitivity for protein detection. In our study, no single 2DGE image yielded > 3000 independent protein spots, which is far fewer than the total number of human proteins predicted from sequencing of the human genome (30,000–40,000 proteins without taking into account the products of alternative RNA splicing). Any changes which are detected in

proteomic studies either due to the disease or treatment are likely to be limited to relatively abundant proteins, albeit they may still be important or biologically significant proteins; e.g. STMN1 is an emerging anti-cancer target [66]. Further improvements in proteomics tools and their application to the direct comparison of protein profiles among background-matched cell fractions prepared from fresh specimens should provide an insight into the intracellular events that underlie malignant transformation in human leukaemias. Our hope then is the translation of that knowledge into clinical applications. Proteomics yield ever greater insights into ALL pathogenesis; one can expect an expanding repertoire of targeted therapies for clinical evaluation.



CHAPTER 3

Altered plasma levels of proteolysis-modulating, carrier and acute phase proteins in B-cell Acute Lymphoblastic Leukemia

3.1. Introduction

Acute lymphoblastic leukemia (ALL), the most common cancer in children, is a malignant (clonal) disease of the bone marrow in which early lymphoid precursors proliferate and replace the normal hematopoietic cells of the marrow. Based on immunophenotype results, it has been found that majority of ALL cases are B-ALL, characterized by an accumulation of blast B-cells. Primary oncogenic events seem, however, to require secondary cooperative changes to generate a fully transformed cell [14]. A comparison of the proteomic profiles in normal and malignant states can not only point out candidate diagnostic markers and/or therapeutic targets of the malignancy, but also elaborate on the mechanism of transformation of the cells.

Blood plasma is a rich source of biochemical products that can indicate physiological or clinical status of a patient [103]. It is the most valuable specimen for protein biomarker determination because it is readily obtainable and contains thousands of protein species secreted from cells and tissues [104, 105]. The discovery of protein biomarkers in plasma for diseases is challenging and requires a highly parallel display and quantization strategy for proteins [106-108] like 2DGE. The protein content of serum however, is dominated by a handful of proteins such as albumin, immunoglobulins, and lipoproteins present across an extraordinary dynamic range of concentration. This exceeds the analytical capabilities of traditional proteomic methods, making detection of lower abundance serum proteins extremely challenging. Reduction of sample complexity is thus an essential first step in the analysis of plasma proteome [109].

There have been three main methods of depleting abundant proteins from serum samples: affinity removal method [103, 106, 110-112]; membrane filtration method to separate low-mass proteins from high-mass ones [109]; and multidimensional chromatographic fractionation [105, 106, 108]. But all these methods are expensive, laborious and time-consuming, as depletion of multiple abundant proteins from each plasma sample requires

multiple technical steps. In our study, we employed ammonium sulfate precipitation with concentrations ranging from 10% to 60% for rapid depletion of multiple abundant proteins from plasma, and obtained best results with 20%. Fountoulakis and coworkers have earlier reported fractionation of plasma proteins with 50% and 70% ammonium sulfate to reduce concentrations of high-abundance components and enrich lower abundant components in plasma 2DGE profiles, thereby facilitating the identification of disease markers [113].

Identification of disease specific markers helps in diagnostic and prognostic monitoring of the malignancy and the associated minimal residual disease, but, disease regulated plasma proteins in B-ALL are still unclear. Here we report the identification of disease-regulated proteins in the plasma for the detection and monitoring of B-ALL. We compared the 2DGE patterns of 20% ammonium sulfate precipitates from plasma of B-ALL patients with those of normal subjects; and proteins were identified by MALDI TOF/TOF mass spectrometry. We could detect differential regulation of 15 proteins in B-ALL blood plasma including several acute phase proteins, carrier/transport proteins, proteolysis modulators, immunoglobulins, iron homeostasis proteins and tissue leakage proteins.

3.2. Materials and Methods

3.2.1. Plasma fractionation with ammonium sulfate

Blood plasma samples of 11 healthy normal volunteers and 12 B-ALL patients on *de novo* diagnosis, from R.K. Mission Hospital and Clinical Hematology Service, Kolkata were collected with written consent of the donors (parents in case of minors). Complete protease inhibitor cocktail (Roche Diagnostics, Germany) was added whenever plasma was stored at -80°C for later use. Plasma samples were centrifuged at 12000g, 4°C, for 30 minutes, and the supernatants diluted with PBS (2.7mM KCl, 1.5mM KH₂PO₄, 137mM NaCl, 8.1mM Na₂HPO₄, pH 7.4) to protein concentrations ≤ 20 mg/ml. Diluted plasma samples were distributed into 1ml

aliquots. Next, 55, 113, 144, 176, 208, 242, 277, 314, and 351 milligrams of $(\text{NH}_4)_2\text{SO}_4$ were added to different aliquots for attaining 10%, 20%, 25%, 30%, 35%, 40%, 45%, 50%, and 55% salt saturations respectively, and incubated on ice for 30 minutes with occasional mixing. The solutions were centrifuged at 12000g, 4°C for 25 minutes, the supernatants taken in fresh tubes and the precipitate dissolved in minimum volume of solubilization buffer (5mM sodium phosphate, 20mM KCl, 1mM EDTA, 0.2mM DTT, and pH-8.0). The starting plasma, the supernatant and the solubilized ammonium sulfate precipitate, all three were dialysed overnight against 10mM Tris, 5mM KCl, pH-7.5, at 4°C.

3.2.2 Two dimensional gel electrophoresis and Image Analysis

After dialysis, the starting plasma, the supernatant and the solubilized ammonium sulfate precipitate, all three were mixed with equal volume of 2D sample buffer containing 8M urea, 2% (w/v) CHAPS, 0.05% Bio-lyte 3-10 ampholyte, 20 mM DTT (Bio-Rad, Hercules, CA) and Protease inhibitor (Roche Diagnostics). The protein concentrations of the samples were estimated using RC DC protein estimation kit (Bio-Rad), and an absolute amount of 1.8 mg for Coomassie staining, or 600 µg for silver staining, or 1.2 mg for SYPRO RUBY staining, was taken in a final volume of 350µl. 17 cm pH 3-10 IPG strips (Bio-Rad) were passively rehydrated or cup-loaded with the plasma samples. IEF was carried out in a Protean IEF cell (Bio-Rad), stepwise up to 120000 Volt-Hours. Equilibration of the strips post IEF was performed following published protocol [114]. The second dimension was run on 8-16% polyacrylamide gradient gels in a Protean II XL electrophoresis module (Bio-Rad). Gels were stained either with Blue Silver Coomassie [32] or SYPRO-RUBY (Sigma) according to manufacturer's instructions, or Silver stain according to the method of Rabilloud [115]. Image captures and analyses were done on Versa Doc series 3000 imaging system using PDQuest software (version 7.1, Bio-Rad). Densitometry analysis of the gel spots of interest was performed using the density tool of PDQuest. Spot volume (intensity) of the desired spot(s) was

normalized as parts per million (ppm) of the total spot volume using the spots that were present in all gels, to calculate the relative abundance of a spot in a sample.

3.2.3. In-Gel tryptic digestion and mass spectrometry

Sequencing grade trypsin was purchased from Promega (Madison, WI). All other reagents were purchased from Pierce (Rockford, USA). The protein spots from Coomassie and SYPRO-RUBY stained 2D gels of normal plasma were excised using a robotic spot-cutter (Bio-Rad). The gel pieces were de-stained with 50% acetonitrile, 25mM ammonium bicarbonate. Subsequent in-gel tryptic digestion, peptide elution, acquisition of MS and MS/MS spectra and database searches were done following our published protocol [116]. Recrystallized CHCA and 2, 5-DHB (Sigma) were used as matrices. MS of the digested peptides was done in positive reflector mode in a MALDI-TOF/TOF tandem mass spectrometer (Applied Biosystems, AB 4700). Autolytic and common keratin peaks were validated and subsequently excluded from MS/MS analysis. Twelve most intense peptides from each spot were subjected to MS/MS analysis. Peak lists were prepared from MS and MS/MS data using GPS explorer V3.6 (Applied Biosystems) software and noise reduction and de-isotoping were performed using default settings. Resulting PMF and MS/MS data were searched against human MSDB and Swiss-Prot databases using in-house MASCOT V2.1 (Matrix Science, UK) server and MOWSE score (with $p < 0.05$) was considered to determine significant hits. For homologous proteins having similar MOWSE scores, preference was given to the protein with best match between theoretical and experimental molecular weight and pI. All MS experiments were repeated at least thrice, with spots excised from three separate gels. The database search parameters included one missed cleavage, error tolerance of ± 100 ppm for PMF and ± 1.2 Da for MS/MS ion search and variable modifications like carbamidomethyl cysteine, methionine oxidation, and N-terminal acetylation.

3.2.4. Western immunoblotting

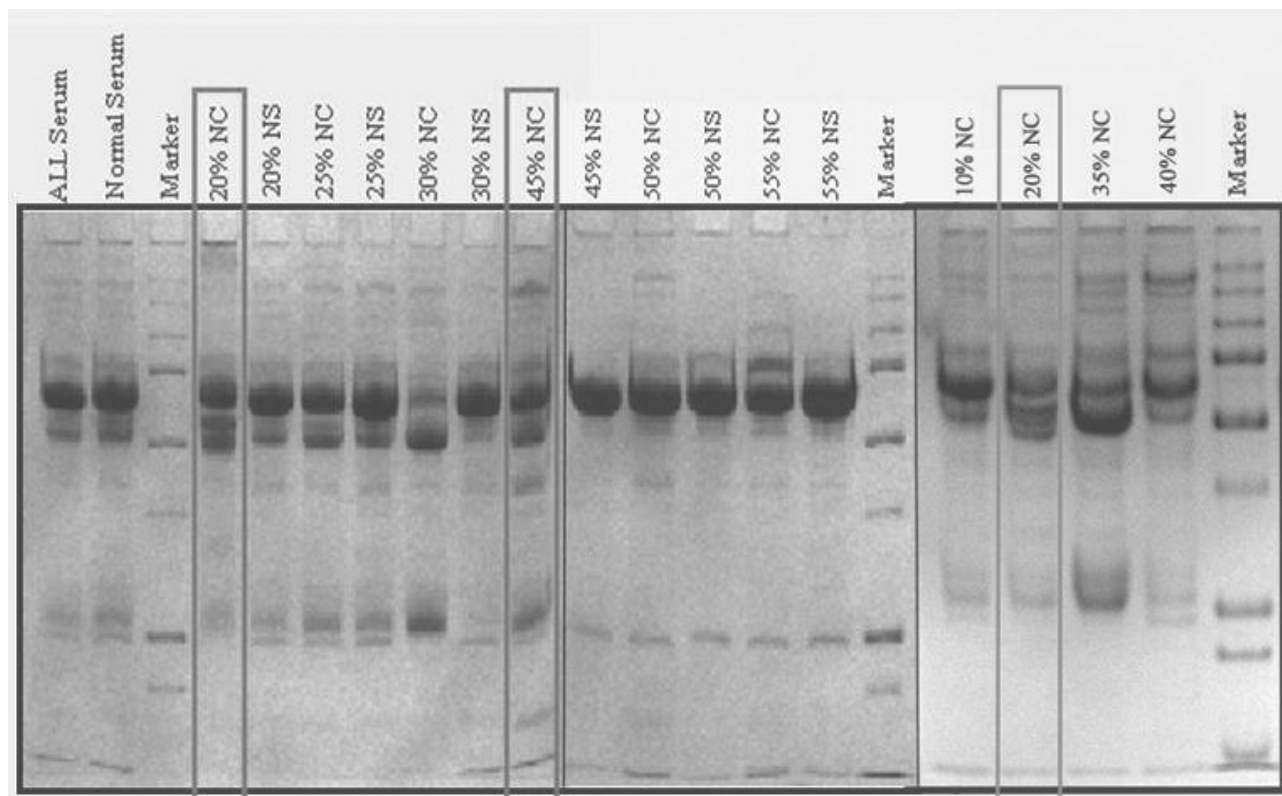
Plasma protein samples (25 µg) were re-suspended in 30 µL SDS-PAGE buffer (2% mercaptoethanol (v/v), 1% SDS, 12% glycerol, 50mM Tris-HCl and a trace amount of bromophenol blue), heated at 95 °C for 5 min, cooled and loaded directly onto 12% gel. 1D-SDS-PAGE was performed in a Mini Protean III-cell (Bio-Rad) using Tris-glycine with 0.1% SDS, following manufacturer's instructions. Proteins separated on gel were blotted onto PVDF membranes and subsequently blocked with Tris-buffer-saline (TBS), 5% non fat dry milk for 2h at room temperature. Primary antibodies (Abcam) were diluted in TBS/0.1% Tween (TBST) following manufacturer's protocol. β -Tubulin was used as loading control. Anti-rabbit or anti-mouse HRP-conjugated IgGs were used as secondary antibodies (Abcam). Membranes were washed with TBST and detected by ECL (Pierce) with either the VersaDoc imager (BioRad) or on X-ray film development.

3.3. Results

3.3.1. Separation of pre-fractionated plasma proteins using 2DGE

1D-SDS-PAGE profiles of raw plasma, ammonium sulfate precipitates and supernatants showed more protein bands in 20% and 45% cuts/precipitates (Figure 3.1) and hence, were chosen for 2DGE. The 2DGE profile of 20% $(\text{NH}_4)_2\text{SO}_4$ cut emerged to precipitate the maximum proportion of lower abundance proteins leaving most of the multiple abundant proteins in solution. From 20 mg protein in raw plasma, 3.5 ± 0.8 mg was obtained in the 20% $(\text{NH}_4)_2\text{SO}_4$ precipitate while the supernatant retained the rest of it (15 ± 1.6 mg estimated). Both 1D and 2DGE profiles of raw diluted plasma, the 20% $(\text{NH}_4)_2\text{SO}_4$ precipitate and the supernatant left after $(\text{NH}_4)_2\text{SO}_4$ precipitation revealed that the salt precipitates a fraction out of the total plasma proteome, that not only has a reduced load of abundant plasma proteins, but is also enriched in various minor proteins, leaving the gel electrophoresis profile of the supernatant almost identical to that of raw plasma.

Figure 3.1: Comparison of 1D-SDS-PAGE profiles of 10-55% (NH₄)₂SO₄ precipitates from normal blood plasma. NC: Normal cut (ammonium sulfate precipitate from normal plasma); NS: Normal sup (supernatant left after ammonium sulfate precipitation from normal plasma)



1D-SDS-PAGE showed depletion of multiple high-abundance proteins including albumin, immunoglobulin, transferrin, fibrinogen, α -2 macroglobulin, haptoglobin and transthyretin; and enrichment/appearance of several low-abundance proteins including tissue leakage proteins like α -fetoprotein in the 20% (NH₄)₂SO₄ precipitate (Figure 3.2).

The high percentage of albumin depletion ensured that many of the other abundant proteins that were obscured by albumin could be resolved well in 2D gels, and minor proteins that were initially hidden by co-migration with albumin or smears became visible (Figure 3.3A-C). The number of spots visible in 2D gels was doubled in 20% (NH₄)₂SO₄ precipitate compared to raw plasma, with various new spots appearing in the pI region 4.5-6.5 and between 10 kD and 50 kD (Figure 3.3D).

Figure 3.2: Coomassie stained 1D SDS-PAGE of raw plasma, its ammonium sulfate precipitate and supernatant. Lane1(from left)- MW marker (M); Lane2- raw normal plasma (NP); Lane 3- supernatant left after 20% $(\text{NH}_4)_2\text{SO}_4$ precipitation from normal plasma (NS), Lane 4- 20% $(\text{NH}_4)_2\text{SO}_4$ precipitate/cut from normal plasma (NC).

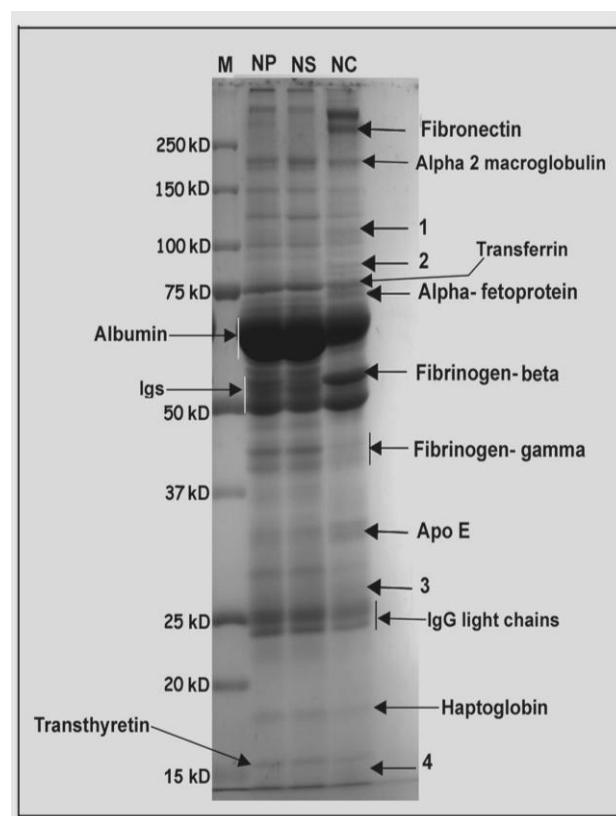
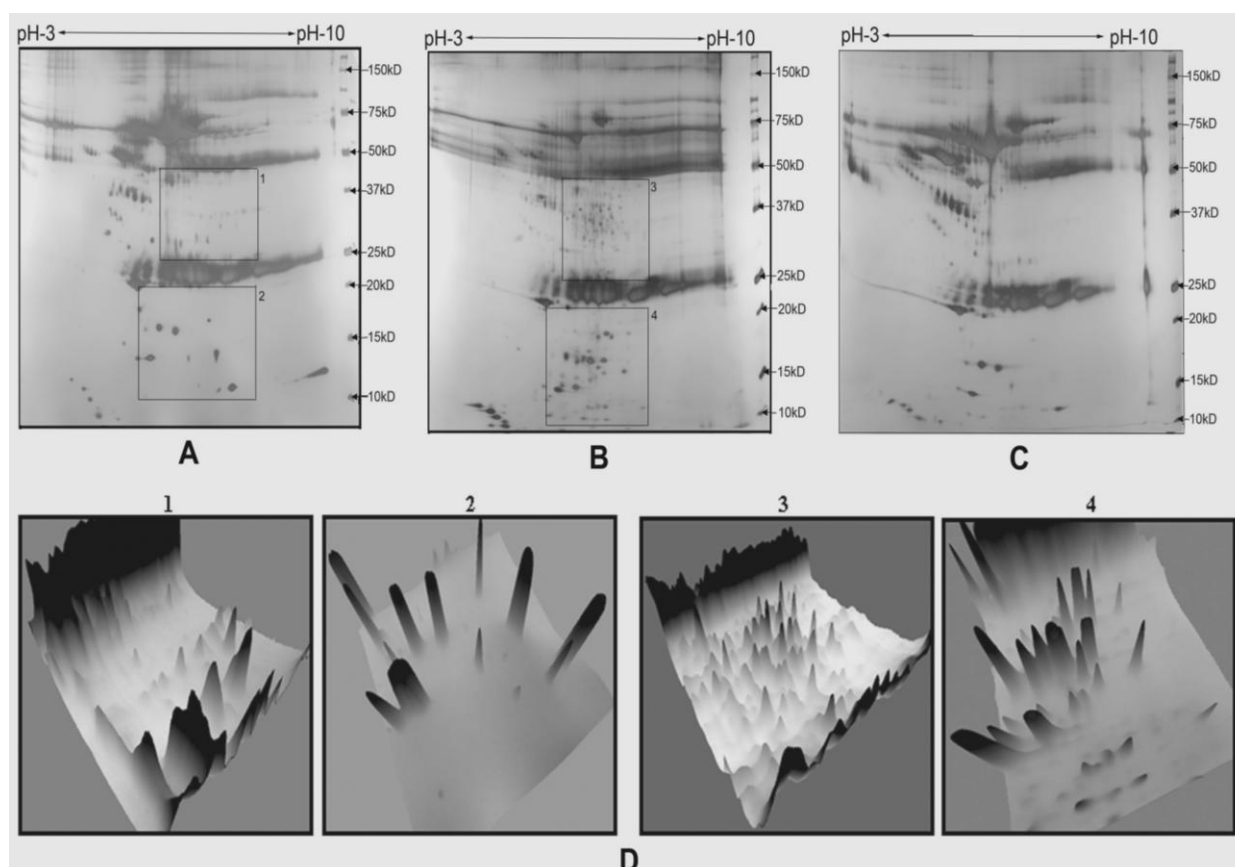


Figure 3.3: A. Silver stained 2DGE profile of raw normal plasma; B. Silver stained 2DGE profile of 20% $(\text{NH}_4)_2\text{SO}_4$ precipitate from normal plasma; C. Silver stained 2DGE profile of supernatant left after 20% $(\text{NH}_4)_2\text{SO}_4$ precipitation; D. 3D view of boxed regions in A and B



3.3.2. Identification of plasma proteins by tandem mass spectrometry

From coomassie and SYPRO-RUBY stained 2D gels of normal plasma, a total of 88 unique proteins were identified by performing MS+MS/MS combined searches as elaborated in Figure 3.4 and Table 3.1. Of these 64 had significant scores ($p \leq 0.05$) in the combined searches. Many of the rest 24 protein identifications were supported by either the published SWISS-2D-PAGE map of human plasma (marked with asterisk '*' in Table 3.1), or ion score ≥ 20 of at least one MS/MS fragment, or other proteomic studies of blood plasma/serum [106, 108, 109] (marked with '**'). All MS and MS/MS spectra together with a detailed description of the identified proteins/peptides are provided in the supplementary material in a CD.

Figure 3.4: Proteome map of 20% $(\text{NH}_4)_2\text{SO}_4$ precipitate obtained from normal plasma.

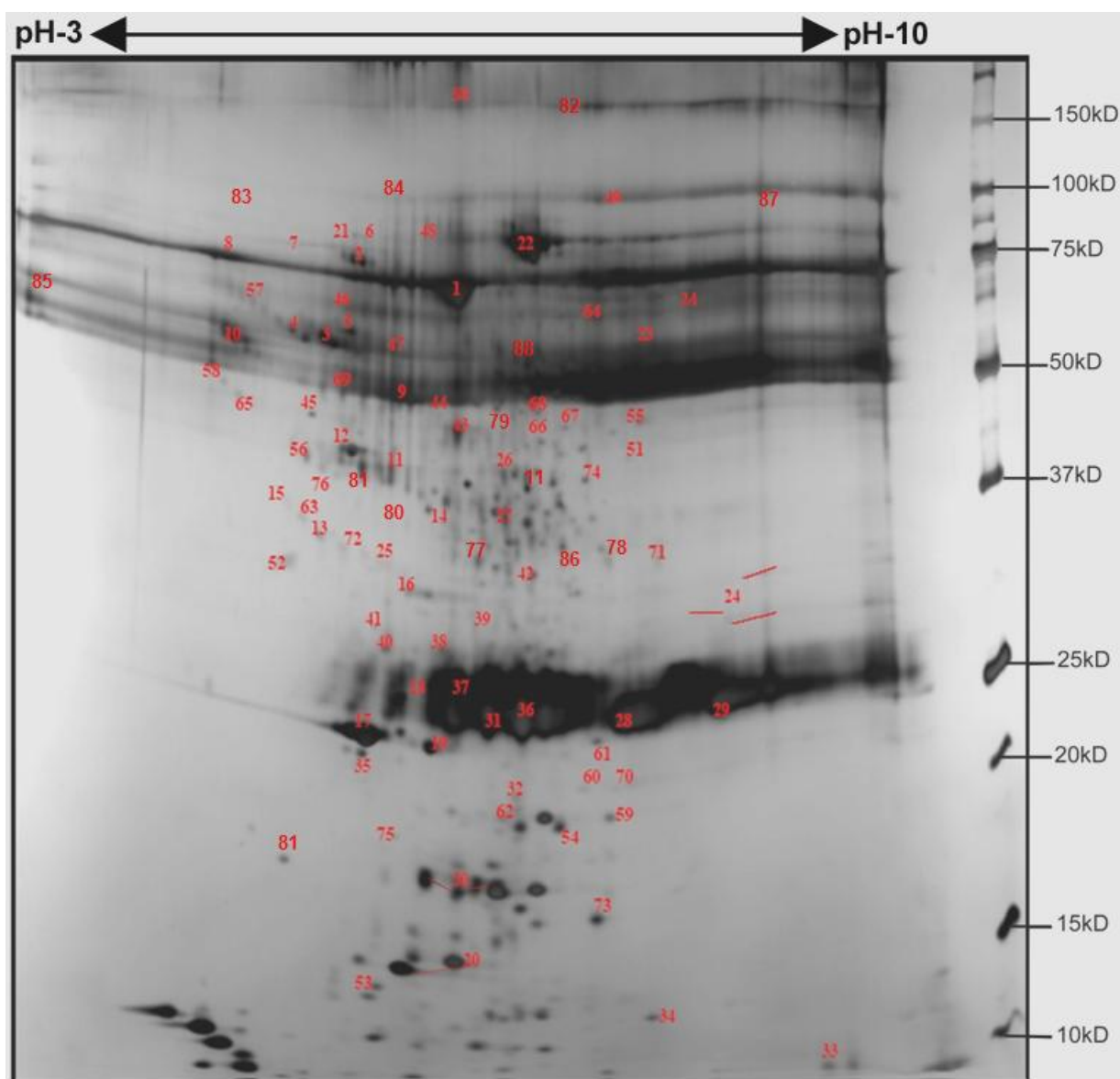


Table 3.1: Mass spectrometry identification details of the 88 protein annotations from 20% (NH₄)₂SO₄ precipitate of normal plasma.

Spot No.	Name of the Protein/Polypeptide	Accession Id.	Mr	pI	Mascot Score	Sequence Coverage	No. of MS/MS matches
1.	Serum Albumin-Human	1BKE	65,993	5.69	191(64)	64%	9
2.	Alpha-1-B-Glycoprotein-Human	Q68CK0_HUMAN	54,220	5.56	160(64)	48%	7
3.	Alpha-1-antitrypsin-Human	AAB59495	46,677	5.43	110(64)	36%	8
4.	Vitronectin precursor-Human	SGHU1V	54,328	5.55	112(64)	23%	5
5.	Kininogen, HMW precursor	KGHUH1	71,900	6.34	115(64)	40%	6
6.	Prothrombin-Human	Q4QZ40_HUMAN	69,920	5.70	202(64)	48%	8
7.	Plasma protease C1 inhibitor (fragment)-Human	Q59EI5_HUMAN	56,695	5.98	116(64)	27%	7
8.	Complement C1 inhibitor precursor-Human	ITHUC1	55,119	6.09	105(64)	29%	5
9.	Vitamin D binding protein-Human	Q53F31_HUMAN	52,916	5.34	221(64)	51%	8
10.	Alpha-2-HS-glycoprotein precursor-Human	WOHU	39,300	5.43	158(64)	40%	5
11.	Haptoglobin precursor-Human	HPHU1	38,427	6.13	242(64)	29%	5
12.	Human apolipoprotein-A-IV	AAA51748	43,358	5.22	494(64)	61%	9

Table 3.1: contd.

Spot No.	Name of the Protein/Polypeptide	Accession Id.	Mr	pI	Mascot Score	Sequence Coverage	No. of MS/MS matches
13.	Complement component C3d-Human	1C3D	32,845	6.34	219(64)	44%	6
*14.	Haptoglobin precursor	HPHU1	38,427	6.13	75(64)	14%	1
*15.	Complement component C3b-Human	S27041	25,280	4.49	49(64)	55%	4
16.	α 1-microglobulin/inter- α -trypsin inhibitor precursor-Human	HCHU	38,974	5.95	95(64)	35%	5
17.	APOA1 protein (fragment)-Human	CAA00975	28,061	5.27	470(64)	81%	11
18.	Serum amyloid P-Human	YLHUP	25,371	6.10	181(64)	30%	4
19.	Preproapolipoprotein A1-Human	LPHUA1	30,759	5.56	173(64)	59%	7
20.	Transthyretin chain A-Human	2TRYA	13,829	5.35	216(64)	94%	5
21.	Human α fetoprotein	E973181	66,358	5.67	264(64)	49%	6
22.	Transferrin-Human	Q53H26_HUMAN	77,030	6.68	339(64)	51%	8
23.	Fibrinogen β chain-Human	FGHUB	55,892	8.54	592(64)	49%	10
24.	Fibrinogen α chain-Human	FGHUA	69,714	8.23	508(64)	38%	8

Table 3.1: contd.

Spot No.	Name of the Protein/Polypeptide	Accession Id.	Mr	pI	Mascot Score	Sequence Coverage	No. of MS/MS matches
25.	Fibrinogen β chain fragment d-Human	1FZAB	35,875	7.66	253(64)	79%	5
26.	Voltage gated Ca channel $\alpha 2\delta 3$ subunit-Human	Q8IZS8_HUMAN	122,933	5.53	65(64)	29%	0
27.	Fibrinogen α chain extended splice form-Human	D44234	94,914	5.70	204(64)	35%	4
28.	Immunoglobulin κ light chain VLJ region-Human	BAC01677	27,574	7.53	160(64)	33%	3
*29.	Immunoglobulin κ chain V-III region (B6)-Human	K3HUB6	11,628	9.34	59(64)	16%	1
30.	Haptoglobin precursor	HPHU2	45,177	6.13	71(64)	53%	5
31.	Immunoglobulin κ chain NIG26 precursor-Human	JEO242	23,504	5.46	203(64)	48%	3
*32.	Immunoglobulin λ light chain variable region (fragment)-Human	AAD16673	11,505	5.67	32(64)	25%	1
33.	Hemoglobin α chain (fragment)-Human	Q9BX3_HUMAN	10,703	7.07	87(64)	60%	3
34.	Hemoglobin β chain-Human	2HBSB	15,827	7.26	143(64)	82%	6

Table 3.1: contd.

Spot No.	Name of the Protein/Polypeptide	Accession Id.	Mr	pI	Mascot Score	Sequence Coverage	No. of MS/MS matches
*35.	Retinol binding protein 4, plasma-Human	Q5VY30_HUMAN	22,929	5.77	22(64)	50%	1
36.	Ig κ light chain VLJ region (fragment)-Human	BAC01701	29,183	8.84	127(64)	39%	4
37.	Anti RhD monoclonal T125 κ light chain precursor-Human	Q5EFE6_HUMAN	25,682	8.70	56(64)	41%	2
38.	Fibrinogen fragment d, chain C-Human	1FZEC	34,457	5.68	64(64)	56%	2
39.	Fibrinogen fragment d, chain B-Human	1FZAB	35,875	7.66	137(64)	53%	5
40.	Fibrinogen fragment d, chain F-Human	1FZEF	34,343	5.68	109(64)	54%	4
41.	Fibrinogen fragment d, chain C-Human	1FZAC	35,144	5.57	91(64)	66%	3
42.	Fibrinogen beta chain precursor	FIBB_HUMAN	55,892	8.54	107(53)	48%	5
43.	Fibrinogen γ A chain precursor-Human	FGHUG	49,465	5.70	313(64)	55%	9
44.	ALB protein (Growth inhibiting protein 20)-Human	Q86YGO_HUMAN	47,330	5.97	170(64)	39%	8
45.	Apolipoprotein-A-IV precursor-Human	LPHUA4	45,307	5.23	107(64)	58%	5

Table 3.1: contd.

Spot No.	Name of the Protein/Polypeptide	Accession Id.	Mr	pI	Mascot Score	Sequence Coverage	No. of MS/MS matches
46.	α 1-antitrypsin precursor-Human	ITHU	46,707	5.37	248(64)	55%	8
47.	Fibrinogen γ B chain precursor-Human	FGHUGB	51,479	5.37	343(64)	64%	8
48.	Coagulation factor XIII chain b precursor-Human	KFHU13	75,442	5.97	94(64)	34%	3
49.	Plasminogen-Human	Q5TEH4_HUMAN	90,510	7.04	90(64)	40%	6
50.	Fibronectin1-Human	Q60FE4_HUMAN	252,848	5.66	224(64)	26%	13
51.	HUMPI5 NID (CDC2-related protein kinase)-Human	AAA60092	35,549	9.02	65(64)	52%	1
52.	Replication licensing factor MCM2-Human	S42228	99,174	5.72	68(64)	21%	0
53.	(P02735) Serum amyloid A protein precursor-Human	SAA_HUMAN	13,524	6.28	157(64)	52%	2
54.	(P01574) Interferon beta precursor (IFN-beta) (Fibroblast interferon)-Human	IFNB_HUMAN	22,279	8.93	53(53)	28%	0
55.	(P61011) Signal recognition particle 54 kDa protein (SRP54)	SRP54_HUMAN	55,668	8.87	53(53)	16%	0

Table 3.1: contd.

Spot No.	Name of the Protein/Polypeptide	Accession Id.	Mr	pI	Mascot Score	Sequence Coverage	No. of MS/MS matches
56.	Hypothetical protein DKFZp779N0926-Human	Q7Z664_HUMAN	45,064	5.76	547(64)	46%	6
**57.	Collagen alpha 1(XI) chain precursor - human	CGHU1E	181,029	5.11	53(64)	21%	2
58.	Nicotinic acetylcholine receptor epsilon chain precursor - human	S34775	54,581	5.09	43(64)	16%	1
**59.	Glutathione S-transferase A2	GSTA2_HUMAN	25,531	8.54	33(64)	85%	1
60.	SET domain, bifurcated 1-Human	Q5SZD8_HUMAN	27,685	4.85	45(64)	24%	1
**61.	Adenylate Kinase 1-Human	Q5T9B7_HUMAN	23,396	8.78	29(64)	29%	2
**62.	Interleukin-14 precursor –Human	A48203	54,723	9.32	26(64)	27%	1
63.	3' Histone mRNA exonuclease1	THEX1_HUMAN	39,907	6.32	45(64)	43%	1
64.	AB009303 NID membrane-type matrix metalloproteinase 3	BAA23742	69,451	8.72	58(64)	34%	1
65.	Leucine-rich PPR motif-containing protein-Human	Q7Z7A6_HUMAN	157,805	5.81	53(64)	17%	1
**66.	Selenoprotein P -Human	AAH15875	43,157	7.59	51(64)	26%	1

Table 3.1: contd.

Spot No.	Name of the Protein/Polypeptide	Accession Id.	Mr	pI	Mascot Score	Sequence Coverage	No. of MS/MS matches
**67.	1-Phosphatidylinositol-4-phosphate 5-kinase-Human	A55967	46,163	7.70	24(64)	9%	1
68.	HSP63G13 NID (p63 protein)-Human	AAG45609	55,652	6.41	60(64)	25%	1
69.	(Q9UPY3) Endoribonuclease Dicer-Human	DICER_HUMAN	217,490	5.45	47(53)	11%	1
70.	(P58340) Myeloid leukemia factor 1	MLF1_HUMAN	30,608	9.46	37(53)	34%	2
71.	Matrix metalloprotease MMP-27	Q9H306_HUMAN	58,986	8.83	36(64)	23%	2
*72.	Apolipoprotein E precursor (ApoE)	APOE_HUMAN	36,132	5.65	284(64)	50%	7
73.	T-cell receptor β -chain precursor	CAA71260	15,318	6.07	46(64)	43%	1
**74.	Homeobox protein CHX10	CHX10_HUMAN	39,386	7.11	33(53)	17%	1
75.	Ephrin-A1 precursor	EFNA1_HUMAN	23,756	6.49	41(53)	36%	1
76.	Intestinal alkaline phosphatase precursor	PPBI_HUMAN	56,776	5.53	36(53)	18%	1
77.	Ficolin 3 precursor	FCN3_HUMAN	32,868	6.20	96(64)	22%	4
78.	Complement component C4 fragment	Q5ST68_HUMAN	32,378	8.50	146(64)	37%	4

Table 3.1: contd.

Spot No.	Name of the Protein/Polypeptide	Accession Id.	Mr	pI	Mascot Score	Sequence Coverage	No. of MS/MS matches
79.	Fibrinogen gamma chain precursor	FIBG_HUMAN	51,479	5.37	226(64)	30%	6
80.	Transthyretin precursor / Prealbumin (multimer)	TTHY_HUMAN	15,877	5.52	214(64)	81%	3
81.	Adrenocorticotrophic hormone (ACTH) (glycosylation shifts Mr and pI)	CAA00890	4,692	8.34	112(64)	78%	1
82.	Alpha-2-macroglobulin precursor (Alpha-2-M)	A2MG_HUMAN	163,175	6.00	74(53)	18%	2
83.	Inter-alpha-trypsin inhibitor heavy chain H4 precursor	ITI4_HUMAN	103,294	6.51	73(53)	26%	3
84.	Complement C3 precursor	CO3_HUMAN	187,046	6.02	80(53)	25%	3
85.	Alpha-1-acid glycoprotein 1 precursor (Orosomucoid 1)	A1AG1_HUMAN	23,497	4.93	130(53)	31%	3
86.	histidine-rich glycoprotein precursor – human (glycosylation shifts pI)	KGHUGH	59,541	7.09	137(64)	22%	4
87.	Sodium/hydrogen exchanger 2 (NHE-2)	SL9A2_HUMAN	91,461	9.20	62(53)	13%	2
88.	C4A2 (C4A3)	Q6U2F0_HUMAN	58,393	5.67	77(64)	35%	6

All the 88 proteins were searched for their molecular function, biological process and localization in the PANTHER classification system database [117]. Figure 3.5 shows the results in form of pie-charts.

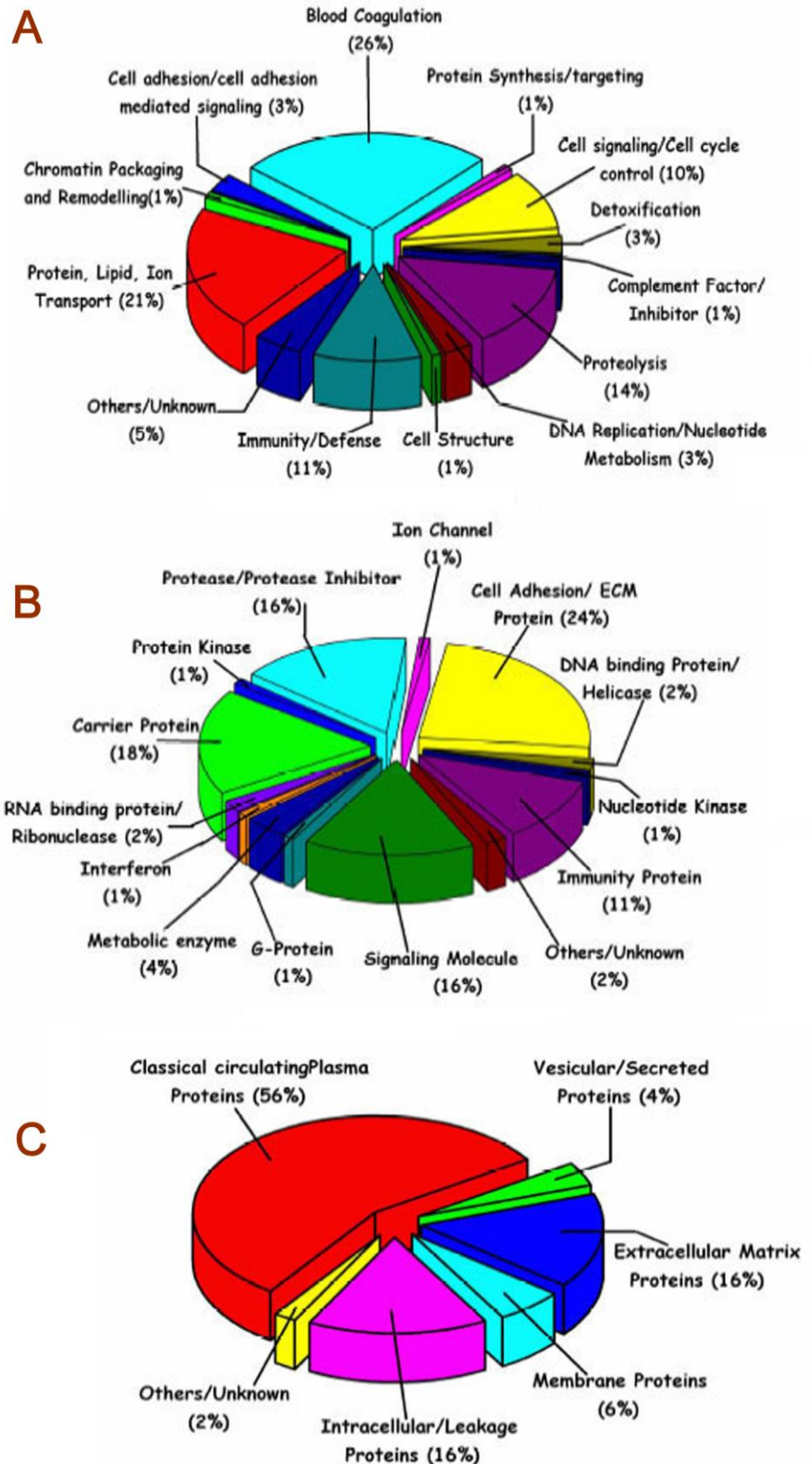


Figure 3.5: Gene Ontology of the identified proteins according to the PANTHER classification system based on-
A. Biological process;
B. Molecular function;
C. Tissue/cellular localization.

3.3.3. Display of differentially regulated proteins in B-ALL plasma

All the ALL blood samples had high percentage of CD10⁺/ CD19⁺ blast cells and were categorized as B-ALL from morphological examination and immunophenotype [14, 118, 119].

The clinical features of B-ALL patients and normal controls are summarized in Table 3.2.

Table 3.2: Clinical Details of Leukemia Patients

Patient Number	Age (Years)	Sex	Clinical Details	Immunophenotype / Classification
B-ALL 1.	33	F	Hb-6.0 g/dL, TLC-3,900 cells/mm ³	87% CD10 ⁺ / CD19 ⁺ cells. Pre-B-ALL
B-ALL 2. *	13	M	Hb-7.9 g/dL, TLC-15,000 cells/mm ³	70.6% CD10 ⁺ / CD19 ⁺ cells. Pre-B-ALL
B-ALL 3.	5	M	Hb-7.5 g/dL, TLC-57,600 cells/ mm ³	78.3% CD10 ⁺ / CD19 ⁺ cells. Pre-B-ALL
B-ALL 4.	2&1/2 months	F	Hb-4.0g/dL, TLC-3,14,000 cells/ mm ³	92.6% CD10 ⁺ / CD19 ⁺ cells. Pre-B-ALL
B-ALL 5.	16	M	Hb-10.1g/dL, TLC-8,500 cells/mm ³	94.6% CD10 ⁺ / CD19 ⁺ cells. Pre-B-ALL
B-ALL 6.	7	F	Hb-3.7 g/dL, TLC-45,000 cells/mm ³	76.2% CD10 ⁺ / CD19 ⁺ cells. Pre-B-ALL
B-ALL 7. *	25	F	Hb-5.5 g/dL, TLC-89,000 cells/mm ³	64.4% CD10 ⁺ / CD19 ⁺ cells. Pre-B-ALL
B-ALL 8.	56	F	TLC-80,600 cells/ mm ³	79.0% CD10 ⁺ / CD19 ⁺ cells. Pre-B-ALL
B-ALL 9.	28	M	Hb-6.8 g/dL, TLC-1,63,000 cells/mm ³	95.0% CD10 ⁺ / CD19 ⁺ cells. Pre-B-ALL
B-ALL 10. *	8	F	Hb-7.9 g/dL, TLC-74,000 cells/mm ³	88.3% CD10 ⁺ / CD19 ⁺ cells. Pre-B-ALL
B-ALL 11. *	16	F	Hb-4.7 g/dL, TLC-1,20,000 cells/mm ³	80.8% CD10 ⁺ / CD19 ⁺ cells. Pre-B-ALL
B-ALL 12.	29	M	Hb-3.6 g/dL, TLC-2,70,000 cells/mm ³	91.1% CD10 ⁺ / CD19 ⁺ cells. Pre-B-ALL
AML 1.	9	M	Hb- 7.8 g/dL, TLC-1, 69,000 cells/mm ³	18% CD19 ⁺ , 6% CD2 ⁺ , 82% CD13 ⁺ , 69% CD33 ⁺ cells. AML
AML 2.	15	F	Hb-2.9 g/dL, TLC- 2, 67,000 cells/mm ³	15% CD19 ⁺ , 2% CD2 ⁺ , 82% CD13 ⁺ , 31% CD33 ⁺ cells. AML (FAB M1)

** Patient samples used in western immunoblots analysis*

As shown in Figure 3.6, a comparison between the 20% $(\text{NH}_4)_2\text{SO}_4$ precipitates obtained from 8 normal and 8 B-ALL blood plasma revealed 15 differentially regulated proteins. Table 3.3 summarizes the results.

Figure 3.6: Display of differentially regulated proteins in B-ALL blood plasma (right) compared to normal (left) A. 20% $(\text{NH}_4)_2\text{SO}_4$ precipitates showing differential regulation of 14 proteins in boxed regions; B. 45% $(\text{NH}_4)_2\text{SO}_4$ precipitates showing differential regulation of retinol binding protein in box 8; C. 3D view of the spots for the 15 differentially regulated proteins in normal and B-ALL plasma proteomes.

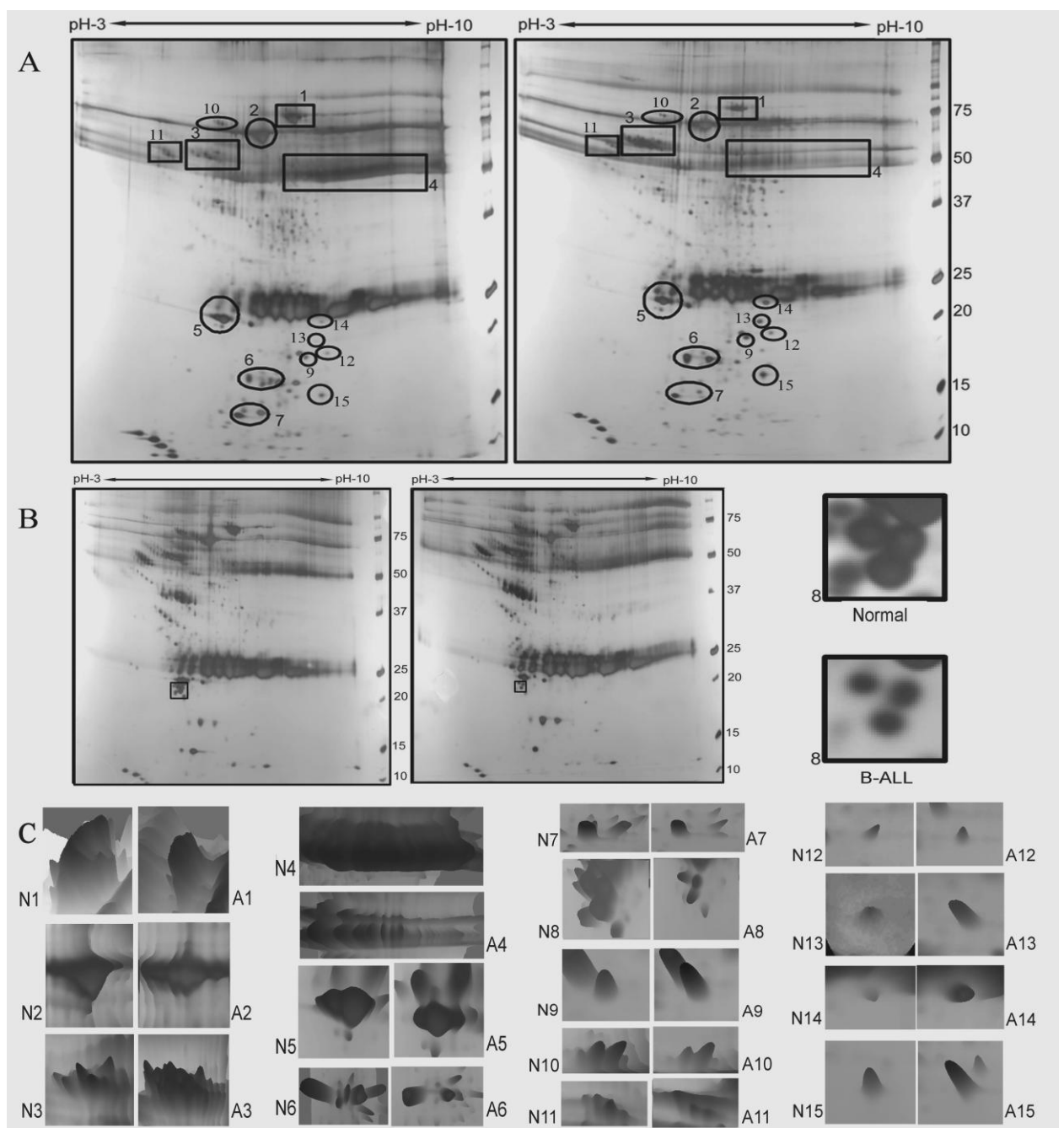


Table 3.3: Statistical evaluation of the spot densities of differentially-regulated proteins in plasma of B-ALL patients.

Name of the Protein	Mascot Score	MS/MS peaks matched	Sequence coverage	ALL		Normal		Change in ALL
				Mean	SEM	Mean	SEM	
Transferrin	339	8	51%	1574.29	110.66	2622.08	123.44	↓↓ (-1.7 fold)
Albumin	191	9	64%	2255.10	110.13	4325.33	97.46	↓↓ (-1.9 fold)
α1-antitrypsin	110	8	36%	4747.58	180.17	2885.75	114.82	↑↑ (+1.6 fold)
IgG Heavy chains*	Plasma Swiss 2D-PAGE			17132.70	2197.63	40228.70	976.26	↓↓↓ (-2.4 fold)
Apolipoprotein A1	470	11	81%	1798.15	54.99	2992.61	96.34	↓↓ (-1.7 fold)
Haptoglobin	71	5	53%	1524.82	84.02	946.58	19.48	↑↑ (+1.6 fold)
Transthyretin	216	5	94%	775.13	28.32	1676.62	22.63	↓↓↓ (-2.2 fold)
Retinol binding protein*	22	1	50%	1062.22	32.26	1576.28	52.83	↓↓ (-1.5 fold)
Interferon β precursor	53 (PMF-based match)			406.14	20.09	227.87	22.61	↑↑ (+1.8 fold)
α1-B-Glycoprotein	160	7	48%	823.35	14.23	1069.96	25.58	↓↓ (-1.3 fold)
α-2-HS-Glycoprotein precursor	158	5	40%	2386.33	34.30	3519.34	53.48	↓↓ (-1.5 fold)
Glutathione-S-transferase**	33	1	85%	300.32	4.67	191.83	10.84	↑↑ (+1.6 fold)
SET domain bifurcated	45	1	24%	416.73	14.15	215.78	4.93	↑↑ (+1.9 fold)
Adenylate Kinase 1**	29	2	29%	335.23	4.36	191.66	3.48	↑↑ (+1.8 fold)
T-cell receptor β-chain- precursor	46	1	43%	470.11	14.45	272.88	5.92	↑↑ (+1.7 fold)

* and ** - protein identification supported by published SWISS-2D-PAGE plasma map and other proteomic studies of blood plasma as described in text.

Table 3.4 lists the raw pixel data for each of the 16 individuals (averaged over triplicate gels for each individual). Differences in mean ppm spot volumes between normal controls and B-ALL cases for all protein spots were subjected to unpaired two-tail student's t-test. Due to the inherent complexity of a 2D gel-based proteomic studies, we have only concentrated on the spots which were very significantly different ($P \leq 0.01$) between normal and B-ALL proteomes.

Table 3.4: PDQuest raw pixel densities from 2DGE profiles, normalization, & statistics

	RAW PIXEL DENSITIES (spot volumes)															
	ALL 1	ALL 2	ALL 3	ALL 4	ALL 5	ALL 6	ALL 7	ALL 8	Normal 1	Normal 2	Normal 3	Normal 4	Normal 5	Normal 6	Normal 7	Normal 8
Total Density	13456.68	14207.36	13549.56	12482.66	14618.09	14399.28	13796.41	13686.09	13839.86	13822.16	12570.89	13676.78	14507.35	13421.56	12976.03	13172.86
Transferrin	22.15	17.85	13.22	20.75	24.44	25.23	22.72	27.14	31.28	32.81	40.19	31.69	42.33	32.02	33.71	38.56
Albumin	35.37	34.88	22.85	24.82	36.35	32.81	33.37	28.72	56.95	58.85	60.98	54.65	62.88	55.29	59.13	57.6
α1-antitrypsin	70.24	52.93	69.15	55.69	73.18	63.45	69.52	68.69	43.34	37.66	31.47	32.15	46.54	39.18	40.29	41.41
IgG Heavy chains	289.58	267.35	245.13	245.45	270.69	274.37	273.65	263.59	523.06	545.49	582.86	532.02	583.69	504.81	531.1	533.9
Apolipoprotein A1	26.71	26.46	22.06	20.1	29.22	27.21	23.37	23.5	36.23	38.52	43.17	41.05	45.79	37.57	37.53	42.85
Haptoglobin	23.83	17.85	19.02	17.25	24.96	23.45			13.6	11.96	12.02	13.03	14.5	12.39		
Transthyretin	12.05	10.32	9.99	8.94	12.29	10.03	11.22		23.79	21.78	21.05	22.19	24.84	22.59	22.7	
Retinol binding protein	14.65	14.99	15.44	13.95	14.7	16.11			21.19	21.66	22.01	21.87	22.44	21.97		
Interferon β precursor	5.82	5.21	5.68						3.34	2.54	3.25					
α1-B-Glycoprotein	10.71	11.75	11.36	9.98			12.2	10.88	13.83	14.03	14.44	14.19			14.72	14.29
α-2-HS-Glycoprotein precursor	32.65	32.63	32	31.91	34.43	32.4	32.75	33.81	47.12	46.18	47.61	48.22	49.09	47.6	47.66	46.01
Glutathione-S-transferase	4.1	4.07	4.11	3.83					2.46	2.89	2.66	2.31				
SET Domain Bifurcated	5.98	5.65	5.53						2.96	2.88	2.83					
Adenylate Kinase 1	4.58	4.64	4.59						2.62	2.59	2.54	2.71				
T-cell receptor β-chain precursor	6.99	6.42	5.89				6.64	6.34	3.71	3.86	3.41				3.31	3.83

STATISTICS FOR NORMAL SAMPLES												
Name of the protein	Normal 1	Normal 2	Normal 3	Normal 4	Normal 5	Normal 6	Normal 7	Normal 8	N_mean	N_SD	N_SEM	
Transferrin	2260.14	2373.72	3197.07	2317.06	2917.83	2385.71	2597.87	2927.23	2622.07875	349.157238	123.44	
Albumin	4114.93	4257.66	4850.89	3995.82	4334.35	4119.49	4556.86	4372.63	4325.32875	275.66347	97.46	
α1-antitrypsin	3131.53	2724.61	2503.4	2350.7	3208.02	2919.18	3104.96	3143.58	2885.7475	324.77438	114.82	
IgG Heavy chains	37793.73	39464.89	46365.85	38899.51	40234.08	37611.87	40929.31	40530.3	40228.6925	2761.30109	976.26	
Apolipoprotein A1	2617.8	2786.83	3434.12	3001.44	3156.33	2799.23	2892.25	3252.9	2992.6125	272.517383	96.34	
Haptoglobin	982.67	865.28	956.18	952.71	999.49	923.14			946.578333	47.7301093	19.48	
Transthyretin	1718.95	1575.73	1674.5	1622.46	1712.24	1683.11	1749.37		1676.62286	59.8774971	22.63	
Retinol binding protein	1356.95	1567.05	1750.87	1599.06	1546.8	1636.92			1576.275	129.412301	52.83	
Interferon β precursor	241.33	183.76	258.53						227.873333	39.1592854	22.61	
α1-B-Glycoprotein	999.29	1015.04	1148.68	1037.52			1134.39	1084.81	1069.955	62.6600264	25.58	
α-2-HS-Glycoprotein precursor	3404.66	3341.01	3787.32	3525.68	3383.8	3546.53	3672.93	3492.78	3519.33875	151.286047	53.48	
Glutathione-S-transferase	177.75	209.08	211.6	168.9					191.8325	21.6982847	10.84	
SET Domain Bifurcated	213.87	208.36	225.12						215.783333	8.5422499	4.93	
Adenylate Kinase 1	189.31	187.38	202.05	187.91					191.6625	6.97269615	3.48	
T-cell receptor β-chain precursor	268.07	279.26	271.26				255.08	290.75	272.884	13.253695	5.92	

Table 3.4: continued.....

	STATISTICS FOR B-ALL SAMPLES										
Name of the protein	ALL 1	ALL 2	ALL 3	ALL 4	ALL 5	ALL 6	ALL 7	ALL 8	A_mean	A_SD	A_SEM
Transferrin	1646.02	1256.39	975.68	1662.3	1671.9	1752.17	1646.8	1983.03	1574.2863	312.9994	110.66
Albumin	2628.43	2455.07	1686.47	1988.36	2486.64	2278.58	2418.74	2098.48	2255.0963	311.52243	110.13
α 1-antitrypsin	5219.71	3725.53	5103.49	4461.39	5006.12	4406.47	5038.99	5018.96	4747.5825	509.59864	180.17
IgG Heavy chains	21519.42	18817.71	18091.36	1966.33	18517.47	19054.42	19834.87	19259.7	17132.66	6215.8418	2197.63
Apolipoprotein A1	1984.89	1862.41	1628.1	1610.23	1998.89	1889.68	1693.92	1717.07	1798.1488	155.53789	54.99
Haptoglobin	1770.87	1256.39	1403.74	1381.92	1707.47	1628.55			1524.8233	205.81398	84.02
Transthyretin	895.47	726.38	737.29	716.19	840.74	696.56	813.26		775.12714	74.939844	28.32
Retinol binding protein	936.75	1055.09	1139.52	1117.55	1005.6	1118.8			1062.2183	79.040974	32.26
Interferon β precursor	432.5	366.71	419.2						406.13667	34.786047	20.09
α 1-B-Glycoprotein	795.89	827.04	838.4	799.51			884.29	794.96	823.34833	34.877475	14.23
α 2-HS-Glycoprotein precursor	2426.3	2296.7	2361.7	2556.35	2355.3	2250.11	2373.8	2470.39	2386.3313	97.017236	34.3
Glutathione-S-transferase	304.68	286.47	303.33	306.82					300.325	9.3477644	4.67
SET Domain Bifurcated	444.39	397.68	408.13						416.73333	24.51467	14.15
Adenylate Kinase 1	340.35	326.59	338.76						335.23333	7.5274453	4.36
T-cell receptor β -chain precursor	519.44	451.88	434.7				481.28	463.24	470.108	32.371344	14.45

We observed down-regulation of transferrin, albumin, immunoglobulin heavy chains, apolipoprotein A1, transthyretin, plasma retinol binding protein (RBP), α 1-B-glycoprotein, α 2-HS-glycoprotein (AHSG); and up-regulation of α 1-antitrypsin, haptoglobin, interferon- β (INF- β), glutathione-s-transferase (GST), SET domain bifurcated (SETDB), adenylate kinase-1 (AK-1), T-cell receptor- β (TCR- β) in the plasma of B-ALL patients as compared to normal plasma; shown as histogram plots in Figure 3.7.

Figure 3.7 (A): Histogram plots of parts per million relative spot densities of individual proteins in 16 2D gel profiles for 8 normal and 8 B-ALL plasma samples. Each of the 16 profiles were assembled using PDQuest, as master images from three replicate 2D gels run for each of the 16 plasma samples.

Gray Bars: B-ALL (n=8), Black bars: Normal (n=8), Hatched bars: AML (n=3), TFN: Transferrin, Alb: Albumin, α 1-ATT: α 1-Antitrypsin, HPG: Haptoglobin, TTR: Transthyretin, RBP: Retinol binding protein, AHSG: α 2-HS Glycoprotein precursor, INF- β : Interferon β , α 1-

BG: α 1-B Glycoprotein, GST: Glutathione-S-Transferase, SET: SET Domain Bifurcated, AK-1: Adenylate Kinase 1, Apo A1: Apolipoprotein A1, TCR- β : T-cell receptor β -chain.

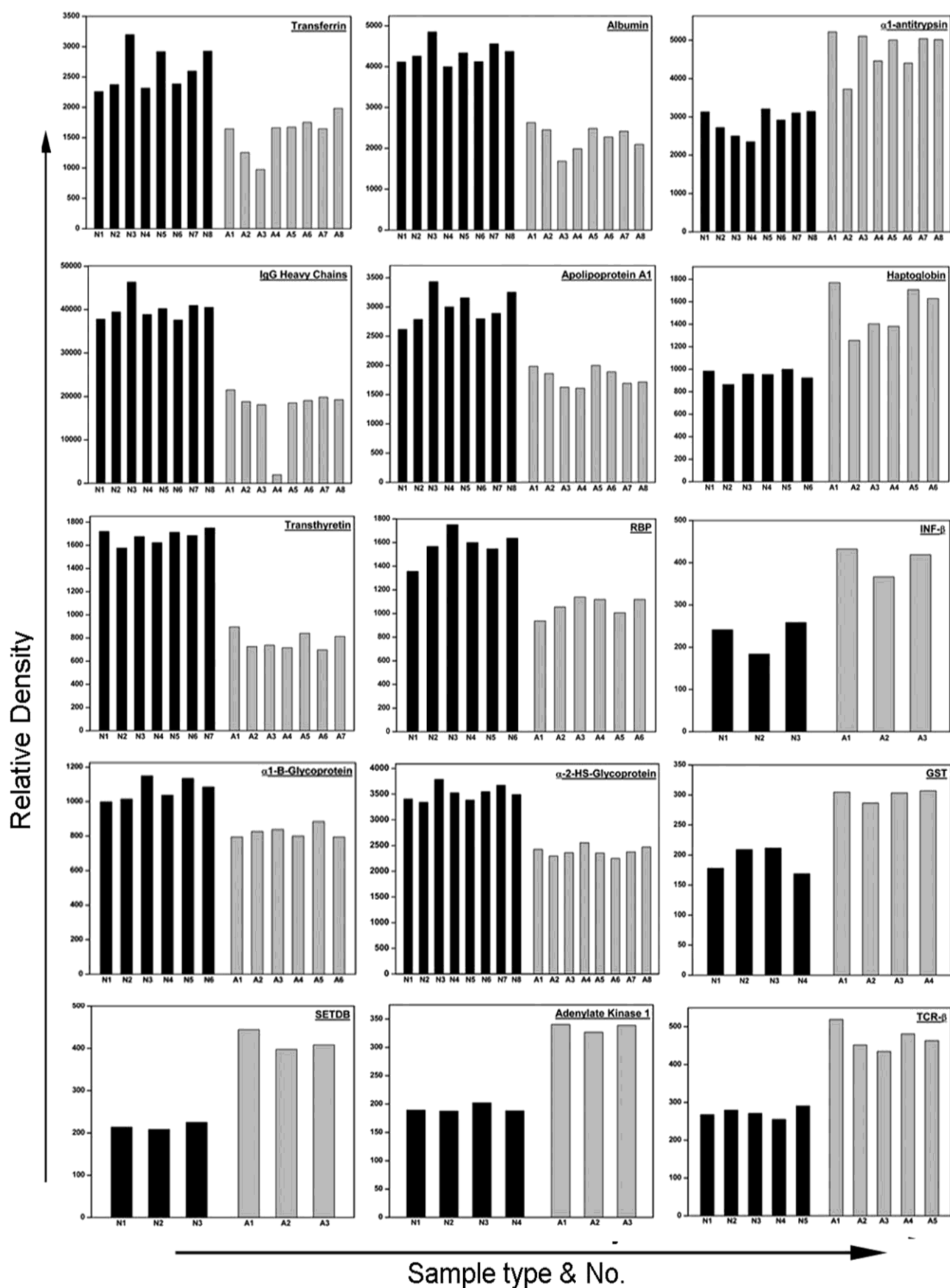
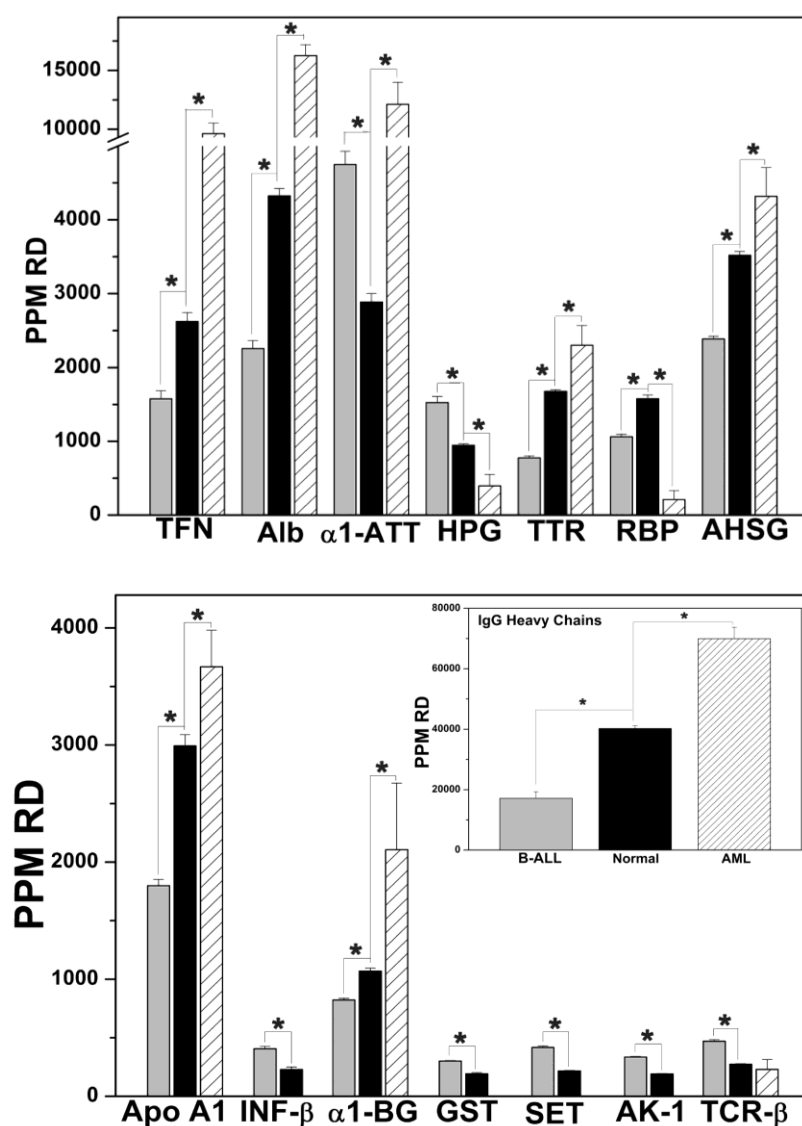


Figure 3.7(B): Histogram plot showing change in ppm relative densities (PPM RD) of the 15 differentially-regulated proteins. The error bars have been derived from densitometry analysis of 2D gels run with eight separate sample sets (normal & B-ALL). All data were subjected to unpaired two-tail student's t-test and the changes were found to be significant ($P \leq 0.01$).

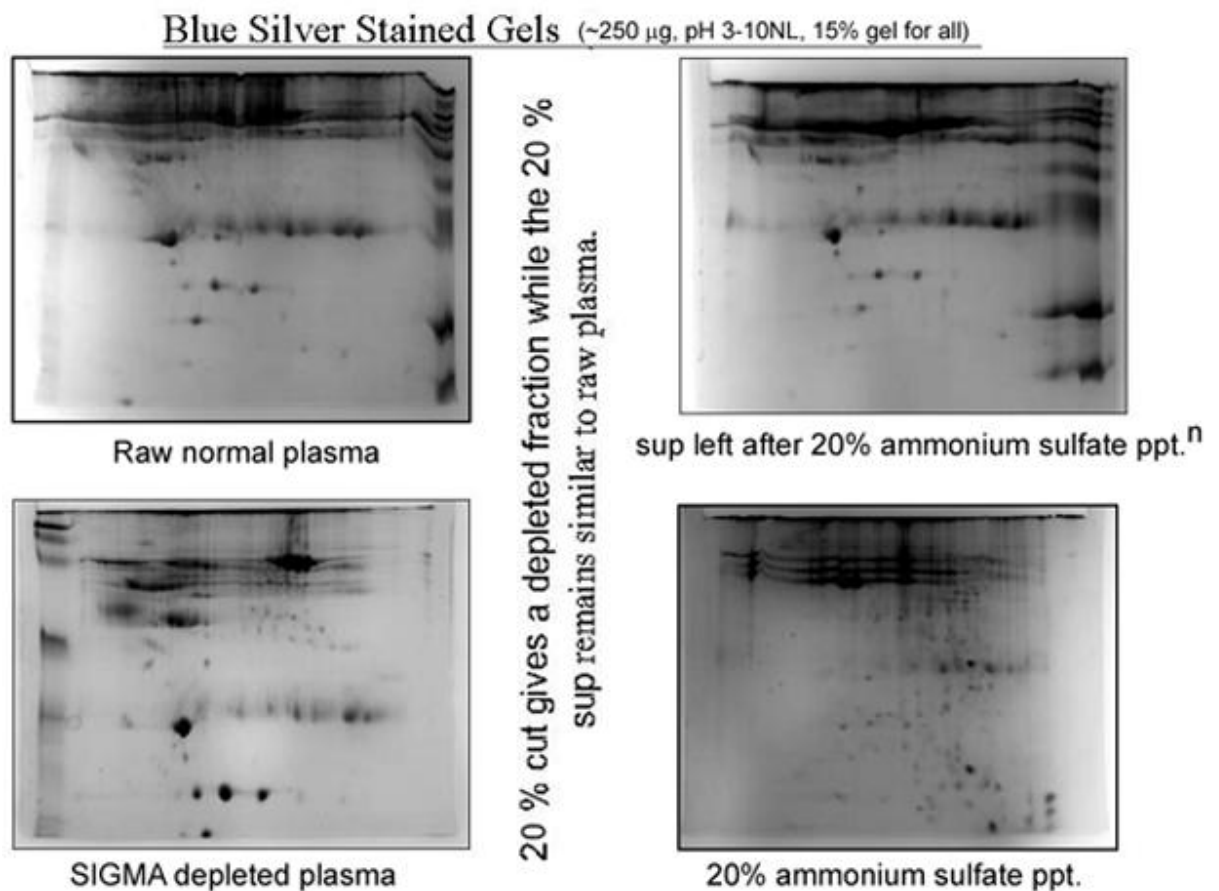
Gray Bars: B-ALL (n=8), Black bars: Normal (n=8), Hatched bars: AML (n=3), TFN: Transferrin, Alb: Albumin, $\alpha 1$ -ATT: $\alpha 1$ -Antitrypsin, HPG: Haptoglobin, TTR: Transthyretin, RBP: Retinol binding protein, AHSG: $\alpha 2$ -HS Glycoprotein precursor, INF- β : Interferon β , $\alpha 1$ -BG: $\alpha 1$ -B Glycoprotein, GST: Glutathione-S-Transferase, SET: SET Domain Bifurcated, AK-1: Adenylate Kinase 1, Apo A1: Apolipoprotein A1, TCR- β : T-cell receptor β -chain.



Of these, differential regulation of RBP was observed in 45% $(\text{NH}_4)_2\text{SO}_4$ precipitates along with similar differences in most of the other proteins, mentioned above (Figure 3.6B). However, in 45% $(\text{NH}_4)_2\text{SO}_4$ precipitates the extent of depletion of abundant proteins was

poorer than 20% precipitates. Figure 3.8 provides 2D SDS-PAGE images that justify the choice of 20% $(\text{NH}_4)_2\text{SO}_4$ precipitate over an expensive commercially available albumin depletion kit (Sigma, St. Louis, MO), for the enrichment of minor proteins in addition to depletion of abundant proteins from plasma.

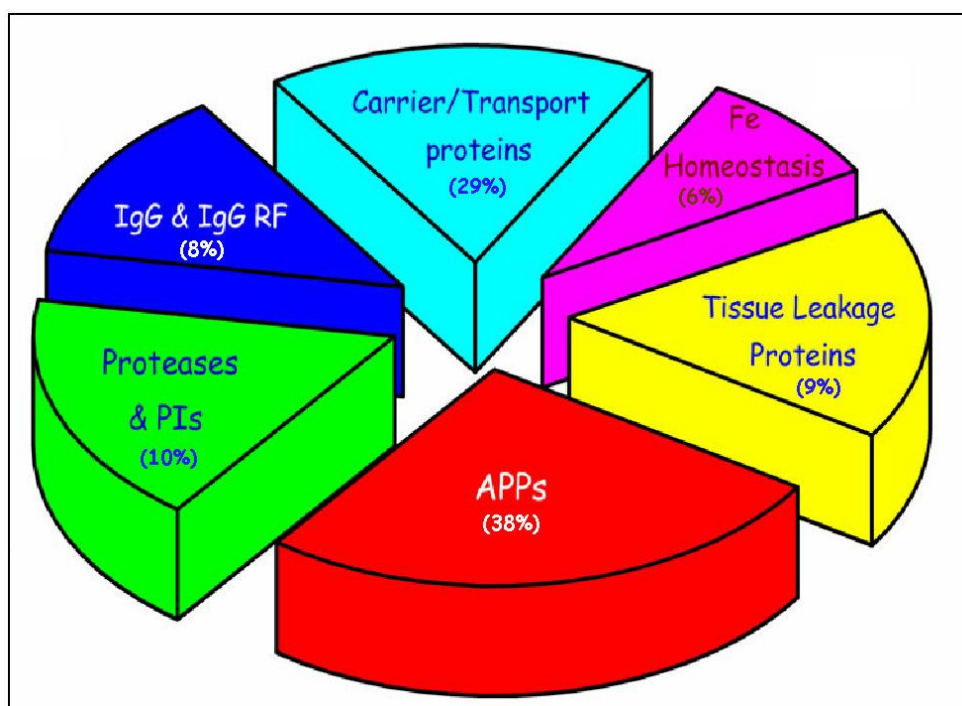
Figure 3.8: Comparison of 20% $(\text{NH}_4)_2\text{SO}_4$ precipitation and Sigma Affi-Gel Blue based depletion of abundant plasma proteins



Six of the 15 differentially-regulated proteins are acute phase plasma proteins (APPs); α -1-antitrypsin and haptoglobin being positive APPs; and transferrin, albumin, transthyretin, RBP amongst negative APPs. APPs are circulating plasma proteins which contribute to the early and nonspecific innate immune response when the body undergoes external or internal challenges such as trauma and infection. GST, SETDB, AK-1 and TCR- β are tissue-leakage proteins; α 1-antitrypsin and haptoglobin are protease inhibitors that are also part of the acute

phase response; and haptoglobin is also involved in iron homeostasis. As most of these proteins participate in multiple physiological processes like proteolysis, cargo-transport and iron homeostasis, their de-regulation might enlighten on the pathophysiology and clinical manifestation of the B-ALL malignancy. Figure 3.9 represents the functional classification of the differentially regulated proteins.

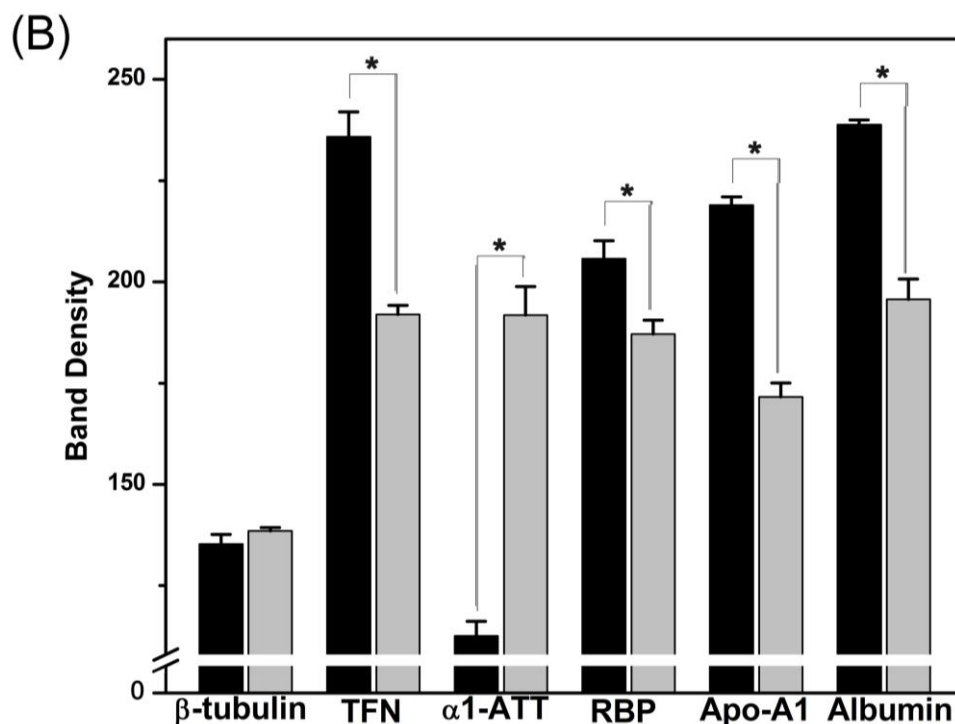
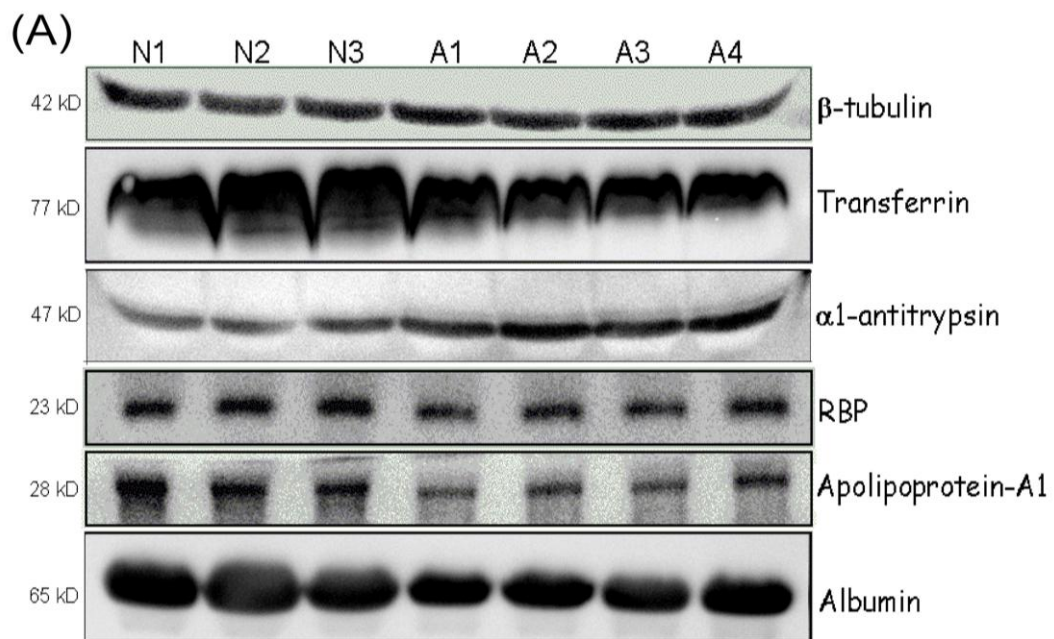
Figure 3.9: Functional classification of the differentially regulated proteins



3.3.4. Validation by western immunoblotting

To confirm the results obtained from 2DGE experiments, we quantitated the amounts of five differentially regulated proteins in raw plasma, obtained from a separate set of 3 normal controls and 4 B-ALL patients, using western immunoblotting. Figure 3.10 shows the immunoblots for 5 proteins with β -tubulin as loading control. The immunoblots clearly support results from 2DGE experiments. The five proteins: transferrin, α 1-antitrypsin, RBP, apolipoprotein-A1 and albumin, were chosen as representatives for proteolysis-modulating, carrier and acute phase proteins exhibiting differential regulation in B-ALL plasma 2DGE profiles.

Figure 3.10: (A) Western immunoblots of 5 differentially regulated proteins in normal and B-ALL raw plasma samples. β -tubulin: loading control, N1- N3: plasma samples from 3 different normal subjects, A1- A4: plasma samples from 4 different B-ALL patients; (B) Histogram plot of the band intensities of the 5 proteins and β -tubulin (loading control) from normal (black bars) and B-ALL (gray bars) raw plasma samples. Error bars indicate standard deviations in the band intensities across the 3 normal or 4 B-ALL sample lanes. All data were subjected to unpaired two-tail student's t-test and the changes were found to be significant ($P \leq 0.05$).



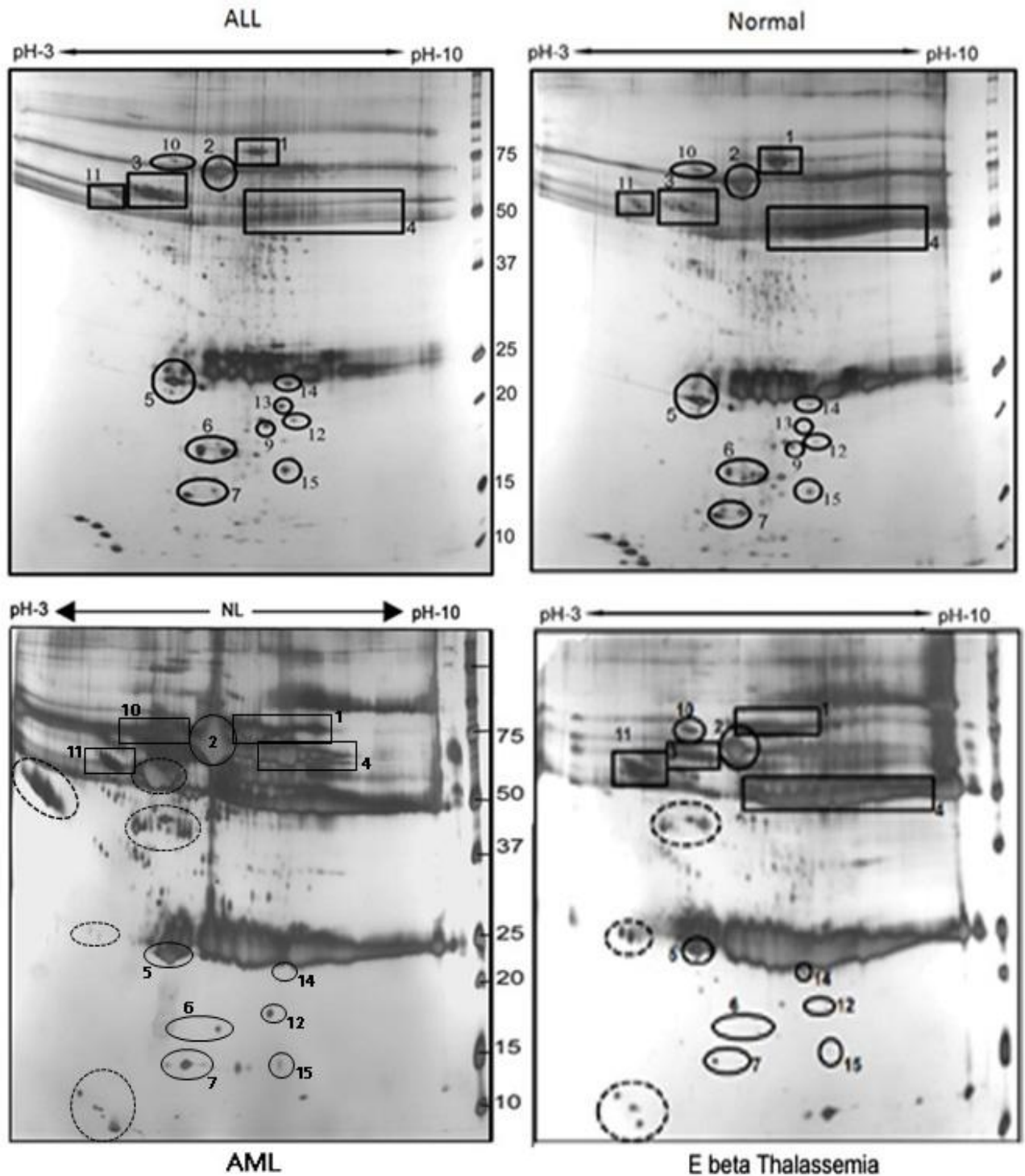
3.4. Discussion

Anderson and coworkers [120] have reported the most exhaustive list of proteins detected and/or identified in plasma till date. $(\text{NH}_4)_2\text{SO}_4$ precipitation helped in reducing concentration of abundant components and in defining spot boundaries in 2DGE profiles of plasma [113]. In our study, 20% $(\text{NH}_4)_2\text{SO}_4$ precipitation led to detection and identification of some proteins in normal blood plasma that were either detectable in LCMS protocols previously, or did not appear in Anderson's list in spite of being important blood plasma constituents (e.g. fibrinogen- γ , IgG light chain- λ). Nonetheless, some proteins are well detected by ESI-MS/MS while poorly ionized by MALDI protocols, as some were in our study [121]. In addition to identification of most of the classical high-abundance plasma proteins, many minor proteins like serum amyloid P, RBP and vitamin D binding protein [106], tissue leakage proteins (e.g. α -fetoprotein), ion channels and hormones were also identified in normal plasma proteome.

Since proteins differ markedly in their solubility at high ionic strength, salting-out has been a useful procedure to assist in enrichment of desired proteins. The advantages of $(\text{NH}_4)_2\text{SO}_4$ are its high water-solubility which allows salt solutions with high ionic strength, and low heat of solvation protecting most proteins from denaturation [122]. The simple inexpensive fractionation of plasma proteins with $(\text{NH}_4)_2\text{SO}_4$ depletes most of albumin and other abundant proteins leading to an increase in low-abundance component signals, as also observed earlier [113]. The composition of the 20% $(\text{NH}_4)_2\text{SO}_4$ precipitate depends primarily on the quantity and solubility of the constituent proteins initially present in the sample, irrespective of the source or nature of the starting material. Our group has also investigated differential regulations in an unrelated blood disorder with similar symptoms, E β -thalassemia [123]. The fact that $(\text{NH}_4)_2\text{SO}_4$ does not differentially deplete plasma proteins from sample to sample has been apparent from the immunoblots shown in Figure 3.10. Furthermore, 2DGE profiles of $(\text{NH}_4)_2\text{SO}_4$ precipitates from acute myeloid leukemia or AML (hatched bars in figure 3.7) and E β -thalassemia (unpublished results) patient plasmas indicated opposite trend of

differential regulation of most of these proteins, pointing towards the specificity of the observations in B-ALL. Figure 3.11 compares representative 2DGE profile of 20% $(\text{NH}_4)_2\text{SO}_4$ precipitate from ALL, Normal, E β -Thalassemia, and AML patient plasma.

Figure 3.11: Comparison of the 2DGE profiles of 20% $(\text{NH}_4)_2\text{SO}_4$ precipitate from ALL, Normal, E β -Thalassemia, and AML patient plasma



Immunoaffinity-based chromatography effectively depletes high-abundance proteins from the plasma [124], but even these expensive, laborious and time consuming commercially available methods fail to completely remove high-abundance components and suffer from their own limitations of specificity [125-128]. Our approach was to use a simple cost-effective method to obtain plasma fractions with somewhat reduced content of abundant proteins and maximum number of well-resolved spots on 2D gels. Although $(\text{NH}_4)_2\text{SO}_4$ fractionation method had a major limitation concerning specificity of the removed proteins, but provided this lack of specificity was not biased with the sample type (normal or patient), it could be effectively used for differential proteomics in clinical studies. Here, the principle of action of peptide ligand libraries holds relevance, which comprise of a mixture of porous beads on which all combinations of hexapeptides are covalently attached. When a complex protein extract is exposed to such a ligand library in large overloading conditions, each bead with affinity to an abundant protein is rapidly saturated, and the vast majority of the same protein remains unbound. In contrast, trace proteins do not saturate the corresponding partner beads, but are captured in progressively increasing amounts as the beads are loaded with additional protein extract. Thus, a solid-phase ligand library enriches for trace proteins, while concomitantly reducing the relative concentration of abundant species [129]. Use of combinatorial peptide ligand libraries for depletion of abundant proteins and accessing low-abundance biomarkers in clinical proteomics studies of blood plasma [130-132] further supports our notion that the objective of any pre-fractionation strategy for plasma should be increased access to disease-markers and not just specific removal of high abundance components.

The acute phase response (APR) normally subsides over 24–48 hours and thereafter the organism returns to normal function. However, this normal pathway can be prolonged and can convert to a chronic phase of inflammation. We observed sustained deregulation of the APPs in the plasma of B-ALL patients collected at different time points from disease onset. The regulation of APPs is reported to be quite different under the condition of the normal short-term

APR and the aberrant more-sustained APR that develops in multiple myeloma [133], autoimmune diseases and other types of cancer [134]. The APP transthyretin, that is down-regulated in B-ALL plasma, interacts with RBP enabling retinol transportation. Low levels of transthyretin coincide with low levels of retinol and RBP, as also reported for ovarian cancer [135]. Reduced levels of RBP have been reported in AML patient sera [136], as also verified in our study. Haptoglobin shows up-regulation in B-ALL plasma. Its up-regulation in AML, CML, and multiple myeloma is reported [133, 136, 137]. While our 2DGE profiles support the up-regulation of haptoglobin β -chain in AML plasma reported by Kwak and co-workers [136], we emphasize on haptoglobin α -chain that exhibits opposite trends of de-regulation in AML and B-ALL (figure 3.7). Additionally, observed de-regulations of α -1-antitrypsin, transferrin and albumin in the plasma of B-ALL patients, together with the available literature suggest that APPs might have important roles in cancer progression.

The altered levels of proteases and their inhibitors in tumor as well as in extracellular fluids have been linked to tumor progression. Many proteases are involved in the degradation of basement membrane and extracellular matrix, leading to tumor cell invasion and metastasis [107]. Figure 3.12 summarizes role of proteases in cancer progression.

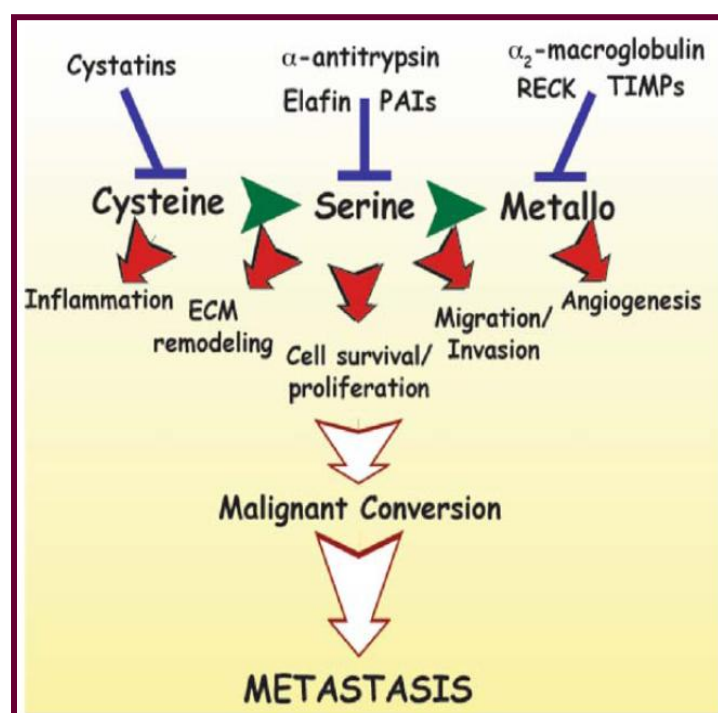
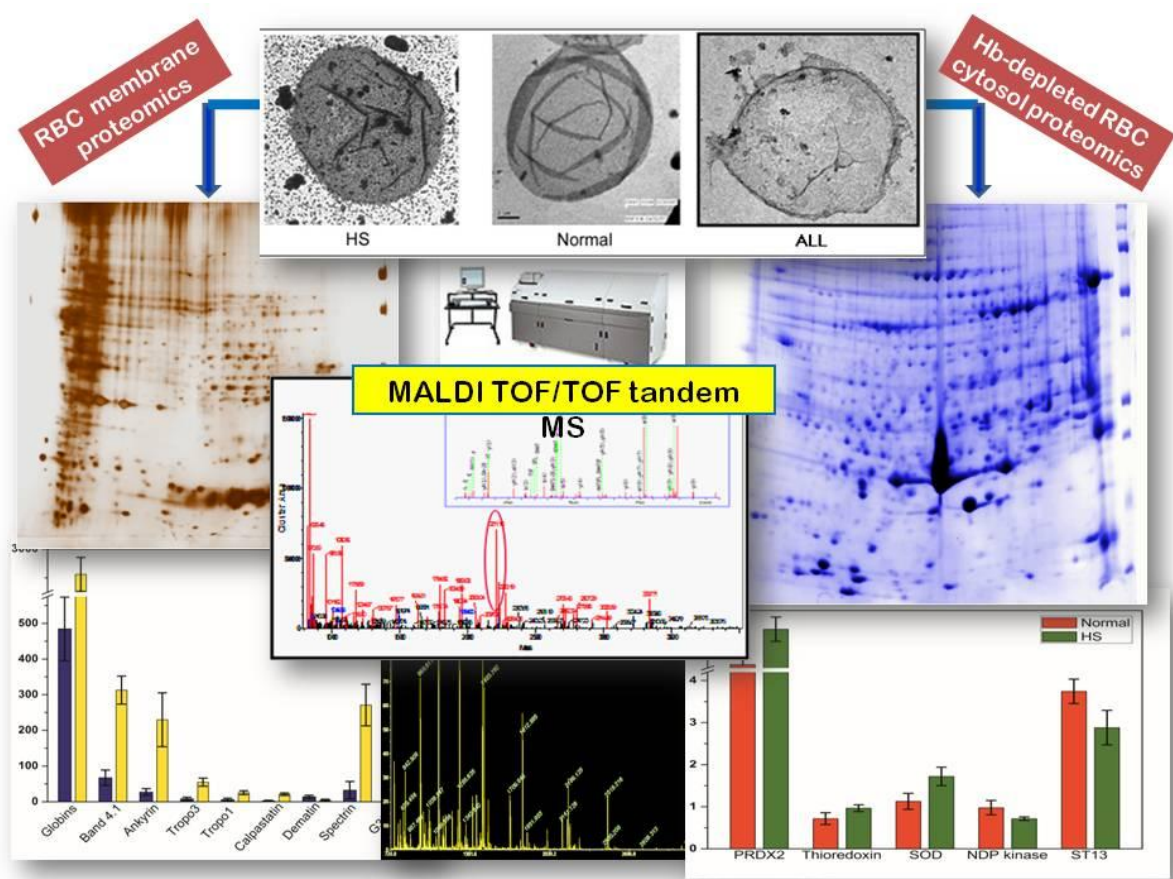


Figure 3.12: Role of proteolysis modifiers in cancer progression

Transferrin and haptoglobin are serine proteases, α -1-antitrypsin is a serine protease inhibitor, while AHSG is a cysteine protease inhibitor. AHSG is reported to be down-regulated in AML, ALL, NHL and multiple myeloma patients [133, 136, 138]. We observed 32% down-regulation of AHSG in B-ALL plasma in contrast to an up-regulation in AML plasma (Figures 3.7 & 3.11). Altered levels of the proteases and protease inhibitors, concurrent with enhanced tumor growth, invasion and metastasis designate these molecules as potential prognostic indicators in cancer. The lymphoblasts fail to mature into antibody-secreting plasma cells in B-ALL. In accordance to this fact, we observed significant down-regulation of immunoglobulin heavy chains in B-ALL patient plasma. In contrast, immunoglobulin heavy chains are up-regulated in AML patient sera [136]; hence they can serve as important biomarkers of B-ALL (Figures 3.7 & 3.11). α -1-B-glycoprotein and TCR- β , belonging to the immunoglobulin receptor family, respectively showed 23% down-regulation and 72% up-regulation in the plasma of B-ALL patients. Carrier proteins transferrin, transthyretin, apolipoprotein A-I and albumin are down-regulated in B-ALL plasma, indicating catabolic protein status. We have observed reduced levels of albumin in B-lymphoblasts obtained from B-ALL patients compared to normal controls (Chapter 2), which might further validate our observations in plasma. Apo-AI is observed to be down-regulated by 40% in B-ALL plasma contrary to the observation in AML (Figures 3.7 & 3.11). Western immunoblots qualitatively supported the 2DGE results but showed quantitative discrepancies in the degrees of deregulation (fold changes) of the proteins, most likely attributable to obvious differences amongst the individuals (normal and patient), differences in the protein loads and detection limits of the two techniques. Confirmation of few of the reported de-regulations in a separate set of B-ALL patients might further emphasize on the prospects of the reported de-regulations as potential diagnostic and prognostic indicators of B-ALL. Transferrin, the major iron transporter protein in plasma, and haptoglobin are known to be involved in iron homeostasis [139]. Differential expression of transferrin and haptoglobin in B-ALL plasma reflects deregulation of iron homeostasis and may emphasize on the connection

between iron and cancer in the leukemia scenario [139]. We observed increased amounts of INF- β , AK-1, GST and a SETDB protein in plasma of B-ALL patients. SETDB is a histone methyltransferase modulating the epigenetic regulation of specific target genes [140]. The observed increases in the leakage of these proteins that are known to play important roles in induction of the acute phase protein response, cellular energy homeostasis, redox regulation and chromatin remodeling [141], might hint towards deregulation of these physiological processes in B-ALL. Hence these areas deserve attention and demand further investigations.

Shi and coworkers have measured serum proteomic profiles of pediatric ALL patients to identify potential protein biomarkers of pediatric ALL [142]. This is the first 2DGE based proteomic study for molecular analysis of B-ALL plasma reporting a relationship between the pathogenesis of B-ALL and the 15 proteins we identified to be differentially expressed in B-ALL. On further validation, a panel of the differentially regulated proteins; for example IgG heavy chains together with haptoglobin; might serve in a less-invasive (than bone-marrow aspiration) diagnostic and prognostic monitoring of B-ALL, and minimal residual disease detection. Through this work, we emphasize upon the assets of proteomic studies over single protein detection assays in revealing differential regulation of different classes of proteins, simultaneously in a disease, which might be a step ahead in cutting through the complexity of heterogeneous diseases and explaining their pathophysiology and clinical manifestation.



CHAPTER 4

Comparison of membrane and hemoglobin-depleted cytosol proteomes of erythrocytes from normal, B-ALL and hereditary spherocytosis blood

4.1. Introduction

Like most of the other leukemic subtypes, B-ALL malignancies are presented with mild to severe anaemia. Several studies have reported abnormalities of the membrane cytoskeleton and enzyme activities of erythrocytes in myeloid as well as lymphoid leukaemias [143-147]. Although myeloid cells and erythrocytes arise from a common progenitor population, the lymphoid cells originate from lymphoid progenitors that are distinct from the myeloid progenitors. Hence a comparative study of the membrane and cytosol proteome of erythrocytes purified from peripheral blood of normal volunteers, B-ALL patients and patients suffering from a non-malignant haematological disorder like hereditary spherocytosis may add insights to our understanding of altered erythrocyte physiology in leukaemia vs. erythroid disorders. Hereditary Spherocytosis (HS) is a common inherited membranopathy characterized by phenotypic and genotypic heterogeneity. It occurs in all racial groups but, is more common in North-European and Japanese populations [148]. HS is commonly associated with dominant inheritance although non-dominant and recessive inheritance is also known. Spheroidal red cells in HS are characterized by decreased deformability and a reduced surface to volume ratio. Several mutations of α - and β -spectrin, ankyrin, band 3 and band 4.2 are known to be associated with HS. The consequence of the primary mutations is loss of vertical linkage between membrane skeleton and lipid bilayer leading to membrane loss and decrease in membrane surface area, compromising normal erythrocyte deformability in circulation [149]. Previous work from our laboratory showed higher loss of transbilayer phospholipid asymmetry in HS erythrocytes compared to normal [150]. Clinical severity of HS ranges from asymptomatic condition to life-threatening anemia with transfusion-dependence and rarely to hydrops fetalis and fetal death. The same protein deficiency may account for a mild or severe disease phenotype. This heterogeneity appears to be related to the coinheritance of modifying genes and secondary protein deficiencies triggered by the primary defect [151-153].

Profiling of erythrocyte proteins has recently gained importance and erythrocyte disorders like sickle cell anemia have been addressed by the proteomic approach [154, 155]. Proteomic analysis of erythrocyte cytosol had been handicapped by the large abundance of hemoglobin, masking majority of the other cytosolic proteins. But in last couple of years, a few novel hemoglobin depletion methods and highly sensitive mass spectrometry have emerged [116, 156-158].

We have found significant changes in B-ALL erythrocyte cytosol and membrane proteomes that may, in part, be responsible for the observed anaemia and may add new insights in understanding the heterogeneous presentation of the disease.

4.2. Materials and Methods

4.2.1. Materials

Sulphopropyl sephadex (SP sephadex), percoll, CHCA (α -cyano-4-hydroxycinnamic acid) MALDI matrix were obtained from Sigma (St. Louis, MO). Electrophoresis reagents were obtained from Bio-Rad (Hercules, CA). Sequencing grade trypsin was obtained from Promega (Madison, WI). Other in-gel tryptic digestion reagents were obtained from Pierce Biotechnologies (Bedford, MA). All other reagents, if not mentioned otherwise, were purchased locally and were of proteomics grade.

4.2.2. Sample Collection

Peripheral blood samples of healthy normal volunteers, B-ALL patients and HS patients, diagnosed for the first time at Department of Hematology, Ramakrishna Mission Seva Pratisthan, Kolkata, India, were collected, with respective consents (parents in case of minors). The institutional ethical review board approved the whole experimental procedure. Red blood cells were purified to >99.5% purity using 75% percoll, as described earlier [116, 123].

4.2.3. Hemoglobin depletion

Hemoglobin depletion was carried out as described earlier [116, 123]. In brief, hemoglobin A

and A2 were kept bound on the SP-sephadex matrix at pH 6.7 while other proteins were obtained in the flow-through.

4.2.4. 2DGE of erythrocyte cytosol

2DGE of hemoglobin-depleted red blood cell cytosol, and staining with CBB or SYPRO-RUBY were essentially the same as described earlier [116, 123]. Densitometry analysis of the gel spots of interest was performed using the density tools of PDQuest (V 7.1) software package. Spot volume (intensity) of the desired spot(s) was normalized as parts per thousand of the total spot volume using the spots that were present in all gels, to find out the relative abundance of a spot in a sample.

4.2.5. 2DGE of Erythrocyte ghost

The erythrocyte ghost membranes were prepared following protocols described earlier [159] with minor modifications. In brief, erythrocytes were lysed in 5mM phosphate buffer, pH 7.4, containing 1mM EDTA and 0.1mM PMSF, overnight at 4°C to obtain erythrocyte ghost membranes. Membranes were washed 5 times with the lysis buffer, pelleted by centrifugation at 30,000g and dissolved in 2D sample buffer containing 20mM Tris, 5M urea, 2M thiourea, 2% (w/v) CHAPS, 2% (w/v) SB 3-10 and 0.2%(w/v) Biolyte 3-10 ampholyte (Bio-Rad) and Protease inhibitor (Roche Diagnostics, Germany). Just prior to IPG strip rehydration, erythrocyte membrane proteins were reduced with 1% (v/v) TBP (Bio-Rad) for 60 minutes at room temperature, and alkylated with 20 mM IAA in dark for 90 minutes at room temperature. 800µg of erythrocyte membrane proteins were focused in 3-10 NL IPG strips (Bio-Rad) up to 1, 20, 000 Volt Hours, followed by SDS-PAGE in 8-16% gradient gels. Resulting 2D gels were silver stained following established protocol. For MS-based identification, SYPRO-RUBY stained gel spots (Bio-Rad) were used. Densitometry analysis of the gel spots of interest was the same as done for erythrocyte cytosol 2D gels.

4.2.6. MALDI TOF/TOF mass spectrometry

The protein spots from CBB and SYPRO RUBY-stained 2D gels were digested with trypsin

according to Shevchenko et al. [36] with minor modifications using Trypsin Gold from Promega (Madison, WI, USA). MS of the digested peptides was carried out in a MALDI-TOF/TOF tandem mass spectrometer (Applied Biosystems, AB 4700). Recrystallized CHCA and 2, 5-dihydroxy-benzoic acid (Sigma) were used as matrices. PMFs were acquired in positive reflector mode. Autotrypsin and common keratin peaks were first validated and subsequently excluded from MS/MS analysis. Ten most intense peptides from CBB-stained gels and seven most intense peptides from SYPRO RUBY-stained gels were subjected to MS/MS analysis. Peak lists were prepared from raw MS and MS/MS data using GPS explorer V3.0 (Applied Biosystems) software and noise reduction and de-isotoping were performed using default settings. The resulting PMF and MS/MS data were searched against human MSDB and Swiss-Prot databases using in-house MASCOT version 2.0.05 (Matrix Science, UK) server and the MOWSE score was considered to determine hits. Proteins with at least two MS/MS hits with $p < 0.05$ were considered a 'true hit'. Also the hit for the next best non-homologous protein was accepted and only the proteins with considerable difference from a nonspecific protein hit were taken into account. For different homologous proteins having the similar MOWSE scores, preference was given to the protein with best match between theoretical and experimental molecular weight and pI. All MS experiments were repeated at least thrice. The database search parameters included one missed cleavage, error tolerance of ± 100 ppm for PMF and ± 1.2 Da for MS/MS ion search. Some common variable modifications like carbamidomethyl cysteine, methionine oxidation, and N-terminal acetylation were included. All MS/MS peaks matched by this method were manually checked and confirmed.

4.2.7. Statistical Analysis

Densitometry data from erythrocyte ghost and cytosol 2D gels were subjected to unpaired two-tail Student's t-test for evaluating significance of the differences observed between normal, B-ALL and HS individuals.

4.2.8. Transmission Electron Microscopy of erythrocyte ghost preparations

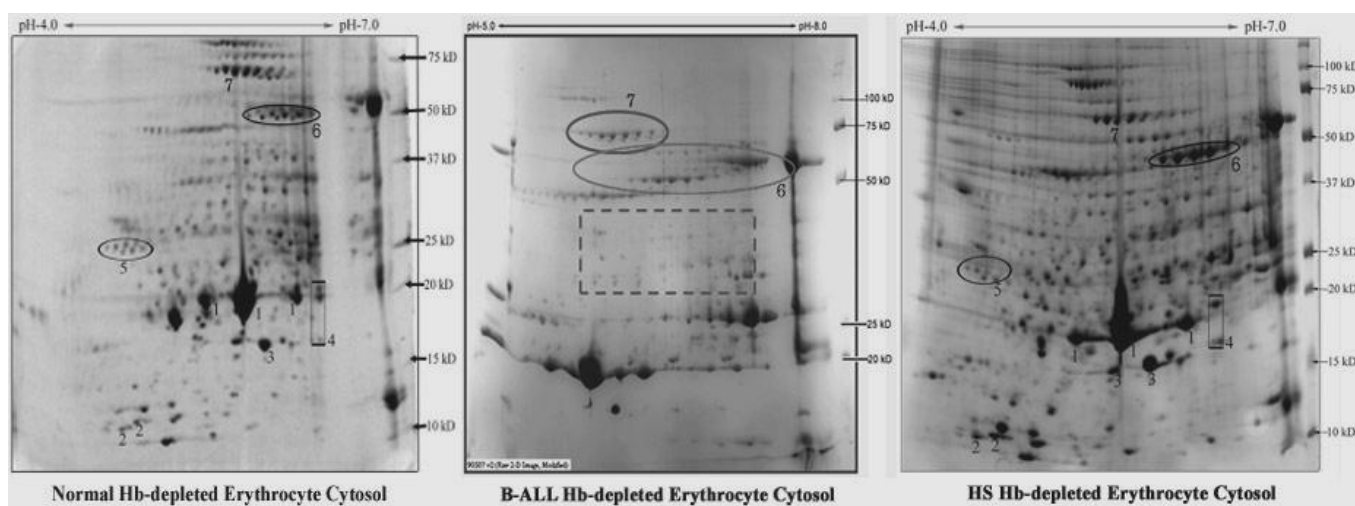
Erythrocyte membrane preparations were laid on formvar/carbon-coated copper grids of 600 meshes and stained with 0.5% (w/v) phosphotungstic acid with a staining time of 25-30 seconds. The grids were dried properly before viewing under the Tecnai S Twin, FEI electron microscope (Eindhoven, The Netherlands) operating at 200 kV accelerating voltage elaborated earlier [160].

4.3. Results

4.3.1. Differences in the erythrocyte cytosol proteomes of B-ALL, HS and normal samples

B-ALL and HS patients, who had never received blood transfusion, were used for erythrocyte cytosol proteome analysis. Representative hemoglobin-depleted erythrocyte cytosol proteomes from a B-ALL patient, an HS patient and a normal control have been shown in Figure 4.1.

Figure 4.1: Representative 2DGE maps of hemoglobin-depleted erythrocyte cytosol from normal, B-ALL and HS individuals. 1- peroxiredoxin 2; 2- thioredoxin; 3- superoxide dismutase; 4- nucleoside di-phosphate kinase; 5- suppressor of tumorigenicity 13; 6- aldehyde dehydrogenase; 7- heat shock protein 70.



The mass spectrometry details of the proteins are given in Table 4.1. The 2D gels of B-ALL and HS cytosol were markedly different from that of normal controls. While HS erythrocyte

cytosol showed up-regulation of redox regulators and down-regulation of a co-chaperone ST13 and a nucleotide kinase NDPK (adjoining histogram plot); the hemoglobin-depleted erythrocyte cytosol proteome of B-ALL patients showed somewhat opposite trends with down-regulation of an oxidoreductase (aldehyde dehydrogenase) and pI shift of a chaperone (HSP-70).

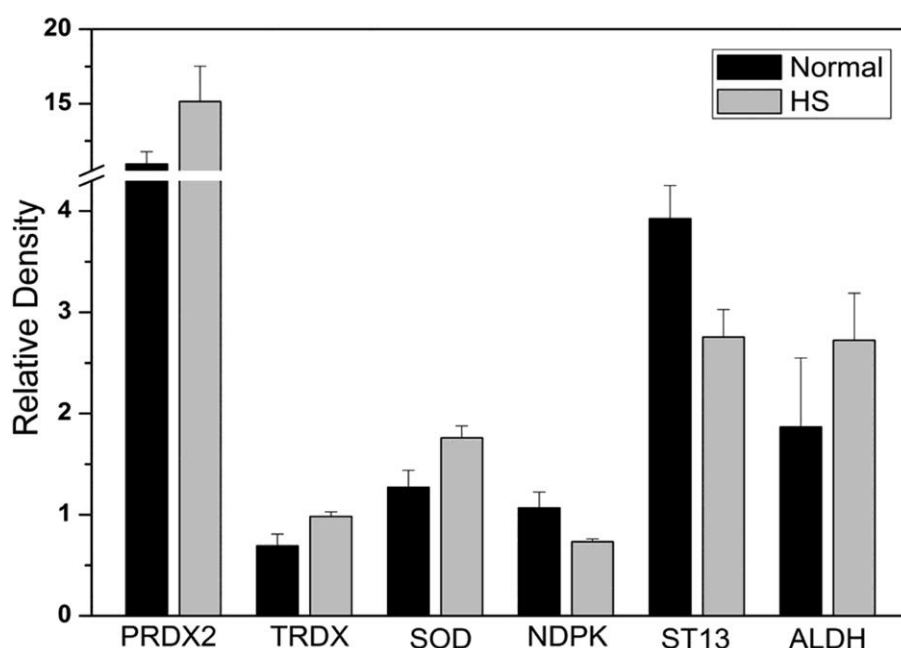


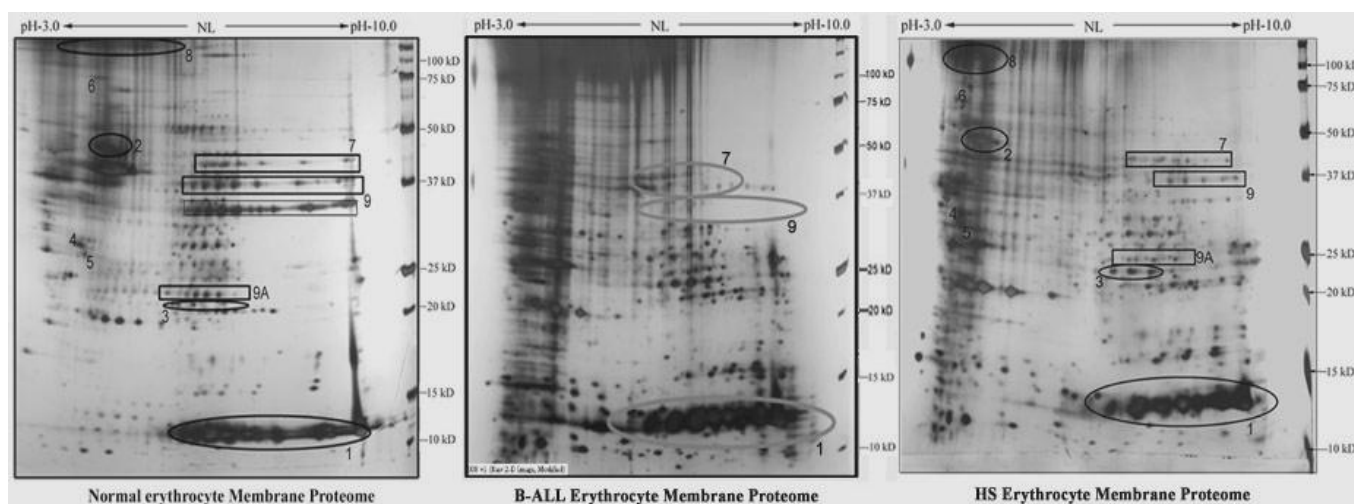
Table 4.1: Identification of differentially regulated proteins by MALDI TOF/TOF mass spectrometry in Hemoglobin-depleted-erythrocyte cytosol proteome

Name of the Protein	Accession ID	MW / pI	Mascot Score	Sequence Coverage	MS/MS peaks matched
Peroxiredoxin 2 (PRDX2)	PRDX2_HUMAN	21.7 / 5.67	216	62%	4
Thioredoxin (TRDX)	P10599	11.6 / 4.8	309	90%	5
Superoxide Dismutase (SOD)	P00441	15.9 / 5.9	465	63%	4
Nucleoside Di-phosphate Kinase (NDPK)	1NSKR	17.3 / 7.0	144	56%	2
Suppression of Tumorigenicity 13 (ST13)	P50502	41.3 / 5.2	206	33%	6
Aldehyde Dehydrogenase 1 (ALDH)	P00352	54.8 / 6.3	147	47%	6

4.3.2. Differences in erythrocyte membrane proteomes of B-ALL, HS and normal samples

B-ALL and HS patients, who had never received blood transfusion, were also used for the erythrocyte ghost proteome analysis. Representative erythrocyte membrane proteomes from a B-ALL patient, an HS patient and a normal control have been shown in Figure 4.2.

Figure 4.2: Representative normal, B-ALL and HS erythrocyte membrane proteomes. 1- Hemoglobin; 2- Band 4.1; 3-Ankyrin; 4- Tropomyosin 3; 5- Tropomyosin 1; 6- Calpastatine; 7- Dematin; 8- Spectrin; 9- Glyceraldehyde 3 phosphate dehydrogenase (G3PD); 9A- G3PD fragments



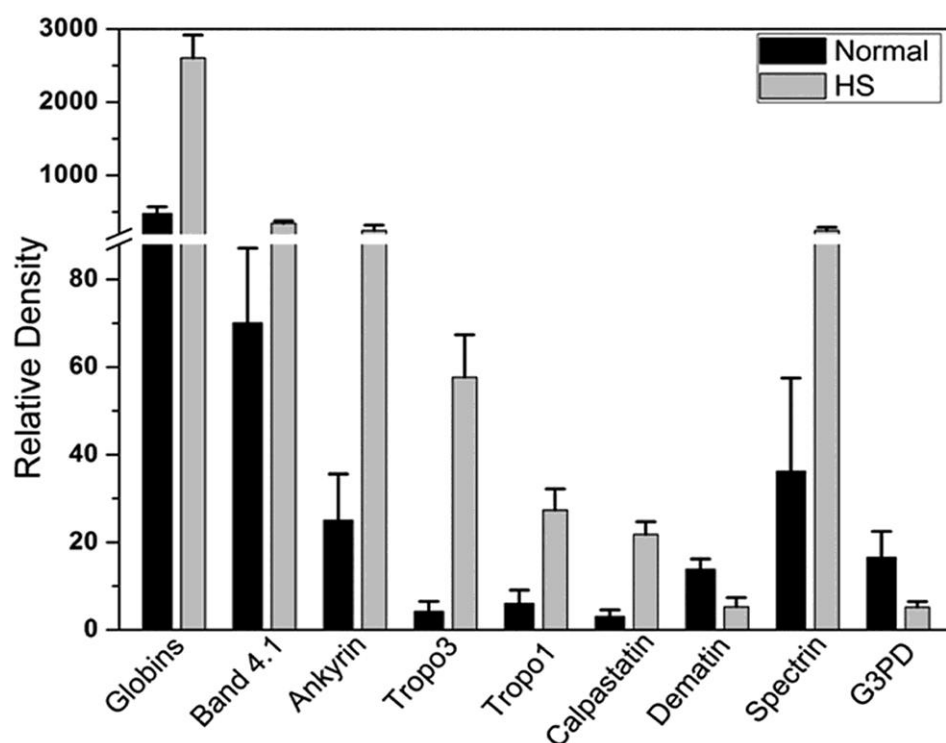
The mass spectrometry details of the proteins are given in Table 4.2.

Table 4.2: Identification of differentially regulated proteins by MALDI TOF/TOF mass spectrometry in erythrocyte membrane proteome

Protein	Accession ID	MW / pI	Mascot Score	Sequence coverage	MS/MS peaks matched
Globins	6HBWB	16.0/7.3	99	78%	4
Band 4.1	MMHUE4	95.2 / 5.37	174	32%	5
Ankyrin	SJHUK	20.6 / 5.65	183	26%	7
Tropomyosin 3	Q5VU58_HUMAN	28.9 / 4.72	241	62%	10
Tropomyosin 1	Q1ZYL5_HUMAN	28.5 / 4.75	138	62%	9
Calpastatine	CAA03059	74.9 / 4.99	86	36%	2
Dematin	DEMA_HUMAN	45.5/8.9	85	42%	4
Spectrin	Q59FP5_HUMAN	246/5.1	275	30%	12
G3PD	DEHUG3	36.0/8.6	151	60%	2

Due to the inherent complexity of a 2D gel-based membrane proteomic studies, we have only concentrated on the spots which were very significantly different ($p < 0.001$) between normal, B-ALL and HS membrane proteomes. Comparison of the erythrocyte membrane proteomes on 2DGE led to the observation of elevated levels of membrane associated globin chains and reduced membrane association of glyceraldehydes-3-phosphate dehydrogenase (G3PD) in both B-ALL and HS patients. While increased association of globin chains with the spherocyte membranes in HS directly indicate severe oxidative stress in the spherocytes, membrane-bound denatured/oxidized hemoglobin and defective erythrocyte cytoskeletal network in B-ALL may be implicated in the erythrocyte destruction in spleen, making the patients anaemic. The HS erythrocyte membrane proteome also displayed increased levels of low molecular weight

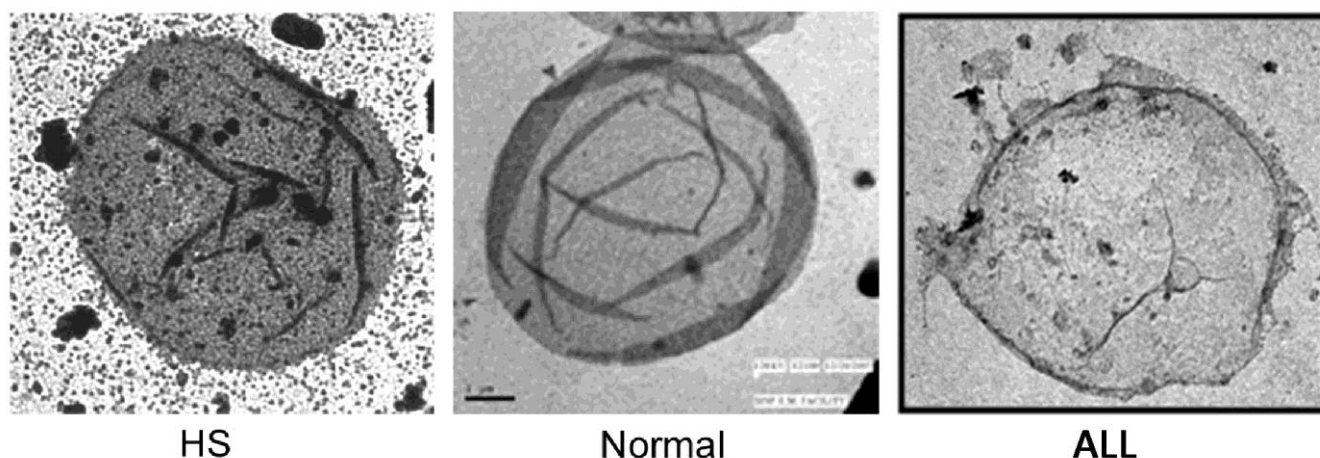
fragments of several major cytoskeletal proteins (adjoining histogram plot).



4.3.3. Alterations in HS erythrocyte ghost morphology

Transmission electron microscopy (TEM) of the sealed erythrocyte ghosts showed significant changes in the ultra-structure of B-ALL and HS erythrocyte membranes with an impression of disrupted membrane skeletal architecture, as shown in Figure 4.3.

Figure 4.3: Transmission electron micrographs of RBC ghost preparations



4.4. Discussion

This proteomic study reveals differential expression of major cytosolic redox regulator proteins in the erythrocyte cytosol from B-ALL and HS samples. Mice expressing low levels of redox enzymes die within three days under high oxidative stress. The lifespan of their erythrocytes under normal conditions is half that of the wild type, suggesting that reactive oxygen species regulate erythrocyte lifespan [161]. SOD deficiency causes anemia in mice [162] and TRDX is up-regulated in sickle cell anemia on hydroxyurea treatment [163]. The elevated level of PRDX2 in HS hints towards its high demand to scavenge elevated levels of reactive oxygen species in the spherocyte. The concomitant up-regulation of two other redox regulators, TRDX and SOD, indicates an adaptive response of spherocytes to oxidative damage. We have previously reported up-regulation of PRDX2, TRDX and SOD also in HbE β -thalassemic erythrocyte cytosol [123]; and hence speculate that the pathophysiology of the two erythrocyte disorders may be significantly related. Aldehyde dehydrogenase (ALDH) constitutes a group of oxidoreductases that catalyse oxidation of aldehydes and include the glycolytic enzyme glyceraldehydes-3-phosphate dehydrogenase (G3PD). About 90% of erythrocyte G3PD is bound to membrane in its inactive form, becoming active when released into the cytoplasm [153]. B-ALL erythrocytes showed reduced levels of membrane associated G3PD and cytosolic

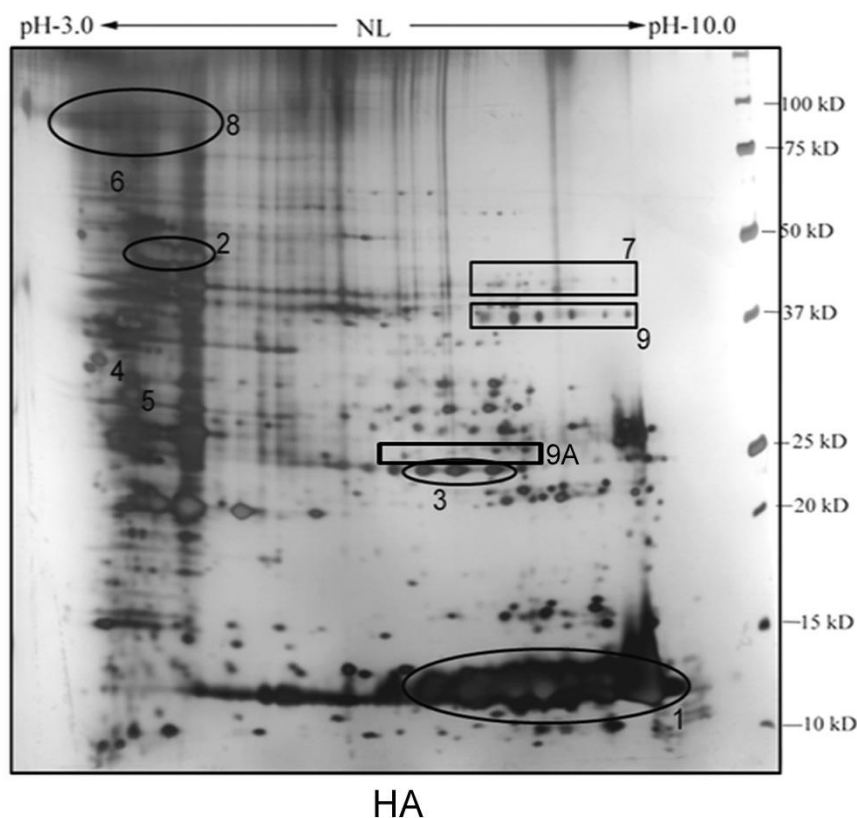
ALDH. Deficiency of G3PD has also been described in case of CML [147]. Altered enzyme activity observed in B-ALL may either be due to intracellular stress with temporary inhibition of red cell glycolysis, posttranslational molecular modification or cyto and karyokinetic abnormalities with loss of functional genetic material governing enzyme synthesis, leading to enzyme abnormality. The red cell enzyme changes may reflect production of an abnormal clone of red blood cell and that these may arise from altered stem cells, has also been suggested by some studies [147]. The defective enzyme activities may be the result of derivation of abnormal cell lines from an abnormal pluripotent stem cell. The presence of such a pluripotent cell has been demonstrated by the presence of a Ph chromosome not only in myeloid precursors but also in erythroid precursors in CML [147].

The observed reduction in membrane associated G3PD and concomitant rise in ALDH amounts in the spherocyte cytosol might reveal a mechanism of erythrocyte metabolic regulation in times of crisis like oxidative stress. The oxidative stress induced time dependent loss of membrane bound G3PD in intact red cells [164] supports the hypothesis.

Membrane bound haemoglobin (MBH) is used as oxidative stress marker [165]. Increased association of globin chains with the erythrocyte membranes in B-ALL and HS emphasize that erythrocytes are subjected to severe oxidative stress in both the haematological disorders. Membrane-bound denatured/oxidized hemoglobin has also been implicated in the proposed erythrocyte clearance mechanism, through the induction of band 3 clustering on the membrane, which in turn leads to autologous IgGs and complement binding and consequent erythro-phagocytosis [152].

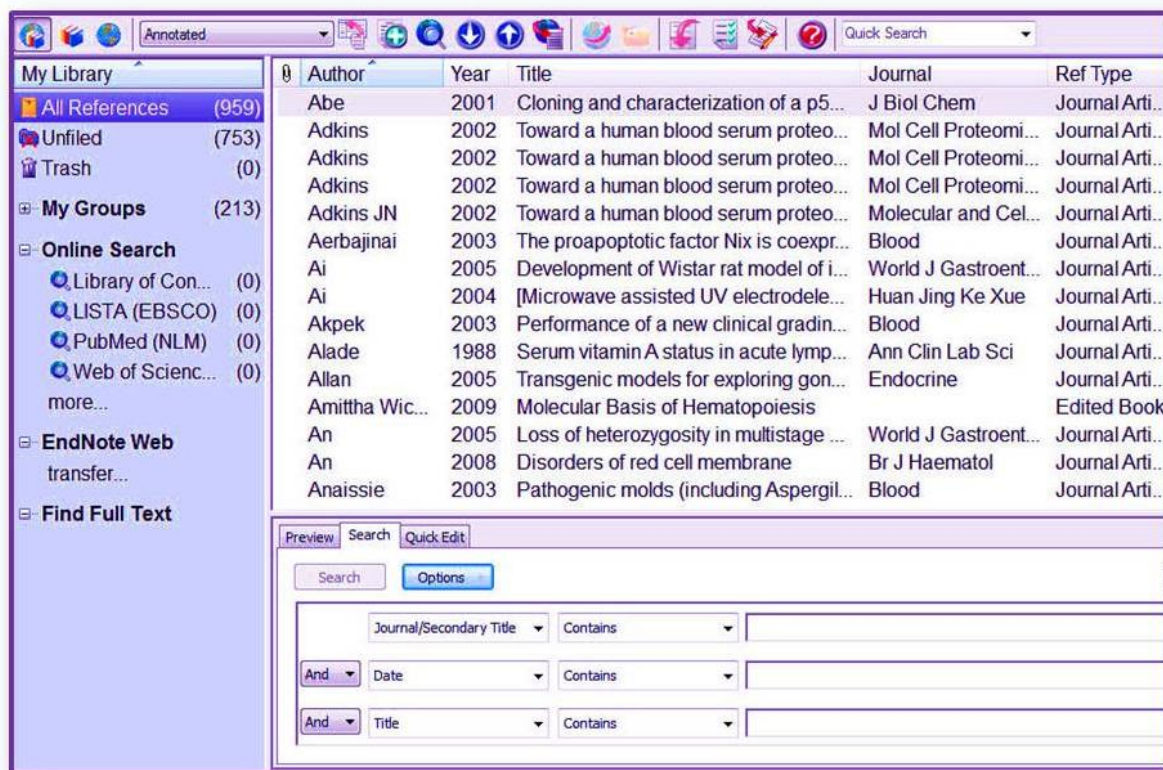
We have also investigated the electron micrograph and membrane proteome of erythrocytes in cases of severe non-HS hemolytic anemia [166], and the profile highly matches with that observed in B-ALL and HS patients. The extent of deregulations in hemolytic anemia is somewhat higher than that in B-ALL or HS. Figure 4.4 shows the 2DGE profile of erythrocyte membrane in a case of severe non-HS hemolytic anemia.

Figure 4.4: Representative erythrocyte membrane proteomes of a non-HS hemolytic anemia case



In conclusion, the present work is the first report of 2DGE based proteomic investigation of B-ALL and HS erythrocyte cytosol, after hemoglobin depletion along with the membrane, and describes a spectrum of secondary protein alterations that accompany the primary defects. Secondary protein deficiencies are often observed and may have serious implications in the clinical outcome of the disease. Changes in the erythrocyte proteomes directly indicate altered redox-regulation, metabolism, protein degradation, cytoskeletal disorganization and oxidative stress. The ultra-structural changes observed in the B-ALL and HS erythrocyte membranes also indicate drastic changes in the architecture of the spectrin-based membrane skeleton. Previous reports support our findings [144]. The aforementioned abnormalities in skeletal, integral or anchoring proteins results in the inability of the erythrocyte to control its surface area or cell volume and causes shortening of erythrocyte survival. Although the examined group of affected individuals is rather small, it is of probable clinical importance that the aberrant electrophoretic profiles were detected in all patients and were similar to that observed in non-HS hemolytic anemia patients. We propose our data to add some new insights in the field of B-ALL pathophysiology, clinical heterogeneity and disease

progression. Since the treatment strategies in B-ALL must address the whole spectrum of the pathophysiology of the disease, much is expected from future studies on erythrocyte proteomes, signaling mechanisms and oxidatively damaged components in B-ALL erythrocyte membrane.



REFERENCES

- [1] J.C. Cambier, S.B. Gauld, K.T. Merrell, B.J. Vilen, B-cell anergy: from transgenic models to naturally occurring anergic B cells?, *Nat Rev Immunol*, 7 (2007) 633-643.
- [2] B.K. Amittha Wickrema, *Molecular Basis of Hematopoiesis*, in, Springer Science, New York, 2009.
- [3] M.A. Teitell, P.P. Pandolfi, Molecular genetics of acute lymphoblastic leukemia, *Annu Rev Pathol*, 4 (2009) 175-198.
- [4] S.L. Nutt, B.L. Kee, The transcriptional regulation of B cell lineage commitment, *Immunity*, 26 (2007) 715-725.
- [5] C. Pridans, M.L. Holmes, M. Polli, J.M. Wettenhall, A. Dakic, L.M. Corcoran, G.K. Smyth, S.L. Nutt, Identification of Pax5 target genes in early B cell differentiation, *J Immunol*, 180 (2008) 1719-1728.
- [6] J.M. Pongubala, D.L. Northrup, D.W. Lancki, K.L. Medina, T. Treiber, E. Bertolino, M. Thomas, R. Grosschedl, D. Allman, H. Singh, Transcription factor EBF restricts alternative lineage options and promotes B cell fate commitment independently of Pax5, *Nat Immunol*, 9 (2008) 203-215.
- [7] G. Fazio, C. Palmi, A. Rolink, A. Biondi, G. Cazzaniga, PAX5/TEL acts as a transcriptional repressor causing down-modulation of CD19, enhances migration to CXCL12, and confers survival advantage in pre-BI cells, *Cancer Res*, 68 (2008) 181-189.
- [8] C.G. Mullighan, S. Goorha, I. Radtke, C.B. Miller, E. Coustan-Smith, J.D. Dalton, K. Girtman, S. Mathew, J. Ma, S.B. Pounds, X. Su, C.H. Pui, M.V. Relling, W.E. Evans, S.A. Shurtleff, J.R. Downing, Genome-wide analysis of genetic alterations in acute lymphoblastic leukaemia, *Nature*, 446 (2007) 758-764.
- [9] C.J.P. Steven A. Corfe, Development of B Lymphocytes, in: B.K. Amittha Wickrema (Ed.) *Molecular Basis of Hematopoiesis*, Springer, New York, 2009, pp. 173-199.
- [10] X. Dai, Y. Chen, L. Di, A. Podd, G. Li, K.D. Bunting, L. Hennighausen, R. Wen, D. Wang, Stat5 is essential for early B cell development but not for B cell maturation and

function, *J Immunol*, 179 (2007) 1068-1079.

[11] W.C. Chou, D.E. Levy, C.K. Lee, STAT3 positively regulates an early step in B-cell development, *Blood*, 108 (2006) 3005-3011.

[12] Y. Kulathu, E. Hobeika, G. Turchinovich, M. Reth, The kinase Syk as an adaptor controlling sustained calcium signalling and B-cell development, *EMBO J*, 27 (2008) 1333-1344.

[13] T. Yasuda, H. Sanjo, G. Pages, Y. Kawano, H. Karasuyama, J. Pouyssegur, M. Ogata, T. Kurosaki, Erk kinases link pre-B cell receptor signaling to transcriptional events required for early B cell expansion, *Immunity*, 28 (2008) 499-508.

[14] C. Cobaleda, I. Sanchez-Garcia, B-cell acute lymphoblastic leukaemia: towards understanding its cellular origin, *Bioessays*, 31 (2009) 600-609.

[15] C.H. Pui, M.V. Relling, J.R. Downing, Acute lymphoblastic leukemia, *N Engl J Med*, 350 (2004) 1535-1548.

[16] C. Cobaleda, W. Jochum, M. Busslinger, Conversion of mature B cells into T cells by dedifferentiation to uncommitted progenitors, *Nature*, 449 (2007) 473-477.

[17] T. Reya, S.J. Morrison, M.F. Clarke, I.L. Weissman, Stem cells, cancer, and cancer stem cells, *Nature*, 414 (2001) 105-111.

[18] S.H. Kroft, Role of flow cytometry in pediatric hematopathology, *Am J Clin Pathol*, 122 Suppl (2004) S19-32.

[19] E.J. Yeoh, M.E. Ross, S.A. Shurtleff, W.K. Williams, D. Patel, R. Mahfouz, F.G. Behm, S.C. Raimondi, M.V. Relling, A. Patel, C. Cheng, D. Campana, D. Wilkins, X. Zhou, J. Li, H. Liu, C.H. Pui, W.E. Evans, C. Naeve, L. Wong, J.R. Downing, Classification, subtype discovery, and prediction of outcome in pediatric acute lymphoblastic leukemia by gene expression profiling, *Cancer Cell*, 1 (2002) 133-143.

[20] M.D. Tabernero, A.M. Bortoluci, I. Alaejos, M.C. Lopez-Berges, A. Rasillo, R. Garcia-Sanz, M. Garcia, J.M. Sayagues, M. Gonzalez, G. Mateo, J.F. San Miguel, A. Orfao, Adult

precursor B-ALL with BCR/ABL gene rearrangements displays a unique immunophenotype based on the pattern of CD10, CD34, CD13 and CD38 expression, *Leukemia*, 15 (2001) 406-414.

[21] C.H. Pui, S. Jeha, New therapeutic strategies for the treatment of acute lymphoblastic leukaemia, *Nat Rev Drug Discov*, 6 (2007) 149-165.

[22] M.R. Wilkins, J.C. Sanchez, A.A. Gooley, R.D. Appel, I. Humphery-Smith, D.F. Hochstrasser, K.L. Williams, Progress with proteome projects: why all proteins expressed by a genome should be identified and how to do it, *Biotechnol Genet Eng Rev*, 13 (1996) 19-50.

[23] D. Penque, Two-dimensional gel electrophoresis and mass spectrometry for biomarker discovery, *Proteomics-Clinical Applications*, 3 (2009) 155-172.

[24] S. Raymond, L. Weintraub, Acrylamide gel as a supporting medium for zone electrophoresis, *Science*, 130 (1959) 711.

[25] M. Capel, B. Redman, D.P. Bourque, Quantitative comparative analysis of complex two-dimensional electropherograms, *Anal Biochem*, 97 (1979) 210-228.

[26] P. Edman, G. Begg, A protein sequenator, *Eur J Biochem*, 1 (1967) 80-91.

[27] B. Bjellqvist, K. Ek, P.G. Righetti, E. Gianazza, A. Gorg, R. Westermeier, W. Postel, Isoelectric focusing in immobilized pH gradients: principle, methodology and some applications, *J Biochem Biophys Methods*, 6 (1982) 317-339.

[28] A. Gorg, W. Postel, S. Gunther, The current state of two-dimensional electrophoresis with immobilized pH gradients, *Electrophoresis*, 9 (1988) 531-546.

[29] M. Karas, F. Hillenkamp, Laser desorption ionization of proteins with molecular masses exceeding 10,000 daltons, *Anal Chem*, 60 (1988) 2299-2301.

[30] C.M. Whitehouse, R.N. Dreyer, M. Yamashita, J.B. Fenn, Electrospray interface for liquid chromatographs and mass spectrometers, *Anal Chem*, 57 (1985) 675-679.

[31] A. Gorg, W. Weiss, M.J. Dunn, Current two-dimensional electrophoresis technology for proteomics, *Proteomics*, 4 (2004) 3665-3685.

- [32] G. Candiano, M. Bruschi, L. Musante, L. Santucci, G.M. Ghiggeri, B. Carnemolla, P. Orecchia, L. Zardi, P.G. Righetti, Blue silver: a very sensitive colloidal Coomassie G-250 staining for proteome analysis, *Electrophoresis*, 25 (2004) 1327-1333.
- [33] C. Fernandez-Patron, L. Castellanos-Serra, P. Rodriguez, Reverse staining of sodium dodecyl sulfate polyacrylamide gels by imidazole-zinc salts: sensitive detection of unmodified proteins, *Biotechniques*, 12 (1992) 564-573.
- [34] L. Castellanos-Serra, W. Proenza, V. Huerta, R.L. Moritz, R.J. Simpson, Proteome analysis of polyacrylamide gel-separated proteins visualized by reversible negative staining using imidazole-zinc salts, *Electrophoresis*, 20 (1999) 732-737.
- [35] P. Sinha, J. Poland, M. Schnolzer, T. Rabilloud, A new silver staining apparatus and procedure for matrix-assisted laser desorption/ionization-time of flight analysis of proteins after two-dimensional electrophoresis, *Proteomics*, 1 (2001) 835-840.
- [36] A. Shevchenko, M. Wilm, O. Vorm, M. Mann, Mass spectrometric sequencing of proteins silver-stained polyacrylamide gels, *Anal Chem*, 68 (1996) 850-858.
- [37] W.F. Patton, A thousand points of light: the application of fluorescence detection technologies to two-dimensional gel electrophoresis and proteomics, *Electrophoresis*, 21 (2000) 1123-1144.
- [38] V.E. Urwin, P. Jackson, Two-dimensional polyacrylamide gel electrophoresis of proteins labeled with the fluorophore monobromobimane prior to first-dimensional isoelectric focusing: imaging of the fluorescent protein spot patterns using a cooled charge-coupled device, *Anal Biochem*, 209 (1993) 57-62.
- [39] M. Unlu, M.E. Morgan, J.S. Minden, Difference gel electrophoresis: a single gel method for detecting changes in protein extracts, *Electrophoresis*, 18 (1997) 2071-2077.
- [40] K.N. Berggren, B. Schulenberg, M.F. Lopez, T.H. Steinberg, A. Bogdanova, G. Smejkal, A. Wang, W.F. Patton, An improved formulation of SYPRO Ruby protein gel stain: comparison with the original formulation and with a ruthenium II tris (bathophenanthroline

disulfonate) formulation, *Proteomics*, 2 (2002) 486-498.

[41] A.W. Dowsey, M.J. Dunn, G.Z. Yang, The role of bioinformatics in two-dimensional gel electrophoresis, *Proteomics*, 3 (2003) 1567-1596.

[42] J.I. Garrels, The QUEST system for quantitative analysis of two-dimensional gels, *J Biol Chem*, 264 (1989) 5269-5282.

[43] J. Fievet, C. Dillmann, G. Lagniel, M. Davanture, L. Negroni, J. Labarre, D. de Vienne, Assessing factors for reliable quantitative proteomics based on two-dimensional gel electrophoresis, *Proteomics*, 4 (2004) 1939-1949.

[44] S. Viswanathan, M. Unlu, J.S. Minden, Two-dimensional difference gel electrophoresis, *Nat Protoc*, 1 (2006) 1351-1358.

[45] A. Görg, Drews, O., Weiss, W., , 1 ed., Cold Spring Harbor Laboratory Press, 2004.

[46] J. Minden, Comparative proteomics and difference gel electrophoresis, *Biotechniques*, 43 (2007) 739, 741, 743 passim.

[47] B. Salih, C. Masselon, R. Zenobi, Matrix-assisted laser desorption/ionization mass spectrometry of noncovalent protein-transition metal ion complexes, *J Mass Spectrom*, 33 (1998) 994-1002.

[48] M. Karas, Bahr, U., Strupat, K., Hillenkamp, F., Tsarbopoulos, A., and Pramanik, B. N., Matrix dependence of metastable fragmentation of glycoproteins in MALDI TOF mass spectrometry., *Anal Chem*, 67 (1995) 675-679.

[49] Y. Dai, R.M. Whittal, L. Li, Two-layer sample preparation: a method for MALDI-MS analysis of complex peptide and protein mixtures, *Anal Chem*, 71 (1999) 1087-1091.

[50] M. Mann, M. Wilm, Error-tolerant identification of peptides in sequence databases by peptide sequence tags, *Anal Chem*, 66 (1994) 4390-4399.

[51] R.S. Brown, J.J. Lennon, Mass resolution improvement by incorporation of pulsed ion extraction in a matrix-assisted laser desorption/ionization linear time-of-flight mass spectrometer, *Anal Chem*, 67 (1995) 1998-2003.

- [52] R.M. Whittal, L. Li, High-resolution matrix-assisted laser desorption/ionization in a linear time-of-flight mass spectrometer, *Anal Chem*, 67 (1995) 1950-1954.
- [53] R. Matthiesen, Mutenda, K.E., Introduction to Proteomics, Mass Spectrometry Data Analysis in Proteomics 1st ed., Humana Press, NY, 2007.
- [54] M. Guilhaus, Principles and instrumentation in time-of-flight mass spectrometry., *J. Mass Spectrom.*, 30 (1995) 1519-1552.
- [55] M.A. Baldwin, Mass spectrometers for the analysis of biomolecules, *Methods Enzymol*, 402 (2005) 3-48.
- [56] E. Stimson, Truong, O., Richter, W. J., Waterfield, M. D., and Burlingame, A. L. , Enhancement of charge remote fragmentation in protonated peptides by high energy CID MALDI-TOF-MS using “cold” matrices., *Int. J. Mass Spectrom. Ion Processes* 169/170 (1997).
- [57] M.L. Vestal, Juhasz, P., and Martin, S. A., Delayed extraction matrix assisted laser desorption time-of-flight mass spectrometry., *Rapid Comm. Mass Spectrom.*, 9 (1995) 1044-1050.
- [58] M.L. Vestal, Juhasz, P., Hines, W., and Martin, S. A., A new delayed extraction MALDI-TOF MS/MS for characterization of protein digests, in: S.A.C. A. L. Burlingame, and M. A. Baldwin (Ed.) *Mass Spectrometry in Biology and Medicine*, Humana Press, NY, 2000, pp. 1-16.
- [59] D.N. Perkins, D.J. Pappin, D.M. Creasy, J.S. Cottrell, Probability-based protein identification by searching sequence databases using mass spectrometry data, *Electrophoresis*, 20 (1999) 3551-3567.
- [60] R.S. Boyd, M.J. Dyer, K. Cain, Proteomic analysis of B-cell malignancies, *J Proteomics*, 73 (2010) 1804-1822.
- [61] J. Boelens, J. Philippe, F. Offner, B-CLL cells from lymph nodes express higher ZAP-70 levels than B-CLL cells from peripheral blood, *Leuk Res*, 31 (2007) 719-720.

- [62] L.A. Smit, D.Y. Hallaert, R. Spijker, B. de Goeij, A. Jaspers, A.P. Kater, M.H. van Oers, C.J. van Noesel, E. Eldering, Differential Noxa/Mcl-1 balance in peripheral versus lymph node chronic lymphocytic leukemia cells correlates with survival capacity, *Blood*, 109 (2007) 1660-1668.
- [63] R. Joubert-Caron, M. Caron, Proteome analysis in the study of lymphoma cells, *Mass Spectrom Rev*, 24 (2005) 455-468.
- [64] S.M. Hanash, J.R. Strahler, R. Kuick, E.H. Chu, D. Nichols, Identification of a polypeptide associated with the malignant phenotype in acute leukemia, *J Biol Chem*, 263 (1988) 12813-12815.
- [65] K. Fujii, T. Kondo, M. Yamada, K. Iwatsuki, S. Hirohashi, Toward a comprehensive quantitative proteome database: protein expression map of lymphoid neoplasms by 2-D DIGE and MS, *Proteomics*, 6 (2006) 4856-4876.
- [66] S. Rana, P.B. Maples, N. Senzer, J. Nemunaitis, Stathmin 1: a novel therapeutic target for anticancer activity, *Expert Rev Anticancer Ther*, 8 (2008) 1461-1470.
- [67] K.S. Rees-Unwin, R. Faragher, R.D. Unwin, J. Adams, P.J. Brown, A.M. Buckle, A. Pettitt, C.V. Hutchinson, S.M. Johnson, K. Pulford, A.H. Banham, A.D. Whetton, G. Lucas, D.Y. Mason, J. Burthem, Ribosome-associated nucleophosmin 1: increased expression and shuttling activity distinguishes prognostic subtypes in chronic lymphocytic leukaemia, *Br J Haematol*, 148 (2010) 534-543.
- [68] I.M. Cristea, S.J. Gaskell, A.D. Whetton, Proteomics techniques and their application to hematology, *Blood*, 103 (2004) 3624-3634.
- [69] M. Vogler, M. Butterworth, A. Majid, R.J. Walewska, X.M. Sun, M.J. Dyer, G.M. Cohen, Concurrent up-regulation of BCL-XL and BCL2A1 induces approximately 1000-fold resistance to ABT-737 in chronic lymphocytic leukemia, *Blood*, 113 (2009) 4403-4413.
- [70] A. Pierce, R.D. Unwin, C.A. Evans, S. Griffiths, L. Carney, L. Zhang, E. Jaworska, C.F. Lee, D. Blinco, M.J. Okoniewski, C.J. Miller, D.A. Bitton, E. Spooncer, A.D. Whetton, Eight-

channel iTRAQ enables comparison of the activity of six leukemogenic tyrosine kinases, *Mol Cell Proteomics*, 7 (2008) 853-863.

[71] Y. Ishihama, Y. Oda, T. Tabata, T. Sato, T. Nagasu, J. Rappsilber, M. Mann, Exponentially modified protein abundance index (emPAI) for estimation of absolute protein amount in proteomics by the number of sequenced peptides per protein, *Mol Cell Proteomics*, 4 (2005) 1265-1272.

[72] J. Malmstrom, M. Beck, A. Schmidt, V. Lange, E.W. Deutsch, R. Aebersold, Proteome-wide cellular protein concentrations of the human pathogen *Leptospira interrogans*, *Nature*, 460 (2009) 762-765.

[73] R.S. Boyd, R. Jukes-Jones, R. Walewska, D. Brown, M.J. Dyer, K. Cain, Protein profiling of plasma membranes defines aberrant signaling pathways in mantle cell lymphoma, *Mol Cell Proteomics*, 8 (2009) 1501-1515.

[74] D. Cecconi, A. Zamo, E. Bianchi, A. Parisi, S. Barbi, A. Milli, S. Rinalducci, A. Rosenwald, E. Hartmann, L. Zolla, M. Chilosì, Signal transduction pathways of mantle cell lymphoma: a phosphoproteome-based study, *Proteomics*, 8 (2008) 4495-4506.

[75] I.M. Ghobrial, D.J. McCormick, S.H. Kaufmann, A.A. Leontovich, D.A. Loegering, N.T. Dai, K.L. Krajnik, M.J. Stenson, M.F. Melhem, A.J. Novak, S.M. Ansell, T.E. Witzig, Proteomic analysis of mantle-cell lymphoma by protein microarray, *Blood*, 105 (2005) 3722-3730.

[76] L. Miguët, R. Bogumil, P. Decloquement, R. Herbrecht, N. Potier, L. Mauvieux, A. Van Dorsselaer, Discovery and identification of potential biomarkers in a prospective study of chronic lymphoid malignancies using SELDI-TOF-MS, *J Proteome Res*, 5 (2006) 2258-2269.

[77] C.G. Mullighan, L.A. Phillips, X. Su, J. Ma, C.B. Miller, S.A. Shurtleff, J.R. Downing, Genomic analysis of the clonal origins of relapsed acute lymphoblastic leukemia, *Science*, 322 (2008) 1377-1380.

[78] S. Li, D. Li, Stem cell and kinase activity-independent pathway in resistance of leukaemia

to BCR-ABL kinase inhibitors, *J Cell Mol Med*, 11 (2007) 1251-1262.

[79] J. Ota, Y. Yamashita, K. Okawa, H. Kisanuki, S. Fujiwara, M. Ishikawa, Y. Lim Choi, S. Ueno, R. Ohki, K. Koinuma, T. Wada, D. Compton, T. Kadoya, H. Mano, Proteomic analysis of hematopoietic stem cell-like fractions in leukemic disorders, *Oncogene*, 22 (2003) 5720-5728.

[80] D. Bhattacharya, S. Saha, S. Basu, S. Chakravarty, A. Chakravarty, D. Banerjee, A. Chakrabarti, Differential regulation of redox proteins and chaperones in HbEbeta-thalassemia erythrocyte proteome, *Proteomics Clin Appl*, 4 (2010) 480-488.

[81] K.N. Jensen, F. Jessen, B.M. Jorgensen, Multivariate data analysis of two-dimensional gel electrophoresis protein patterns from few samples, *J Proteome Res*, 7 (2008) 1288-1296.

[82] H. Kovarova, M. Hajduch, G. Korinkova, P. Halada, S. Krupickova, A. Gouldsworthy, N. Zhelev, M. Strnad, Proteomics approach in classifying the biochemical basis of the anticancer activity of the new olomoucine-derived synthetic cyclin-dependent kinase inhibitor, bohemine, *Electrophoresis*, 21 (2000) 3757-3764.

[83] J. Li, D.P. Sejas, R. Rani, T. Koretsky, G.C. Bagby, Q. Pang, Nucleophosmin regulates cell cycle progression and stress response in hematopoietic stem/progenitor cells, *J Biol Chem*, 281 (2006) 16536-16545.

[84] P. Brown, E. McIntyre, R. Rau, S. Meshinchi, N. Lacayo, G. Dahl, T.A. Alonzo, M. Chang, R.J. Arceci, D. Small, The incidence and clinical significance of nucleophosmin mutations in childhood AML, *Blood*, 110 (2007) 979-985.

[85] S.P. Cullen, I.S. Afonina, R. Donadini, A.U. Luthi, J.P. Medema, P.I. Bird, S.J. Martin, Nucleophosmin is cleaved and inactivated by the cytotoxic granule protease granzyme M during natural killer cell-mediated killing, *J Biol Chem*, 284 (2009) 5137-5147.

[86] A. Kumar, S. Agarwal, J.A. Heyman, S. Matson, M. Heidtman, S. Piccirillo, L. Umansky, A. Drawid, R. Jansen, Y. Liu, K.H. Cheung, P. Miller, M. Gerstein, G.S. Roeder, M. Snyder, Subcellular localization of the yeast proteome, *Genes Dev*, 16 (2002) 707-719.

- [87] D. Campana, F.G. Behm, Immunophenotyping of leukemia, *J Immunol Methods*, 243 (2000) 59-75.
- [88] L. De Zen, A. Orfao, G. Cazzaniga, L. Masiero, M.G. Cocito, M. Spinelli, A. Rivolta, A. Biondi, L. Zanesco, G. Basso, Quantitative multiparametric immunophenotyping in acute lymphoblastic leukemia: correlation with specific genotype. I. ETV6/AML1 ALLs identification, *Leukemia*, 14 (2000) 1225-1231.
- [89] J.W. Cui, J. Wang, K. He, B.F. Jin, H.X. Wang, W. Li, L.H. Kang, M.R. Hu, H.Y. Li, M. Yu, B.F. Shen, G.J. Wang, X.M. Zhang, Two-dimensional electrophoresis protein profiling as an analytical tool for human acute leukemia classification, *Electrophoresis*, 26 (2005) 268-279.
- [90] H. Parkinson, U. Sarkans, N. Kolesnikov, N. Abeygunawardena, T. Burdett, M. Dylag, I. Emam, A. Farne, E. Hastings, E. Holloway, N. Kurbatova, M. Lukk, J. Malone, R. Mani, E. Pilicheva, G. Rustici, A. Sharma, E. Williams, T. Adamusiak, M. Brandizi, N. Sklyar, A. Brazma, ArrayExpress update--an archive of microarray and high-throughput sequencing-based functional genomics experiments, *Nucleic Acids Res*, 39 (2011) D1002-1004.
- [91] S. Kazemi, Z. Mounir, D. Baltzis, J.F. Raven, S. Wang, J.L. Krishnamoorthy, O. Pluquet, J. Pelletier, A.E. Koromilas, A novel function of eIF2 α kinases as inducers of the phosphoinositide-3 kinase signaling pathway, *Mol Biol Cell*, 18 (2007) 3635-3644.
- [92] S. Grisendi, C. Mecucci, B. Falini, P.P. Pandolfi, Nucleophosmin and cancer, *Nat Rev Cancer*, 6 (2006) 493-505.
- [93] K. Nakamura, M. Fujimoto, T. Tanaka, Y. Fujikura, Differential expression of nucleophosmin and stathmin in human T lymphoblastic cell lines, CCRF-CEM and JURKAT analyzed by two-dimensional gel electrophoresis, *Electrophoresis*, 16 (1995) 1530-1535.
- [94] A.S. Lee, GRP78 induction in cancer: therapeutic and prognostic implications, *Cancer Res*, 67 (2007) 3496-3499.
- [95] F.M. Uckun, S. Qazi, Z. Ozer, A.L. Garner, J. Pitt, H. Ma, K.D. Janda, Inducing apoptosis in chemotherapy-resistant B-lineage acute lymphoblastic leukaemia cells by targeting HSPA5,

a master regulator of the anti-apoptotic unfolded protein response signalling network, *Br J Haematol*, 153 (2011) 741-752.

[96] C. Choudhary, C. Kumar, F. Gnad, M.L. Nielsen, M. Rehman, T.C. Walther, J.V. Olsen, M. Mann, Lysine acetylation targets protein complexes and co-regulates major cellular functions, *Science*, 325 (2009) 834-840.

[97] D. Szklarczyk, A. Franceschini, M. Kuhn, M. Simonovic, A. Roth, P. Minguéz, T. Doerks, M. Stark, J. Muller, P. Bork, L.J. Jensen, C. von Mering, The STRING database in 2011: functional interaction networks of proteins, globally integrated and scored, *Nucleic Acids Res*, 39 (2011) D561-568.

[98] R. Maddaly, G. Pai, S. Balaji, P. Sivaramakrishnan, L. Srinivasan, S.S. Sunder, S.F. Paul, Receptors and signaling mechanisms for B-lymphocyte activation, proliferation and differentiation--insights from both in vivo and in vitro approaches, *FEBS Lett*, 584 (2010) 4883-4894.

[99] H. Niiro, E.A. Clark, Regulation of B-cell fate by antigen-receptor signals, *Nat Rev Immunol*, 2 (2002) 945-956.

[100] H. Jumaa, R.W. Hendriks, M. Reth, B cell signaling and tumorigenesis, *Annu Rev Immunol*, 23 (2005) 415-445.

[101] N. Cheung, C.W. So, Transcriptional and epigenetic networks in haematological malignancy, *FEBS Lett*, 585 (2011) 2100-2111.

[102] N. Feldhahn, P. Rio, B.N. Soh, S. Liedtke, M. Sprangers, F. Klein, P. Wernet, H. Jumaa, W.K. Hofmann, H. Hanenberg, J.D. Rowley, M. Muschen, Deficiency of Bruton's tyrosine kinase in B cell precursor leukemia cells, *Proc Natl Acad Sci U S A*, 102 (2005) 13266-13271.

[103] L.F. Steel, M.G. Trotter, P.B. Nakajima, T.S. Mattu, G. Gonye, T. Block, Efficient and specific removal of albumin from human serum samples, *Mol Cell Proteomics*, 2 (2003) 262-270.

[104] N.L. Anderson, N.G. Anderson, The human plasma proteome: history, character, and

diagnostic prospects, *Mol Cell Proteomics*, 1 (2002) 845-867.

[105] Y. Tanaka, H. Akiyama, T. Kuroda, G. Jung, K. Tanahashi, H. Sugaya, J. Utsumi, H. Kawasaki, H. Hirano, A novel approach and protocol for discovering extremely low-abundance proteins in serum, *Proteomics*, 6 (2006) 4845-4855.

[106] R. Pieper, C.L. Gatlin, A.J. Makusky, P.S. Russo, C.R. Schatz, S.S. Miller, Q. Su, A.M. McGrath, M.A. Estock, P.P. Parmar, M. Zhao, S.T. Huang, J. Zhou, F. Wang, R. Esquer-Blasco, N.L. Anderson, J. Taylor, S. Steiner, The human serum proteome: display of nearly 3700 chromatographically separated protein spots on two-dimensional electrophoresis gels and identification of 325 distinct proteins, *Proteomics*, 3 (2003) 1345-1364.

[107] M.F. Ullah, M. Aatif, The footprints of cancer development: Cancer biomarkers, *Cancer Treat Rev*, 35 (2009) 193-200.

[108] J.N. Adkins, S.M. Varnum, K.J. Auberry, R.J. Moore, N.H. Angell, R.D. Smith, D.L. Springer, J.G. Pounds, Toward a human blood serum proteome: analysis by multidimensional separation coupled with mass spectrometry, *Mol Cell Proteomics*, 1 (2002) 947-955.

[109] R.S. Tirumalai, K.C. Chan, D.A. Prieto, H.J. Issaq, T.P. Conrads, T.D. Veenstra, Characterization of the low molecular weight human serum proteome, *Mol Cell Proteomics*, 2 (2003) 1096-1103.

[110] T. Baussant, L. Bougueleret, A. Johnson, J. Rogers, L. Menin, M. Hall, P.M. Aberg, K. Rose, Effective depletion of albumin using a new peptide-based affinity medium, *Proteomics*, 5 (2005) 973-977.

[111] A. Ettorre, C. Rosli, M. Silacci, S. Brack, G. McCombie, R. Knochenmuss, G. Elia, D. Neri, Recombinant antibodies for the depletion of abundant proteins from human serum, *Proteomics*, 6 (2006) 4496-4505.

[112] C. Greenough, R.E. Jenkins, N.R. Kitteringham, M. Pirmohamed, B.K. Park, S.R. Pennington, A method for the rapid depletion of albumin and immunoglobulin from human plasma, *Proteomics*, 4 (2004) 3107-3111.

- [113] L. Jiang, L. He, M. Fountoulakis, Comparison of protein precipitation methods for sample preparation prior to proteomic analysis, *J Chromatogr A*, 1023 (2004) 317-320.
- [114] T. Rabilloud, C. Valette, J.J. Lawrence, Sample application by in-gel rehydration improves the resolution of two-dimensional electrophoresis with immobilized pH gradients in the first dimension, *Electrophoresis*, 15 (1994) 1552-1558.
- [115] T. Rabilloud, A comparison between low background silver diammine and silver nitrate protein stains, *Electrophoresis*, 13 (1992) 429-439.
- [116] M.D. Bhattacharya D, Chakrabarti A. , Hemoglobin depletion from red blood cell cytosol reveals new proteins in 2-D gel-based proteomics study *Proteomics-Clin Appl.* , 1 (2007) 561-564.
- [117] P.D. Thomas, M.J. Campbell, A. Kejariwal, H. Mi, B. Karlak, R. Daverman, K. Diemer, A. Muruganujan, A. Narechania, PANTHER: a library of protein families and subfamilies indexed by function, *Genome Res*, 13 (2003) 2129-2141.
- [118] R. Komrokji, J. Lancet, R. Felgar, N. Wang, J.M. Bennett, Burkitt's leukemia with precursor B-cell immunophenotype and atypical morphology (atypical Burkitt's leukemia/lymphoma): case report and review of literature, *Leuk Res*, 27 (2003) 561-566.
- [119] O. Hrusak, A. Porwit-MacDonald, Antigen expression patterns reflecting genotype of acute leukemias, *Leukemia*, 16 (2002) 1233-1258.
- [120] N.L. Anderson, M. Polanski, R. Pieper, T. Gatlin, R.S. Tirumalai, T.P. Conrads, T.D. Veenstra, J.N. Adkins, J.G. Pounds, R. Fagan, A. Lohley, The human plasma proteome: a nonredundant list developed by combination of four separate sources, *Mol Cell Proteomics*, 3 (2004) 311-326.
- [121] D. Molle, J. Jardin, M. Piot, M. Pasco, J. Leonil, V. Gagnaire, Comparison of electrospray and matrix-assisted laser desorption ionization on the same hybrid quadrupole time-of-flight tandem mass spectrometer: application to bidimensional liquid chromatography of proteins from bovine milk fraction, *J Chromatogr A*, 1216 (2009) 2424-2432.

- [122] R.R. Burgess, Protein precipitation techniques, *Methods Enzymol*, 463 (2009) 331-342.
- [123] Bhattacharya D, Saha S, Basu S, Chakravarty S, Chakravarty A, Banerjee D, Chakrabarti A, Differential regulation of redox proteins and chaperones in HbEbeta-thalassemia erythrocyte proteome, *Proteomics - Clin App*, 4 (2010) 480-488.
- [124] K.S. Choi, L. Song, Y.M. Park, J. Marshall, A.L. Lund, H. Shion, E.M. Park, H.Z. Chae, J.H. Park, Analysis of human plasma proteome by 2DE- and 2D nanoLC-based mass spectrometry, *Prep Biochem Biotechnol*, 36 (2006) 3-17.
- [125] C. Tu, P.A. Rudnick, M.Y. Martinez, K.L. Cheek, S.E. Stein, R.J. Slebos, D.C. Liebler, Depletion of abundant plasma proteins and limitations of plasma proteomics, *J Proteome Res*, 9 (2010) 4982-4991.
- [126] E. Bellei, S. Bergamini, E. Monari, L.I. Fantoni, A. Cuoghi, T. Ozben, A. Tomasi, High-abundance proteins depletion for serum proteomic analysis: concomitant removal of non-targeted proteins, *Amino Acids*, 40 (2011) 145-156.
- [127] Y. Gong, X. Li, B. Yang, W. Ying, D. Li, Y. Zhang, S. Dai, Y. Cai, J. Wang, F. He, X. Qian, Different immunoaffinity fractionation strategies to characterize the human plasma proteome, *J Proteome Res*, 5 (2006) 1379-1387.
- [128] T. Linke, S. Doraiswamy, E.H. Harrison, Rat plasma proteomics: effects of abundant protein depletion on proteomic analysis, *J Chromatogr B Analyt Technol Biomed Life Sci*, 849 (2007) 273-281.
- [129] P.G. Righetti, E. Boschetti, A. Zanella, E. Fasoli, A. Citterio, Plucking, pillaging and plundering proteomes with combinatorial peptide ligand libraries, *J Chromatogr A*, 1217 (2010) 893-900.
- [130] P.G. Righetti, E. Fasoli, E. Boschetti, Combinatorial peptide ligand libraries: The conquest of the 'hidden proteome' advances at great strides, *Electrophoresis*, 32 (2011) 960-966.
- [131] T. Leger, D. Lavigne, J.P. Le Caer, L. Guerrier, E. Boschetti, J. Fareh, L. Feldman, O.

Laprevote, O. Meilhac, Solid-phase hexapeptide ligand libraries open up new perspectives in the discovery of biomarkers in human plasma, *Clin Chim Acta*, 412 (2011) 740-747.

[132] M. Fertin, O. Beseme, S. Duban, P. Amouyel, C. Bauters, F. Pinet, Deep plasma proteomic analysis of patients with left ventricular remodeling after a first myocardial infarction, *Proteomics Clin Appl*, 4 (2010) 654-673.

[133] L. Biro, G. Domjan, A. Falus, L. Jakab, K. Cseh, L. Kalabay, G. Tarkovacs, J. Tresch, E. Malle, J. Kramer, Z. Prohaszka, J. Jako, G. Fust, A. Csaszar, Cytokine regulation of the acute-phase protein levels in multiple myeloma, *Eur J Clin Invest*, 28 (1998) 679-686.

[134] O. Gallo, A.M. Gori, M. Attanasio, F. Martini, B. Giusti, T. Brunelli, E. Gallina, Interleukin-6 and acute-phase proteins in head and neck cancer, *Eur Arch Otorhinolaryngol*, 252 (1995) 159-162.

[135] A.M. van Bennekum, S. Wei, M.V. Gamble, S. Vogel, R. Piantedosi, M. Gottesman, V. Episkopou, W.S. Blaner, Biochemical basis for depressed serum retinol levels in transthyretin-deficient mice, *J Biol Chem*, 276 (2001) 1107-1113.

[136] J.Y. Kwak, T.Z. Ma, M.J. Yoo, B.H. Choi, H.G. Kim, S.R. Kim, C.Y. Yim, Y.G. Kwak, The comparative analysis of serum proteomes for the discovery of biomarkers for acute myeloid leukemia, *Exp Hematol*, 32 (2004) 836-842.

[137] Y. Kaneta, Y. Kagami, T. Tsunoda, R. Ohno, Y. Nakamura, T. Katagiri, Genome-wide analysis of gene-expression profiles in chronic myeloid leukemia cells using a cDNA microarray, *Int J Oncol*, 23 (2003) 681-691.

[138] L. Kalabay, K. Cseh, S. Benedek, S. Fekete, T. Masszi, K. Herjeczki, T. Pozsonyi, L. Jakab, Serum alpha 2-HS glycoprotein concentration in patients with hematological malignancies. A follow-up study, *Ann Hematol*, 63 (1991) 264-269.

[139] M.T. Dorak, A.K. Burnett, M. Worwood, HFE gene mutations in susceptibility to childhood leukemia: HuGE review, *Genet Med*, 7 (2005) 159-168.

[140] I. Takada, M. Mihara, M. Suzawa, F. Ohtake, S. Kobayashi, M. Igarashi, M.Y. Youn, K.

- Takeyama, T. Nakamura, Y. Mezaki, S. Takezawa, Y. Yogiashi, H. Kitagawa, G. Yamada, S. Takada, Y. Minami, H. Shibuya, K. Matsumoto, S. Kato, A histone lysine methyltransferase activated by non-canonical Wnt signalling suppresses PPAR-gamma transactivation, *Nat Cell Biol*, 9 (2007) 1273-1285.
- [141] J. Gauldie, C. Richards, D. Harnish, P. Lansdorp, H. Baumann, Interferon beta 2/B-cell stimulatory factor type 2 shares identity with monocyte-derived hepatocyte-stimulating factor and regulates the major acute phase protein response in liver cells, *Proc Natl Acad Sci U S A*, 84 (1987) 7251-7255.
- [142] L. Shi, J. Zhang, P. Wu, K. Feng, J. Li, Z. Xie, P. Xue, T. Cai, Z. Cui, X. Chen, J. Hou, F. Yang, Discovery and identification of potential biomarkers of pediatric acute lymphoblastic leukemia, *Proteome Sci*, 7 (2009) 7.
- [143] J. Basu, M. Kundu, M.M. Rakshit, P. Chakrabarti, Abnormalities of the erythrocyte membrane in chronic myelogenous leukemia, *Biotechnol Appl Biochem*, 12 (1990) 501-505.
- [144] M. Kundu, J. Basu, P. Chakrabarti, M.M. Rakshit, Abnormalities in the erythrocyte membrane in acute lymphoid leukaemia, *Biochem J*, 258 (1989) 903-906.
- [145] A. Kumar, C.M. Gupta, Red cell membrane abnormalities in chronic myeloid leukaemia, *Nature*, 303 (1983) 632-633.
- [146] M. Kundu, J. Basu, M. Fujimagari, P. Williamson, R.A. Schlegel, P. Chakrabarti, Altered erythrocyte protein kinase C activity and membrane protein phosphorylation in chronic myelogenous leukemia, *Biochim Biophys Acta*, 1096 (1991) 205-208.
- [147] S. Sharma, H.P. Pati, Erythrocyte enzyme abnormalities in leukemias, *J Assoc Physicians India*, 54 (2006) 453-457.
- [148] J. Delaunay, The molecular basis of hereditary red cell membrane disorders, *Blood Rev*, 21 (2007) 1-20.
- [149] S. Perrotta, P.G. Gallagher, N. Mohandas, Hereditary spherocytosis, *Lancet*, 372 (2008) 1411-1426.

- [150] S. Basu, D. Banerjee, S. Chandra, A. Chakrabarti, Eryptosis in hereditary spherocytosis and thalassemia: role of glycoconjugates, *Glycoconj J*, 27 (2010) 717-722.
- [151] A. Iolascon, R.A. Avvisati, C. Piscopo, Hereditary spherocytosis, *Transfus Clin Biol*, 17 (2010) 138-142.
- [152] P. Margetis, M. Antonelou, F. Karababa, A. Loutradi, L. Margaritis, I. Papassideri, Physiologically important secondary modifications of red cell membrane in hereditary spherocytosis-evidence for in vivo oxidation and lipid rafts protein variations, *Blood Cells Mol Dis*, 38 (2007) 210-220.
- [153] S. Rocha, E. Costa, P. Rocha-Pereira, F. Ferreira, E. Cleto, J. Barbot, A. Quintanilha, L. Belo, A. Santos-Silva, Erythrocyte membrane protein destabilization versus clinical outcome in 160 Portuguese Hereditary Spherocytosis patients, *Br J Haematol*, 149 (2010) 785-794.
- [154] D.G. Kakhniashvili, N.B. Griko, L.A. Bulla, Jr., S.R. Goodman, The proteomics of sickle cell disease: profiling of erythrocyte membrane proteins by 2D-DIGE and tandem mass spectrometry, *Exp Biol Med*, 230 (2005) 787-792.
- [155] A. Biondani, Turrini, F., Carta, F., et al., Heat-shock protein-27, -70 and peroxiredoxin-II show molecular chaperone function in sickle red cells: Evidence from transgenic sickle cell mouse model., *Proteomics-Clin App*, 2 (2008) 706-719.
- [156] E.M. Pasini, M. Kirkegaard, P. Mortensen, H.U. Lutz, A.W. Thomas, M. Mann, In-depth analysis of the membrane and cytosolic proteome of red blood cells, *Blood*, 108 (2006) 791-801.
- [157] F. Roux-Dalvai, A. Gonzalez de Peredo, C. Simo, L. Guerrier, D. Bouyssie, A. Zanella, A. Citterio, O. Burlet-Schiltz, E. Boschetti, P.G. Righetti, B. Monsarrat, Extensive analysis of the cytoplasmic proteome of human erythrocytes using the peptide ligand library technology and advanced mass spectrometry, *Mol Cell Proteomics*, 7 (2008) 2254-2269.
- [158] J.H. Ringrose, W.W. van Solinge, S. Mohammed, M.C. O'Flaherty, R. van Wijk, A.J. Heck, M. Slijper, Highly efficient depletion strategy for the two most abundant erythrocyte

soluble proteins improves proteome coverage dramatically, *J Proteome Res*, 7 (2008) 3060-3063.

[159] M. Bhattacharyya, S. Ray, S. Bhattacharya, A. Chakrabarti, Chaperone activity and prodan binding at the self-associating domain of erythroid spectrin, *J Biol Chem*, 279 (2004) 55080-55088.

[160] D. Majumder, D. Banerjee, S. Chandra, S. Banerjee, A. Chakrabarti, Red cell morphology in leukemia, hypoplastic anemia and myelodysplastic syndrome, *Pathophysiology*, 13 (2006) 217-225.

[161] E.M. Pasini, H.U. Lutz, M. Mann, A.W. Thomas, Red blood cell (RBC) membrane proteomics--Part II: Comparative proteomics and RBC patho-physiology, *J Proteomics*, 73 (2009) 421-435.

[162] Y. Iuchi, F. Okada, K. Onuma, T. Onoda, H. Asao, M. Kobayashi, J. Fujii, Elevated oxidative stress in erythrocytes due to a SOD1 deficiency causes anaemia and triggers autoantibody production, *Biochem J*, 402 (2007) 219-227.

[163] S.S. Ghatpande, P.K. Choudhary, C.T. Quinn, S.R. Goodman, Pharmacoproteomic study of hydroxyurea-induced modifications in the sickle red blood cell membrane proteome, *Exp Biol Med (Maywood)*, 233 (2008) 1510-1517.

[164] C. Mallozzi, A.M. Di Stasi, M. Minetti, Free radicals induce reversible membrane-cytoplasm translocation of glyceraldehyde-3-phosphate dehydrogenase in human erythrocytes, *Arch Biochem Biophys*, 321 (1995) 345-352.

[165] S. Rocha, R.M. Vitorino, F.M. Lemos-Amado, E.B. Castro, P. Rocha-Pereira, J. Barbot, E. Cleto, F. Ferreira, A. Quintanilha, L. Belo, A. Santos-Silva, Presence of cytosolic peroxiredoxin 2 in the erythrocyte membrane of patients with hereditary spherocytosis, *Blood Cells Mol Dis*, 41 (2008) 5-9.

[166] D. Banerjee, S. Saha, A. Chakrabarti, Porous red cell ultrastructure and loss of membrane asymmetry in a novel case of hemolytic anemia, *Eur J Haematol*, 81 (2008) 399-402.



CONCLUDING REMARKS

B-cell acute lymphoblastic leukaemia (B-ALL) is the most common cancer in children and constitutes the major class of lymphoid leukemia. At the same time, it constitutes a class of hematological malignancies with pretty high survival rates. The overall cure rate in children is about 80%, and about 45%-60% of adults have long-term disease-free survival. The identification of the genetic abnormalities associated with B-ALL has led to an improved understanding of B-ALL pathophysiology and consequent successful remissions in most of the cases. But, the mechanisms responsible for the B-cell developmental arrest are unknown. Nevertheless, the primary oncogenic events seem to require secondary cooperative changes to generate a fully transformed cell. Like those for most oncological diseases and malignancies, the popular treatment strategies for B-ALL include conventional chemotherapeutic anti-metabolites and nucleoside analogues that interfere with either different stages of DNA and protein synthesis or the integrity of mitotic spindle apparatus. These conventional treatment regimens exploit the 'rapid proliferation' property of cancer cells. However, although contemporary treatments cure more than 80% of children with B-ALL, some patients fall in high risk and/or poor prognosis classes requiring intensive treatment, others exhibit drug resistance and many patients still develop serious acute and late complications like pancytopenia, CNS relapses, etc. owing to the side effects of the treatments. Furthermore, the survival rate for adults with B-ALL remains below 40% despite the use of transplantation, and treatment outcome is poor among patients who relapse on current front-line ALL regimens. The majority of relapse cases have a clear relationship to the diagnosis leukemic clone, either arising through the acquisition of additional genetic lesions or, more commonly, arising from an ancestral (pre-diagnosis) clone. The initial excitement generated by the phenomenal success of a kinase inhibitor - imatinib, led to the expectation that other targeted therapeutics would be equally successful. But subsequent results indicated that in spite of some anti-leukemic activity shown by molecularly targeted agents, the responses they induce are seldom durable and certainly do not extend to all patients. This sobering fact emphasizes the need to link targeted

therapeutics to effective molecular profiling studies that show prospects of delineating the signalling pathway(s) that drive(s) leukemogenic progression of the disease. Additionally, such studies may assess the efficacy of available targeted therapies and propose novel effective therapeutic interventions. The choices for molecular profiling studies include genetic, transcriptomic and proteomic investigations. The proteome of a cell is dynamic unlike its genome, as it shows characteristic perturbations in response to disease and physiological state of the cell. Nonetheless, the knowledge that transcriptome data produces on genome-wide expression does not necessarily translate through to protein expression. Discrepancies between protein and mRNA abundances arise from post-translation modifications and epigenetic regulations, for e.g. by micro RNAs. Hence, proteomics wins over genomics and/or transcriptomic methodologies in investigating the states and/or abundances of the actual functional mediators of cellular physiology i.e. 'proteins'. When the goal of the proteomic experiment is to provide a list of proteins showing differential expressions in the sample of interest that was essentially the primary objective of our study, 2D gel electrophoresis followed by mass spectrometry is the best approach. 2D gels serve as molecular profile fingerprints and a thorough comparison of the proteomic profiles of normal and malignant cells can not only point out candidate diagnostic markers and/or therapeutic targets of the malignancy, but also throw light on the mechanism of transformation of the cells. Difference gel electrophoresis (DIGE) is feathered with the advantages of high-sensitivity and wide dynamic range of detection. However, a compromise in sensitivity, as in non-DIGE 2D gel electrophoresis, has the hidden profit of detecting only high-confidence 'true' differences. Parallel use of 2D gel electrophoresis and DIGE approaches can serve in validating the observations. With a preliminary two-dimensional gel electrophoresis (2DGE) followed by MALDI ToF/ToF tandem mass spectrometry approach and DIGE followed by tandem mass spectrometry validation studies, our comparative proteomic study of a homogeneous population of background matched CD19⁺ cells from B-ALL patients led to the identification of more than 75

differentially regulated proteins in the malignant CD19⁺ cells compared to normal primary CD19⁺ cells. Gene ontology (GO) annotation of the differentially regulated proteins revealed significant deregulation of proteins participating in protein metabolism, protein folding, protein translocation, transcriptional regulation, bioenergetics, redox homeostasis, cytoskeletal organization, RNA splicing, carbohydrate metabolism, signal transduction and DNA replication, in the malignant cells. Several of the proteins identified could be linked to specific signal transduction pathways relevant to leukemogenesis. Our data also implicate a number of novel proteins and pathways mediating ‘fine-tuning’ of B-cell signalling and leukemogenesis in B-ALL. Comparison of our data with microarray based gene expression profiles of B-ALL cells, available in ArrayExpress, NCBI revealed ~75% agreement between proteomic and transcriptomic trends. The interactome of the observed de-regulations could propose research avenues for addressing the leukemogenic B-cell biology. Furthermore, candidate proteins which exhibit opposite trends of de-regulations in myeloid vs. lymphoid leukemia might not only point out prospective biomarkers but also enhance our knowledge on the regulation of commitment and differentiation of the hematopoietic stem cell into myeloid or lymphoid lineages. Multivariate statistical analysis highlights existence of a correlation between genetic lesions and protein expression patterns that can be extrapolated to the association of characteristic protein expression patterns with good or poor prognosis genotypes known in B-ALL etiology. B-ALL is scantily addressed by the research community and the major reason for it is successful remissions and high survival rates for this class of leukemia. But, it is noteworthy that a study of the molecular profile of such good prognosis leukemia and comparison with that of the poor outcome leukemias will pave the way to identifying the causes of prognostic stratifications. Furthermore, significant differences between primary tumour cells and immortalised cell lines emphasizes the importance of obtaining protein profiling data from primary malignant B-cells, rather than immortalised cell lines.

Blood plasma is an easily accessible patient specimen and contains a dynamic load of mediators of various cellular responses, thereby comprehensively sampling the state of the body in disease. But definitive diagnostic plasma biomarkers of B-ALL are still unclear. This motivated us to study the plasma proteome of B-ALL patients and to identify differentially regulated protein biomarkers. The protein content of plasma however, is dominated by a handful of proteins such as albumin, immunoglobulins, and lipoproteins present across an extraordinary dynamic range of concentration. This exceeds the analytical capabilities of traditional proteomic methods, making detection of lower abundance disease-markers extremely challenging. Reduction of sample complexity is thus an essential first step in the analysis of plasma proteome. Previously available methods of depleting abundant proteins from plasma samples are expensive, laborious and time intensive and hence are unsuitable for high throughput screening of patient samples. We have employed ammonium sulfate precipitation based fractionation of plasma for depleting multiple high-abundance proteins that led to the detection of several low-abundance components in 2D gels. Like the previously available methods, our fractionation strategy fails to completely remove high-abundance components and suffered from limitations of specificity. However, since lack of specificity of our method is not biased with the sample type (normal or patient), and thereby can be effectively used for differential proteomics in clinical studies. Use of combinatorial peptide ligand libraries for depletion of abundant proteins and accessing low-abundance biomarkers in clinical proteomics studies of blood plasma further supports our notion that the objective of any pre-fractionation strategy for plasma is 'increased access to disease-markers' and not just 'specific removal of high abundance components'. Nonetheless, our method being simple, fast and inexpensive can actually be taken from 'bench' to 'bedside'. 2D gel electrophoresis of the pre-fractionated normal and B-ALL plasma samples followed by MALDI-TOF/TOF tandem mass spectrometry for identification of protein spots led to the identification of 15 disease-regulated proteins. Functional annotation of the identified proteins revealed differential regulation of chiefly

carrier proteins and proteolysis modulators along with several acute phase and tissue-leakage proteins including a histone deacetylase. The 2D proteome profiles can serve in a less-invasive (than bone-marrow aspiration) prognostic and minimal residual disease (MRD) monitoring of B-ALL. As most of the de-regulated proteins are involved in multiple physiological processes like proteolysis, cellular epigenetic regulation, cargo-transport and iron homeostasis, proteomic studies of blood plasma shows prospects of elucidating the pathophysiology and/or clinical manifestation of the B-ALL malignancy.

Like most of the other leukemic subtypes, B-ALL malignancies are presented with mild to severe anaemia. Several studies have reported abnormalities of the membrane cytoskeleton and enzyme activities of erythrocytes in myeloid as well as lymphoid leukaemias. Although myeloid cells and erythrocytes arise from a common progenitor population, the lymphoid cells originate from lymphoid progenitors that are distinct from the myeloid progenitors. Thus anaemic manifestation in B-ALL sounds intriguing. A comparative study of the membrane and cytosol proteome of erythrocytes purified from peripheral blood of normal volunteers, B-ALL patients and patients suffering from a non-malignant haematological disorder like hereditary spherocytosis (HS) can add beneficial insights to our understanding of altered erythrocyte physiology in leukaemia vs. erythroid disorders. Major difficulty of a proteomic analysis of erythrocyte cytosol is the large abundance of hemoglobin masking majority of the other cytosolic proteins. This issue had earlier been addressed in our laboratory with the development of an ion-exchange chromatography based hemoglobin depletion protocol. We have employed the same in this study for obtaining hemoglobin-depleted erythrocyte cytosol proteome. 2D gel electrophoresis and MALDI-ToF/ToF tandem mass spectrometry based proteomic investigation of normal, B-ALL and HS erythrocyte membrane and cytosol proteome revealed disease specific differential regulations. While HS erythrocyte cytosol showed up-regulation of redox regulators, B-ALL patients showed down-regulation of an oxidoreductase (aldehyde dehydrogenase). Redox regulators occupy a huge proportion of erythrocyte cytosol proteins,

just next to hemoglobin, indicating their major role in erythrocyte physiology. Discrepancies between B-ALL and HS redox enzyme levels hint towards different erythrocyte metabolic regulation schemes to adapt to crisis conditions of oxidative stress. The erythrocyte enzyme changes in B-ALL reflect possibilities of production of an abnormal clone of red blood cells derived from an abnormal pluripotent stem cell. 2D erythrocyte membrane proteome profiles led to the observation of elevated levels of membrane associated globin chains and reduced membrane association of glyceraldehydes-3-phosphate dehydrogenase (G3PD) in both B-ALL and HS patients. Membrane bound haemoglobin (MBH) is used as oxidative stress marker. Increased association of globin chains with the erythrocyte membranes in B-ALL and HS emphasize that erythrocytes are subjected to severe oxidative stress in both the haematological disorders. Membrane-bound denatured/oxidized hemoglobin has also been implicated in the proposed erythrocyte clearance mechanism, through the induction of band 3 clustering on the membrane, which in turn leads to autologous IgGs and complement binding and consequent erythro-phagocytosis. The ultra-structural changes observed in the B-ALL and HS erythrocyte membranes also indicate drastic changes in the architecture of the spectrin-based membrane skeleton that further assists in hemolysis and subsequent anaemia.